



National Library
of Canada

Acquisitions and
Bibliographic Services Branch

395 Wellington Street
Ottawa, Ontario
K1A 0N4

Bibliothèque nationale
du Canada

Direction des acquisitions et
des services bibliographiques

395, rue Wellington
Ottawa (Ontario)
K1A 0N4

Your file *Votre référence*

Our file *Notre référence*

NOTICE

The quality of this microform is heavily dependent upon the quality of the original thesis submitted for microfilming. Every effort has been made to ensure the highest quality of reproduction possible.

If pages are missing, contact the university which granted the degree.

Some pages may have indistinct print especially if the original pages were typed with a poor typewriter ribbon or if the university sent us an inferior photocopy.

Reproduction in full or in part of this microform is governed by the Canadian Copyright Act, R.S.C. 1970, c. C-30, and subsequent amendments.

AVIS

La qualité de cette microforme dépend grandement de la qualité de la thèse soumise au microfilmage. Nous avons tout fait pour assurer une qualité supérieure de reproduction.

S'il manque des pages, veuillez communiquer avec l'université qui a conféré le grade.

La qualité d'impression de certaines pages peut laisser à désirer, surtout si les pages originales ont été dactylographiées à l'aide d'un ruban usé ou si l'université nous a fait parvenir une photocopie de qualité inférieure.

La reproduction, même partielle, de cette microforme est soumise à la Loi canadienne sur le droit d'auteur, SRC 1970, c. C-30, et ses amendements subséquents.

Canada

Production of Domoic Acid, a Neurotoxin, by the Diatom
Pseudonitzschia pungens f. multiseriis Hasle
Under Phosphate and Silicate Limitation

by
Youlian Pan

A thesis submitted in partial fulfilment of the requirements for
the Degree of Doctor of Philosophy

at

Dalhousie University
Halifax, Nova Scotia, Canada

May, 1994

©Copyright by Youlian Pan, 1994



National Library
of Canada

Acquisitions and
Bibliographic Services Branch

395 Wellington Street
Ottawa, Ontario
K1A 0N4

Bibliothèque nationale
du Canada

Direction des acquisitions et
des services bibliographiques

395, rue Wellington
Ottawa (Ontario)
K1A 0N4

Your file *Votre référence*

Our file *Notre référence*

THE AUTHOR HAS GRANTED AN IRREVOCABLE NON-EXCLUSIVE LICENCE ALLOWING THE NATIONAL LIBRARY OF CANADA TO REPRODUCE, LOAN, DISTRIBUTE OR SELL COPIES OF HIS/HER THESIS BY ANY MEANS AND IN ANY FORM OR FORMAT, MAKING THIS THESIS AVAILABLE TO INTERESTED PERSONS.

L'AUTEUR A ACCORDE UNE LICENCE IRREVOCABLE ET NON EXCLUSIVE PERMETTANT A LA BIBLIOTHEQUE NATIONALE DU CANADA DE REPRODUIRE, PRETER, DISTRIBUER OU VENDRE DES COPIES DE SA THESE DE QUELQUE MANIERE ET SOUS QUELQUE FORME QUE CE SOIT POUR METTRE DES EXEMPLAIRES DE CETTE THESE A LA DISPOSITION DES PERSONNE INTERESSEES.

THE AUTHOR RETAINS OWNERSHIP OF THE COPYRIGHT IN HIS/HER THESIS. NEITHER THE THESIS NOR SUBSTANTIAL EXTRACTS FROM IT MAY BE PRINTED OR OTHERWISE REPRODUCED WITHOUT HIS/HER PERMISSION.

L'AUTEUR CONSERVE LA PROPRIETE DU DROIT D'AUTEUR QUI PROTEGE SA THESE. NI LA THESE NI DES EXTRAITS SUBSTANTIELS DE CELLE-CI NE DOIVENT ETRE IMPRIMES OU AUTREMENT REPRODUITS SANS SON AUTORISATION.

ISBN 0-315-98919-X

Canada

Name YOU LIAN PAN

Dissertation Abstracts International is arranged by broad, general subject categories. Please select the one subject which most nearly describes the content of your dissertation. Enter the corresponding four-digit code in the spaces provided.

Biological Oceanography

0416

U·M·I

SUBJECT TERM

SUBJECT CODE

Subject Categories

THE HUMANITIES AND SOCIAL SCIENCES

COMMUNICATIONS AND THE ARTS
 Architecture 0729
 Art History 0377
 Art 0900
 Cinema 0378
 Dance 0357
 Fine Arts 0723
 Information Science 0291
 Music 0413
 Speech Communication 0459
 Theater 0465

EDUCATION
 General 0515
 Administration 0514
 Adult and Continuing 0516
 Agricultural 0517
 Art 0273
 Bilingual and Multicultural 0282
 Business 0488
 Early Childhood 0518
 Elementary 0524
 Finance 0277
 Guidance and Counseling 0519
 Health 0680
 Higher 0745
 History of 0520
 Home Economics 0278
 Industrial 0521
 Language and Literature 0279
 Mathematics 0280
 Music 0522
 Philosophy of 0998
 Physical 0523

Psychology 0525
 Reading 0535
 Religious 0527
 Sciences 0714
 Secondary 0533
 Social Sciences 0534
 Sociology of 0340
 Special 0529
 Teacher Training 0530
 Technology 0710
 Tests and Measurements 0288
 Vocational 0747

LANGUAGE, LITERATURE AND LINGUISTICS
 Language 0679
 General 0289
 Ancient 0290
 Linguistics 0291
 Modern 0401
 Literature 0294
 General 0295
 Classical 0297
 Comparative 0298
 Medieval 0299
 Modern 0316
 African 0591
 American 0305
 Asian 0352
 Canadian (English) 0355
 Canadian (French) 0593
 English 0311
 Germanic 0312
 Latin American 0315
 Middle Eastern 0313
 Romance 0314
 Slavic and East European 0314

PHILOSOPHY, RELIGION AND THEOLOGY
 Philosophy 0422
 Religion 0318
 General 0321
 Biblical Studies 0319
 Clergy 0320
 History of 0322
 Philosophy of 0469
 Theology

SOCIAL SCIENCES
 American Studies 0323
 Anthropology 0324
 Archaeology 0326
 Cultural 0327
 Physical
 Business Administration 0310
 General 0272
 Accounting 0770
 Banking 0454
 Management 0338
 Marketing 0385
 Canadian Studies
 Economics 0501
 General 0503
 Agricultural 0505
 Commerce Business 0508
 Finance 0509
 History 0510
 Labor 0511
 Theory 0358
 Folklore 0351
 Geography 0578
 Gerontology
 History
 General

Ancient 0579
 Medieval 0581
 Modern 0582
 Black 0328
 African 0331
 Asia, Australia and Oceania 0332
 Canadian 0334
 European 0335
 Latin American 0336
 Middle Eastern 0333
 United States 0337
 History of Science 0585
 Law 0398
 Political Science
 General 0615
 International Law and Relations 0616
 Public Administration 0617
 Recreation 0814
 Social Work 0452
 Sociology
 General 0626
 Criminology and Penology 0627
 Demography 0938
 Ethnic and Racial Studies 0631
 Individual and Family Studies 0628
 Industrial and Labor Relations 0629
 Public and Social Welfare 0630
 Social Structure and Development 0700
 Theory and Methods 0344
 Transportation 0709
 Urban and Regional Planning 0999
 Women's Studies 0453

THE SCIENCES AND ENGINEERING

BIOLOGICAL SCIENCES
 Agriculture 0473
 General 0285
 Agronomy
 Animal Culture and Nutrition 0475
 Animal Pathology 0476
 Food Science and Technology 0359
 Forestry and Wildlife 0478
 Plant Culture 0479
 Plant Pathology 0480
 Plant Physiology 0817
 Range Management 0777
 Wood Technology 0746
 Biology 0306
 General 0287
 Anatomy 0308
 Biostatistics 0309
 Botany 0379
 Cell 0329
 Ecology 0353
 Entomology 0369
 Genetics 0793
 Limnology 0410
 Microbiology 0307
 Molecular 0317
 Neuroscience 0416
 Oceanography 0433
 Physiology 0821
 Radiation 0778
 Veterinary Science 0472
 Zoology
 Biophysics 0786
 General 0760
 Medical

EARTH SCIENCES
 Biogeochemistry 0425
 Geochemistry 0996

Geodesy 0370
 Geology 0372
 Geophysics 0373
 Hydrology 0388
 Mineralogy 0411
 Paleobotany 0345
 Paleocology 0426
 Paleontology 0418
 Paleozoology 0985
 Palynology 0427
 Physical Geography 0368
 Physical Oceanography 0415

HEALTH AND ENVIRONMENTAL SCIENCES
 Environmental Sciences 0768
 Health Sciences
 General 0566
 Audiology 0300
 Chemotherapy 0992
 Dentistry 0567
 Education 0350
 Hospital Management 0769
 Human Development 0758
 Immunology 0982
 Medicine and Surgery 0564
 Mental Health 0347
 Nursing 0569
 Nutrition 0570
 Obstetrics and Gynecology 0380
 Occupational Health and Therapy 0354
 Ophthalmology 0381
 Pathology 0571
 Pharmacology 0419
 Pharmacy 0572
 Physical Therapy 0382
 Public Health 0573
 Radiology 0574
 Recreation 0575

Speech Pathology 0460
 Toxicology 0383
 Home Economics 0386

PHYSICAL SCIENCES
 Pure Sciences
 Chemistry 0485
 General 0749
 Agricultural 0486
 Analytical 0487
 Biochemistry 0488
 Inorganic 0738
 Nuclear 0490
 Organic 0491
 Pharmaceutical 0494
 Physical 0495
 Polymer 0754
 Radiation 0405
 Mathematic
 Physics 0605
 General 0986
 Acoustics
 Astronomy and Astrophysics 0606
 Atmospheric Science 0608
 Atomic 0748
 Electronics and Electricity 0607
 Elementary Particles and High Energy 0798
 Fluid and Plasma 0759
 Molecular 0609
 Nuclear 0610
 Optics 0752
 Radiation 0756
 Solid State 0611
 Statistics 0463
 Applied Sciences
 Applied Mechanics 0346
 Computer Science 0984

Engineering 0537
 General 0538
 Aerospace 0539
 Agricultural 0540
 Automotive 0541
 Electronics and Electrical 0544
 Heat and Thermodynamics 0348
 Hydraulic 0545
 Industrial 0546
 Marine 0547
 Materials Science 0794
 Mechanical 0548
 Metallurgy 0743
 Mining 0551
 Nuclear 0552
 Packaging 0549
 Petroleum 0765
 Sanitary and Municipal 0554
 System Science 0790
 Geotechnology 0428
 Operations Research 0796
 Fast Technology 0795
 Textile Technology 0994

PSYCHOLOGY
 General 0621
 Behavioral 0384
 Clinical 0622
 Developmental 0620
 Experimental 0623
 Industrial 0624
 Personality 0625
 Physiological 0989
 Psychobiology 0349
 Psychometrics 0632
 Social 0451



献给我的父母

To my parents

CONTENTS

CONTENTS	v
LIST OF FIGURES	xii
LIST OF TABLES	xviii
ABSTRACT	xx
SYMBOLS AND ABBREVIATIONS	xxi
ACKNOWLEDGEMENTS	xxv
CHAPTER 1. GENERAL INTRODUCTION	1
1.1. The problems	1
1.2. The approaches	2
1.3. Literature review	8
1.3.1. History of <i>Pseudonitzschia pungens</i>	8
1.3.2. Distribution of <i>Pseudonitzschia pungens</i>	10
1.3.3. Domoic acid poisoning	11
1.3.4. Physiological and ecological studies	13
CHAPTER 2. GENERAL METHODS	16
2.1. Organisms and culture	16
2.2. Culture media	16
2.2.1. Medium F	17
2.2.2. Medium FE	18
2.2.3. Medium H	19

2.3. Measurement of biomass	19
2.4. Chlorophyll <i>a</i> analysis	20
2.5. Nutrient analyses	20
2.5.1. Particulate carbon and nitrogen	20
2.5.2. Particulate phosphorus and silicon	21
2.5.2.1. Oxidation	21
2.5.2.2. Analysis	21
2.5.3. Dissolved phosphorus and silicon	22
2.5.4. Dissolved inorganic nutrients	22
2.5.5. Dissolved carbon dioxide	23
2.6. Analysis of domoic acid	23
2.7. Measurements of Adenosine triphosphate (ATP) and adenyl energy charge (EC)	24
2.7.1. Reagents	25
2.7.1.1. Inorganic compounds	25
2.7.1.2. Tris buffer	25
2.7.1.3. Organic compounds and enzymes	25
2.7.2. Filtration and extraction (enzyme inactivation)	27
2.7.3. Assay	27
2.8. Measurements of alkaline phosphatase activity	29
2.8.1. Reagents	29
2.8.2. Assay	30

2.9. Relationships between photosynthesis and photosynthetic photon flux density (PPFD)	31
2.10. Chemostat continuous culture system	33
2.11. Growth	35
2.11.1. Batch culture	35
2.11.2. Continuous culture	36
CHAPTER 3. PHOTOSYNTHESIS AND GROWTH	37
3.1. Introduction	37
3.2. Materials and methods	39
3.2.1. Determination of particulate chlorophyll <i>a</i> , carbon and nitrogen, dissolved inorganic nutrients and light	39
3.2.2. Growth rate	40
3.2.3. Experiment A: effects of culture age	40
3.2.4. Experiment B: light dependence	41
3.2.5. Experiment C: temperature dependence	41
3.3. Results	42
3.3.1. Dependence of photosynthesis and growth on age of the cultures	42
3.3.1.1. Growth and cellular chemical composition	42
3.3.1.2. Photosynthesis	49
3.3.2. Photosynthesis and growth under different PPFD levels	54
3.3.2.1. Growth and cellular chemical composition	54
3.3.2.2. Photosynthesis	60
3.3.3. Temperature dependence of photosynthesis and growth	63

3.3.3.1. Growth and cellular chemical composition	63
3.3.3.2. Photosynthesis	67
3.4. Discussion	70
3.4.1. Growth	70
3.4.2. Chemical composition	74
3.4.3. Photosynthesis	78
3.4.4. Overview	82
CHAPTER 4. EFFECTS OF SILICATE LIMITATION ON GROWTH AND DOMOIC ACID PRODUCTION IN BATCH CULTURES	85
4.1. Introduction	85
4.2. Materials and methods	86
4.3. Results	88
4.3.1. In medium F (Treatment A)	94
4.3.2. In high-Si medium (Treatment B)	95
4.3.3. In low-Si medium (Treatments C and D)	97
4.3.4. Silicate perturbation	97
4.4. Discussion	99
4.4.1. Growth	99
4.4.2. Cellular silicon	101
4.4.3. Roles of silicon in cell metabolism	102
4.4.4. Production of domoic acid in relation to silicate limitation	105

CHAPTER 5.	SILICATE LIMITATION AND DOMOIC ACID PRODUCTION IN CHEMOSTAT CONTINUOUS CULTURES	109
5.1.	Introduction	109
5.2.	Materials and methods	110
5.2.1.	Chemostat system	110
5.2.2.	Preparation of culture medium and stock culture	110
5.2.3.	Procedures for experiments	113
5.3.	Results	115
5.3.1.	Experiment I: continuous culture	115
5.3.2.	Experiment II: continuous culture	123
5.3.3.	Experiment III: extended batch culture	127
5.3.4.	Growth kinetics	130
5.4.	Discussion	134
5.4.1.	Growth and uptake kinetics in relation to domoic acid production	134
5.4.2.	Cellular chemical composition and DA production	141
5.4.3.	Domoic acid production in relation to nutrient metabolism	146
CHAPTER 6.	PHOSPHATE LIMITATION AND DOMOIC ACID PRODUCTION IN CHEMOSTAT CONTINUOUS CULTURE	151
6.1.	Introduction	151
6.2.	Materials and methods	152
6.2.1.	Chemostat system	152
6.2.2.	Preparation of culture medium and stock culture	152

6.2.3. Procedures for experiments	153
6.3. Results	155
6.3.1. Steady states in continuous cultures	155
6.3.2. Principal component analysis	162
6.3.3. Extended batch mode	168
6.4. Discussion	175
6.4.1. Growth and DA production	175
6.4.2. N:P ratios and DA production	178
6.4.3. Phosphate limitation and cellular chemical composition	182
6.4.4. Alkaline phosphatase activity and DA production	184
6.4.5. Relationships between DA production and other primary metabolism (energy partitioning)	186
CHAPTER 7. GENERAL DISCUSSION: BIOCHEMICAL AND ECOLOGICAL PERSPECTIVES	189
7.1. Biochemical perspectives	190
7.2. Bioenergetics in relation to DA production	194
7.3. Ecological perspectives	196
7.3.1. Effects of light and temperature	196
7.3.2. Implication of abnormal nutrient ratios	198
7.3.3. Implication of heavy precipitation and freshwater discharge	203
7.3.4. Population dynamics of <i>P. pungens</i> f. <i>multiseries</i> and DA production	207
CHAPTER 8. CONCLUSIONS	209

APPENDICES		213
Appendix A1.	List of publications	214
Appendix B1.	One example of standard curves for particulate (A) phosphorus and (B) silicon measurements (Chapter 2).	216
Appendix B2.	Examples for the standard curves for the measurements of ATP, ATP+ADP, ATP+ADP+AMP (Chapter 2).	217
Appendix B3.	Examples for the measurements of alkaline phosphatase activity. (A) standard curve, (B) one example (July 13, chamber 2; Chapters 2, 6).	218
Appendix B4.	Sensitivity and coefficient of variation of various methods used (Chapter 2)	219
Appendix C1.	Silicate concentrations (μM) of the control and the reservoir during the silicate limited continuous culture experiments (Chapter 5).	220
Appendix C2.	Silicate limited steady state experiments (Chapter 5). (A) DA concentrations (left: DA in cultures, right: DA per cell) and (B) DA production, in relation to bacterial abundance.	221
Appendix C3.	Bacterial effects on DA production (Chapter 5).	222
Appendix D1.	Future developments	225
	D1.1. Domoic acid as a valuable compound	225
	D1.2. Further research potential	226
REFERENCES		227

LIST OF FIGURES

Fig. 1.1.	<i>Pseudonitzschia pungens</i> f. <i>multiseries</i> , a pennate diatom bloomed in the fall-winter of 1987 in Cardigan Bay, Prince Edward Island (PEI). (Top) colonies of <i>P. pungens</i> f. <i>multiseries</i> (scale: 1 cm = 40 μ m), (Bottom) map of PEI.	3
Fig. 1.2.	Domoic acid and related compounds.	4
Fig. 1.3.	Amnesic shellfish poisoning occurred in Cardigan Bay PEI and resulted in 105 cases of human poisonings and \$3 x 10 ⁶ economic loss (Addison and Stewart, 1989).	5
Fig. 1.4.	Potential pathway of domoic acid biosynthesis (refers to Luckner, 1984, Laycock <i>et al.</i> , 1989 and Douglas <i>et al.</i> , 1992).	12
Fig. 2.1.	Schematic display of chemostat system. 1 = chemostat culture chamber, 2 = thermostat water jacket, 3 = stir bar, 4 = effluent, 5 = polycarbonate buffer cylinder, 6 = sterile air filter (0.2 μ m), 7 = cotton filters, 8 = activated charcoal to remove organic compounds in the air, 9 = measuring cylinder for effluent measurements, 10 = stopcock.	34
Fig. 3.1.	Growth curves based on different indices of biomass fitted by Gompertz equation (2.11).	43
Fig. 3.2.	Modelled (Equation 2.12) growth rates (μ , d ⁻¹) based on different indices of biomass during the first 15 days of the culture.	46
Fig. 3.3.	Variations with time in the cellular (A) carbon, (B) nitrogen, and (C) chlorophyll <i>a</i> . Error bar = 1 standard deviation. Absent of error bar means it is smaller than the symbol. The curves are the ratios of the corresponding lines in Fig. 3.1.	47
Fig. 3.4.	Changes with time in the ratios of (A) carbon to chlorophyll <i>a</i> (by weight) and (B) carbon to nitrogen (atomic). The curves are the ratios of corresponding lines in Fig. 3.1.	48
Fig. 3.5.	Relationships between photosynthesis and PPFD in cultures after 4 days growth. (A) normalized to chlorophyll <i>a</i> (μ g C [μ g Chl <i>a</i>] ⁻¹ h ⁻¹), (B) normalized to carbon (μ g C [μ g C] ⁻¹ h ⁻¹). The curves	

	are fitted by Equation 2.6.	50
Fig. 3.6.	Variations of α^B in various phases of batch culture. (A) normalized to chlorophyll <i>a</i> ($\mu\text{g C } [\mu\text{g Chl } a]^{-1} \text{ h}^{-1} [\mu\text{mol m}^{-2} \text{ s}^{-1}]^{-1}$), (B) normalized to carbon ($\mu\text{g C } [\mu\text{g C}]^{-1} \text{ h}^{-1} [\mu\text{mol m}^{-2} \text{ s}^{-1}]^{-1}$).	52
Fig. 3.7.	Variation of P_m^B in various phases of batch culture. (A) normalized to chlorophyll <i>a</i> ($\mu\text{g C } [\mu\text{g Chl } a]^{-1} \text{ h}^{-1}$), (B) normalized to carbon ($\mu\text{g C } [\mu\text{g C}]^{-1} \text{ h}^{-1}$).	53
Fig. 3.8.	Growth curves of <i>P. pungens</i> f. <i>multiseries</i> under various PPFD levels ($\mu\text{mol m}^{-2} \text{ s}^{-1}$) fitted by Gompertz equation (2.11).	55
Fig. 3.9.	Variations with PPFD levels in (A) the maximal growth (the solid curve is fitted by Equations 3.7 to the 5 filled points only and the broken line is fitted to all the 8 data points), (B) the duration of lag phase and (C) the time when maximal growth reached (fitted by Equation 3.8).	57
Fig. 3.10.	Variations with PPFD levels in the cellular (A) carbon, (B) nitrogen and (C) chlorophyll <i>a</i> . The lines are linear regressions.	58
Fig. 3.11.	Variations with PPFD levels in the ratios of (A) carbon to chlorophyll <i>a</i> (by weight) and (B) carbon to nitrogen (atomic).	59
Fig. 3.12.	Variations of α^B with PPFD levels. (A) normalized to chlorophyll <i>a</i> , (B) normalized to carbon. The curves are fitted by exponential functions.	61
Fig. 3.13.	Variations of P_m^B with PPFD levels. (A) normalized to chlorophyll <i>a</i> , (B) normalized to carbon. The lines are linear regressions.	62
Fig. 3.14.	Growth rate of <i>P. pungens</i> f. <i>multiseries</i> at different temperatures. The curve is fitted by eye.	64
Fig. 3.15.	Effect of temperature on the cellular (A) carbon, (B) nitrogen and (C) chlorophyll <i>a</i> . The curves are fitted by eye.	65
Fig. 3.16.	Effect of temperature on the ratios of (A) carbon to chlorophyll <i>a</i> (by weight) and (B) carbon to nitrogen (atomic). The curves are fitted by eye.	66
Fig. 3.17.	Relationships between photosynthesis and photosynthetic photon	

	flux density (P-I curves, Equation 2.6) at (A) 0° to 25°C, (B) 15°C and (C) 0°C.	68
Fig. 3.18.	Variations of (A) P_m^B and (B) α^B with temperature. The curves are fitted by eye.	69
Fig. 3.19.	Relationships of (A) growth rates and (B) photosynthetic rate (P_m^B) with cellular chlorophyll <i>a</i> . The lines are linear regressions.	77
Fig. 3.20.	Relationship between growth rate (μ) and photosynthetic rate (P_m^B). (A) P_m^B is normalized to chlorophyll <i>a</i> , (B) P_m^B is normalized to carbon. The lines are linear regressions.	79
Fig. 4.1.	Experimental design. Four treatments: (A) control, the initial DISi was 95 μ M; (B) high initial DISi 190 μ M; (C) low initial DISi = 61 μ M, 65 μ M Si spiked on day 14; (D) low initial DISi = 65 μ M, 120 μ M Si added on day 25. Each treatment was in triplicate. The curves are plotted by eye.	87
Fig. 4.2.	Treatment A. Variations in (A) cell concentrations, (B) dissolved inorganic silicate, (C) particulate silicon, (D) chlorophyll <i>a</i> and (E) domoic acid concentrations during the growth cycle. Error bar = 1 standard deviation. Absence of error bar means the standard deviation was smaller than the symbol. The curve in A is fitted by Equation 2.11.	90
Fig. 4.3.	Treatment B. Legend as in Fig. 4.2.	91
Fig. 4.4.	Treatment C. (B) Silicate (65 μ M) was added on day 14. Other legends as in Fig. 4.2.	92
Fig. 4.5.	Treatment D. (B) Silicate (120 μ M) was added on day 25. Other legends as in Fig. 4.2.	93
Fig. 4.6.	Relationship between cellular domoic acid and growth rate during the DISi perturbation experiments. The solid curves are the slopes of curves in Figs. 4.4A (A) and 4.5A (B) respectively.	98
Fig. 4.7.	Relationship of maximum DA concentrations in the culture and DA per cell with silicate supply. The lines are linear regressions.	106
Fig. 5.1.	Schematic procedures for experiments. See text for details.	112

Fig. 5.2.	Experiment I. Variations with growth rate: (A) DA concentration, (B) cellular DA, (C) DA production rate, and (D) DISi. Silicate concentration in the reservoir was 165.4 (± 9.0) μM . The curves in A, B, C, are fitted by Equation 5.1.	121
Fig. 5.3.	Experiment I. Relationships of domoic acid with (A) silicate, (B) phosphate in the culture medium, and (C) ATP concentrations in the cells. The curves in A and B are fitted by an exponential function like Equation 5.1 and the line in C is a linear regression.	122
Fig. 5.4.	Experiment II. Variations with growth rate: (A) DA concentration, (B) cellular DA, (C) DA production rate, (D) bacterial abundance, and (E) DISi and DSi. Silicate concentration in the reservoir was 56.2 (± 3.4) μM . The curves are fitted by Equation 5.1 or by eye.	124
Fig. 5.5.	Experiments I + II. Domoic acid concentration (filtrate + cells) in relation to growth rate. The curve is fitted by Equation 5.1.	126
Fig. 5.6.	Experiment III. Variations with time in (A) cell concentration, (B) DA per cell, (C) DA in filtrate, (D) DA in cells + filtrate, (E) bacterial abundance, and (F) DISi.	128
Fig. 5.7.	Growth kinetics fitted with Droop's cell quota model: $\mu = \mu_{max}' (Q - K_q)/Q$. (A) Experiments I and II, (B) Experiment I, and (C) Experiment II.	131
Fig. 5.8.	Growth kinetics fitted with Goldman equation: $\mu = \mu_{max}' U/(K_U + U)$. (A) both Experiments I and II, (B) Experiment I, and (C) Experiment II.	133
Fig. 5.9.	Domoic acid in relation to silicate uptake rate. (A) DA in the whole culture, (B) DA in cells, and (C) DA production rate. Curves fitted by Equation 5.1.	138
Fig. 5.10.	Relationships between domoic acid production and cell chemical composition. The curve in A is fitted by Equation 5.1.	144
Fig. 5.11.	ATP concentrations in relation to (A) growth rate, (B) silicate uptake, and (C) DA production. The lines are linear regressions, broken lines corresponding to open triangles, solid line to filled circles.	147

Fig. 5.12.	Relationships between domoic acid concentration and other cell metabolism. The curve in A is fitted by an exponential function, as in Equation 5.1. The lines in B and C are linear regressions corresponding to open triangles (broken) and filled circles (solid).	148
Fig. 6.1.	Schematic illustration of procedures for experiments. See text for details.	154
Fig. 6.2.	Relationship of growth rate and phosphate uptake rate during the continuous culture. μ_m' is fixed at 1.10 d^{-1} (the maximum μ_m' from Chapter 5). $\mu = \mu_m' U/(K_U+U)$.	158
Fig. 6.3.	Variation with growth rate in the steady state experiments. (A) domoic acid concentration, (B) cellular DA and its production, (C) alkaline phosphatase activity (APA, $\text{ng P } [\mu\text{g Chl } a]^{-1} \text{ h}^{-1}$), and (D) dissolved phosphorus. The curves in A, B, C are fitted by Equation 5.1 and those in D are fitted by eye.	159
Fig. 6.4.	Relationships between alkaline phosphatase activity (APA) and dissolved inorganic phosphate. The curve is fitted by Equation 5.1.	161
Fig. 6.5.	Relationships of alkaline phosphatase activity to (A) DA production, (B) cellular DA, (C) DA in the filtrate, and (D) total DA in continuous cultures. The lines are linear regressions.	163
Fig. 6.6.	Relationships of N:P (atomic) ratios to (A) DA production, (B) cellular DA, and (C) total DA in continuous cultures. Curves fitted by eye.	164
Fig. 6.7.	Relationships of cellular DA (filled circle) and DA production (open triangles) with (A) carbon assimilation, uptake of (B) phosphate, (C) nitrate and (D) silicate in continuous cultures. Curves fitted by Equation 5.1.	165
Fig. 6.8.	Relationships of growth rate to (A) ATP, (B) ATP+ADP+AMP, and (C) adenylate energy charge (EC) in continuous cultures. Curves fitted by eye.	166
Fig. 6.9.	Variations of (A) growth rate, (B) total DA in the culture and (C) DA production in relation to the scores of first principle component (PC1) in continuous cultures. The line in A is linear regression and the curves in B and C are fitted by Equation 5.1.	169

Fig. 6.10	Chamber 1 in the extended batch mode. Variations with time in (A) biomass [concentrations of cell (left) and chlorophyll a (right)], (B) DA [cellular DA (left) and its production (right)], (C) APA ($\text{ng P } [\mu\text{g Chl } a]^{-1} \text{ h}^{-1}$, left) and percentage of DA in the medium, and (D) dissolved phosphorus (left) and silicate (right).	170
Fig. 6.11.	Chamber 6 in the extended batch mode. Legend as Fig. 6.10. (D) 61 μM phosphate was added to the culture on day 4.	172
Fig. 6.12.	Chamber 2 in the extended batch mode. Legend as Fig. 6.10. (D) 142 μM of silicate was added to the culture on day 1 and 50 μM phosphate on day 4.	174
Fig. 7.1.	The study area. The surface circulation pattern as described by Lauzier (1965).	204
Fig. 7.2.	Proposed explanation for the toxigenic blooms of <i>Pseudo-nitzschia pungens</i> f. <i>multiseries</i> in Cardigan Bay PEI.	206

LIST OF TABLES

Table 1.1.	Known distribution of <i>Pseudonitzschia pungens</i> in the world oceans.	6
Table 1.2.	Comparison of the two different forma of <i>Pseudonitzschia pungens</i> . Values in the parenthesis are means.	9
Table 2.1.	Composition of medium F.	17
Table 2.2.	Composition of medium H.	18
Table 3.1.	Nutrient concentrations (μM) in culture medium during growth of <i>P. pungens</i> f. <i>multiseries</i> in Experiment A.	44
Table 3.2.	Changes in photoadaptive parameters of <i>P. pungens</i> f. <i>multiseries</i> with time at two PPFD levels in Experiment A.	51
Table 3.3.	Values of parameters in Equation 3.8.	56
Table 3.4.	Changes in photoadaptive parameters I_m , I_k and I_s ($\mu\text{mol m}^{-2} \text{s}^{-1}$) during growth at different PPFDs in Experiment B.	63
Table 3.5.	Initial slopes of μ -I curves in selected diatoms and dinoflagellates. $\alpha_g = 10^{-3} \text{ d}^{-1} [\mu\text{mol m}^{-1} \text{s}^{-1}]^{-1}$.	74
Table 4.1.	Maximum growth rates, chlorophyll <i>a</i> , cell concentration, particulate silicon and DA concentration during growth of <i>P. pungens</i> f. <i>multiseries</i> under 4 different conditions. Values in parentheses give the ages (day) of the culture when these measurements were made.	89
Table 4.2.	Variation in the cellular silicon content in selected diatom species.	103
Table 5.1a.	Experiment I: measured variable, their statistics and their correlation with growth rate, DA production and concentrations.	117
Table 5.1b.	Experiment II: legend as Table 5.1a.	118
Table 5.2a.	Experiment I: cellular chemical compositions of <i>P. pungens</i> f. <i>multiseries</i> expressed as ratios at various growth rates, their	

	correlations (R) with DA production ($\mu\text{g DA l}^{-1} \text{d}^{-1}$) and concentration ($\mu\text{g DA l}^{-1}$).	119
Table 5.2b.	Experiment II: legend as Table 5.2a.	120
Table 5.3.	Common changes of chemical properties in Experiments I and II as a result of increase in growth rate.	125
Table 5.4.	Growth kinetics in chemostat cultures (function: $\mu = \mu_{\text{max}}' (Q - k_q)/Q$). Values in parentheses are standard deviations.	130
Table 5.5.	Growth kinetics in chemostat cultures. Data were from the direct fitting equation 5.3 to experimental data points. Values in parentheses are standard deviations.	132
Table 5.6.	Growth kinetics in chemostat cultures. Data were determined first by performing linear regression on Q vs. U . and then by fine-tune fitting equation 5.3 to experimental data points. Values in parentheses are standard deviations.	134
Table 5.7.	Comparison of DA production in steady-state continuous cultures with the production in batch cultures under silicate limitation.	139
Table 6.1.	Steady state experiments: measured variables, their statistics and their correlations with growth rate, DA production and concentration.	157
Table 6.2.	Fitted values of Fig 6.2. During fitting, an up-limit of 1.10 d^{-1} (the μ_m' value from Chapter 5) was applied in comparison with the values obtained by directly fitting. Values in the parentheses are standard deviations of fitting.	158
Table 6.3.	Steady state experiments: results of principal component analysis of observed variables showing percentage of variance and correlation coefficients (n=19, significant level = 0.43).	167
Table 6.4.	Steady state cultures: cellular chemical compositions and their correlations with growth rate, domoic acid and its production. Values of C:Chla, N:Chla, Si:Chla and P:Chla are $\mu\text{g}:\mu\text{g}$, and the rest are molar ratios.	181
Table 7.1.	Characteristics of two types of conditions for DA production.	193

ABSTRACT

Pseudonitzschia pungens f. *multiseries* Hasle is the first diatom to have been implicated in an episode of shellfish poisoning. In 1987, 150 people became sick and 3 died after consuming mussels, *Mytilus edulis*, from Cardigan Bay, Prince Edward Island (Addison and Stewart, 1989). It was discovered that the mussels had been feeding on a monospecific bloom of *P. pungens* f. *multiseries*, and the toxin involved was domoic acid (DA, Subba Rao *et al.*, 1988a). This thesis reports an investigation of the physiology of the diatom, with particular emphasis on factors that lead to DA production.

Photosynthesis, phosphate (P) and silicate (Si) uptake, and domoic acid production were studied in batch and chemostat continuous cultures. The photosynthetic carbon assimilation rate of *P. pungens* f. *multiseries* was low compared to other diatoms, especially when the cultures progressed into stationary phase and were nutrient limited. Luxury uptake of P and Si occurred when the culture populations were perturbed with these nutrients after being starved of them. Domoic acid was produced both in dividing and non-dividing populations and the production rates correlated with the severity of P or Si limitation. Production of DA was significantly enhanced when overall cell metabolism declined due to nutrient limitation. In the batch cultures, there were two stages of DA production. The first stage corresponded to the decline of population growth, and the second stage to nutrient limitation. These two stages are believed to be controlled by self-limiting factors and external stress respectively. In continuous culture, the same two stages were detected. Under severe limitation of either P or Si, DA production rose to maximum levels around $200 \mu\text{g l}^{-1} \text{d}^{-1}$ ($3.17 \text{ pg DA cell}^{-1} \text{d}^{-1}$) and the maximum DA levels attained were $11.9 \text{ pg DA cell}^{-1}$ in cells and $1118 \mu\text{g l}^{-1}$ in whole culture. The main conclusions are (i) the self-limiting control associated with decline of population growth is an essential prerequisite to DA production, but the main control is external nutrient stress; (ii) the major cell mechanism regulating DA production is a change in partitioning of energy and precursors between primary and secondary metabolism; (iii) the domoic acid poisoning episodes in Cardigan Bay were likely caused by abnormal nutrient ratios in the sea water.

SYMBOLS AND ABBREVIATIONS

α^B	The initial slope of the P^B -I curve ($\text{ng C } [\mu\text{g Chl } a]^{-1} \text{ h}^{-1} [\mu\text{mol m}^{-2} \text{ s}^{-1}]^{-1}$ or $\text{ng C } [\mu\text{g C}]^{-1} \text{ h}^{-1} [\mu\text{mol m}^{-2} \text{ s}^{-1}]^{-1}$).
α_g	The initial slope of the μ_m -I curve ($\text{d}^{-1} [\mu\text{mol m}^{-2} \text{ s}^{-1}]^{-1}$).
β^B	The photoinhibition index (same units as α^B).
μ	(Specific) growth rate (d^{-1}).
μ_m	Maximum growth rate (d^{-1}).
$\mu_{m(m)}$	Maximum growth rate at optimal PPFD levels (d^{-1}).
0-MF	3-0-methylfluorescein.
0-MFP	3-0-methylfluorescein phosphate.
ADP	Adenosine diphosphate.
AMP	Adenosine monophosphate.
AP	Alkaline phosphatase.
APA	Alkaline phosphatase activity.
ASP	Amnesic shellfish poisoning.
ATP	Adenosine triphosphate.
C	Carbon.
Chl	Chlorophyll.
CHN	Carbon, hydrogen and nitrogen.
d	day.
D	Dilution rate in chemostat continuous culture (d^{-1}).
DA	Domoic acid.

DAD	Diode array detector (one method for DA analysis).
DAPI	Diamidino-2-phenyl-indole dihydrochloride.
DCMU	3-(3,4-dichlorophenyl)-1,1-dimethylurea.
DIP	Dissolved inorganic phosphate.
DISi	Dissolved inorganic silicate.
DNA	Deoxyribonucleic acid.
DP	Total dissolved phosphorus.
DSi	Total dissolved silicon.
EC	Adenyl energy charge (Equation 2.4).
EDTA	Ethylene diamine tetraacetic acid.
f	The negative initial slope of t_m -I curve (Equation 3.8).
fg	femtogram (10^{-15} gram).
FMOG	9-fluoromethyl-methoxycarbonyl (one method for DA analysis).
GF/F	Glass fibre filter, grade F.
HL	High light ($1100 \mu\text{mol m}^{-2} \text{s}^{-1}$).
I	Photosynthetic photon flux density ($\mu\text{mol m}^{-2} \text{s}^{-1}$).
I_k	Photo-adaptive index (Equation 2.9).
I_m	I corresponding to the maximum photosynthetic rate P_m^B (Equation 2.8).
I_s	I corresponding to P_s^B (Equation 2.10).
LL	Low light ($105 \mu\text{mol m}^{-2} \text{s}^{-1}$).
MK	Myokinase (or Adenylate kinase).
MW	Molecular weight.
N	Nitrogen.

N_1, N_2	Biomass at times 1 and 2 respectively (Equation 3.1)
N_0	Initial biomass.
N_t	Cell number at time t .
ng	nanogram (10^{-9} gram).
Pi	Phosphate.
P	Phosphorus.
P^B	Biomass normalized photosynthetic rate ($\mu\text{g C } [\mu\text{g C}^{-1} \cdot \text{a}]^{-1} \text{ h}^{-1}$ or $\mu\text{g C } [\mu\text{g C}]^{-1} \text{ h}^{-1}$, Equation 2.6).
P^B_d	The intercept of the P^B -I curve on the Y-axis (same units as P^B , Equation 2.6).
P^B_m	P^B at optimum I (Equation 2.7).
P^B_s	The maximum <i>potential</i> P^B in the absence of photoinhibition (same units as P^B , Equation 2.6).
PC	Particulate carbon.
PC1	Principal component 1.
PC2	Principal component 2.
PC3	Principal component 3.
PC4	Principal component 4.
PC5	Principal component 5.
PEI	Prince Edward Island.
PEP	Phosphoenolpyruvate.
pg	picogram (10^{-12} gram).
PK	Pyruvate kinase.
PIP	Particulate inorganic phosphorus.

PISi	Particulate inorganic silicon.
PC	Particulate carbon.
PN	Particulate nitrogen.
PP	Particulate phosphorus.
PPFD	Photosynthetic photon flux density ($\mu\text{mol m}^{-2} \text{s}^{-1}$).
PSi	Particulate silicon.
PSP	Paralytic shellfish poisoning.
Q_{10}	Ratios of metabolic rates at the temperatures of 10°C difference.
R	Correlation coefficient.
R_a	Chlorophyll <i>a</i> fluorescence after acidification.
R_b	Chlorophyll <i>a</i> fluorescence before acidification.
RNA	Ribonucleic acid.
rpm	Revolutions per minute.
Std	Standard deviation.
μg	microgram (10^{-6} gram).
T	Temperature ($^{\circ}\text{C}$).
t	Time (day).
t_1, t_2	Times 1 and 2 respectively (Equation 3.1)
t_d	Maximum t_m (day), when the culture is in the dark (Equation 3.8).
t_m	The time (day) needed to reach μ_m (Equation 3.8).
Tris	Trishydroxymethylaminomethane.
Y	Magnitude of change in biomass ($\text{Ln}(N_t/N_0)$, Equation 2.11). N_t = biomass at time t, N_0 = biomass at time 0.

ACKNOWLEDGEMENTS

It would be impossible for a long journey like a Ph.D. program to reach its destination without the support from various sources. My guru, Subba Rao Durvasula has been a continuous source of humour and logistic support, Ken Mann has been an excellent English teacher and continuous source of financial support, and along with other committee members Bob Brown, Glen Harrison and Bill Li provided stimulating guidance and criticism throughout the research and writing of the thesis. I am indebted to my committee.

Don Gordon, Jim Stewart and Mike Sinclair helped and encouraged me throughout. Subba Rao Durvasula isolated and supplied NPBIO strain, and K. Pauley isolated KP-59 stain, of *Pseudonitzschia pungens* f. *multiseries*. The KP-59 strain was supplied by Jim Stewart. Both strains were confirmed by the taxonomic authorities G. Hasle and G. A. Fryxell. Leo Vining and Jeff Wright gave me criticism on the potential pathway of domoic acid synthesis (Fig. 1.4) and enriched my knowledge of secondary metabolism. Wade Blanchard (Dalhousie Statistical Consulting Service) gave me critical evaluation of various statistical methods used. Trevor Platt took time to discuss with me the P-I model. Roddy Warnock instructed me and let me use his photosynthetron. Steve Bates provided me with his unpublished manuscripts when I was writing the thesis. Richard Gallant (PEI Department of Fisheries and Aquaculture) provided reports of a PEI mussel monitoring program. Roger Pocklington and his crew, Jeff Wright (Jr.), Krista Pronk and Jim Leonard analyzed domoic acid throughout. Bill Li and Paul Dickie kindly collected mid-Atlantic sea water for me during their 1991 JGOFS cruise, taught me the DAPI method for bacterial quantification and helped in many other experimental issues. Yonghong Guan enumerated bacteria epifluorescent samples. Lorne Lea (DFO, Charlottetown) and Peter Vass assisted in collecting Cardigan Bay seawater and helped in many other ways. Peter Strain and Pierre Clement analyzed nutrients at the initial stage. Mark Hodgson, Leslie Harris and Brian Irwin provided instruction and let me use their CHN analyzer and spectrophotometers. Peter Vass, Jim Frost, Brian Irwin, Bill Li, Ron O'Dor and Jim Novitski loaned me equipment. Paul Keizer let me use his office during the renovation period of 1992. Paul Boudreau loaned me his computer. Gary Wohlgeschaffen, Ann Orr, Joanne Jellett, Linda Marks and Zhiming Yu gave me support as both friends and colleagues. Sharon Morgan (Bedford Institute) and Steve Fry, Donna Healy, Finn Sander and Barbara Cossar (Dalhousie University) gave me technical and administrative support. Art Cosgrove and Heinz Wiele (Bedford Institute) assisted with graphics and slides for presentation. People in the Biology Department at Dalhousie and the Biological Science Branch at BIO supported me physically and

morally. My parents, my wife Yonghong, my children Elysia and Eric gave me constant support and encouragement. I sincerely appreciate the efforts of, and extend gratitude to, all these people.

Dalhousie University and Bedford Institute of Oceanography afforded me space and facilities for these studies. This work has been funded by research grants from the Natural Sciences and Engineering Research Council of Canada (NSERC) to Ken Mann, Graduate Scholarships from Dalhousie University to Y. Pan and by grants from the phycotoxin program in the Department of Fisheries and Oceans, Canada (DFO) to Subba Rao Durvasula. I received Lett bursary for a travel grant and a personal emergency support.

Parts of the results of Chapter 3 have been published (Appendix A1, Nos. 7 and 11). Copyright permission has been obtained from Elsevier Scientific Publishers B. V., Amsterdam for the reproduction.

CHAPTER 1

GENERAL INTRODUCTION

1.1. The problems

Production of phycotoxin by diatom blooms was unknown until 1987. In 1987, a monospecific bloom of a pennate diatom *Pseudonitzschia pungens* f. *multiseriis* Hasle (formerly *Nitzschia pungens* f. *multiseriis* Grunow, Fig. 1.1) occurred in Cardigan Bay, Prince Edward Island (PEI). This diatom produced a neurotoxin, domoic acid (DA, Fig. 1.2), which was accumulated by the blue mussel (*Mytilus edulis* Linnaeus). Subsequently, consumption of the toxin-laden mussels resulted in amnesic shellfish poisoning (ASP). It caused economic losses of approximately \$3 x 10⁶ (Fig. 1.3) due to the closure of shellfisheries and 105 cases of human poisonings, of which 3 were fatal (Addison and Stewart, 1989).

P. pungens f. *multiseriis* is an ubiquitous diatom distributed from 60 °N to 40 °S in both Atlantic and Pacific (Table 1.1). The physiology and ecology of this diatom, which bloomed in the fall and winter, unlike most other diatom blooms which occur in the spring, was not much known before the outbreak of the toxigenic blooms in 1987. *P. pungens* f. *multiseriis* is the first diatom reported toxigenic and its toxigenesis only occurs in certain waters of the world oceans. This raised several questions, i.e. (i) Under

what conditions, does it become toxigenic and what are the triggers of the toxin synthesis? (ii) How can it bloom in the late fall and winter when the natural conditions are obviously not favoured for other diatom blooms?

1.2. The approaches

In *P. pungens* f. *multiseries*, DA production usually started when the active growth declined, and toxicity in nature occurred 7-10 days after the peak of the bloom (Silvert and Subba Rao, 1992). This suggests that DA production is associated with physiological stresses, such as nutrient limitation. Natural marine ecosystems are very complex because of the interaction of physical, chemical and biological factors, so it is very difficult to pinpoint the main factors that regulate a specific algal bloom and induce the toxin production. This is true for any other toxigenic algal blooms. Therefore in the present studies I used cultures as analogues of natural blooms, controlling a few environmental factors and simulating the bloom conditions in the PEI bays to study the physiology, ecology and toxigenesis of *P. pungens* f. *multiseries*.

In this thesis I investigated: 1) the physiological ecology of *P. pungens* f. *multiseries*; 2) the role of nutrients in the development and decline of the monospecific toxigenic blooms; and 3) the role of physiological stress due to nutrient limitation in the DA production. The hypothesis is tested that *P. pungens* f. *multiseries* produces domoic acid when stressed by nutrient limitation. After description of methodology (Chapter 2), photosynthesis and growth of this diatom in relation to physiological stages, light history

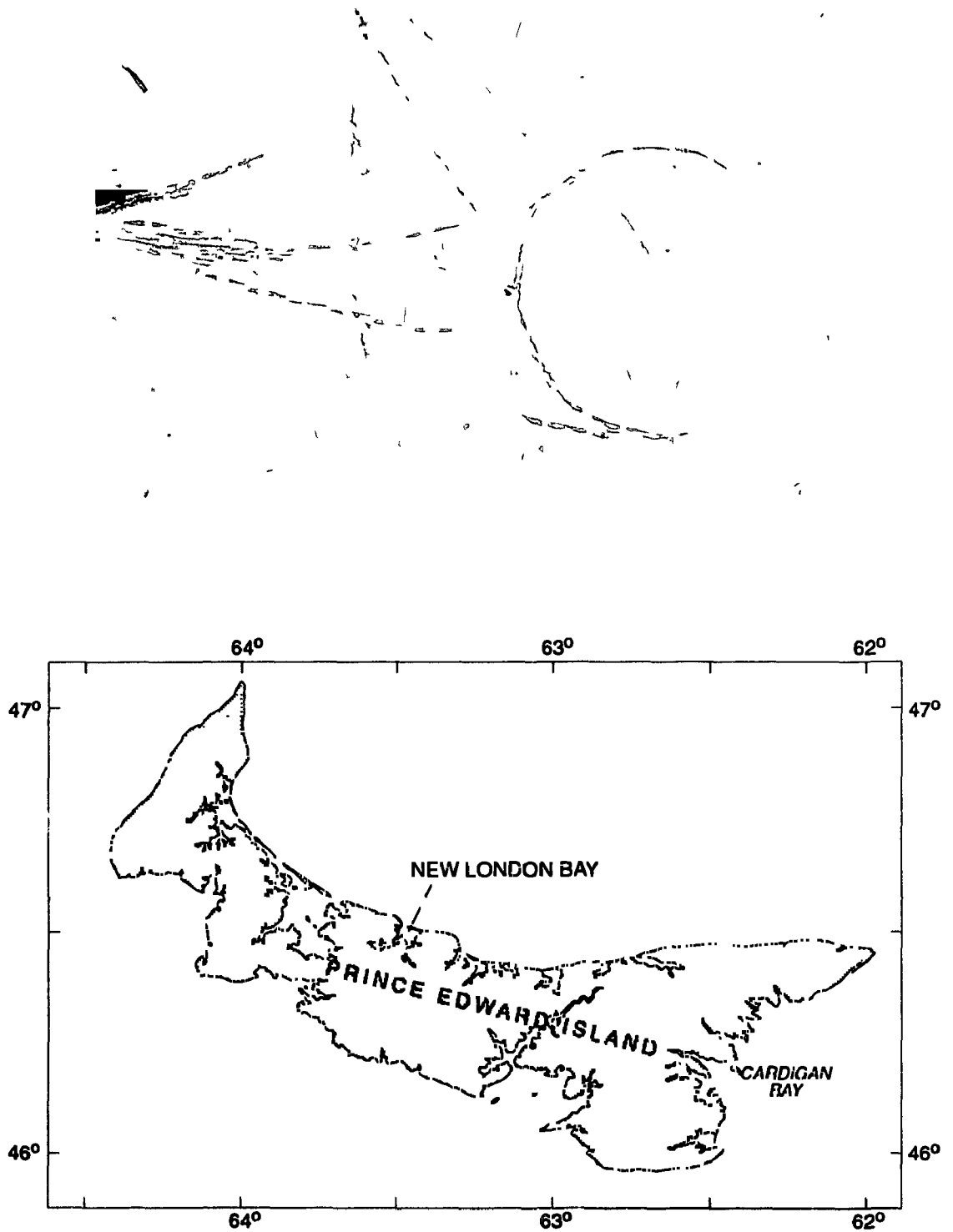


Fig. 1.1. *Pseudonitzschia pungens* f. *multiseriis*, a pennate diatom bloomed in the fall-winter of 1987 in Cardigan Bay, Prince Edward Island. (Top) colonies of *P. pungens* f. *multiseriis* (scale: 1 cm = 40 μ m), (Bottom) map of PEI.

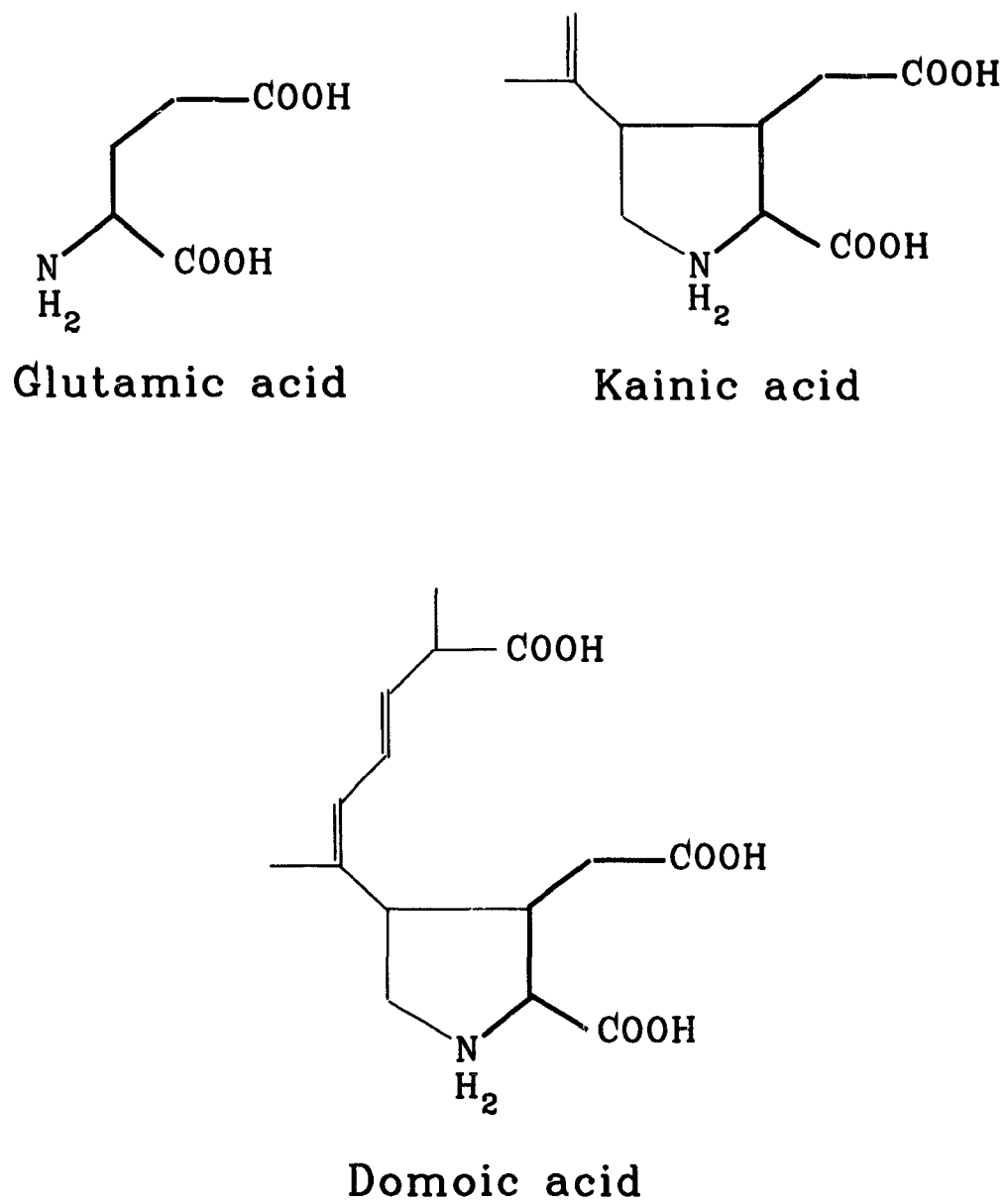


Fig. 1.2. Domoic acid and related compounds.

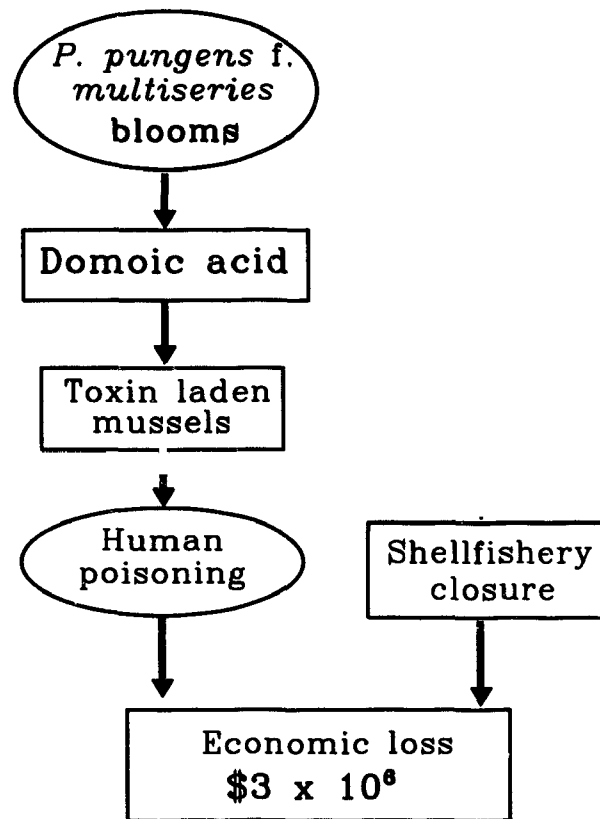


Fig. 1.3. Amnesic shellfish poisoning occurred in Cardigan Bay PEI and resulted in 105 cases of human poisonings and $\$3 \times 10^6$ economic loss (Addison and Stewart, 1989).

Table 1.1. Known distribution of *Pseudonitzschia pungens* in the world oceans. Forma m = f. *multiseries*, p = f. *pungens*.

Region	Ocean	Location	Abundance (10 ³ cells l ⁻¹)	Forma (m/p)	References	
Cardigan Bay, Canada	Atlantic	46°15'N, 62°30'W	10-15000	m	Bates <i>et al.</i> , 1939	
Nova Scotia, Canada		43-47°N, 50-60°W	0.08-100	m and p	Subba Rao., unpublished	
Gulf of Mexico, USA		30°N, 85-90°W		m	Dickey <i>et al.</i> , 1992	
New York Bight, USA		40°N, 74°W	0.12-2.95		Marshall and Cohn, 1987b	
Eastern coast, USA		35-45°N, 66-76°W	0.10-19.50		Marshall and Ranasinghe, 1989	
Chesapeake Bay, USA		37°15'N, 76°25'W		m	Cupp, 1943	
Norwegian Sea		62°N			Hasle, 1972	
Drobak, Norway		59°40'N, 10°40'E		m	Hasle, 1965	
Cabo Frio, Brazil		23°S, 42°W			Gonzalez-Rodriguez <i>et al.</i> , 1985	
Atlantida, Uruguay		34°46'S, 55°45'W		m	Hasle, 1965	
Quequen, Argentina		38°30'S, 59°W		m	Hasle, 1965	
British Columbia, Canada		Pacific	48-53°N, 126-131°W	3700-10600		Forbes and Denman, 1991
British Columbia, Canada			49°45'-50°N, 124°W			Sancetta, 1989
West coast, USA	33-45°N, 117-125°W				Cupp, 1943	
Oregon, USA	32-46°N, 124-125°W			m	Hasle, 1965	

Table 1.1. Continued

Region	Ocean	Location	Abundance (10 ³ cells l ⁻¹)	Forma (m/p)	References
Chile	Pacific	30-50°S, 72-77°W			Rivera, 1985
Wellington Harbour, New Zealand		41°S, 174°E			Hasle, 1972
Western North Pacific		20-34°N, 139-155°E			Furuya and Marumo, 1983
Hachijo Island, Japan		32-40°N, 140°E	10.1%		Furuya <i>et al.</i> , 1986
Ofunato - Atsumi Bays, Japan		35-39°N, 137-141°E		p and m	Takano and Kuroki, 1977
Yeddo Bay, Japan		N E			Grunow, 1988
Meizhou Bay, China		24°N, 118°E			Lin <i>et al.</i> , 1991
Eastern China Sea		24-42°N, 112-124°E			Zou <i>et al.</i> , 1993
Kori, Korea					Yoo and Lee, 1982
Gulf of Santa Fe	Caribbean				Breeuwer de Ramirez, 1977
Cayo Enrique-Gata, Puerto Rico		22°N, 66°W			Navarro, 1983
Mithapur, India	Indian				Ram <i>et al.</i> , 1989
Banyuls-sur-Mer, France	Mediterranean	42°29'N, 03°18'W			Cahet <i>et al.</i> , 1972
Golf du lion					Fiala <i>et al.</i> , 1976
Indian Sector	Antarctic	61-65°S, 100-120°E			Kawamura and Ichikawa, 1984

and temperature are studied in Chapter 3. Onset of the stationary phase is coincident with silicate depletion in the medium. Chapters 4 and 5 deal with physiology and toxigenesis of the diatom under silicate stress, showing that toxin production is greatly enhanced when silicate is depleted in the cultures. To further demonstrate the roles of nutrient stress in DA production, bioenergetics and phosphate stress are studied in Chapter 6. Biochemical and ecological perspectives on the formation of the toxigenic blooms in nature are presented in Chapter 7. The major contributions to physiological ecology of *P. pungens* f. *multiseries* are concluded in Chapter 8.

1.3. Literature review

1.3.1. History of *Pseudonitzschia pungens*

Pseudonitzschia pungens was first found by Grunow (1882) from Yeddo Bay in Japan and reported as *Homoeccladia pungens* Grunow. Cleve (1897) characterized it as having "linear-lanceolate, acute" valves. It has a synonym of *Nitzschia pungens* var. *atlantica* Cleve (Cupp, 1943). Hasle (1965) recorded forma *multiseries* of this species in the samples from Drobak in Norway, Chesapeake Bay and Oregon in the United States, Atlantida in Uruguay, and Quequen in Argentina. Takano and Kuroki (1977) observed forma *pungens* of this species co-occurring with forma *multiseries* and some other members of *Pseudonitzschia* group from Japanese coastal waters.

Pseudonitzschia pungens is a pennate, colony-forming diatom. Because of the

similarity in the shapes of frustule and colony between *P. pungens* on one hand and *P. seriata* Cleve and five other closely related species on the other, Hasle (1965) grouped them as *Nitzschia seriata*-complex in genus *Nitzschia* (Hasle, 1965). The unique type of colony-formation and the shape of frustule readily indicate this complex as a member of *Pseudonitzschia* Peragallo, which was considered to be subdivisional group in the Genus *Nitzschia* Hasle, Bacillariophyceae before 1993. Since 1993, this group is now promoted to be the Genus *Pseudonitzschia* Peragallo (Hasle, 1993).

Table 1.2. Comparison of two different forma of *Pseudonitzschia pungens*. Values in the parentheses are means.

Measurement	<i>f. multiseriata</i>	<i>f. pungens</i>
Length (μm)	68-140 (100)	81-151 (106)
Width (μm)	4-5	3.1-5 (4)
Transapical costae in 10 μm	10-13	11-14
Poroids	Fine, 4-6 in 1 μm or 2-4 rows between costae	Round, usually 2 rows, one at each side of costa
References	Hasle, 1965; Takano & Kuroki, 1977	Takano & Kuroki, 1977

There are two forma in the species of *P. pungens*, *f. multiseriata* and *f. pungens*. Of these two forma, only *f. multiseriata* is toxigenic (Subba Rao *et al.*, 1988a, 1990; Bates *et al.*, 1989; Smith *et al.*, 1990a). Differences between these two forma can only be seen under the electron microscope (Table 1.2). The main differences are the size and the number of rows of poroids: usually fine poroids, 4-6 in 1 μm (Hasle, 1965) or 2-4 rows

between costae (Takano and Kuroki, 1977) for forma *multiseries*; and round poroids, usually 2, one row at each side of a costa, for forma *pungens*. Changes in morphology have been observed for f. *multiseries* under different physiological conditions (Subba Rao and Wohlgeschaffen, 1990) or in different stages of the life cycle (Subba Rao *et al.*, 1991).

1.3.2. Distribution of *Pseudonitzschia pungens*

Pseudonitzschia pungens is an ubiquitous species distributed from 62 °N (Hasle, 1965) to 65 °S (Kawamura and Ichikawa, 1984). It has been found in the Pacific (Takano and Kuroki, 1977; Forbes and Denman, 1990), Atlantic (Hasle, 1965, 1972; Marshall and Ranasinghe, 1989), Indian (Ram *et al.*, 1989), Antarctica (Kawamura and Ichikawa, 1984) and Mediterranean (Cahet *et al.*, 1972). Its cell concentration ranged from a few cells per litre to 15×10^6 cells per litre (Table 1.1).

Pseudonitzschia pungens f. *multiseries* occurs between 60 °N and 40 °S in the Atlantic and Pacific oceans (Table 1.1). Most recently, it has been reported toxigenic in the northwest Atlantic coasts from Cardigan Bay, Prince Edward Island (PEI) (Subba Rao *et al.*, 1988a, 1990; Bates *et al.*, 1989) in the north (46 °N) to the Gulf of Mexico (Dickey *et al.*, 1992) in the south (15 °N); and in the northeast Pacific (Scholin *et al.*, 1994; Whyte *et al.*, 1994 and personal communication, October, 1993).

On the Northwest Atlantic coasts, this species has been recorded since 1965 and appeared year-round. Cell concentrations ranged from a few cells (Marshall and his associates, 1983-1989) to 15 million cells l⁻¹ (Bates *et al.*, 1989). The relative rank of

abundance of this species was usually higher in the fall and winter than in spring and summer, more in near-shore than in offshore (Marshall and Cohn, 1987a, b). In the PEI bays also, the toxigenic form, *Pseudonitzschia pungens* f. *multiseries* was most abundant in the fall and winter, but very low in the summer (Bates *et al.*, 1989).

1.3.3. Domoic acid poisonings

P. pungens f. *multiseries* caused amnesic shellfish poisoning (ASP) in PEI bays in 1987, 1988 (Silvert and Subba Rao, 1991) and also during 1989, 1990 (Smith, unpublished) and 1991. This diatom was most abundant during the winter of 1987 and the poisoning was most severe. The mussels accumulated DA produced by *P. pungens* f. *multiseries* (Subba Rao *et al.*, 1988a, 1990, Bates, *et al.* 1989, Wohlgeschaffen *et al.*, 1992).

More recently, DA was detected in *P. pungens* f. *multiseries* from the Gulf of Mexico (Dickey *et al.*, 1992), in *P. australis* Frenguelli (= *Nitzschia pseudoseriata* Hasle, Fritz *et al.*, 1992; Garrison *et al.*, 1992) and in *P. pungens* f. *multiseries* (Scholin *et al.*, 1994) from Monterey Bay, California. Domoic acid poisoning, which was believed to be related to *P. australis* or *P. pungens* f. *multiseries*, was also reported from California (Work *et al.*, 1993) and Oregon coasts (Wood and Shapiro, 1993). In the fall of 1993, DA poisoning also occurred along the Canadian Pacific coasts attributable to the toxigenic *P. pungens* f. *multiseries* (Whyte, personal communication, October, 1993). Earlier, DA was isolated from two red algae, *Chondria armata* Okamura in Japan and nearby waters (Takemoto and Daigo, 1958) and *Alsidium corallinum* C. Agardh in Mediterranean

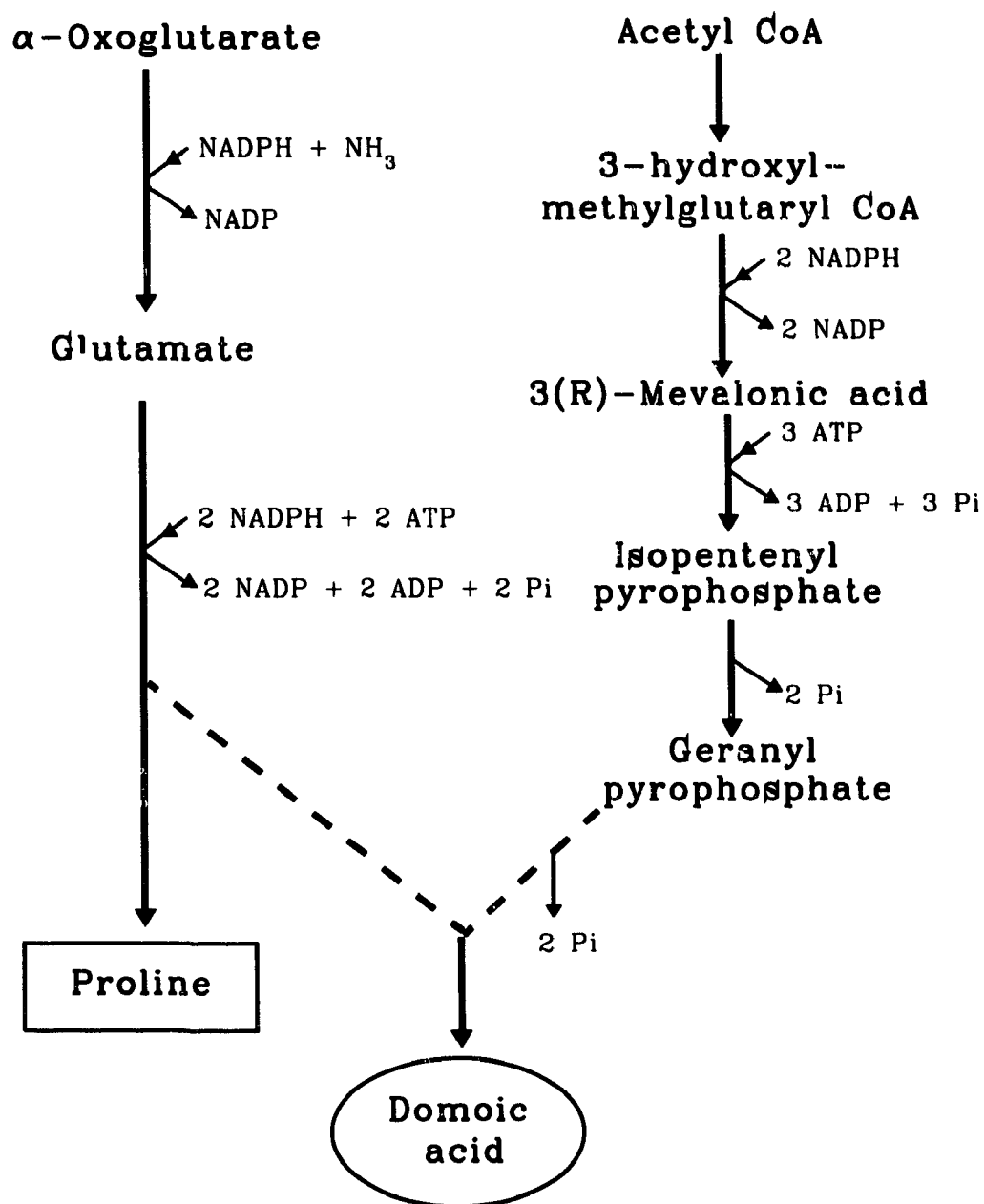


Fig. 1.4. Potential pathway of domoic acid biosynthesis (refers to Luckner, 1984, Laycock *et al.*, 1989 and Douglas *et al.*, 1992).

(Impellizzeri *et al.*, 1975).

Domoic acid (Fig. 1.2) is a naturally occurring, excitatory amino acid, first isolated by Daigo (1959) from *Chondria armata*. Its name was derived from the Japanese name of this alga, *domoi*. Domoic acid is closely related to kainic acid (Fig. 1.2) and probably acts as an agonist to glutamate, a neurotransmitter in the central nervous system (Hampson and Wenthold, 1988). Human poisoning by DA result in short-term memory loss and more severely in death (Addison and Stewart, 1989).

Domoic acid consists of two parts. One is the proline-like ring and the other is an isoprenoid structure (Fig. 1.2). Part of the former probably originally derived from glutamate which is from α -oxoglutarate in the Krebs cycle (Fig. 1.4). Synthesis of proline from glutamate requires 2 NADPH and 2 ATP. The latter may be derived from geranyl pyrophosphate, which is originally from acetyl-CoA (Luckner, 1984). Three ATP and 2 NADPH are required during the biochemical process from acetyl-CoA to geranyl pyrophosphate. These two parts probably condense to form domoic acid under certain physiological conditions, which are under investigations. Details of the condensation procedures remain obscure.

1.3.4. Physiological and ecological studies

The production and storage of toxins of an individual isolate of *P. pungens* f. *multiseries* vary with light, temperature, growth rate and physiological stage of the cells. Generally, the toxin content in *P. pungens* f. *multiseries* is lowest or undetectable in the mid-exponential phase, increases after cells enter the stationary phase and attains a

maximum in the advanced stationary phase (Subba Rao *et al.*, 1990; Bates *et al.*, 1991)

Light is required in the production of domoic acid (Bates, *et al.*, 1991). In the stationary phase of *P. pungens* f. *multiseries*, DA production ceased during the period of darkness; it resumed immediately after the transition from dark to light (Bates *et al.*, 1991). Addition of photosynthetic inhibitor DCMU stopped DA production (Bates *et al.*, 1991). Hence, photosynthesis (specifically photochemical processes), the primary energy source for carbon assimilation, mediates DA production as well.

Production of toxin as a secondary metabolite may compete with the primary metabolism for photosynthesized energy. Production of DA in the batch culture of *P. pungens* f. *multiseries* has only been found in the lag phase (Douglas and Bates, 1992) or stationary phase (Subba Rao *et al.*, 1990; Bates *et al.*, 1991) when the carbon assimilation rate was drastically reduced to ~3-15% of that in the exponential phase (Pan *et al.*, 1991). It seems that some of the photosynthesized energy has been channelled into DA production instead of carbon assimilation. In saxitoxin production, physiological stress such as lowering the temperature resulted in an enhancement of toxicity and content of saxitoxins (STX and its derivatives) per cell of *Alexandrium* spp. Lowering temperature results in decrease in carbon assimilation (Pan *et al.*, 1993) and growth rate (Boyer *et al.*, 1985; Pan *et al.*, 1993). It reduces the competition of the primary metabolism for the photosynthesized energy. Dark reaction (carbon assimilation) rate is reduced because low temperature lessens enzyme activity, whereas light reaction (energy assimilation) is somewhat independent of temperature. Therefore, energy is made available for toxin production.

In *P. pungens f. multiseriis*, onset of stationary phase corresponded to the silicate deficiency (Pan *et al.*, 1991) and initiation of DA production. Cultures grown with initial silicate concentrations of 5-30 μM contained approximate 35% more DA per cell than those grown with 55-105 μM (Bates *et al.*, 1991), which according to the authors is attributed to the differences in the duration in the stationary phase because cells grown in lower silicate concentration entered stationary phase earlier.

DA is not detected in the sexual phases of *P. pungens f. multiseriis*, i.e. gametes and zygotes, and resulting cells grown for 16 days do not have DA (Subba Rao *et al.*, 1991). Cells must go through several generations of asexual reproduction after finishing the sexual cycle before they can produce DA. This provides a possible explanation why *P. pungens f. multiseriis* produces DA in one place but not in another.

CHAPTER 2

GENERAL METHODS

2.1. Organism - culture

Two strains of *Pseudonitzschia pungens* (Grunow) f. *multiseries* (Hasle) were used in these studies. Strain NPBIO was isolated from Cardigan Bay, Prince Edward Island (PEI) in December of 1987 when the toxigenic bloom caused by this diatom was first reported. Strain KP-59 was isolated from New London Bay, PEI, in October of 1991. Both strains are confirmed by the taxonomy authorities G. Hasle and G. A. Fryxell respectively. Stock cultures have been maintained in medium FE (Section 2.2.2, Subba Rao *et al.*, 1988) under continuous light of up to $410 \mu\text{mol m}^{-2} \text{s}^{-1}$ and at temperatures between 3-10 °C. Cultures were suitably acclimated to a given condition of light, temperature and nutrient by sub-culturing 2 or 3 times at 5-7 days intervals to meet the requirements of the experimental protocol as detailed in each chapter.

2.2. Culture media

Media were made using aged sea water from Cardigan Bay, where blooms of toxigenic *P. pungens* f. *multiseries* were reported, or from the Atlantic Ocean (36°N,

63°30'W). Seawater was filtered through 153 µm nitex to remove large zooplankton and other large marine organisms and stored in plastic containers for a period of one year or more. The seawater was enriched for each medium as described below and autoclaved at 15-20 Psi (121-131 °C) for 15-30 minutes as detailed in each chapter.

2.2.1. Medium F

The recipe of Medium F is described in Table 2.1 (Guillard and Ryther, 1962).

Table 2.1. Composition of medium F

Enrichments	Formula	Concentration (µM)
Macronutrients		
NO ₃	NaNO ₃	1765.000
PO ₄	NaH ₂ PO ₄ .H ₂ O	72.500
Si	Na ₂ SiO ₃ .9H ₂ O	123.000
Micronutrient		
Fe	C ₆ H ₅ O ₇ Fe.3H ₂ O	23.300
Cu	CuSO ₄ .5H ₂ O	0.079
Zn	ZnSO ₄ .7H ₂ O	0.153
Co	CoCl ₂ .6H ₂ O	0.085
Mn	MnCl ₂ .4H ₂ O	1.830
Mo	NaMoO ₄ .2H ₂ O	0.052
EDTA	Na ₂ EDTA	38.249
Vitamins		
Thiamine.HCl	C ₁₂ H ₁₇ N ₄ OSCl.HCl	0.593
Biotin	C ₁₀ H ₁₆ N ₂ O ₃ S	4.1x10 ⁻³
VB ₁₂	C ₆₃ H ₈₈ CoN ₁₄ O ₁₄ P	7.35x10 ⁻⁴

Table 2.2. Composition of medium H

Enrichments	Formula	Concentration (μM)
Macronutrients		
NO_3	NaNO_3	1765.000
PO_4	$\text{NaH}_2\text{PO}_4 \cdot \text{H}_2\text{O}$	72.500
Si	$\text{NaSiO}_3 \cdot 9\text{H}_2\text{O}$	123.000
Micronutrient		
Fe	$\text{C}_6\text{H}_5\text{O}_7\text{Fe} \cdot 3\text{H}_2\text{O}$	30.100
Cu	$\text{CuSO}_4 \cdot 5\text{H}_2\text{O}$	0.079
Zn	$\text{ZnSO}_4 \cdot 7\text{H}_2\text{O}$	0.153
Co	$\text{CoCl}_2 \cdot 6\text{H}_2\text{O}$	0.090
Mn	$\text{MnCl}_2 \cdot 4\text{H}_2\text{O}$	2.000
Mo	$\text{NaMoO}_4 \cdot 2\text{H}_2\text{O}$	0.124
Citric acid	$\text{C}(\text{OH})(\text{COOH})(\text{CH}_2\text{COOH})_2 \cdot \text{H}_2\text{O}$	42.800
Vitamins		
Thiamine.HCl	$\text{C}_{12}\text{H}_{17}\text{N}_4\text{OSCl} \cdot \text{HCl}$	0.593
Biotin	$\text{C}_{10}\text{H}_{16}\text{N}_2\text{O}_3\text{S}$	4.1×10^{-3}
VB_{12}	$\text{C}_{63}\text{H}_{88}\text{CoN}_{14}\text{O}_{14}\text{P}$	7.35×10^{-4}

2.2.2. Medium FE

Medium FE was a modification of medium F (Subba Rao *et al.*, 1988a). To medium F described above, 2% (v/v) soil extract was added. The soil extract was prepared using soil from Cardigan Bay area and fortified by NaNO_3 and $\text{Na}_2\text{HPO}_4 \cdot 12\text{H}_2\text{O}$ as described below. In woods near Cardigan Bay, a deep pit was dug and a large quantity of soil was collected to a level 0.5 m below the ground and stored in plastic bags in the

dark at room temperature. To 1 kg soil, 1 litre distilled water was added and the mixture was autoclaved for 25 minutes at 131 °C. The soil extract was filtered through Whatman GF/C filter or centrifuged at 1000 rpm (~150 g) for 10 minutes. After cooling down, the filtrate or the supernatant fluid was adjusted to 1 litre using distilled water and enriched by 4 g NaNO₃ and 0.6 g Na₂HPO₄ 12H₂O. Aliquots (20 ml) were dispensed into clean plastic vials and deep frozen. To prepare medium FE, one vial was added to 1 litre medium F, and the medium was autoclaved.

2.2.3. Medium H

Medium H was a modification of medium F, in which EDTA was replaced by citric acid and other changes were made as described in Table 2.2 (Humphrey, 1963; Humphrey and Subba Rao, 1967).

2.3. Measurement of biomass

Biomass was usually determined by cell concentrations. Culture samples (10-15 ml) were preserved by 1% (v/v) of the water solution mixture (1%:1%) of paraformaldehyde and glutaraldehyde and enumerated using an inverted microscope. In addition, particulate chlorophyll *a*, carbon, nitrogen, silicon and phosphorus were also used as biomass indices; *in vivo* chlorophyll *a* fluorescence was used for monitoring population size in the continuous culture (Section 2.10).

2.4. Chlorophyll *a* analysis

Chlorophyll *a* was determined by fluorometry (Strickland and Parsons, 1972). A culture sample (usually 20 ml) was filtered onto a 25 mm Whatman GF/F filter (average pore size = 0.7 μm), the funnel and the filter were rinsed with isotonic saline (NaCl solution of the same ionic strength as the culture medium). Then the filter was transferred into a glass vial containing 90% acetone (10 ml) and refrigerated at 0-5 °C for 24-36 hours. The extract was analyzed for chlorophyll *a* using a Turner Model 10 fluorometer. The fluorometric readings were taken before (R_b) and after (R_a) acidification by 1 or 2 drops of 1 N HCl. The chlorophyll *a* concentration was calculated from the difference between R_b and R_a based on a calibration for each scale using the standard chlorophyll *a* supplied by Sigma Chemical Inc. (Sigma-C6144). Chlorophyll *a* values are an average of two determinations.

2.5. Nutrient analyses

2.5.1. *Particulate carbon and nitrogen*

Particulate carbon and nitrogen were analyzed using either a Perkin-Elmer Model 240B or Model 2400 CHN Elemental Analyzer. A culture sample (30 or 40 ml) was filtered onto a 25 mm Whatman GF/F filter, which had been previously baked at 550 °C for 3 hours. The cells on the filter were rinsed twice by isotonic saline. Samples were stored in plastic petri dishes frozen at -20 °C until analyzed (< 3 months). The cells on

the filter were dried at 60 °C overnight and then manually rolled using clean stainless tweezers into a silver filter (for Model 240B) or a tin disk (for Model 2400) before combustion (Strickland and Parsons, 1972). Particulate carbon and nitrogen values are averages of two determinations.

2.5.2. Particulate phosphorus and silicon

Culture samples (20 or 10 ml) were filtered in duplicate onto nuclepore filters (pore size = 1 µm, 25 mm diameter), which had been previously rinsed twice using distilled water. Cells on the filter were rinsed twice with isotonic saline immediately upon the completion of filtration. The samples were kept in plastic petri dishes stored frozen at -20 °C until analysis (30-80 days) using the procedures described below.

2.5.2.1. Oxidation Oxidation was carried out in a 60-ml polypropylene plastic bottle using alkaline persulphate as oxidant (Koroleff, 1983b). The filter was transferred to a polypropylene bottle containing distilled water (30 ml) and oxidizing solution (3 ml). The bottle was closed tightly and autoclaved at 15-20 Psi (126-131 °C) for 60 minutes, then allowed to stand at room temperature for ~12 hours. Standard solutions of Na₂SiO₃ and NaH₂PO₄ were simultaneously treated for calibration (Appendix B1).

2.5.2.2. Analysis Samples were taken from the bottle for phosphorus and silicon measurements. For phosphorus determination, 4 ml of the oxidized solution (or its dilutions) was transferred to a 5-ml Vacutainer tube. Mixed reagent (Strickland and

Parsons, 1972; 0.5 ml) was added to the tube using an Eppendorf Repeater pipette. Absorbency at 885 nm was measured using a Phillips Model PU8625 UV/VIS spectrophotometer between 10 and 30 minutes after the addition of mixed reagent. Phosphorus concentration was extrapolated from a standard curve determined simultaneously.

For silicon, 6 ml of the oxidized solution (or its dilution) was transferred to a 10-ml plastic tube and 0.25 ml of acid molybdate solution (Koroleff, 1983a) was added using an Eppendorf Repeater pipette and mixed. After 15 (\pm 1) minutes, oxalic acid (0.25 ml, 0.8 M) and ascorbic acid (0.05 ml, 0.32 M) were added and mixed well. Full colour development was allowed to proceed for 60 minutes. Absorbency at 810 nm was measured within 3 hours. Silicon concentration was extrapolated from a standard curve determined simultaneously.

2.5.3. Dissolved phosphorus and silicon

A culture sample was filtered through a nuclepore filter (1.0 μ m) and the filtrate (30 ml) transferred to a 60-ml polypropylene bottle and stored frozen. For analysis, the filtrate was thawed and 3 ml oxidation solution were added. The mixture was autoclaved for 60 minutes. Phosphorus and silicon were determined following the same procedures as described in Section 2.5.2.2.

2.5.4. Dissolved inorganic nutrients

Culture filtrate was collected in a 40-ml polypropylene bottle following the same procedures described in Section 2.5.3. Samples for Chapter 3 were analyzed for nitrate,

nitrite, phosphate and silicate using an Autoanalyzer II (Strickland and Parsons, 1972) by Mr. P. Clement in Marine Chemistry Division, Bedford Institute of Oceanography. The remaining samples were analyzed for phosphate and silicate using spectrophotometry (Strickland and Parsons, 1972) following the same procedures described in Section 2.5.2.2.

2.5.5. *Dissolved carbon dioxide*

Total dissolved CO₂ in the cultures was calculated from alkalinity determinations (Strickland and Parsons, 1972) based on salinity determined with Guildline Salinometer and pH with an Orion Research microprocessor ion-analyzer 901 at room temperature.

2.6. Analysis of domoic acid

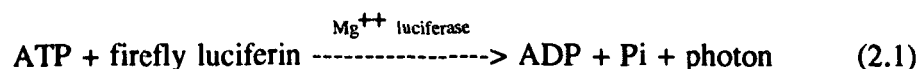
Culture samples were filtered onto nuclepore filters (25 mm, pore size = 1.0 µm). The filters were kept in plastic petri dishes and the filtrates (10 ml) were kept in 20-ml plastic vials. Both the filters and filtrates were stored frozen (-20 °C) until analyzed (5-100 days). The samples were analyzed using high performance liquid chromatography (HPLC, Pocklington *et al.*, 1990, Wright *et al.*, 1989) by Dr. R. Pocklington and his associates, Marine Chemistry Division, Bedford Institute of Oceanography. Before analysis, a filter sample was transferred to a vial. The petri dish was rinsed twice with 1 ml of filtered (0.2 µm nuclepore filter) seawater, and the rinsed fluid added to the vial. The vial was capped and left in a sonic water bath (Sonic 300 Dismembrator, Artek, 20

+ 0.4 kHz) for 15 minutes to rupture the cells and release DA into the solution. The contents were then filtered through a Millipore Millex-HV filter (0.45 μm). For the filtrate sample, direct filtration through a Millipore Millex-HV filter was applied.

Two methods were used for analysis depending on DA concentrations present in the samples. At low levels (detection limit = 2 ng), DA was determined using the 9-fluorenyl-methoxycarbonyl (FMOC) method. Domoic acid first reacted with 9-fluorenylmethyl-chloroformate to form a fluorescent derivative that was then separated by HPLC and finally measured using a fluorescence detector (Pocklington *et al.*, 1990). At high level (> 0.5 μg), a 5 μl portion was injected and separated by HPLC (5 μm Vydac 201 TP column, 25 cm x 2.1 mm ID at 40 $^{\circ}\text{C}$, isocratic elution with 0.5 ml min^{-1} 10% acetonitrile in water plus 0.1% trifluoroacetic acid) and the ultraviolet absorbency of DA at its characteristic wavelength of 242 nm was measured by diode array detector (DAD, Wright *et al.*, 1989). The value of DA is an average of duplicates.

2.7. Measurement of adenosine triphosphate (ATP) and adenyl energy charge (EC)

Among the various techniques for separating and measuring ATP, the firefly bioluminescent reaction is one of the most specific, sensitive and reproducible assay procedures known. This method makes use of the fact that firefly luciferin and luciferase react with ATP in the presence of Mg^{++} and oxygen to yield one photon of light for every ATP molecule hydrolysed (McElroy *et al.*, 1969).



2.7.1. Reagents

2.7.1.1. Inorganic compounds

1. MgSO₄ (0.04 M): prepared in the laboratory.
2. KHAsO₄ (pH 7.4, 0.1 M): obtained commercially from Sigma Chemical Inc. St. Louis US. (Sigma FF-As-100)
3. Mixture of MgCl₂ (15 mM) and potassium phosphate buffer (pH 7.4, 75 mM)
4. Mixture of MgCl₂ (30 mM) and potassium phosphate buffer (pH 7.4, 150 mM).

2.7.1.2. Tris buffer (Sigma Trizma base, No. T-1503, FW=121.1; 0.02 M)

5. pH = 7.75. Trishydroxymethylaminomethane (Tris, 7.5 g) was dissolved in 3000 ml of distilled water and pH of the buffer was adjusted to 7.75 by drop-wise addition of concentrated HCl. The solution was autoclaved at 15 Psi for 15 minutes and then dispensed (50 ml) to 60-ml sterile plastic flasks when it was hot. The buffer was kept in fridge until being used for extraction.
6. pH = 7.55. Following the same procedures for reagent 5 but adjusted the pH to 7.55.

2.7.1.3. Organic compounds and enzymes (from Sigma Chemical, St. Louis, U.S.)

7. ATP standard (Sigma A5349): Stock solution was prepared at the concentration of 1 μM in Tris buffer (reagent 5, pH = 7.75).
8. ADP standard (Sigma A1782): Stock solution was prepared at the concentration 0.1 mM in Tris buffer (reagent 5, pH = 7.75).

9. AMP standard (Sigma A1752): Stock solution was prepared at the concentration 0.05 mM in Tris buffer (reagent 5, pH = 7.75).
10. Phosphoenolpyruvate - Na (PEP-Na, 5 mM): 95 mg PEP-Na (FW=190, Sigma P9303) were dissolved in 100 ml Tris buffer (reagent 6, pH 7.55).
11. Pyruvate kinase (PK, Sigma P1506): A solution of 1,000 units was diluted to 50 ml with Tris buffer (reagent 6, pH 7.55). The final concentration in the stock solution was 20 units ml⁻¹ (>0.2 units per sample).
12. Myokinase (MK, or Adenylate kinase; Sigma M3003): 20,000 units were diluted to 5 ml with Tris buffer (reagent 6, pH 7.55). The final concentration in the stock solution is 4,000 units ml⁻¹ (20 unit per sample).
13. Firefly lantern extract: Lyophilized firefly lantern extracts were obtained commercially (Sigma FLE-50) stored frozen and desiccated (< -5 °C) prior to use. At assay *a*) each vial of the enzyme extract was rehydrated with 5 ml distilled water and allowed an ageing period of 2-3 hours at room temperature; then *b*) equal volumes of MgSO₄ (reagent 1) and KHASO₄ (reagent 2) were added to 25 ml in each vial; *c*) several vials of the solution were combined if the number of samples was over 25 and more vials of enzymes were needed; *d*) this enzyme solution was centrifuged at 1,000 rpm (~150 g) for 10 minutes and the supernatant fluid was used for assay.

2.7.2. Filtration and extraction (enzyme Inactivation)

The culture sample (30 - 50 ml) was filtered through a Whatman GF/F filter at

vacuum pressure less than 180 mm Hg. The filter was sucked dry but not rinsed (rinsing will create an unpredictable error). Immediately, the filter was transferred into a 5-ml vacutainer tube containing boiling Tris buffer (4 ml, Reagent 5, pH=7.75) and the tube left in a boiling water bath for 2.5-3 minutes (the sample should not be extracted for more than 3 minutes). The tube was transferred to an icy water bath and then stored in the dark at -20 °C until analysis.

2.7.3. Assay

The assay was carried out using an integrated photometer (ATP Photometer). Before assay, ADP and AMP were both converted to ATP by enzyme reactions (2.2) and (2.3) given below. To determine ATP, reagent 3 (50 µl) was mixed with sample or standard (0.2 ml) in a 10-ml cylindrical vial. The vial was manually transferred into the photometer before 1 ml firefly lantern extract (reagent 13) was added using an automatic dispenser. The peak height method with a 3 second delay (Karl and Holm-Hansen, 1980) was used for the measurement of photon flux densities.



For ADP+ATP determination, *a*) Reagent 4 (2.5 ml) was mixed with PEP-Na (Reagent 10, 1 ml) and PK (reagent 11, 1.5 ml); *b*) this mixture (50 µl) was added to samples or standards (0.2 ml) in a cylindrical vial and allowed to react for 30 minutes in

a water bath at 30 °C to convert ADP to ATP (Equation 2.2); c) the vial was transferred to a boiling water bath for 2 min to inactivate the enzymes and d) assayed as ATP after it cooled.

To determine AMP+ADP+ATP, a) Reagent 4 (2.5 ml) was mixed with PEP-Na (Reagent 10, 1 ml), PK (Reagent 11, 1 ml) and MK (Reagent 12, 0.5 ml) and then taken through the steps b) (Equations 2.2, 2.3), c) and d) described for ADP+ATP measurement.

For the measurement of blanks, 0.2 ml Tris buffer (Reagent 5) was used instead of the sample. The procedures for treatment and assay were the same as for the samples. A standard curve was obtained for each set (less than 40) samples and the levels of ATP, ADP+ATP and AMP+ADP+ATP were extrapolated from the standard curves obtained simultaneously. Averages of 3 determinations was reported.

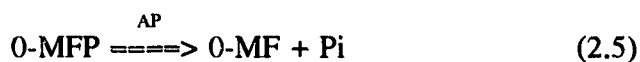
All the glassware used during the preparation of reagents and samples and during the assay was washed using a mixture (0.5% 1:1) of JAVEX bleach and EXTRAN MN-1 soap and then rinsed thoroughly. The glassware was finally baked at 550 °C for >3 hours to eliminate any organic contaminant as any negligence of the cleanliness of the glassware would result in unpredictable errors.

Adenyl energy charge (EC) is defined as (Karl and Holm-Hansen, 1980):

$$EC = \frac{ATP + 1/2 ADP}{ATP + ADP + AMP} \quad (2.4)$$

2.8. Measurements of alkaline phosphatase activity

The underlying principle for the determination of alkaline phosphatase activity is that many microorganisms produce phosphatase associated with the cell membrane surface when phosphorus becomes limiting in a culture or in sea water. These phosphatases are capable of hydrolysing organic phosphate bonds. Examination for the presence of alkaline phosphatase (AP) has been used to determine the phosphate limitations in limnological and oceanographical investigations (Perry, 1972 and the references therein). The assay used in the experiments was based on the hydrolysis of the monophosphate ester bond of 3-0-methylfluorescein phosphate (0-MFP) by this enzyme.



2.8.1. Reagents

1. Tris Buffer (10 mM, pH=8.5): Tris (2.42 g) was dissolved in distilled water (2000 ml) and the pH was adjusted to 8.5 by adding concentrated HCl. The buffer was autoclaved at 15 Psi for 15 min and then aseptically dispensed into small stocks (50 ml) in sterile plastic culture flasks (60 ml) when it was hot.
2. Substrate: 3-0-methylfluorescein phosphate (0-MFP, MW=511, 1.0 mM). The substrate was obtained commercially from Sigma Chemical Inc. (Sigma M2629, St. Louis, U. S.). 0-MFP (5.11) was dissolved in Tris buffer (10.0 ml, Reagent 1, pH=8.5) and dispensed (1 ml each) to 15-ml plastic culture tubes stored frozen until assay. The stock was thawed at 5 °C and diluted 10x with the same Tris

buffer for a working solution for the assay.

3. Standard: 3-O-methylfluorescein (O-MF, MW=346, 0.1 mM). O-MF (1.73 mg, Sigma M7004) was dissolved in absolute methanol (50 ml) and dispensed (1 ml each) to plastic tubes store at -5.0°C . For a working solution, 1 ml of the stock solution was diluted to 100 ml with 0.05 N NaOH to get 1.0 μM and further diluted with distilled water to various concentrations. A linear relationship existed between the intensity of fluorescence of O-MF and its concentration (Appendix B3).

2.8.2. Assay

A culture sample was collected, a portion of it was filtered through nuclepore filter (1.0 μm) and the filtrate was collected. Before assay, the culture (4 ml), filtrate (4 ml) and fresh medium (4 ml) were transferred to 6-ml vacutainer tubes and the tubes were positioned in a water bath (37°C) and allowed to condition for 5 - 10 minutes before addition of the substrate.

A Turner model 111 fluorometer was equipped with No. F4T5 lamp, a primary filter of Wratten No. 47B (395-477 nm, the same as chlorophyll *a* measurement) and a secondary filter of Wratten No. 2A-12 combination (visible above 507 nm). After adding the substrate (0.5 ml, Reagent 2), the contents were mixed thoroughly using a Vortex-Genie mixer and its fluorescence was determined immediately. The tubes were left in the water bath before the next fluorescence readings were taken. The contents were mixed before each measurement of fluorescence and 6 to 8 measurements were obtained during 60 to 80 minutes. Alkaline phosphatase activity (APA) was determined by the slope of

the increments of fluorescence in the culture or filtrate minus that in the fresh medium. APA in the filtrate usually was negligible compared to that in the culture sample (<5%). Values presented were averages of two determinations.

All glassware used in the preparation and the assay was cleaned using a mixture (0.5% 1:1) of JAVEX bleach and EXTRAN MN-1 soap and rinsed thoroughly using tap water and distilled water, then autoclaved at 15 Psi for 15 minutes. Contact with any phosphate based detergent would result in unpredictable errors and has been avoided.

2.9. Relationships between photosynthesis and photosynthetic photon flux density (PPFD)

The photosynthesis-PPFD (P^B -I) relationships were determined using the ^{14}C method (Steemann-Nielsen, 1952). High specific activity $\text{H}^{14}\text{CO}_3^-$ (111-222 K Bq ml⁻¹ depending on cell density) was added to about 65 ml culture and after mixing thoroughly, 1 ml aliquots of the culture were dispensed into 48 clean glass vials in a photosynthetron incubator and incubated for 30 minutes at different PPFDs ranging from 11 to 5000 $\mu\text{mol m}^{-2} \text{s}^{-1}$ (Lewis *et al.*, 1985). The radioactivity added was determined in 5 μl of the ^{14}C -containing incubation medium using 5 ml Aquasol scintillation fluid containing NaOH (10 μl 6N). Incubations of the cells with the radioactive bicarbonate were terminated by addition of HCl (250 μl 6N). The vials were shaken for more than 1 hour to remove residual $\text{H}^{14}\text{CO}_3^-$. A Beckman two-channel scintillation counter was used to determine radioactivity. Photosynthesis was determined by the ratios of radioactivity assimilated by

the cells during the 30 minutes to the total radioactivity added multiplied by CO₂ concentration in the culture medium (Section 2.5.5). The relationship between photosynthesis (P^B : $\mu\text{g C } [\mu\text{g Chl a}]^{-1} \text{ h}^{-1}$ or $\mu\text{g C } [\mu\text{g C}]^{-1} \text{ h}^{-1}$) and PPFD (I : $\mu\text{mol m}^{-2} \text{ s}^{-1}$) could be described by the photoinhibition model of Platt *et al.* (1980) with the addition of a single parameter, P_d^B :

$$P^B = [P_s^B (1 - \exp(-\alpha^B I / P_s^B)) \exp(-\beta^B I / P_s^B)] + P_d^B \quad (2.6)$$

In this formulation, P_s^B (same units as P^B) is the maximum *potential* photosynthesis in the absence of photoinhibition; α^B ($\text{ng C } [\mu\text{g Chl a}]^{-1} \text{ h}^{-1} [\mu\text{mol m}^{-2} \text{ s}^{-1}]^{-1}$ or $\text{ng C } [\mu\text{g C}]^{-1} \text{ h}^{-1} [\mu\text{mol m}^{-2} \text{ s}^{-1}]^{-1}$) is the initial slope of the P^B - I curve, that is, photon efficiency or photosynthesis per unit PPFD, β^B (same units as α^B) is the photoinhibition index, P_d^B (same units as P^B) is the intercept of the P^B - I curve on the Y-axis. The additional parameter P_d^B was necessary to account for a background uptake of ¹⁴C in all samples. P_s^B , P_d^B , α^B , β^B were calculated by fitting Equation 2.6 to experimental data points by non-linear regression using a commercial package employing the Marquardt algorithm (Marquardt, 1963). All the points were equally weighted. P_m^B , I_m , I_k , I_s , were calculated from P_s , α , β following the relationship among these parameters suggested by Platt *et al.* (1980):

P_m^B , the maximum biomass normalized photosynthetic rates (same units as P^B):

$$P_m^B = P_s^B \left(\frac{\alpha^B}{\alpha^B + \beta^B} \right) \left(\frac{\beta^B}{\alpha^B + \beta^B} \right)^{\beta/\alpha} \quad (2.7)$$

I_m , I corresponding to the maximum photosynthetic rate P_m^B :

$$I_m = \frac{P_s^B}{\alpha^B} \ln \left(\frac{\alpha^B + \beta^B}{\beta^B} \right) \quad (2.8)$$

I_k , photo-adaptive index:

$$I_k = P_m^B / \alpha^B \quad (2.9)$$

I_s , I corresponding to the maximum *potential* photosynthetic rate (P_s^B) in the absence of photoinhibition:

$$I_s = P_s^B / \alpha \quad (2.10)$$

Where, I_m , I_k , I_s have the same units as I .

2.10. Chemostat continuous culture system

The continuous culture system is shown in Fig. 2.1. The Pyrex glass chemostat culture chamber of 1.5 litre (1) was surrounded by a thermostat water jacket (2), which was connected and circulated with a thermostat water bath. Temperature was maintained at 15 (± 0.2) °C. The culture was agitated at about 100 rpm by a magnetic stirrer (3) at the bottom of the chamber and aerated by sterile air at 30 (± 10) bubbles per minutes. Reservoir medium was added continuously by a peristaltic pump. Effluent was collected in a plastic flask (4). The flow rate (dilution rate) was confirmed by measuring the effluent (9) every day. Six chemostats were set up simultaneously. The chemostats were exposed to a bank of 290 (± 50) $\mu\text{mol m}^{-2} \text{s}^{-1}$ continuous cool white fluorescent light.

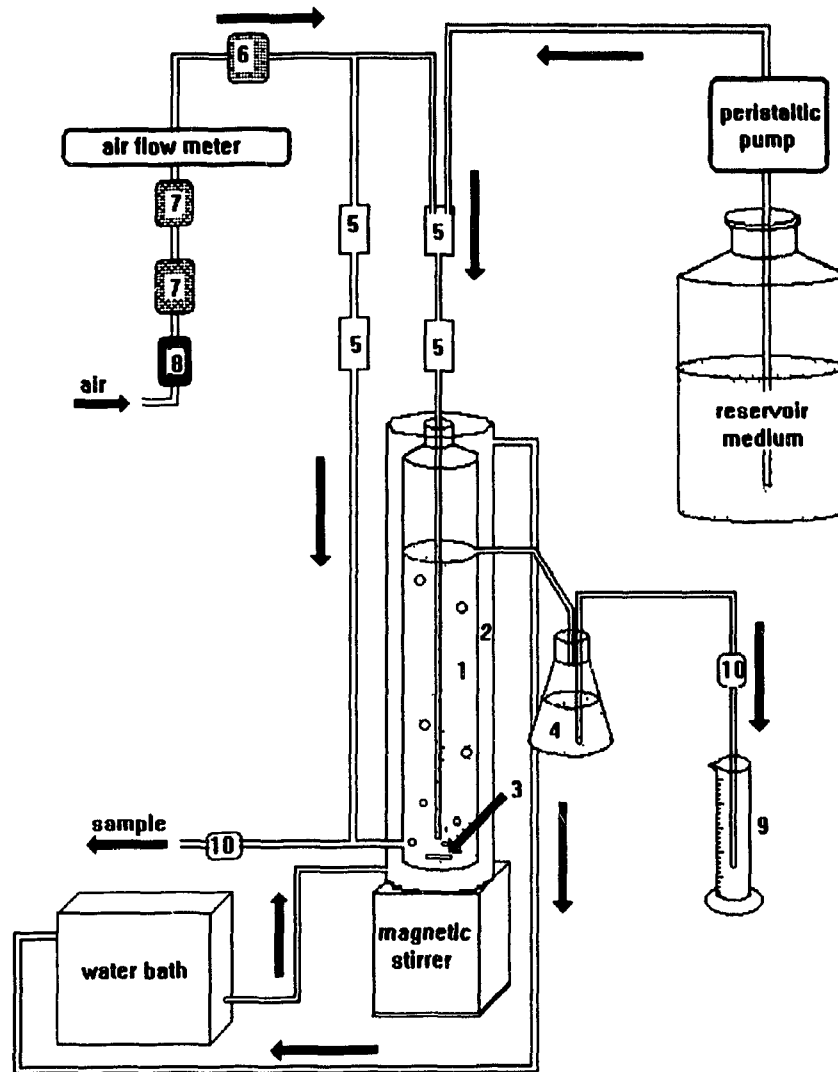


Fig. 2.1. Schematic display of chemostat system. 1 = chemostat culture chamber, 2 = thermostat water jacket, 3 = stir bar, 4 = effluent, 5 = polycarbonate buffer cylinder, 6 = sterile air filter (0.2 μm), 7 = cotton filters, 8 = activated charcoal to remove organic compounds in the air, 9 = measuring cylinder for effluent measurements, 10 = stopcock.

All the glassware and tubing were washed using a mixture (0.5% 1:1) of JAVEX bleach and EXTRAN MN-1 soap then rinsed thoroughly using tap water (>5 times) and distilled water (> 5 times). Parts (chemostat, effluent flask, tubing and buffer cylinders to supply medium and air, etc) were connected before or immediately after (inside the autoclave chamber) being autoclaved at 15 Psi for 20-30 minutes. The system was then aseptically connected with sterile air and medium supply soon after being mounted on the shelf.

The culture population was monitored daily by measuring *in vivo* chlorophyll *a* fluorescence. After measurement of fluorescence, a 10-ml sample was preserved (Section 2.3) in a 20-ml plastic vial and served as the backup for population size determination. Steady state was defined as a period of 5 days during which the coefficient of variation of the chlorophyll *a* fluorescence was not greater than 5%.

2.11. Growth

2.11.1. Batch culture

Growth of *P. pungens* f. *multiseries* in batch culture was described by the Gompertz growth model (Zwietering *et al.*, 1990). Growth is defined in terms of the logarithm of cell concentrations (or other biomass index) as a function of time. Changes in growth rate result in a sigmoidal curve: an initial lag phase, an exponential growth phase, and finally a stationary phase. The Gompertz equation may be expressed as:

$$Y = a \exp[-\exp(b-ct)] \quad (2.11)$$

where $Y = \ln(N_t/N_0)$, N_t is the cell concentration at time t and N_0 is the initial cell concentration. The parameters a , b and c describe the shape of the curve. They are mathematical parameters rather than biological ones. However, the biological meanings can be described by the values derived from these parameters. The maximum growth rate (μ_{\max}) is given by ac/e where 'e' is the base of Napierian logarithms (~ 2.718). The duration of the lag phase is given by $(b-1)/c$ (Zwietering *et al.*, 1990). Changes in growth rates as a function of time were normalized to cell concentration and other biomass indices and fitted by non-linear regression (Marquardt, 1963). Growth rates throughout the culture experiments were computed from the derivative of Equation (2.11) with respect to time:

$$\frac{dY}{dt} = ac \exp[-\exp(b-ct)] \exp(b-ct) \quad (2.12)$$

using the estimates of parameter a , b , and c obtained from non-linear regression of Equation (2.11).

2.11.2. Continuous culture

At the steady state when the culture population remains constant. The growth rate (μ) of the culture population was determined by the dilution rate (D):

$$\mu = D = \frac{dv}{V dt} \quad (2.13)$$

Throughout the thesis, the term *growth rate* (μ) is equivalent to the *specific growth rate* in the literature.

CHAPTER 3

PHOTOSYNTHESIS AND GROWTH

3.1. Introduction

Photosynthesis and growth are basic physiological processes of phytoplankton. Photosynthesis is not only the essential process for primary metabolism, but is also required for toxin production. For example, the yield of saxitoxins per cell in *Alexandrium catenella*, a dinoflagellate implicated in paralytic shellfish poisoning, was proportional to hours of light per day (Proctor *et al.*, 1975). In stationary phase, domoic acid production by *Pseudonitzschia pungens* f. *multiseriis* ceased during periods of darkness; however, the toxin production resumed immediately after the transition from dark to light (Bates *et al.*, 1991). Production of domoic acid was also inhibited by addition of the photosynthetic inhibitor DCMU (Bates *et al.*, 1991). Hence, photosynthesis, the primary energy source for carbon assimilation, is necessary for DA production as well.

Variations in light intensity have less effect on the production of phycotoxins (Ogata *et al.*, 1987, 1989; Boyer *et al.*, 1985; Bates *et al.*, 1991). Differences in the initial DA production rate between light intensities of 45 and 145 $\mu\text{mol m}^{-2} \text{s}^{-1}$ were not significant (Bates *et al.*, 1991).

Physiological stress, such as low temperature, resulted in an enhancement of saxitoxin production by *Alexandrium* spp. Toxicity and the content of saxitoxins (STX and its derivatives) per cell increased under sub-optimal growth temperature (Proctor *et al.*, 1975; Hall, 1982; Boyer *et al.*, 1985; Ogata *et al.*, 1987; Anderson *et al.*, 1990). Transferring the culture to a lower temperature (from 15 to 10 °C) increased toxin production, but decreasing light intensity (from 113 to 19 $\mu\text{mol m}^{-2} \text{s}^{-1}$) did not have a similar effect (Ogata *et al.*, 1987). Low temperature limited the photosynthesis and growth of *P. pungens* f. *multiseries* (Pan *et al.*, 1993, Lewis *et al.*, 1993), but did not limit DA production (Lewis *et al.*, 1993).

A study of the relationship of photosynthesis and photosynthetic photon flux density (PPFD = I) is essential to understand the physiological ecology of algae. To describe the relationship between photosynthesis and incident PPFD, Blackman (1905) first produced an ideal model. Thirty years later, Baly (1935) and Smith (1936) developed mathematical formulations to fit experimental data on phytoplankton. Steel (1962), Webb *et al.* (1974), and Platt *et al.* (1975), Platt and Jassby (1976), and Platt *et al.* (1980) have produced alternative formulations to define the P vs I curve.

The initial slope of the P-I curve, α^B , is one of the two important parameters in all models. It is a relative measure of light absorption and maximum quantum efficiency of photosynthesis at low light. This parameter depends on the type of chlorophyll and accessory pigments of the cell, the absorption characteristics of the cell and its pigments. Simply stated, α^B is the photochemical parameter in the models.

P_m^B , the maximum carbon assimilation rate, is the other important parameter,

indicating algal physiological activity. Thus P_m^B is dependent on physiological stage, light, temperature and overall cell metabolism. Therefore, cell division and photosynthesis are ultimately regulated by the environmental factors affecting these processes.

Studies on photosynthesis and growth of *Pseudonitzschia pungens* f. *multiseries* under different environmental conditions are important in understanding the development of a toxic bloom. In this chapter, I study photosynthesis and growth of *Pseudonitzschia pungens* f. *multiseries* and examine their relationship to culture age, photosynthetic photon flux density (PPFD), temperature, cellular carbon, nitrogen and chlorophyll *a*.

3.2. Materials and Methods

Non-axenic *P. pungens* f. *multiseries* isolated from Cardigan Bay, PEI (strain NPBIO) were grown as clonal batch cultures in medium FE (Section 2.2.2), at 0-25 °C under continuous cool white fluorescence light of 53 to 1100 $\mu\text{mol m}^{-2} \text{s}^{-1}$. Growth, photosynthesis, and cellular chemical composition were determined *a*) in different growth phases, *b*) for cultures under different PPFD, and *c*) at different temperatures.

3.2.1. Determination of particulate chlorophyll *a*, carbon and nitrogen, dissolved inorganic nutrients and light

Chlorophyll *a* was determined fluorometrically (Section 2.4). Particulate carbon and nitrogen were analyzed by combustion (Section 2.5.1). Growth PPFD was measured

with a LICOR model Li-185B light meter. Inorganic nitrate, phosphate and silicate concentrations in the medium were measured using a Technicon Autoanalyzer II (Section 2.5.4).

3.2.2. *Growth rate*

Growth rates were determined using the Gompertz growth model (Section 3.11.1) except for experiment C. In this case growth rates were determined by Equation 3.1 (see Section 3.2.5).

3.2.3. *Experiment A: effects of culture age*

For stock cultures, 500-ml flasks each containing medium FE (200 ml, Section 2.2.2) were seeded with culture in exponential growth phase (25 ml each). Cultures were routinely grown at two levels of PPFD (105 and 1100 $\mu\text{mol m}^{-2} \text{s}^{-1}$) and were sub-cultured every 5 days for 10 days using fresh medium. At the beginning of the experiments, 3-litre Fernbach flasks containing FE medium (2 litre) were seeded with exponentially growing *P. pungens* f. *multiseries* (5-day old, 200 ml) adapted to the experimental PPFD. Cultures grown at 105 and 1100 $\mu\text{mol m}^{-2} \text{s}^{-1}$ were designated as low light (LL) and high light (HL) cultures respectively. The photosynthesis-PPFD (P-I) relationship was determined using the ^{14}C method (Section 2.9). Samples were analyzed for cell concentration, chlorophyll *a*, particulate carbon and nitrogen after 1, 4, 8, 15, 25 and 34 days growth at 10 °C.

3.2.4. Experiment B: light dependence

Stock cultures were grown under 5 PPFD levels (53, 250, 410, 815 and 1100 $\mu\text{mol m}^{-2} \text{s}^{-1}$) at 10 - 12 °C. After subculturing twice (in 10 days), exponentially growing cells were inoculated into a 3-litre Fernbach flask at a 1:10 ratio as in experiment A for each PPFD level. P-I characteristics of the culture, cell concentration, chlorophyll *a*, particulate carbon and nitrogen were measured on day 4 and day 12.

3.2.5. Experiment C: temperature dependence

A stock culture was grown at 10-12 °C under continuous cool white fluorescence light of 410 $\mu\text{mol m}^{-2} \text{s}^{-1}$. To measure temperature dependence, exponentially growing culture of *P. pungens* f. *multiseries* (5 days, 200 ml) was inoculated into a 3-litre Fernbach flask containing FE medium (2 litre). On the third day of growth, the culture in 250 ml aliquots was dispensed into each of 6 autoclaved flasks, which were transferred to 0, 5, 10, 15, 20 and 25 °C with photosynthetic photon flux density (PPFD) ranging from 350 to 440 $\mu\text{mol m}^{-2} \text{s}^{-1}$. P-I relationships were determined at corresponding temperatures for cells harvested on the 4th day. Cell concentration, chlorophyll *a*, particulate carbon and nitrogen were measured at the same time. Cell concentrations were also measured on days 0, 1, 3.

Growth rates (μ) of *P. pungens* f. *multiseries* in all the cultures were calculated using Equation 3.1 (Guillard, 1973):

$$\mu = \text{Ln} (N_2/N_1) / (t_2-t_1) \quad (3.1)$$

based on the cell concentration (N_1 , N_2) on day 3 (t_1) and day 4 (t_2).

3.3. Results

3.3.1. *Dependence of photosynthesis and growth on age of the cultures*

3.3.1.1. Growth and cellular chemical composition Both low light (LL) and high light (HL) cultures grew exponentially for 8 days attaining a maximum of 1.56 and 1.41 $\times 10^8$ cells l^{-1} respectively by day 15. Thereafter, there was no marked change in cell concentration (Fig. 3.1A).

Chlorophyll *a* concentrations increased with increasing age of the culture for the first 4 days (Fig. 3.1B). The maximum chlorophyll *a* concentrations attained were 40.2 $\mu g\ l^{-1}$ in the HL culture and 103.3 $\mu g\ l^{-1}$ in the LL culture. The HL cells contained less chlorophyll *a* than LL cells although similar cell concentrations were obtained in both HL and LL cultures (Figs. 3.1A, B).

Particulate carbon and nitrogen increased with time at both levels of PPFD for the first 8 days (Figs. 3.1C, D). The following are the features of interest: *i*) accumulation of carbon seemed to be more rapid than nitrogen (Figs. 3.1C, D) and *ii*) the lag phase for the accumulation of nitrogen was longer in HL cells (Fig. 3.1D).

PO_4 and NO_2+NO_3 were abundant over the entire 34 days of growth. However, SiO_3 was reduced to 11% and 8% of the initial levels (84-86 μM) in the HL and LL cultures respectively by day 8 due to utilization by the diatom for frustule formation (Table 3.1). This low level of SiO_3 corresponded with the onset of the stationary phase.

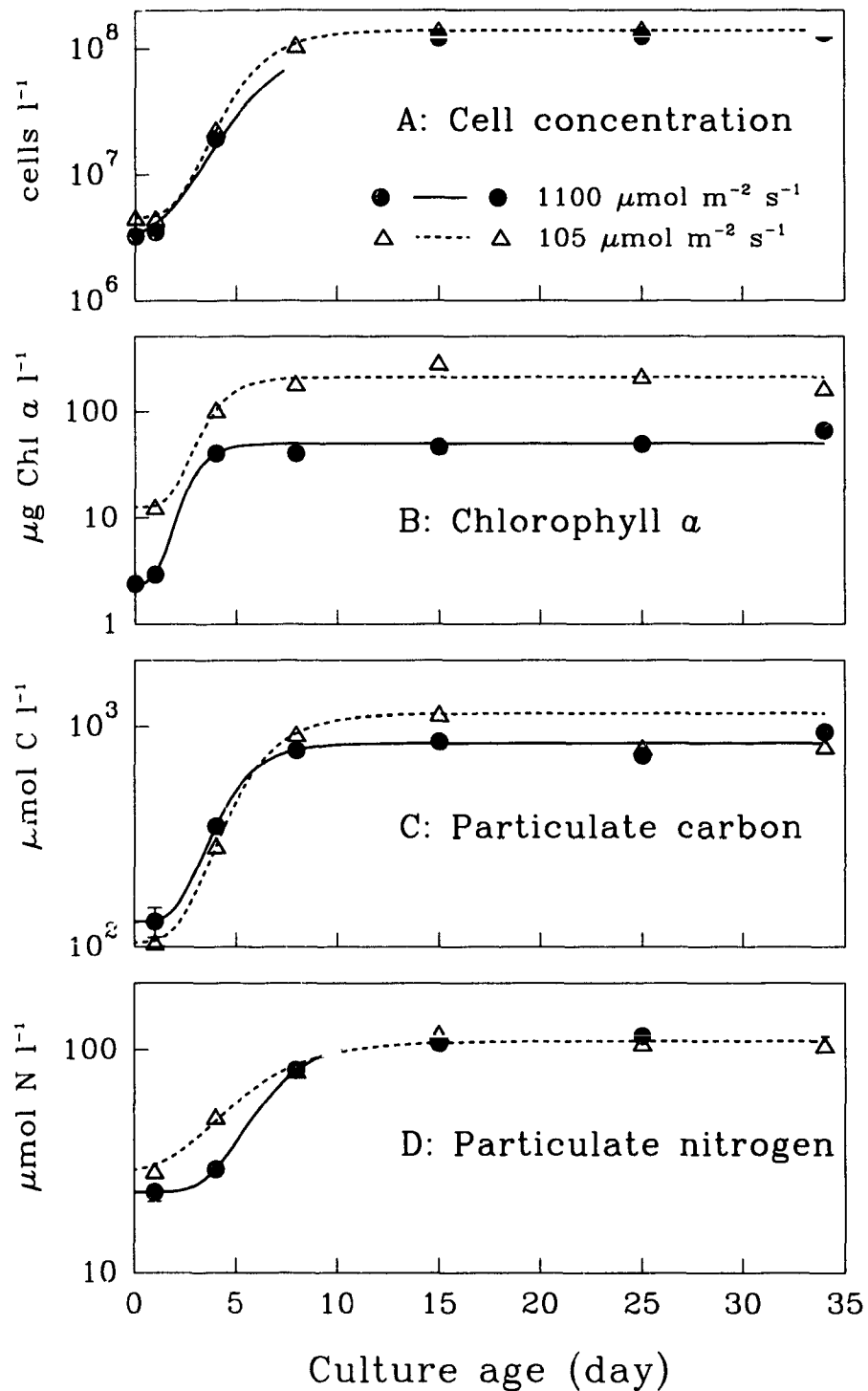


Fig. 3.1. Growth curves based on different indices of biomass fitted by Gompertz equation (2.11).

The decrease in silicate concentrations between days 1 and 15 was 72 μM (HL) and 73 μM (LL), and resulted in cell concentrations of 100×10^6 cells l^{-1} and 114×10^6 cells l^{-1} respectively. Based on this yield, a cellular silicon of 20.2 pg cell^{-1} (HL) and 15.5 pg cell^{-1} (LL) were calculated. The quantity of silicate (2.1-3.2 μM) available beyond day 15 was probably insufficient for further division of the cells.

Table 3.1. Nutrient concentrations (μM) in culture medium during growth of *P. pungens* f. *multiseries* in Experiment A.

PPFD ($\mu\text{mol m}^{-2} \text{s}^{-1}$)	Age (day)	SiO_3	PO_4	$\text{NO}_2 + \text{NO}_3$
1100	1	75.30	102.0	3028
	4	49.30	53.3	3001
	8	9.26	63.4	2961
	15	3.19	47.3	2813
	25	3.72	59.1	2892
	34	5.64	80.4	2770
105	1	75.60	101.0	3085
	4	55.80	77.3	2941
	8	6.06	62.9	3032
	15	2.05	70.4	2987
	25	9.25	89.7	2937
	34	6.42	84.9	2969

Using the derivative (Equation 2.12) of the Gompertz equation, growth rates (μ) were calculated based on all indices of biomass. Because of the scarcity of data points during the exponential phase, caution should be applied when interpreting these values.

The maximum growth rate (μ_m) based on an increase in cell numbers was 0.56 d^{-1} for the HL culture with a lag phase of 1 day. The corresponding values for the LL culture were 0.74 d^{-1} and 2 days (Fig. 3.2A).

Variations in the accumulation rate of chlorophyll *a*, particulate carbon and nitrogen were observed. Measuring growth rates using chlorophyll *a*, μ_m was calculated as 0.95 (LL) and $1.34 \text{ (HL)} \text{ d}^{-1}$ (Fig. 3.2B). The maximum growth rates based on chlorophyll *a* were much higher and occurred much earlier as compared to the μ_m calculated using other biomass indices (Fig. 3.2). The μ_m obtained using particulate nitrogen was $0.2\text{-}0.3 \text{ d}^{-1}$ (Fig. 3.2D). Besides resulting in the lowest μ_m , use of particulate nitrogen resulted in the longest lag phase compared to other growth indicators (Figs. 3.1D, 3.2D).

Cellular carbon and nitrogen were at their maximum on day 1 and drastically decreased by day 4 but there was no marked difference between cells grown under HL and LL (Figs. 3.3A, B). In general, cellular chlorophyll *a* was low initially, then increased in 3.2-3.5 days to a maximum (Fig. 3.3C). However, cellular chlorophyll *a* levels were always higher (by a factor of 1.8-5.4) in LL cells than in HL cells. Carbon:chlorophyll *a* ratio was highest in the lag phase, lowest in the exponential phase and slightly increased in the stationary phase. This ratio was consistently lower in LL than in HL cells (Fig. 3.4A). The C:N of cells was low at the beginning, peaked by day 4 in HL and by day 8 in LL cells, followed by a gradual decrease (Fig. 3.4B). In the exponential phase, C:N ratio was higher in HL cultures than in LL cultures, whereas in the stationary phase, C:N ratio was lower in HL cultures than in LL cultures.

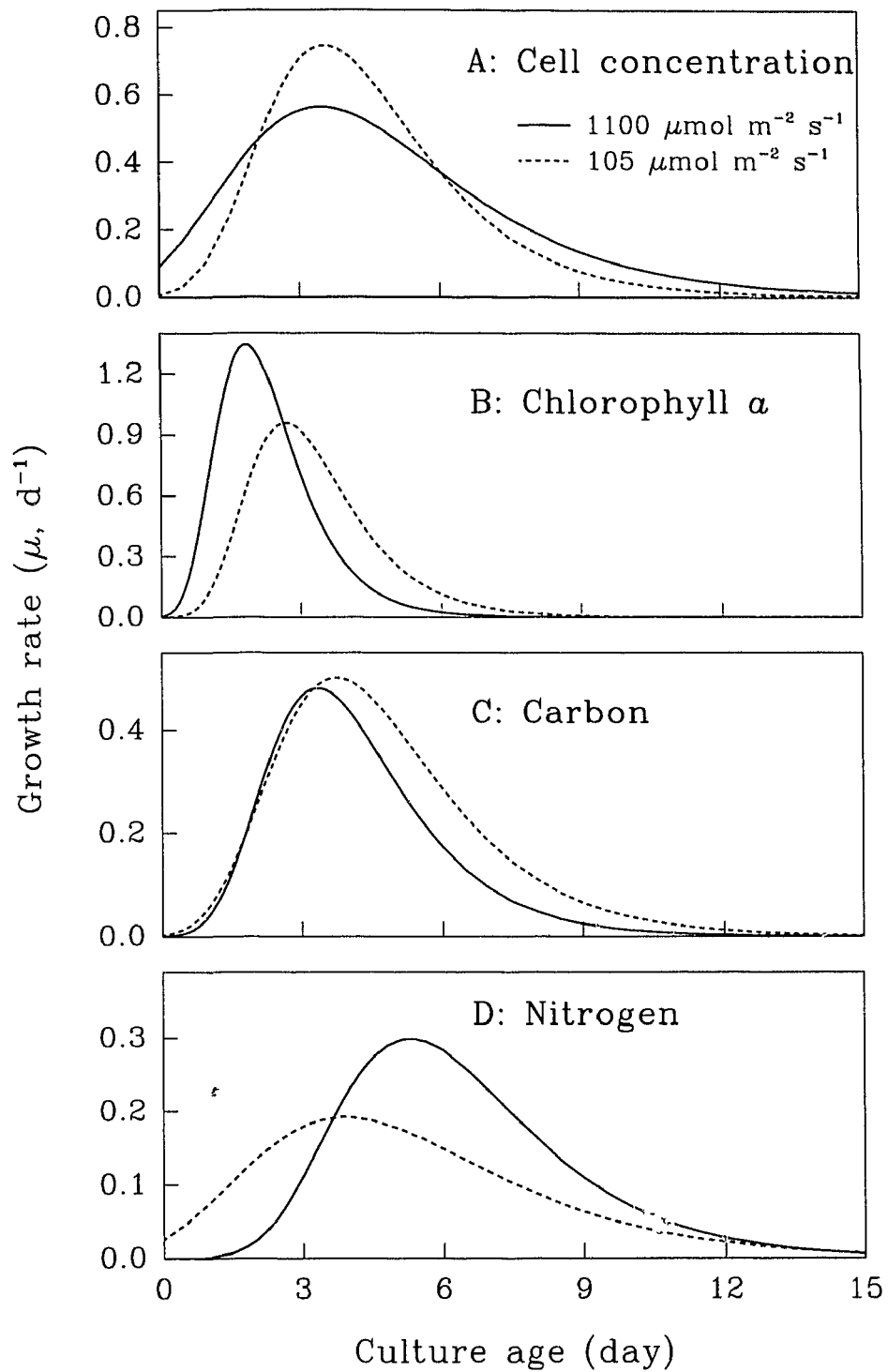


Fig. 3.2. Modelled (Equation 2.12) growth rates (d^{-1}) based on different indices of biomass during the first 15 days of the cultures.

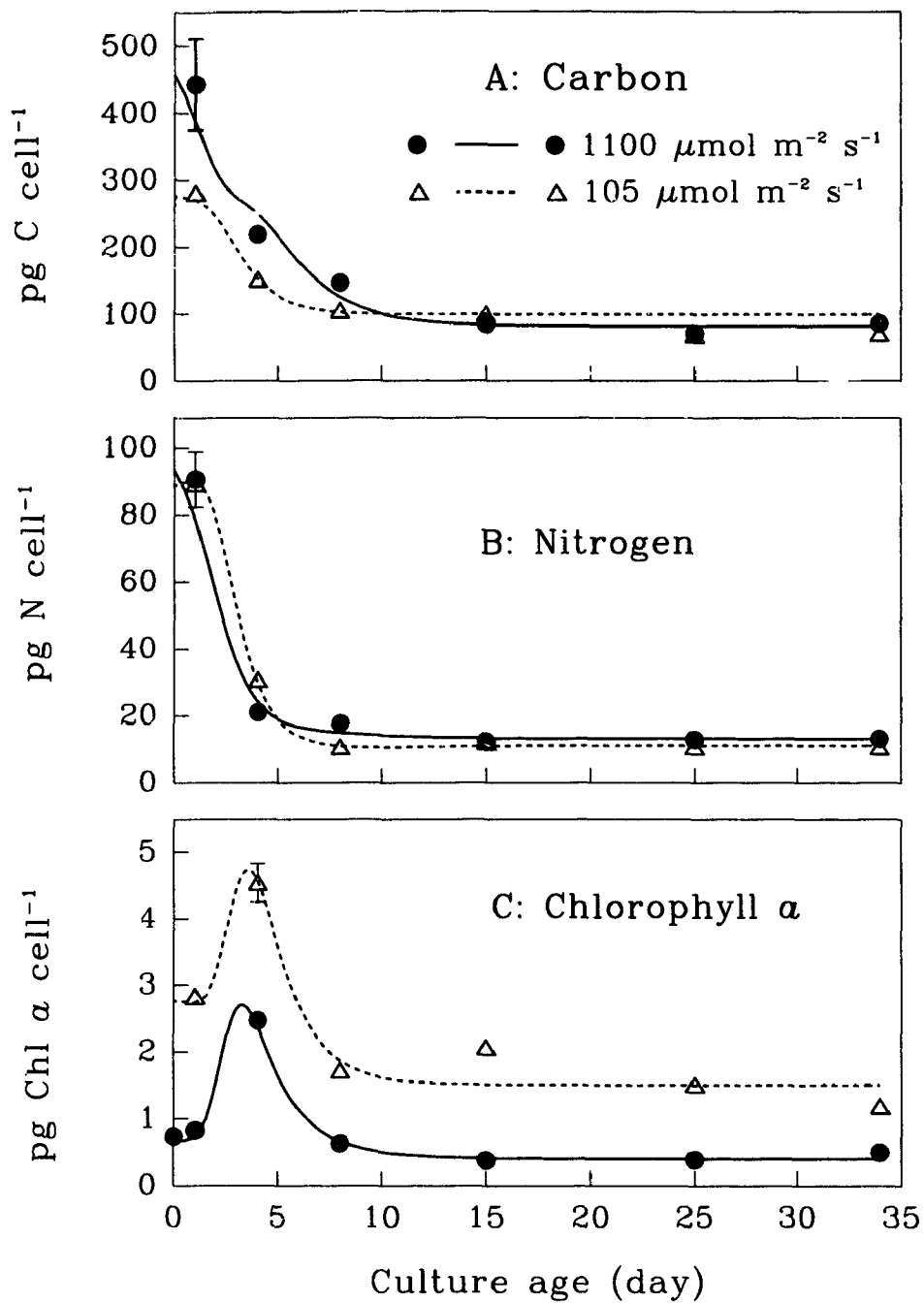


Fig. 3.3. Variations with time in the cellular (A) carbon, (B) nitrogen, and (C) chlorophyll *a*. Error bar = 1 standard deviation. Absent of error bar means it is smaller than the symbol. The curves are the ratios of the corresponding lines in Fig. 3.1.

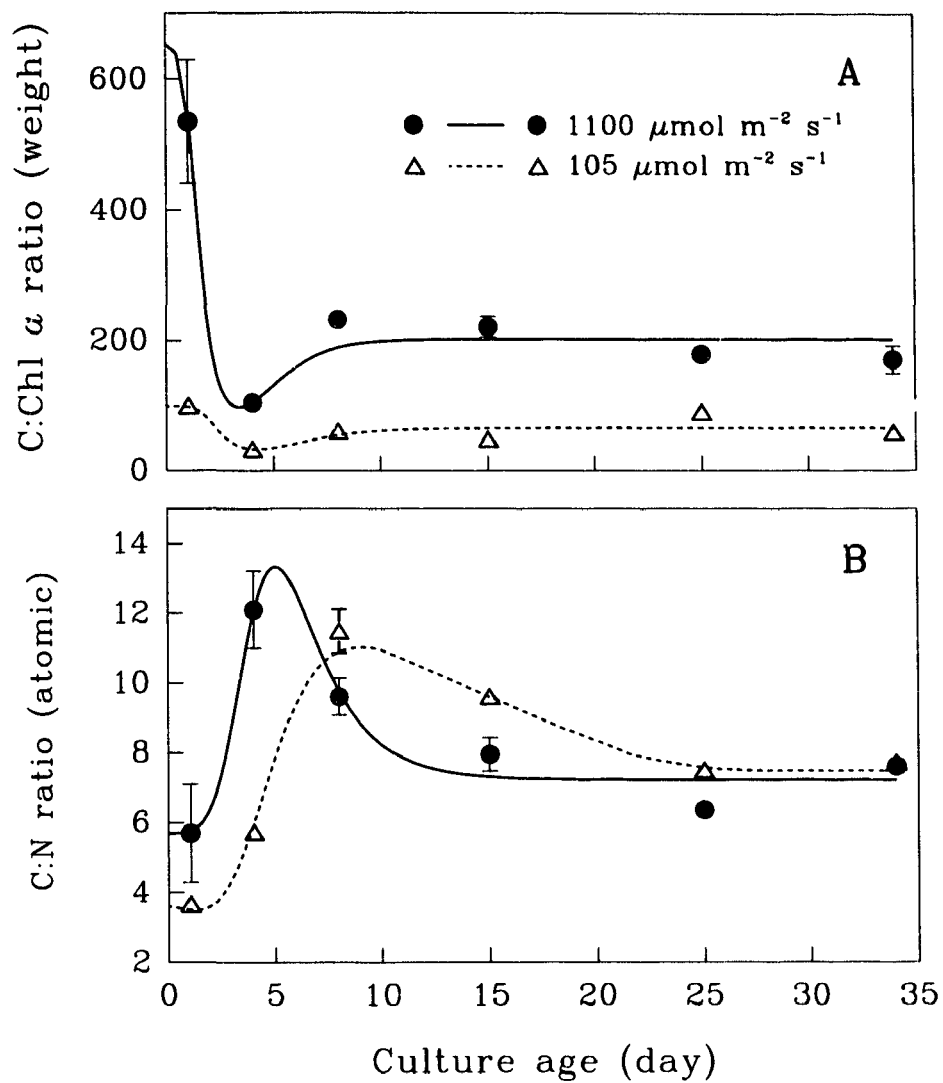


Fig. 3.4. Changes with time in the ratios of (A) carbon to chlorophyll a (by weight) and (B) carbon to nitrogen (atomic). The curves are the ratios of corresponding lines in Fig. 3.1.

3.3.1.2. Photosynthesis Photosynthetic rates increased as PPFD level increased but were inhibited at higher PPFD (Fig. 3.5). The empirical formula of Platt *et al.* (1980) provided with an additional parameter (P_d^B , Equation 2.6) described my data well. Photosynthetic rates were corrected for background uptake, P_d^B , because the data showed that P_d^B varied significantly with the age of the culture: in exponentially growing cultures, it was < 10% of the maximum corrected photosynthesis (P_m^B), in post-exponential cultures, on the other hand, it was 3-4 times higher than the corrected photosynthesis, similar to the findings of Laws and Caperon (1976) who studied cultures of the flagellate *Monochrysis lutheri*.

Interpretation of the P-I responses in HL and LL depended upon the biomass index used. For example in exponentially growing cells, if photosynthesis is normalized to chlorophyll *a* (Fig. 3.5A), HL cells achieved a greater maximum photosynthetic rate (P_m^B : assimilation number) than the LL cells (2.2 compared to 1.7 $\mu\text{g C} [\mu\text{g Chl } a]^{-1} \text{ h}^{-1}$). In contrast, when normalized to carbon (Fig. 3.5B), HL cells attain a P_m^B that is only 40% of that of LL cells (0.02 compared to 0.05 $\mu\text{g C} [\mu\text{g C}]^{-1} \text{ h}^{-1}$). This was a consequence of differences in the C:Chl *a* ratio in HL and LL cells.

Regardless of biomass index chosen, HL cells attained P_m^B at a higher PPFD than LL cells ($I_{m(\text{HL})} = 1272$, $I_{m(\text{LL})} = 489 \mu\text{mol m}^{-2} \text{ s}^{-1}$). The photoadaptive parameters I_m , I_k and I_s were independent of the biomass index chosen (Table 3.2). Consistent differences existed between the HL and LL cells. The I_m of HL cells was always higher (by a factor of 1.7-5.3) than those of LL cells; for I_k the factor was 2 to 6.2. This differences was also true for I_s except for day 1.

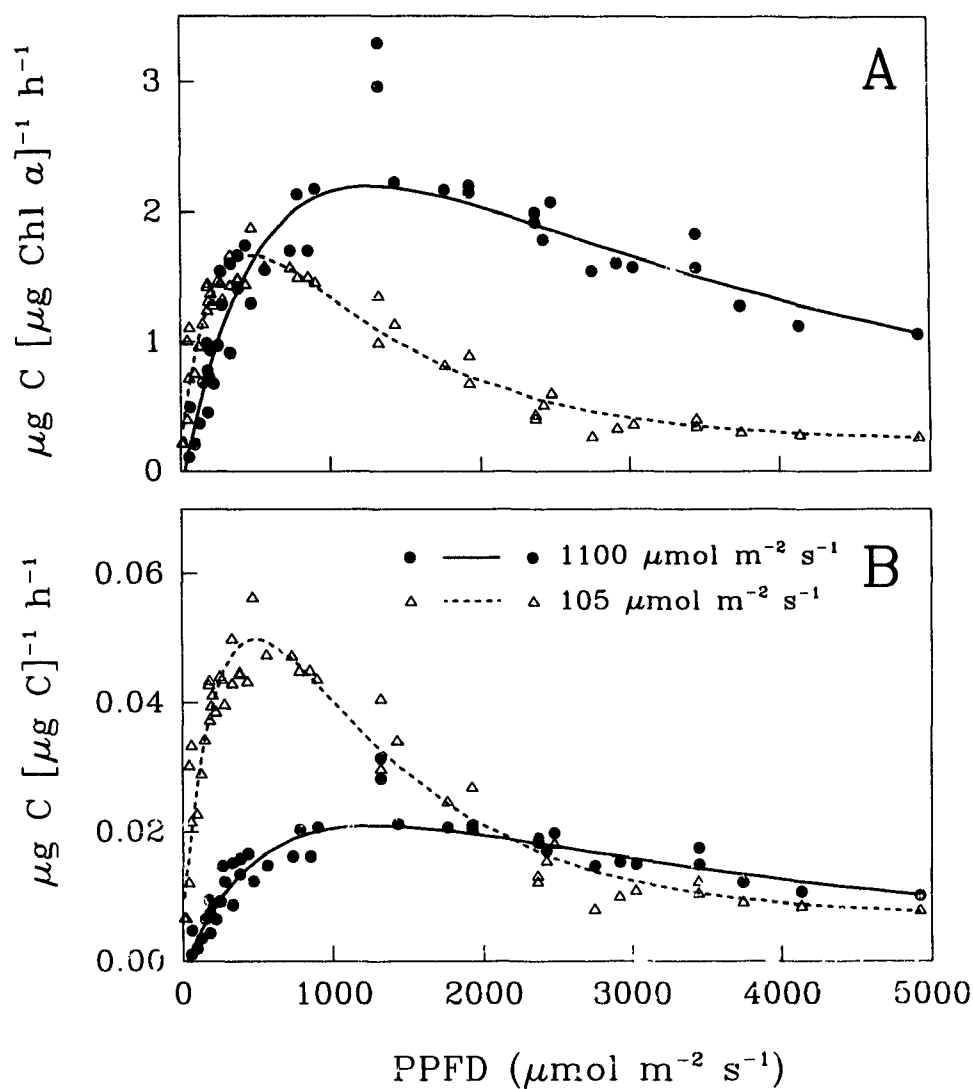


Fig. 3.5. Relationships between photosynthesis and PPFD in cultures after 4 days growth. (A) normalized to chlorophyll *a* ($\mu\text{g C} [\mu\text{g Chl } a]^{-1} \text{h}^{-1}$), (B) normalized to carbon ($\mu\text{g C} [\mu\text{g C}]^{-1} \text{h}^{-1}$). The curves are fitted by Equation 2.6.

Table 3.2. Changes in photoadaptive parameters of *P. pungens* f. *multiseries* with time at two PPFD levels in Experiment A.

PPFD ($\mu\text{mol m}^{-2} \text{s}^{-1}$)	Age (days)	I_m	I_k	I_s
		($\mu\text{mol m}^{-2} \text{s}^{-1}$)		
1100	1	1006	172	212
	4	1272	415	569
	8	1716	399	427
	15	1049	217	239
	25	1086	244	346
	34	593	156	154
105	1	599	86	311
	4	489	140	339
	8	379	102	134
	15	197	35	31
	25	426	114	106
	34	276	46	42

The photosynthetic response to PPFD varied systematically with the age of the culture in both HL and LL cells. With increasing culture age, the photochemical parameter (the initial slope of P-I curve, α^B) increased to attain a maximum on day 4 (6.06 ng C [$\mu\text{g Chl } a$] $^{-1}$ h $^{-1}$ [$\mu\text{mol m}^{-2} \text{s}^{-1}$] $^{-1}$ at HL, and 8.69 ng C [$\mu\text{g Chl } a$] $^{-1}$ h $^{-1}$ [$\mu\text{mol m}^{-2} \text{s}^{-1}$] $^{-1}$ at LL, Fig. 3.6A), after which there was a drastic decrease. α^B continuously decreased in the stationary phase (Fig. 3.6). When normalized to chlorophyll *a* (Fig. 3.6A), α^B values were comparable between HL and LL cells. In terms of cellular carbon, however, the α^B value in HL cells was usually lower (Fig. 3.6B) because of the high

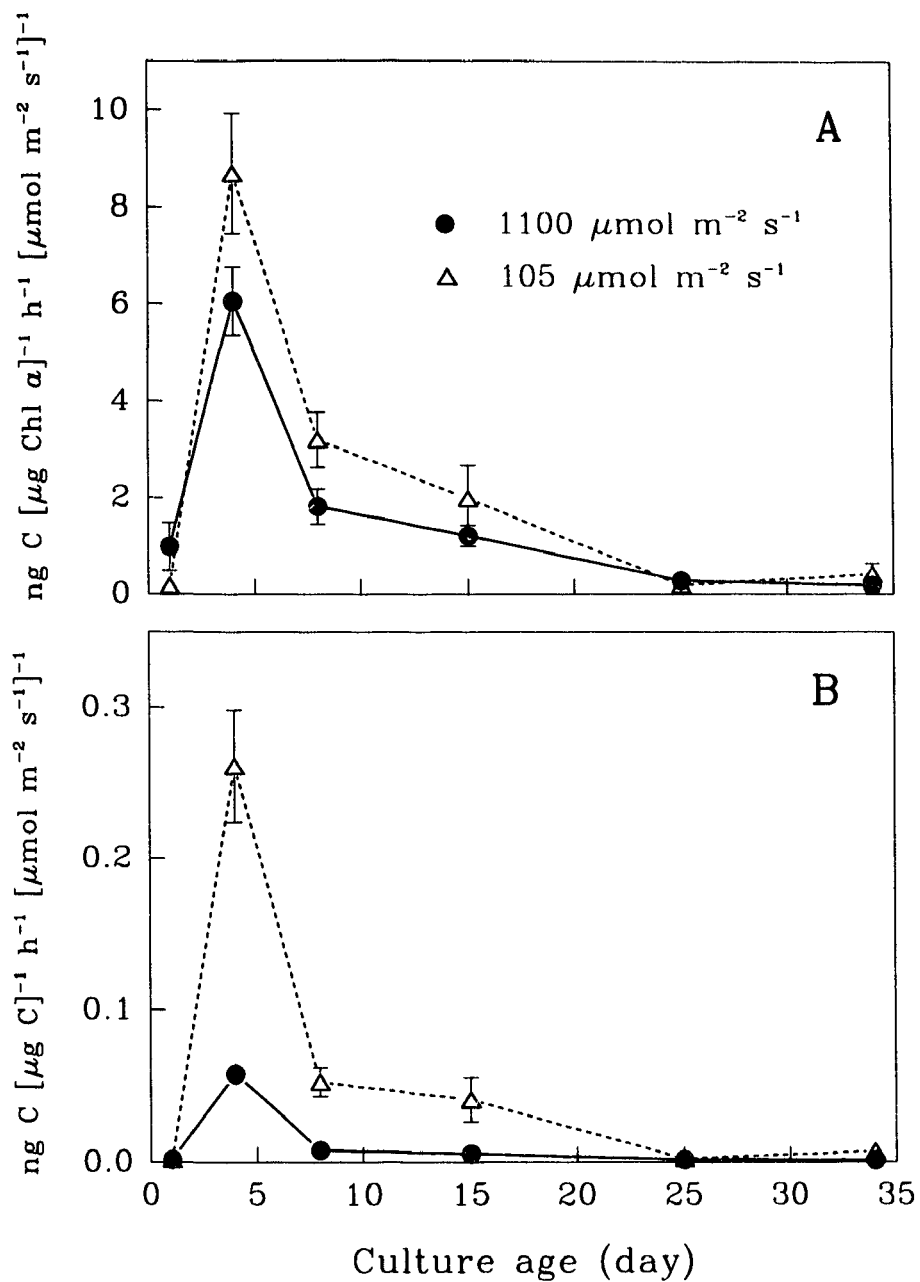


Fig. 3.6. Variations of α^B in various phases of batch cultures. (A) normalized to chlorophyll *a* ($\mu\text{g C } [\mu\text{g Chl } a]^{-1} \text{ h}^{-1} [\mu\text{mol m}^{-2} \text{ s}^{-1}]^{-1}$), (B) normalized to carbon ($\mu\text{g C } [\mu\text{g C}]^{-1} \text{ h}^{-1} [\mu\text{mol m}^{-2} \text{ s}^{-1}]^{-1}$).

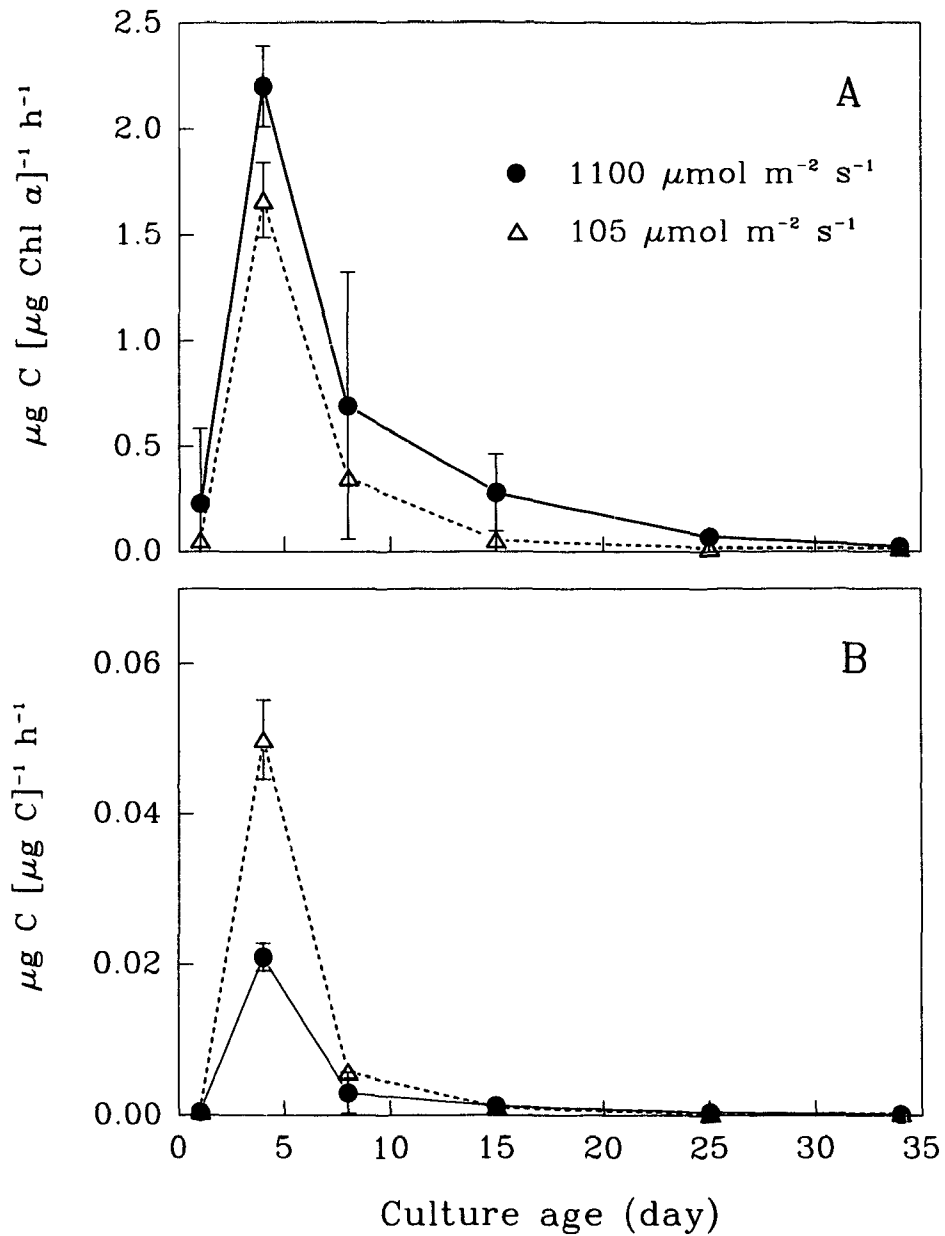


Fig. 3.7. Variation of P_m^B in various phases of batch cultures. (A) normalized to chlorophyll *a* ($\mu\text{g C} [\mu\text{g Chl } a]^{-1} \text{h}^{-1}$), (B) normalized to carbon ($\mu\text{g C} [\mu\text{g C}]^{-1} \text{h}^{-1}$).

C:Chl *a* ratio in HL cells (Fig. 3.4A).

The variations of P_m^B over time were similar to those of α^B , i.e. they attained a maximum on day 4 ($2.2 \mu\text{g C } [\mu\text{g Chl } a]^{-1} \text{ h}^{-1}$ in HL $1.7 \mu\text{g C } [\mu\text{g Chl } a]^{-1} \text{ h}^{-1}$ in LL) and subsequently decreased (Fig. 3.7A).

3.3.2. *Photosynthesis and growth under different PPFD levels*

3.3.2.1. Growth and cellular chemical composition The cultures grew at different rates with different lag phases under various PPFD levels (Fig. 3.8). Generally, cultures entered exponential phase earlier and grew faster at higher PPFD. For example, the culture at $1100 \mu\text{mol m}^{-2} \text{ s}^{-1}$ entered stationary phase on day 4, while the culture at $53 \mu\text{mol m}^{-2} \text{ s}^{-1}$ was still in the exponential phase on day 12.

Maximal growth rates and the duration of lag phase were determined by fitting data to the Gompertz model (Equation 2.11, Figs. 3.9A, B). Maximal growth rates (μ_m) ranged from 0.21 to 0.84 d^{-1} and were saturation functions (Equation 3.7) of PPFD levels. At $410 \mu\text{mol m}^{-2} \text{ s}^{-1}$, there was a scarcity of data points in the exponential phase (Fig. 3.8C) and a large standard deviation in the lag phase (Fig. 3.9B), which resulted in an abnormally high value of μ_m .

$$\mu_m = \mu_{m(m)} [1 - \exp(-\alpha_g I)] \quad (3.7)$$

In equation 3.7, $\mu_{m(m)}$ is the maximal growth rate at PPFD for optimal growth, α_g is the initial slope of the μ_m -I curve ($\text{d}^{-1} [\mu\text{mol m}^{-2} \text{ s}^{-1}]^{-1}$).

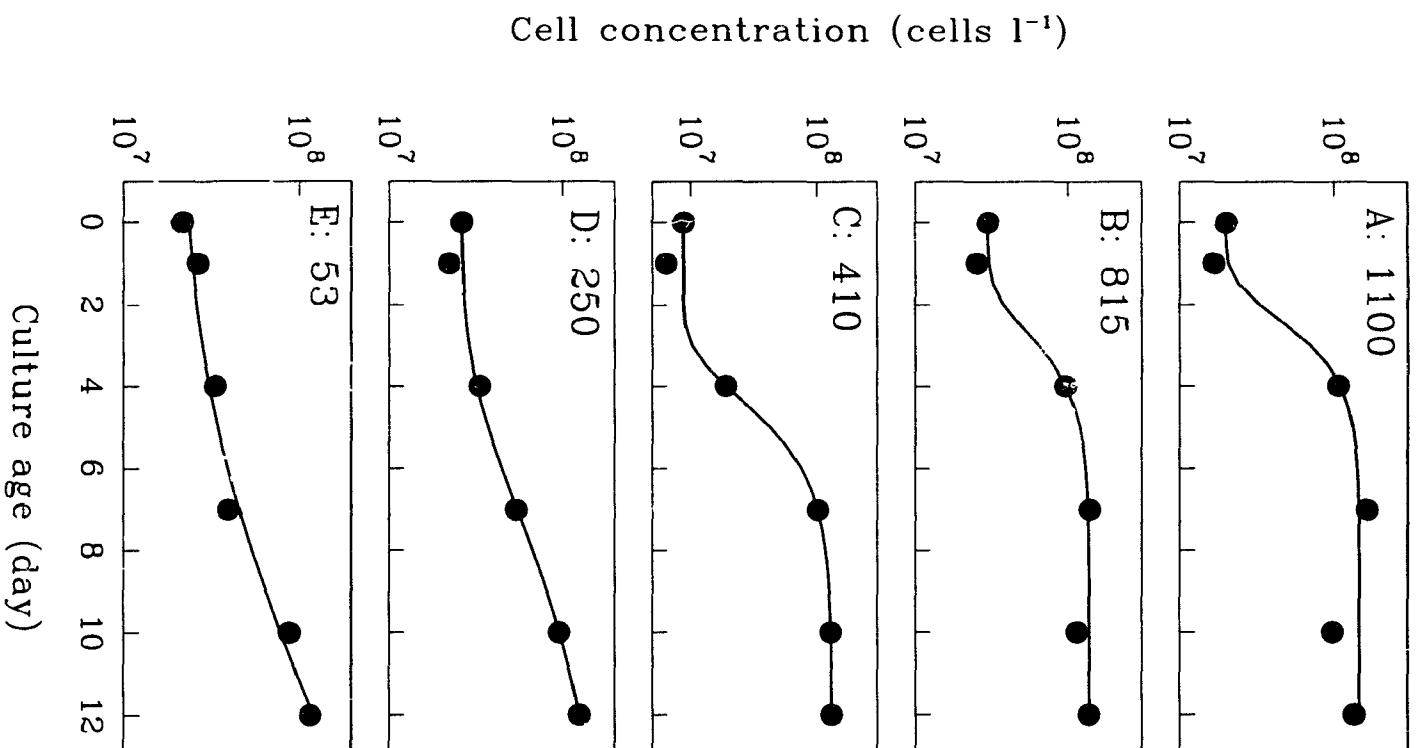


Fig. 3.8.

Growth curves of *P. pungens* f. *multiseries* under various PPFD levels ($\mu\text{mol m}^{-2} \text{s}^{-1}$) fitted by Gompertz equation (2.11).

Replacing a , b , c in Equation 2.11 with the fitted values, the time (t_m , in days) when the culture reached μ_m was determined. Surprisingly, t_m was a typical exponentially decreasing function of PPFD, under which cells were grown (Fig. 3.9). The relationship was well described by Equation 3.8:

$$t_m = (t_d - g) \exp(-fI) + g \quad (3.8)$$

Where, t_d (same unit as t_m) is the maximum t_m when the culture is in the dark, f (day $[\mu\text{mol m}^{-2} \text{s}^{-1}]^{-1}$) is the negative initial slope at $I \rightarrow 0$, and g describes the asymptote (t_m at $I \rightarrow \infty$). Based on the data of t_m (Fig. 3.9C), fitted values are as in Table 3.3.

Table 3.3. Values of parameters in Equation 3.8

Parameter	Value	Standard deviation
t_d (day)	18.16	0.21
f (day $[\mu\text{mol m}^{-2} \text{s}^{-1}]^{-1}$)	0.004905	0.000143
g (day)	2.24	0.096

In the exponential phase (day 4), cellular carbon, nitrogen and chlorophyll a decreased as PPFD increased (Fig. 3.10). In the stationary phase (day 12), on the other hand, cellular carbon and nitrogen became relatively constant (Figs. 3.10A, B) while chlorophyll a decreased as PPFD increased (Fig. 3.10C). This was consistent with the results from experiment A (Fig. 3.3).

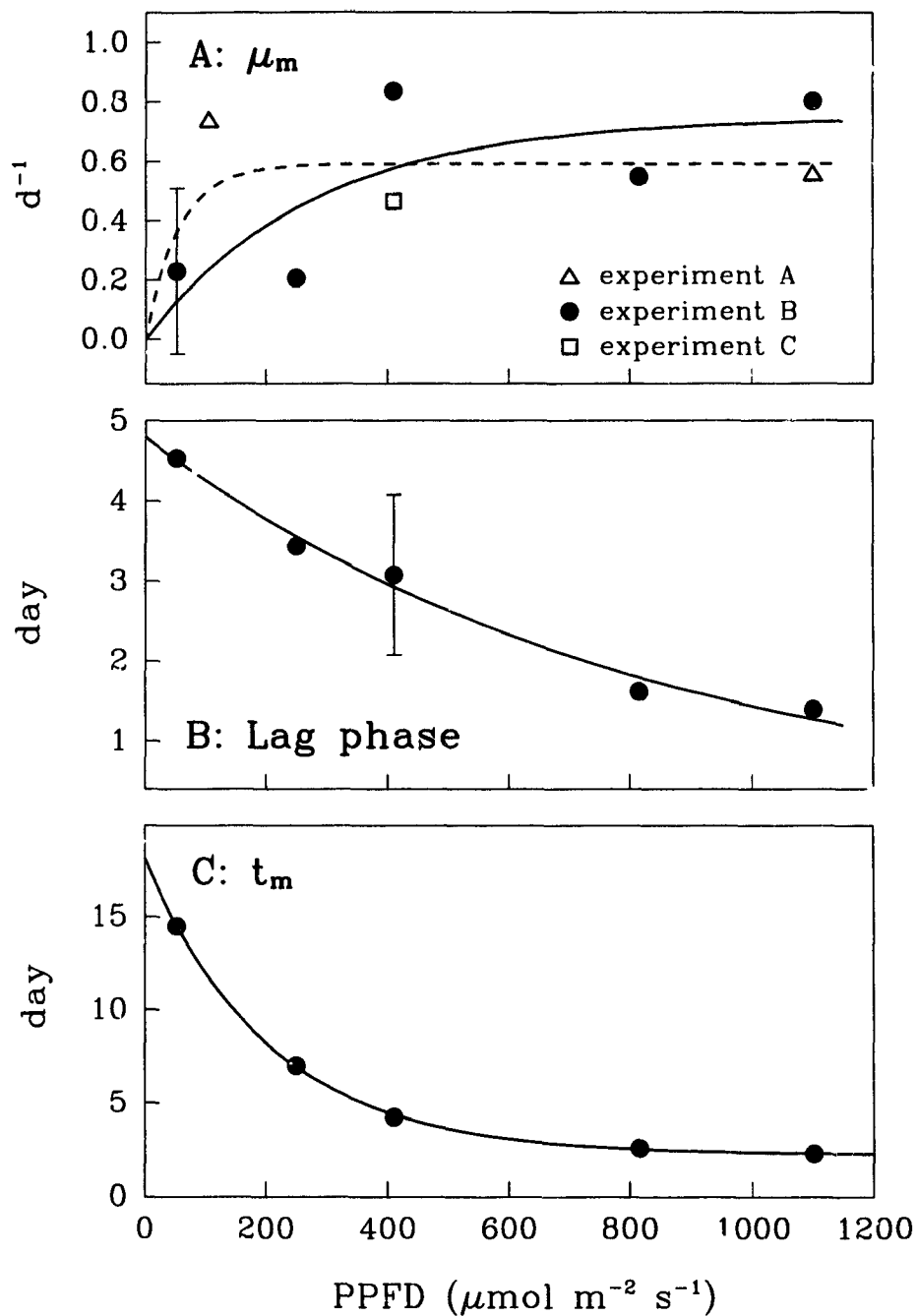


Fig. 3.9. Variations with PPFD levels in (A) the maximal growth (the solid curve is fitted by Equations 3.7 to the 5 filled points only and the broken line is fitted to all the 8 data points), (B) the duration of lag phase and (C) the time when maximal growth reached (fitted by Equation 3.8).

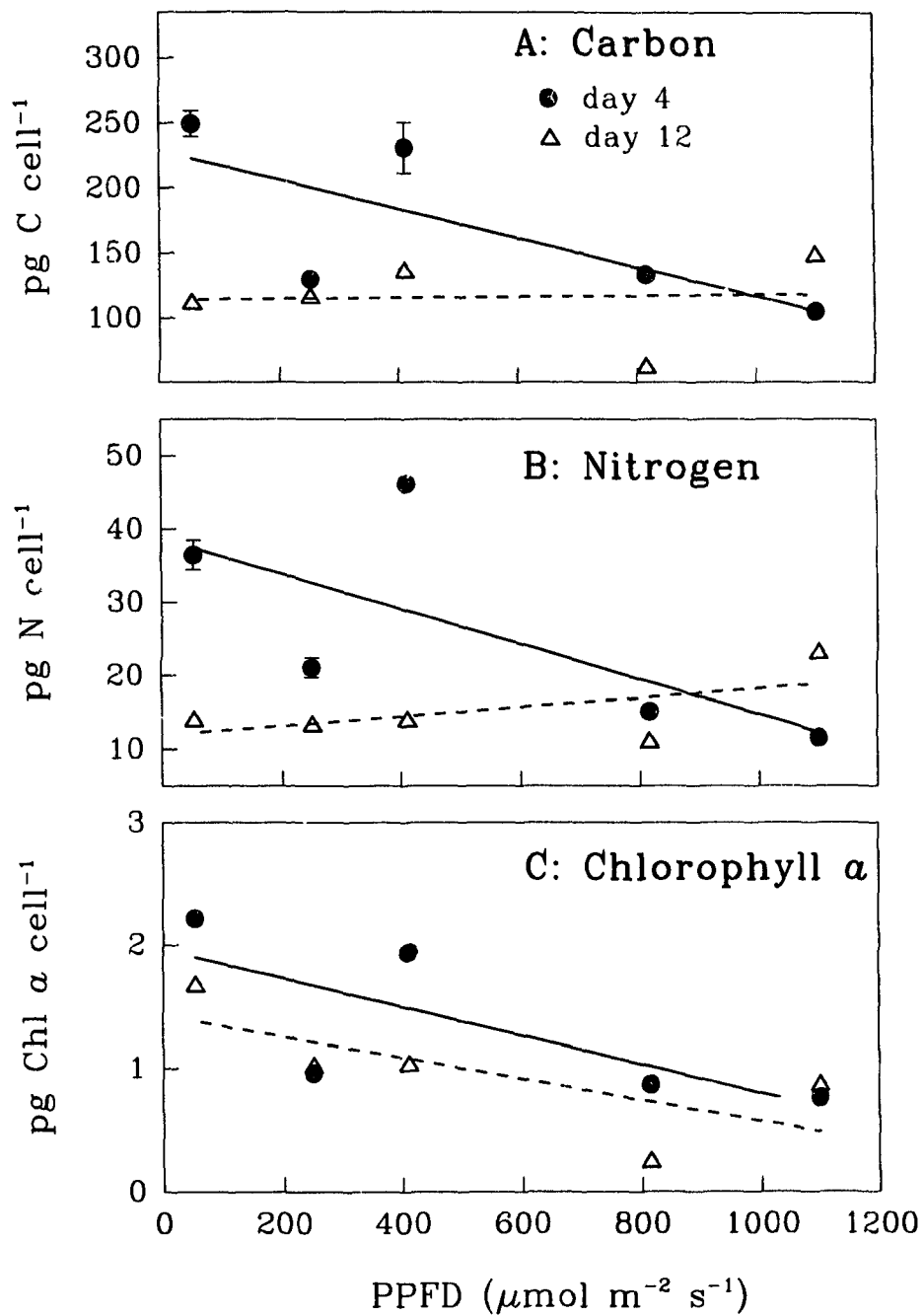


Fig. 3.10. Variations with PPFD levels in the cellular (A) carbon, (B) nitrogen and (C) chlorophyll *a*. The lines are linear regressions.

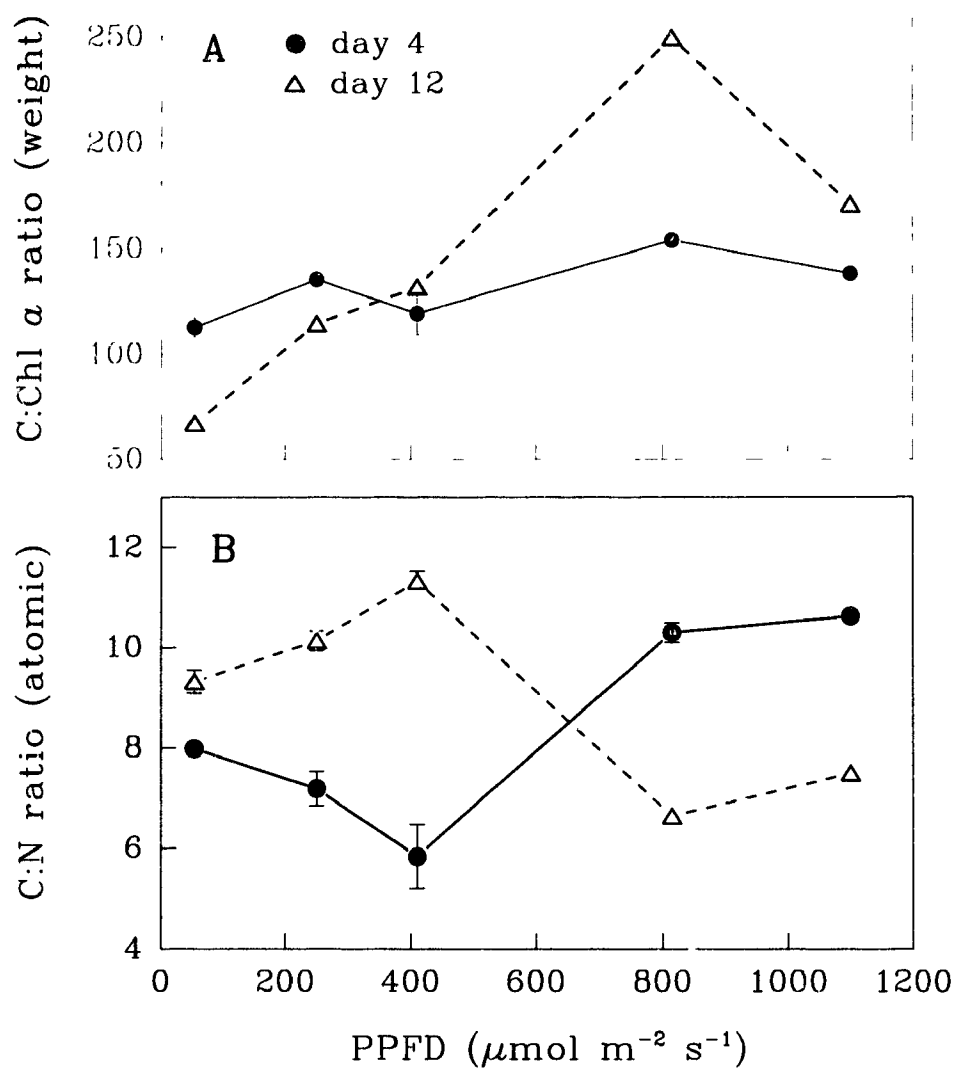


Fig. 3.11. Variations with PPFD levels in the ratios of (A) carbon to chlorophyll *a* (by weight) and (B) carbon to nitrogen (atomic).

The patterns of change in C:Chl *a* were similar on day 4 and day 12 (Fig. 3.11A). However, the magnitude of change in this ratio was higher on day 12 than day 4. C:Chl *a* slightly increased from 113 to 153 on day 4 as a result of increasing PPFD (Fig. 3.11A). A more significant increase occurred on day 12, from 67 at 53 $\mu\text{mol m}^{-2} \text{s}^{-1}$ to 249 at 815 $\mu\text{mol m}^{-2} \text{s}^{-1}$. At higher PPFD ($>815 \mu\text{mol m}^{-2} \text{s}^{-1}$), C:Chl *a* ratio decreased both on day 4 and day 12.

The ratio of carbon to nitrogen was variable and ranged from 5.84 to 11.33. On day 4, the C:N ratio decreased from 7.98 to 5.84 when PPFD increased from 53 to 410 $\mu\text{mol m}^{-2} \text{s}^{-1}$ and then increased again as PPFD further increased (Fig. 3.11B). In contrast, the C:N ratio on day 12 was a mirror image of that on day 4.

3.3.2.2. Photosynthesis Photosynthetic characteristics also varied with different PPFD levels. The initial slope α^B ranged from 0.40 to 6.22 $\text{ng C} [\mu\text{g Chl } a]^{-1} \text{h}^{-1} [\mu\text{mol m}^{-2} \text{s}^{-1}]^{-1}$ (Fig. 3.12A) while P_m^B ranged from 0.10 to 1.16 $\mu\text{g C} [\mu\text{g Chl } a]^{-1} \text{h}^{-1}$ (Fig. 3.13A). Regardless of the biomass indices used for normalization, α^B increased on day 4, and decreased on day 12 as PPFD increased (Fig. 3.12). These variations were more pronounced on day 12 than on day 4.

In the exponential phase (day 4), P_m^B (normalized to chlorophyll *a*) increased as PPFD increased from 53 to 250 $\mu\text{mol m}^{-2} \text{s}^{-1}$ and remained approximately constant between 250 and 410 $\mu\text{mol m}^{-2} \text{s}^{-1}$. As PPFD further increased, P_m^B slightly decreased showing a photoinhibition at high PPFD levels (Fig. 3.13A). When normalized to carbon, photoinhibition was not evident (Fig. 3.13B). In the stationary phase (day 12), on the

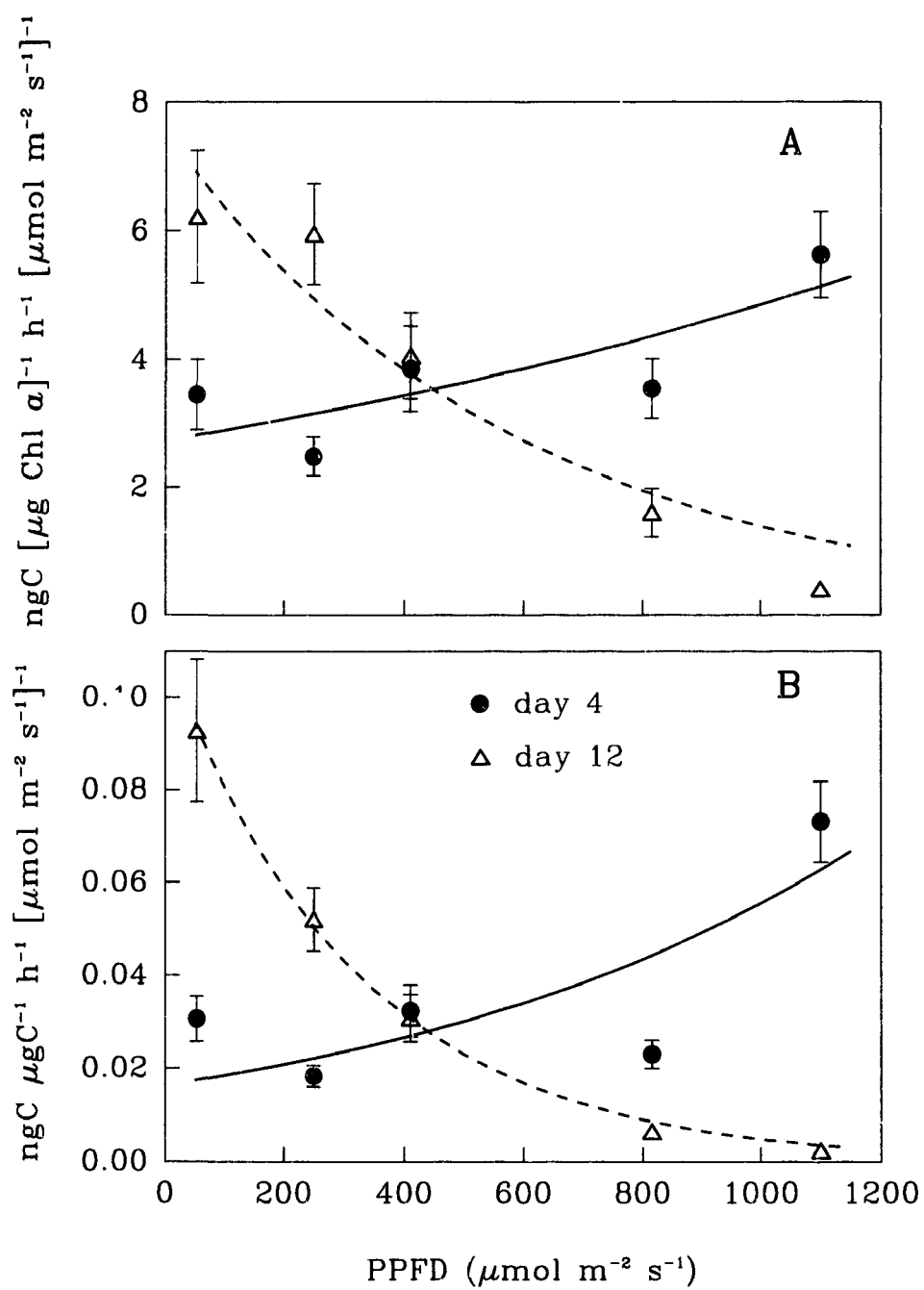


Fig. 3.12. Variations of α^B with PPFD levels. (A) normalized to chlorophyll *a*, (B) normalized to carbon. The curves are fitted by exponential functions.

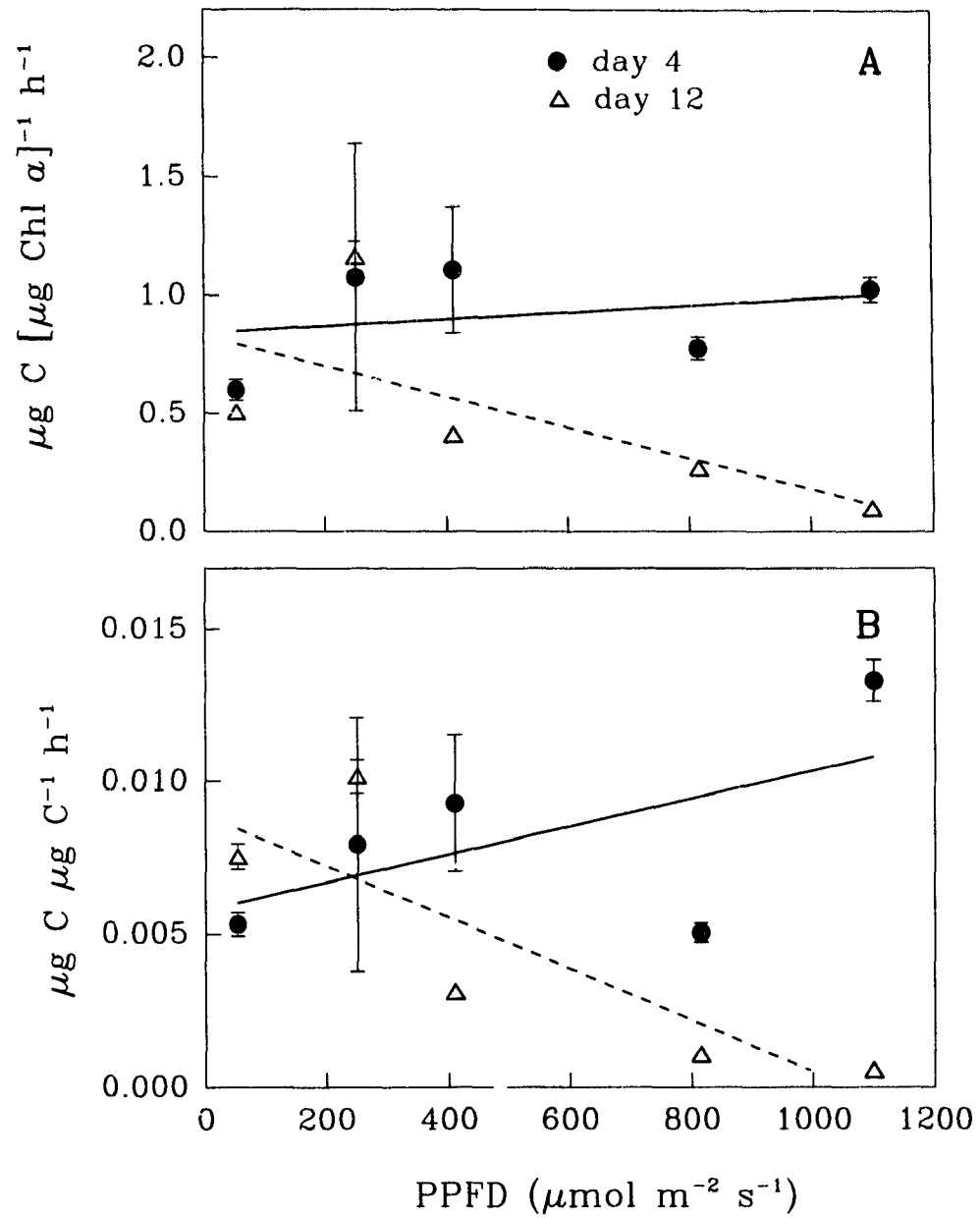


Fig. 3.13. Variations of P_m^B with PPFD levels. (A) normalized to chlorophyll a , (B) normalized to carbon. The lines are linear regressions.

other hand, photoinhibition was significant at high PPFD.

The photoadaptive parameter I_m generally corresponded to the growth PPFD (Table 3.4). Cultures grown at higher PPFD had higher I_m values. For individual cultures, however, the I_m value was higher on day 4 than day 12. Nevertheless, I_k and I_s did not follow the variation of PPFD.

Table 3.4. Changes in photoadaptive parameters I_m , I_k and I_s ($\mu\text{mol m}^{-2} \text{s}^{-1}$) during growth at different PPFDs in Experiment B

PPFD ($\mu\text{mol m}^{-2} \text{s}^{-1}$)	Day 4			Day 12		
	I_m	I_k	I_s	I_m	I_k	I_s
1100	1320	198	217	900	218	222
815	1430	231	249	560	186	155
410	730	278	1029	430	112	120
250	900	431	4132	780	201	209
53	500	175	212	430	93	99

3.3.3. Temperature dependence of photosynthesis and growth

3.3.3.1. Growth and cellular chemical composition

Over the temperature range investigated, cells grew at different rates at different temperatures. The growth rates ranged from 0.21 to 1.25 d^{-1} reaching a plateau at 15 °C and remaining relatively constant between 15 and 25 °C. A Q_{10} of 2.8 was determined between 5 and 15 °C (Fig. 3.14). Cellular carbon and nitrogen decreased by 56% and 45% respectively (Figs. 3.15A, B) when the growth rate increased from 0.21 d^{-1} at 0 °C to 1.18 d^{-1} at 15 °C. Growth rates were positively correlated with cellular chlorophyll *a* levels ($r = 0.8$, $p < 0.05$). There

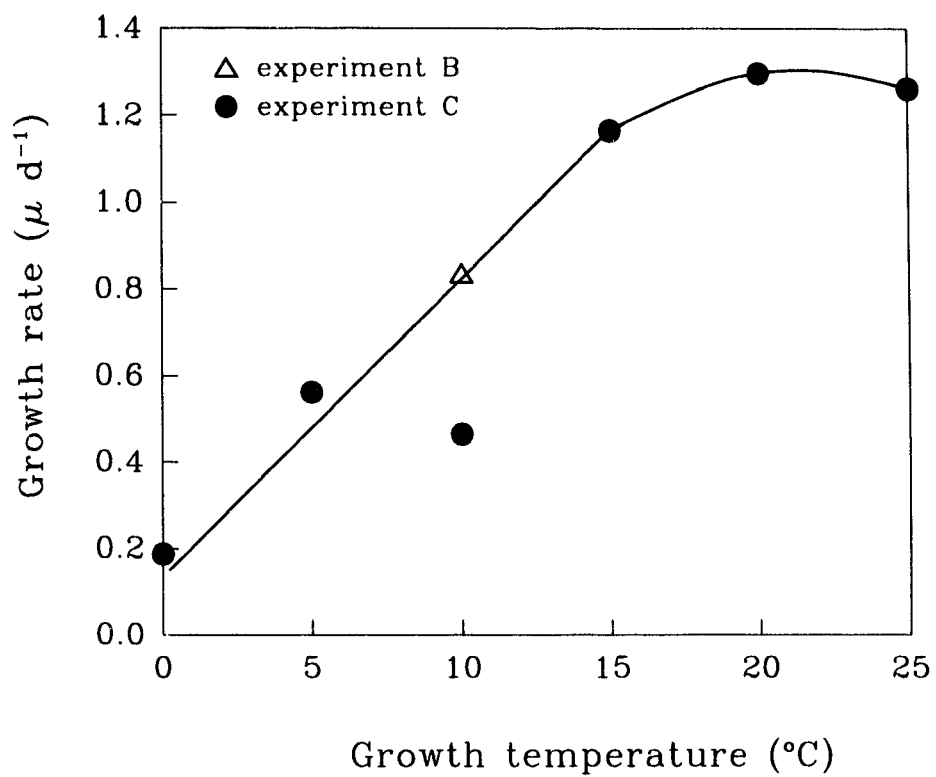


Fig. 3.14. Growth rate of *P. pungens* f. *multiseriis* at different temperatures. The curve is fitted by eye.

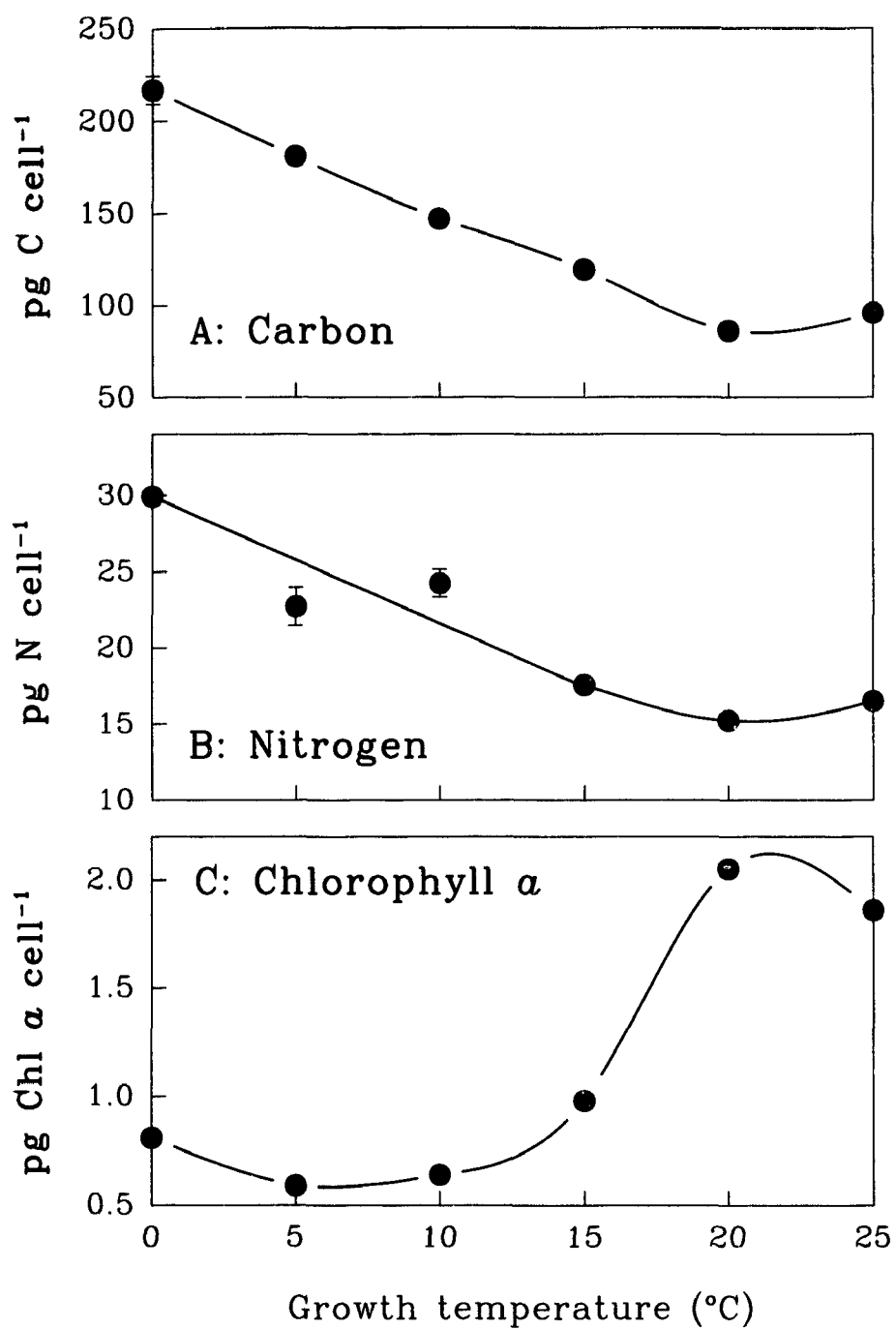


Fig. 3.15. Effects of temperature on the cellular (A) carbon, (B) nitrogen and (C) chlorophyll *a*. The curves are fitted by eye.

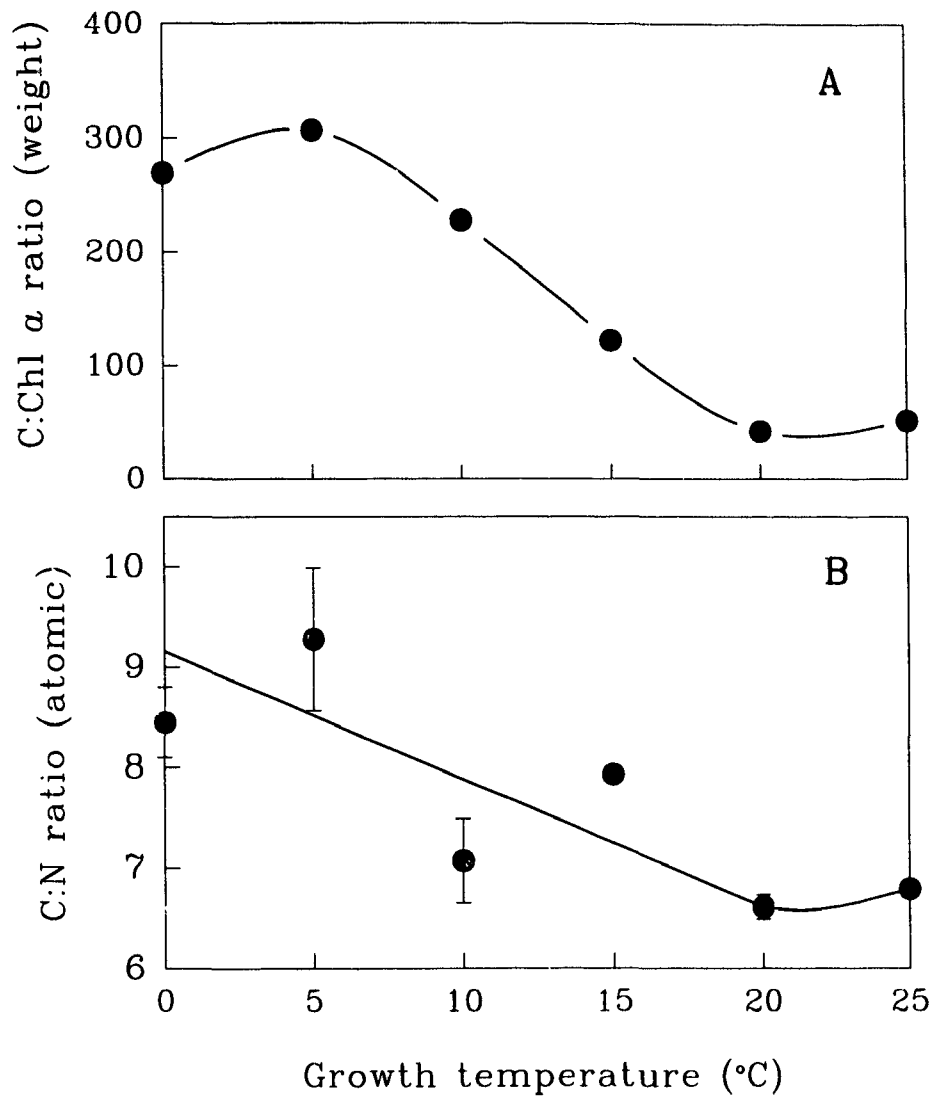


Fig. 3.16. Effects of temperature on the ratios of (A) carbon to chlorophyll *a* (by weight) and (B) carbon to nitrogen (atomic). The curves are fitted by eye.

was a parallel increase in growth rate and cellular chlorophyll *a* in the temperature range 10 - 15 °C (Figs. 3.14, 3.15C). The C:Chl *a* ratio (by weight) decreased drastically from 306 to 52 (Fig. 3.16A), while the C:N ratio decreased slightly from 9.4 to 6.6 as growth rate and temperature increased (Fig. 3.16B).

Nutrient concentrations in the medium remained high throughout the experiment. Nitrate were 2.32 - 2.70 mM, phosphate 72 - 91 µM and silicate 106 - 154 µM, therefore, none of the major nutrients limited growth.

3.3.3.2. Photosynthesis The shapes of the P-I curves were generally similar at all temperatures (Fig. 3.17). The maximum P_m^B was $3.42 \mu\text{g C } [\mu\text{g Chl } a]^{-1} \text{ h}^{-1}$ at 15 °C whereas the minimum P_m^B was $0.08 \mu\text{g C } [\mu\text{g Chl } a]^{-1} \text{ h}^{-1}$ at 0 °C. At 15 °C, the optimal temperature for photosynthesis (Figs. 3.17A, B), P-I relationships were well described. However, when cells were stressed after transferring from 10 to 0 °C, P_m^B was very low ($0.08 \mu\text{g C } [\mu\text{g Chl } a]^{-1} \text{ h}^{-1}$) and the P-I data points were scattered (Fig. 3.17C).

The temperature dependence of the P-I responses was related to the biomass index chosen (Fig. 3.18). For example, if photosynthesis was normalized to chlorophyll *a*, P_m^B ($\mu\text{g C } [\mu\text{g Chl } a]^{-1} \text{ h}^{-1}$) increased exponentially from 0.08 at 0 °C to 3.42 at 15 °C with a Q_{10} of 10.8 between 5 and 15 °C and then decreased at temperatures >15 °C (Fig. 3.18A). Normalized to carbon, the maximum photosynthetic rate showed a plateau between 15 and 25 °C.

The initial slope of P-I curve (α^B) increased exponentially from $0.17 \text{ ng C } [\mu\text{g Chl } a]^{-1} \text{ h}^{-1} [\mu\text{mol m}^{-2} \text{ s}^{-1}]^{-1}$ at 0 °C to $6.5 \text{ ng C } [\mu\text{g Chl } a]^{-1} \text{ h}^{-1} [\mu\text{mol m}^{-2} \text{ s}^{-1}]^{-1}$ at 20 °C with

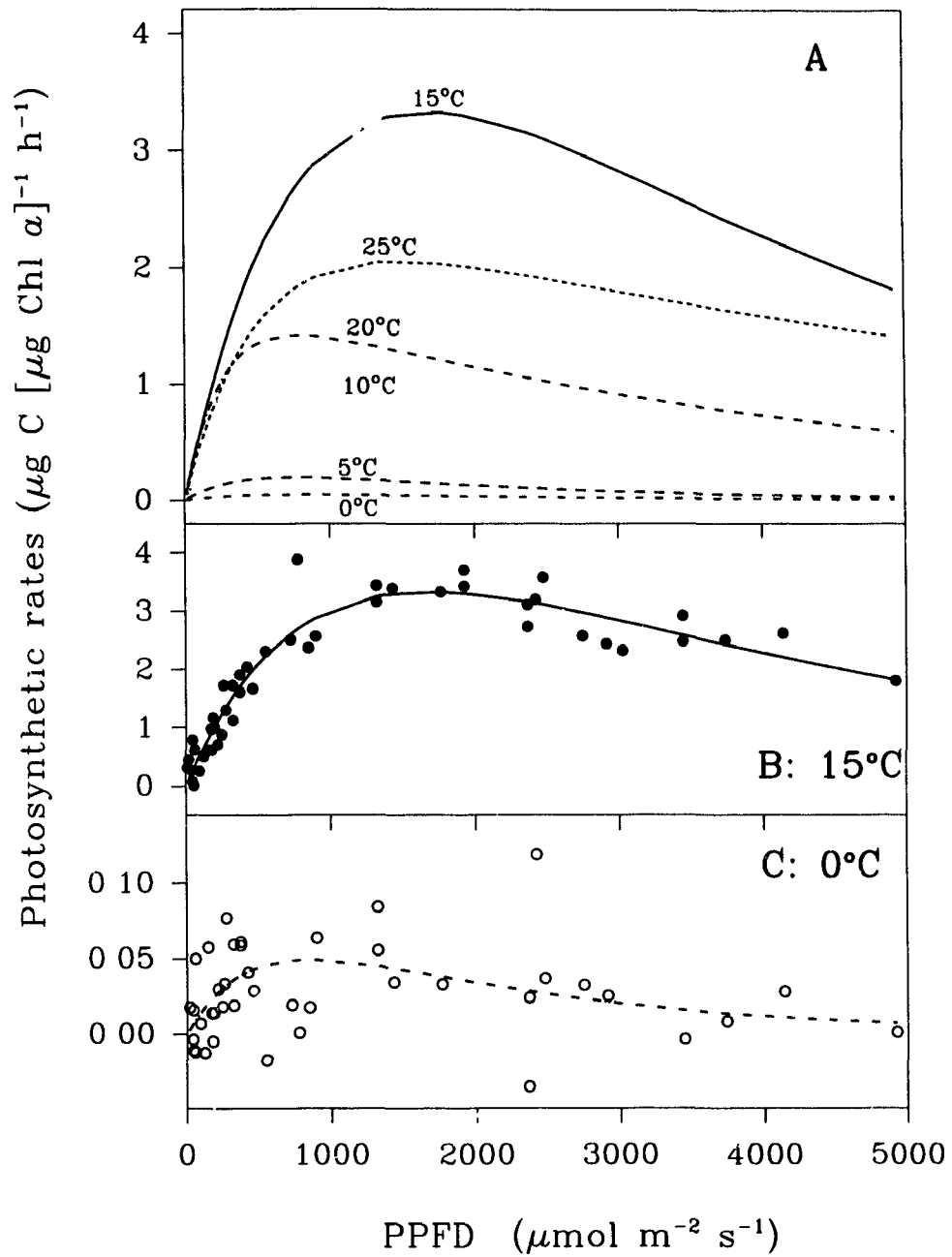


Fig. 3.17. Relationships between photosynthesis and photosynthetic photon flux density (P-I curves, Equation 2.6) at (A) 0° to 25°C, (B) 15°C and (C) 0°C.

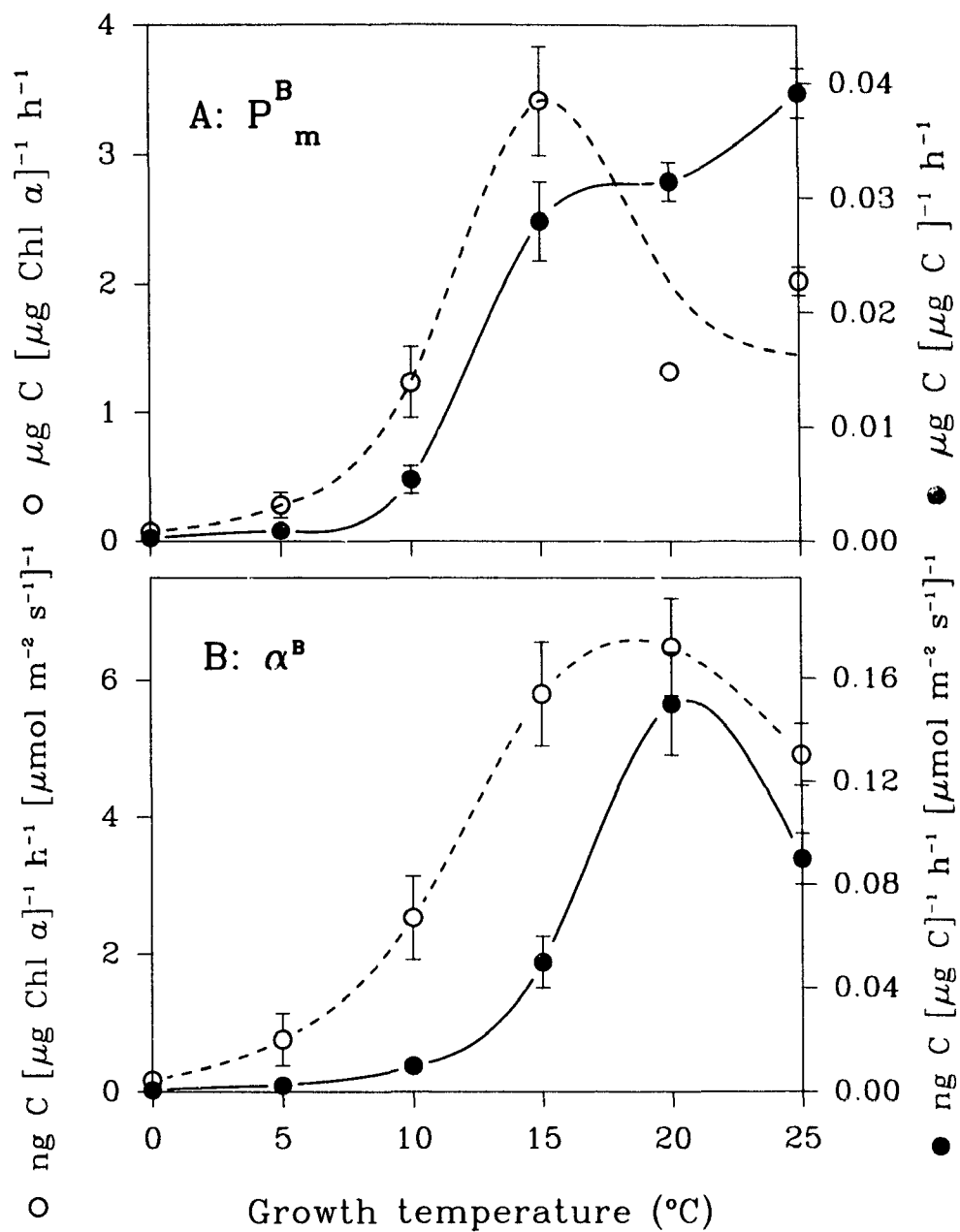


Fig. 3.18. Variations of (A) P_m^B and (B) α^B with temperature. The curves are fitted by eye.

a Q_{10} of 16.9 between 5 and 15 °C. The patterns of changes on α^B at different temperature were similar between these two biomass normalizations of carbon and chlorophyll *a*, although there was a temperature difference of 5 °C between the two curves in Fig. 3.18B.

3.4. Discussion

3.4.1. Growth

Pseudonitzschia pungens f. *multiseries* grew at different rates depending on the physiological states. Upon inoculating into a fresh medium, *P. pungens* f. *multiseries* usually experienced a lag phase with a duration of 0-4 days. The growth rates increased gradually and attained a maximum after cells entered exponentially phase, and decreased afterwards. Growth rates changed with various levels of PPFD and temperature. This fits the general growth model of phytoplankton (Fogg and Thake, 1987).

A variety of cell functions changed as the batch-culture population aged. Signs of aging in *P. pungens* f. *multiseries* appeared before the cells reached the stationary phase. Both cellular carbon and nitrogen were highest on day 1 and decreased gradually as the cells approached the stationary phase by day 8 or later (Figs. 3.3A, B). Chlorophyll *a* changed similarly (Fig. 3.3C).

The decrease in cellular chlorophyll *a* in the aged *P. pungens* f. *multiseries* cells, especially in the HL culture (Fig. 3.1B), might be due to breakdown of photosynthetic membrane, as was shown in *Gonyaulax polyedra* (Prézelin, 1982) and *Ptychodiscus brevis*

(Steidinger, 1979). In *P. pungens* f. *multiseries*, the chloroplasts were clearly seen under the photo-microscope to be heavily pigmented in the exponentially growing cells but neither the shape of chloroplasts nor the pigmentation were clearly seen in the aged cells. Prézelin (1982) found *Gonyaulax polyedra* cells began to break down their photosynthetic membranes in order to sustain cell metabolic requirements. Taylor (1968) noted a decrease in chloroplast lamella and a reduction in stroma in old zooxanthellae cells.

Faster growth due to higher PPFD accelerated aging of *P. pungens* f. *multiseries*. Cultures had a shorter lag period, grew faster and reached stationary phase earlier under higher PPFD (Fig. 3.8). This was similar to the observations of Bates *et al.* (1991). The signs of delay in aging were found in the cultures at low PPFD, which had higher cell content of carbon, nitrogen and chlorophyll *a* (Fig. 3.10) compared to high light cells on day 4. Similar features were shown in the culture of *Gonyaulax polyedra* (Prézelin, 1982).

Applying the same exponential decreasing function as Equation 3.8 to the duration of lag phase, a similar curve was obtained (Fig. 3.9B). The *g* value was very small (<0.3 day) and its standard deviation was more than 3 times higher. This suggests that the duration of lag phase would approach 0 if the PPFD was further increased. Similar changes in the duration of the lag+exponential phase under different PPFD was reported for the same diatom by Bates *et al.* (1991). In their experiment, stationary phase was reached 10 days earlier in the high light ($145 \mu\text{mol m}^{-2} \text{s}^{-1}$) culture than those in low light ($45 \mu\text{mol m}^{-2} \text{s}^{-1}$). They also found a delay in domoic acid production in the low light grown cultures.

The time for *P. pungens f. multiseriis* culture to reach its maximal growth was a typical exponential function of growth PPF_D (Fig. 3.9C). The cultures grew faster and reached their maximal growth earlier at higher PPF_D. These cultures would approach their minimum t_m (2.24) if PPF_D levels were higher.

Extrapolating the exponential curve in Fig. 3.9C to the point $I=0$, a maximal value of t_m was obtained. A negative value of compensation PPF_D (I_c) and a positive intercept on Y-axis were also obtained by supplying an additional parameter of I_c to the μ -I model (Equation 3.7). Although a negative I_c is physiologically meaningless, a positive intercept on Y-axis together with a t_m value of 18.2 days suggested that *P. pungens f. multiseriis* might be able to grow in the dark in the presence of some energy source other than light. Observation of Subba Rao and Wohlgeschaffen (unpublished data) showed growth of *P. pungens f. multiseriis* in the dark in the presence of a variety of organic substrates. This suggests that this alga is both photo- and heterotrophic. Heterotrophic growth has also been found in other diatoms such as *Nitzschia laevis* (Lewin and Hellebust, 1978), and *Phaeodactylum tricornutum* (Flynn and Syrett, 1986).

Maximal growth (μ_m) was a saturation function of PPF_D levels (Fig. 3.9A). The PPF_D levels for the optimal growth in *P. pungens f. multiseriis* was 410-1100 $\mu\text{mol m}^{-2} \text{s}^{-1}$, which was consistent with the variation of P_m^B (Fig. 3.13A). Similar saturation functions between growth and incident PPF_D exist in most other diatoms and dinoflagellates (Keifer and Mitchell, 1983; Falkowski *et al.*, 1985 and Langdon, 1987). For example, in the diatoms *Ditylum brightwellii* and *Pseudonitzschia turgidula* (Paasche, 1968), and dinoflagellate *Gonyaulax polyedra* (Rivkin *et al.*, 1982a), growth rates

increased as a saturation function of PPFD. Langdon (1987) found an α_g of $17 \times 10^3 \text{ d}^{-1} [\mu\text{mol m}^{-2} \text{ s}^{-1}]^{-1}$ for *Skeletonema costatum* grown at 20 °C. In the present study on *P. pungens* f. *multiseries*, α_g was $2.7(\pm 1.9) \times 10^{-3} \text{ d}^{-1} [\mu\text{mol m}^{-2} \text{ s}^{-1}]^{-1}$ which was generally low compared to other diatoms but comparable to dinoflagellates (Table 3.5). However, because of the scarcity and scattering of data points in Fig. 3.9A, caution should be applied when comparing these data with the literature values. For example, after introducing the 3 points from experiments A and C, the α_g value increased to $18 (\pm 16) \times 10^{-3} \text{ d}^{-1} [\mu\text{mol m}^{-2} \text{ s}^{-1}]^{-1}$, which was comparable to other diatoms.

Table 3.5. Initial slopes of μ - I curves in selected diatoms and dinoflagellates. $\alpha_g = 10^{-3} \text{ d}^{-1} [\mu\text{mol m}^{-2} \text{ s}^{-1}]^{-1}$

Taxa	T °C	α_g	References
Diatoms			
<i>P. pungens</i> f. <i>multiseries</i>	10	2.7-18	Present study
<i>Skeletonema costatum</i>	15	17.00	Langdon, 1987
<i>Thalassiosira weissflogii</i>	20	20.10	Laws and Bannister, 1980
	18	9.29	Falkowski <i>et al.</i> , 1985
<i>Leptocylindrus danicus</i>	10	11.78	Verity, 1981
<i>Chaetoceros protuberans</i>	19	7.07	Morel <i>et al.</i> , 1981
<i>Phaeodactylum tricornutum</i>	22-24	25.00	Geider <i>et al.</i> , 1985
Dinoflagellates			
<i>Gonyaulax polyedra</i>	23	2.63	Rivkin <i>et al.</i> , 1982a
<i>Alexandrium tamarense</i>	15	3.40	Langdon, 1987
<i>Prorocentrum micans</i>	18	0.35	Falkowski <i>et al.</i> , 1985
<i>Gyrodinium cf. aureolum</i>	20	17.33	Garcia and Purdie, 1992
<i>Pyrocystis noctiluca</i>	23	1.73	Rivkin <i>et al.</i> , 1982b

There are no data on acclimation of *P. pungens* f. *multiseries*. It would have well acclimated at the time of the experiments after two subculturings (>5 generation times) under the new PPFD. Rivkin *et al.* (1982a) showed that *Gonyaulax polyedra* can retain its maximal growth for up to two generation times during exposure to sub-optimal PPFD. This suggests that this dinoflagellate needs a transition time of at least two generation to acclimate to a new PPFD.

The acclimation time of phytoplankton to different temperatures varies from 0 to more than 100 hours, and from 0 to 4 divisions (Li, 1980). If *P. pungens* f. *multiseries* adapted to the new temperatures after one generation (one division), the cultures at 10°, 15°, 20° and 25 °C in experiment C would have been acclimated to the new temperature before the P-I experiments and the one at 5 °C would be almost acclimated (0.8 division).

3.4.2. Chemical composition

Growth is the expression of overall metabolism of an organism or a population and is related to the variation in chemical composition of algae. Comparison of growth rates in experiment A based on the 4 biomass indices, i.e. chlorophyll *a*, cell number, carbon, and nitrogen showed that cell division was not internally consistent with intracellular chemical constituents (Fig. 3.2). In HL, for example, chlorophyll *a* based growth rate increased and reached its maximum after 1.8 days. Cells were actively dividing as the photosynthetic capacity increased resulting from the rapid increase of chlorophyll *a* per unit volume (Figs. 3.1B, 3.2B) and reached the maximal cell division after 3.5 days, i.e. 1.7 days later than chlorophyll *a* based rate. Growth rate measured by

particulate carbon reached a maximum in 4.4 days, and that by particulate nitrogen reached a maximum in 5.2 days. The magnitudes of μ_{\max} attained, based on the 4 biomass indices differed as well (Fig. 3.2). In LL culture, the maximal growth based on chlorophyll *a* was attained after 2.7 days as compared to 1.8 days at HL (Table 3.4). A similar unbalanced growth in cellular constituents was found by other researchers. For example, Caperon and Meyer (1972a, b) demonstrated that μ based on ^{14}C , carbon or chlorophyll *a* cannot be equated to the growth prediction based on nutrient uptake. Shuter (1979) divided the cellular carbon into 4 compartments (carbohydrate, protein, lipid and nucleotide) and emphasized that differences in the flows of material between compartments and between cells would result in unbalanced growth.

Chemical composition is influenced by growth rate. In experiment A, for example, cellular carbon and nitrogen in *P. pungens* were highest at the beginning of the batch cultures (Fig. 3.3A), but decreased substantially as the cells entered the exponential phase. Cellular levels of carbon and nitrogen did not recover when the cells entered the stationary phase although carbon and nitrogen sources in the medium were not limiting. In experiment B, on day 4, growth rate increased as PPFD increased and reached a plateau; but cellular carbon and nitrogen decreased. Similarly, in experiment C, the highest cellular carbon and nitrogen occurred at 0 °C when the growth of *P. pungens* was restricted by the low temperature. Both cellular carbon ($r = -0.94$, $p < 0.01$) and nitrogen ($r = -0.98$, $p < 0.01$) were negatively correlated with the growth rate of *P. pungens* f. *multiseries* at various temperatures.

Cellular chlorophyll *a*, on the other hand, positively correlated with growth rate

and maximum photosynthetic rate (Fig. 3.19). In experiment A, for example, cellular chlorophyll *a* was initially low, it increased and reached a maximum at 3.2 days for HL culture and 3.5 days for LL cultures corresponding to the maximal growth at 3.5 day (HL) and 3.6 day (LL) respectively. In experiment C, increase in cellular chlorophyll *a* was similar to the increase in growth and photosynthetic rate. In experiment B, however, this feature was different. Growth rate increased while cellular chlorophyll *a* decreased with increasing PPFD. This was due to the photoadaptation mechanism. Systematic differences in cellular chlorophyll *a* existed in the cultures under different PPFD no matter how fast the cells grew (Fig. 3.3C).

Upon transfer from 10 °C to higher temperatures, cellular chlorophyll *a* increased immediately, more than double within a day, coincident with the obvious increases in growth and photosynthetic rates. The C:Chl *a* ratio decreased with increase in temperature, consistent with observations on *Phaeodactylum tricornutum* (Li, 1980), *Skeletonema costatum* (Sakshaug, 1977; Yoder, 1979) and *Dunaliella tertiolecta* (Eppley and Sloan, 1966). When transferred to lower temperatures, on the other hand, variations in cellular chlorophyll *a* were very small, even though growth and photosynthetic rates decreased. However, my data showed that in temperature controlled batch cultures of *P. pungens* f. *multiseries*, growth rate was significantly correlated to cellular chlorophyll *a* ($r = 0.81$, $n = 6$).

Temperature limited cultures showed that the C:N ratio decreased approaching the Redfield ratio (6.25) when growth rates increased as a result of increasing temperature (Figs. 3.14, 3.16). This was similar to the negative correlation between C:N ratio and

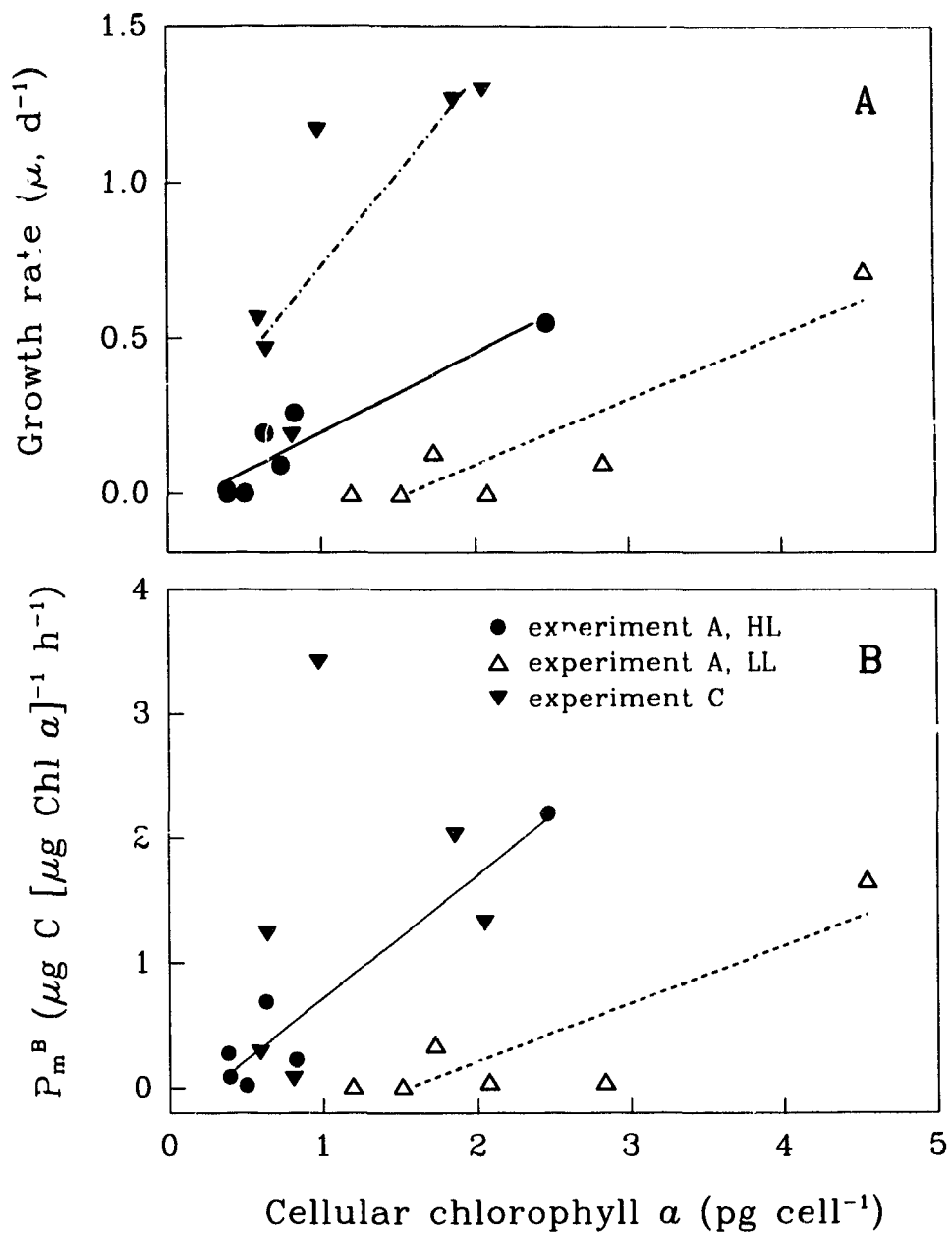


Fig. 3.19. Relationships of (A) growth rates and (B) photosynthetic rate (P_m^B) with cellular chlorophyll a . The lines are linear regressions.

growth rate of the chrysophyte *Monochrysis lutei* under P-limitation, the diatom *Thalassiosira pseudonana* 3H under NH_4 limitation and the chlorophyte *Dunaliella tertiolecta* under P- and N-limitation (Goldman *et al.*, 1979). Goldman *et al.* (1979) found as a common feature that the Redfield ratio (C:N:P=106:16:1) was approached only at high growth rates ($>90\mu_{\text{max}}$) regardless of the N:P ratio in the medium. However, this feature was not applicable to the data from experiments A and B. The C:N ratio increased with increasing growth rate in the exponential phase of the HL culture of experiment A (Fig. 3.4) and then decreased as the cells approaching stationary phase. In the LL culture, on the other hand, the ratio increased and did approach the Redfield ratio when cells approached μ_m , but the ratio further increased in the late exponential phase and then decreased after cells entered stationary phase.

3.4.3. Photosynthesis

The growth rate was positively correlated with the maximum photosynthetic rate regardless of the growth conditions (Fig. 3.20). For example in experiment A, the maximal P_m^B attained on day 4 (Fig. 3.7) corresponds to the mid-exponential phase (Fig. 3.1). The P_m^B decreased as growth rate decreased when the cultures aged, which is consistent with that of *Nitzschia closterium* (Humphrey and Subba Rao, 1967) and some other microalgae (Glover, 1980). The relative magnitudes of P_m^B occurring during the exponential phase compared to that in the early stationary phase ($P_m^B_{(\text{day } 4)} : P_m^B_{(\text{day } 8)}$) were 4.7 for HL and 3.2 for LL cells respectively in the experiment A. The corresponding ratios for growth rates were 2.8 (HL) and 5.4 (LL) respectively. A similar

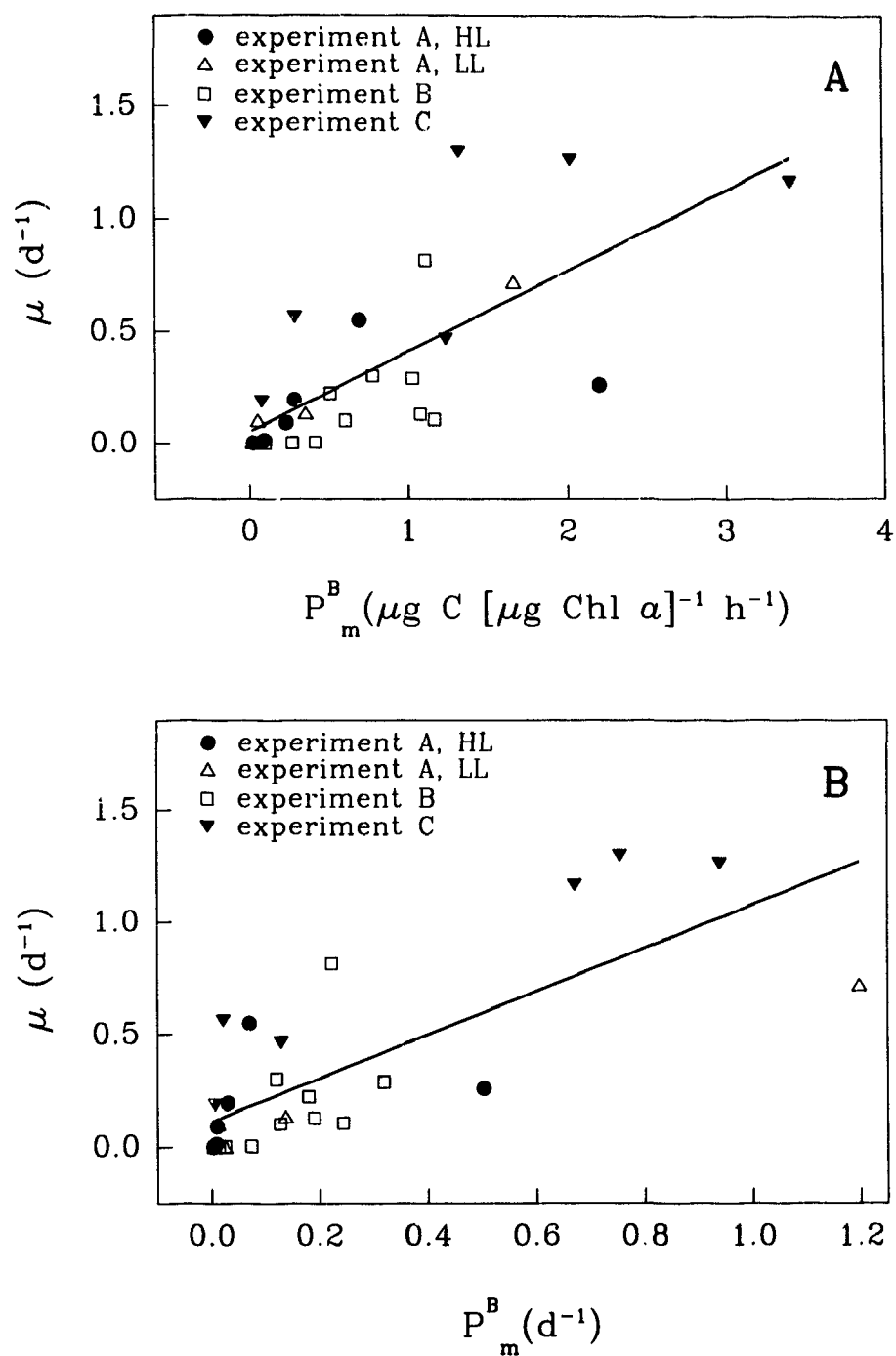


Fig. 3.20. Relationship between growth rate (μ) and photosynthetic rate (P_m^B). (A) P_m^B is normalized to chlorophyll *a*, (B) P_m^B is normalized to carbon. The lines are linear regressions.

tendency was seen in experiment B (Fig. 3.13). This was in agreement with previous studies on other diatoms. For example, *Thalassiosira pseudonana* 3H grown at 18 °C and 200 $\mu\text{mol m}^{-2} \text{s}^{-1}$ (Glover, 1980) had the corresponding ratio of 6.0 for photosynthesis.

The HL cultures in Experiment A yielded higher P_m^B than those grown at PPFD an order of magnitude less. This phenomenon was tested further in Experiment B. Normalized to carbon, P_m^B increased as PPFD increased on day 4; on the other hand, it was an exponential decreasing function of PPFD on day 12 (Fig. 3.13B). The physiological states of cultures under various PPFD levels were different on both day 4 and day 12. On day 4, for example, the cultures at 250 and 410 $\mu\text{mol m}^{-2} \text{s}^{-1}$ were approaching α in the period of maximal growth (Fig. 3.8); but the culture at 53 $\mu\text{mol m}^{-2} \text{s}^{-1}$ was still in the lag phase and those at 810 and 1100 $\mu\text{mol m}^{-2} \text{s}^{-1}$ had already passed the period of maximal growth and were approaching stationary phase. Similarly, as PPFD increased, α^B increase on day 4, but decrease on day 12. Generally, in the exponential phase, P_m^B was larger for the cultures under higher PPFD; in the stationary phase, on the other hand, the cultures grown at low PPFD had higher P_m^B and α^B . This was consistent with the aging effects of high PPFD discussed above (section 3.4.1) and also suggests cells survive better under low PPFD.

The initial slopes α^B were low when normalized to cell concentration; but were comparable to those of *Pseudonitzschia delicatissima* (Erga, 1989) and *Nitzschia americana* (Miller and Kamykowski, 1986b) when normalized to chlorophyll *a*. The chlorophyll *a* normalized P_m^B of *P. pungens* f. *multiseriis* was also comparable with those of other diatoms and dinoflagellates (Pan *et al.*, 1991; Subba Rao, 1988). When

normalized to carbon they were of the same magnitude as other pennate diatoms but were low compared to *Amphiprora paradoxa* (Glover 1980). P_m^B based on particulate carbon were two orders of magnitude lower than *Fragilaria* sp (Taguchi, 1976) and *Gonyaulax polyedra* (Prézelin and Matlick, 1983).

In experiment A, P_m^B ($\mu\text{g C } [\mu\text{g Chl } a]^{-1} \text{ h}^{-1}$) increased between day 1 and day 4 corresponding with a decrease in C:Chl *a* ratio. Following this, P_m^B decreased rapidly while the C:Chl *a* slightly increased and then remained relatively constant in stationary phase (Figs. 3.7A, 3.4A). The variation of C:N ratio in the HL culture of experiment A was similar to that of P_m^B , but not the LL culture. This relationship of P_m^B ($\mu\text{g C } [\mu\text{g Chl } a]^{-1} \text{ h}^{-1}$) with C:Chl *a* or with C:N for *P. pungens* f. *multiseries* also differed from those for *Leptocylindrus danicus* (Verity, 1981) and could be attributed to the effects of physiological stage of the cells. On day 4 in experiment B, P_m^B , C:Chl *a* ratio, N:Chl *a* increased with an increase in PPFD; which was consistent with the observations on *L. danicus* (Verity, 1981).

Growth and photosynthesis were promoted as a result of increase in temperature from 10 to 15 °C (Figs. 3.14, 3.18A,B); and the cells responded consistently to the increasing PPFD (Fig. 3.17). When temperature decreased from 10 to 0 °C, on the other hand, the cells were stressed, growth and photosynthetic rates were drastically reduced, and no clear P-I relationship was established (Fig. 3.17C).

Photosynthetic rates (Fig. 3.18A) of *P. pungens* f. *multiseries* increased with temperature up to 20 °C. The exponential increase of P_m^B from 0.08 at 0 °C to 3.42 at 15 °C was similar to that reported for well acclimated, temperate microphytoplankton (Li

and Dickie, 1987). But the Q_{10} of P_m^B was much higher than some well acclimated coastal phytoplankton (Harrison and Platt, 1980). The Q_{10} of photosynthesis at low temperatures ($<10^\circ\text{C}$) may be as high as 16 (Harris, 1978). Harris and Piccinin (1977) reported a $Q_{10} = 16.0$, between 2.5°C and 5°C , for photosynthesis of natural phytoplankton populations.

The relative photon efficiency, α^B , varied significantly (Fig. 3.18B) in the growth temperature range of 0° to 15°C . α^B increased exponentially with increasing temperature, similar to the sigmoid pattern of *Leptocylindrus danicus* (Verity, 1982), but the magnitude of temperature dependent variations of α^B for *P. pungens* was much higher than that for *L. danicus* (Verity, 1981). For *Nitzschia americana*, at salinity lower than 30‰, Q_{10} for α^B was variable, the maximum was 13.1 between 10° and 20°C at 8‰ (Miller and Kamykowski, 1986a).

3.4.4. Overview

Photosynthesis and growth were coupled (Fig. 3.20B). After integrating all the data from Experiments A, B and C, a regression analysis showed that the specific rates of growth (μ) and photosynthesis (P_m^B) were positively correlated (Equation 3.9), which is consistent with the results discussed in Section 3.4.3 on the maximum photosynthesis and growth.

$$\mu = 0.966 P_m^B + 0.112, \quad (n=28, p < 0.001) \quad (3.9)$$

A positive intercept of μ when P_m^B is 0 further suggests that this diatom might be able to grow heterotrophically as discussed earlier.

The physiological activity of *P. pungens* f. *multiseries* decreased as the culture progressed from exponential to stationary phase, which is consistent with other diatoms and dinoflagellates. Growth and photosynthetic characteristics were comparable to other diatoms and dinoflagellates. Although similarities exist between *P. pungens* f. *multiseries* and other diatoms in these variations, production of domoic acid initiated at the beginning of stationary phase (Subba Rao *et al.*, 1990, Bates *et al.*, 1989) implies that the factors inducing stationary phase might also induce the production of domoic acid.

Photosynthesis and growth decline in low light. However cells adapt to decreasing PPFD levels by increasing chlorophyll content and photon efficiency in the low PPFD. Therefore, decreasing light would have less impact on overall cell metabolism than changes of other environmental factors such as temperature and nutrient concentrations.

Lowering temperature, on the other hand, results in a decrease in enzyme activity and thus reduces the overall metabolism. It reduces the demands from primary metabolism for energy and precursors. As a result of lowering temperature, a distinction between dark reaction and light reaction must be made (Prézelin, 1981). Dark reaction (carbon assimilation) rate is reduced because many enzyme reactions are involved; light reaction (energy assimilation), however, is somewhat independent of temperature.

The chlorophyll content of a cell is an indicator of physiological activity, being positively correlated to growth rate and photosynthesis (Fig. 3.19). Carbon and nitrogen contents of exponential growing cells, however, are somehow inversely related to growth

rate and photosynthesis.

Domoic acid is produced when overall cell metabolic rate declines (Subba Rao *et al.*, 1990; Bates *et al.*, 1991). Thus, stress resulting from lowering temperature or nutrient limitations would have greater impact on enhancing toxin production than from lowering light. However, decreasing light to a very low level would limit the energy supply, hence limit primary metabolism as well as toxin production.

The depletion of silicate in the medium coincided with initiation of stationary phase, suggesting that depletion of silicate limits overall cell metabolism and might also initiate the production of domoic acid.

CHAPTER 4

**EFFECTS OF SILICATE LIMITATION ON
GROWTH AND DOMOIC ACID PRODUCTION
IN BATCH CULTURES**

4.1. Introduction

The availability of dissolved silicon in sea water regulates the growth of diatom populations because silicon is required for diatom frustule construction. Decrease of silicate concentration to low or undetectable levels in marine and freshwater habitats during diatom blooms has been well documented (Paasche, 1973a; Sommer and Stabel, 1983; Egge and Aksnes, 1992 and Harrison *et al.*, 1993). The magnitude of a diatom bloom is often directly related to the availability of silicon in sea water.

In diatom culture, silicate concentrations in the medium can regulate the cell yield (Taguchi *et al.*, 1987). Cessation of cell division, which may be due to cessation of DNA synthesis (Darley and Volcani, 1969; Sullivan and Volcani, 1973), was found to accompany depletion of silicon in the culture media (Lewin, 1955; Lewin and Chen, 1968; Vaultot *et al.*, 1987; Brzezinski *et al.*, 1990). Concomitantly, cells tend to accumulate lipid under silicate limitation (Shifrin and Chisholm, 1981; Enright *et al.*,

1986; Taguchi *et al.*, 1987; Lombardi and Wangersky, 1991).

Uptake of silicate by the diatom *Navicula pelliculosa* is related to aerobic respiration (Lewin, 1955). In Si-deficient cells, addition of silicate stimulated respiration as did organic substrates such as glucose, fructose, lactate, citrate, glycerol which also stimulated cell division.

Pseudonitzschia pungens f. multiseriis produces domoic acid during the stationary phase (Subba Rao *et al.*, 1990; Bates *et al.*, 1991). The onset of the stationary phase was found to coincide with low levels of silicate in the medium (Pan *et al.*, 1991). The linkage between DA production and silicon depletion is not understood. Initiation of the stationary phase in *P. pungens f. multiseriis*, can be caused by self-inhibition factors, such as shading, accumulation of metabolic wastes in the medium or deficiency of essential nutrients such as silicate (Fogg and Thake, 1987).

In this chapter, production of domoic acid by *P. pungens f. multiseriis* grown in media with different silicate concentrations is studied to test the hypothesis that DA production is triggered by silicate limitation.

4.2. Materials and Methods

Pseudonitzschia pungens f. multiseriis (clone NPBIO) was cultured at 15 (± 1) °C under 410 (± 80) $\mu\text{mol m}^{-2} \text{s}^{-1}$ continuous cold-white-fluorescent light. The stock culture was originally grown in medium FE (Section 2.2.2) and transferred to medium F (Section 2.2.1) 15 days before the experiment started. This stock culture was further sub-cultured

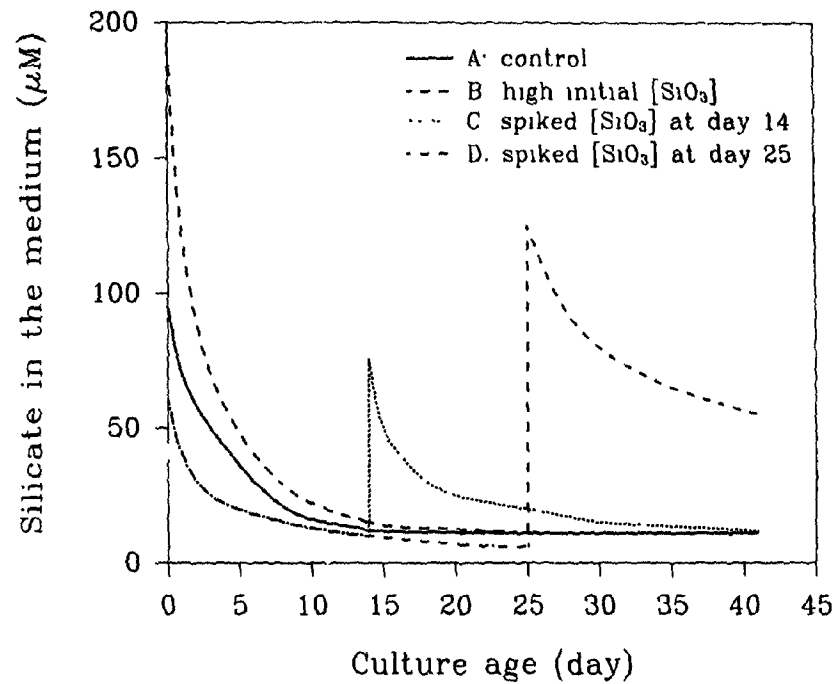


Fig. 4.1. Experimental design. Four treatments: (A) control, the initial DISi was 95 µM; (B) high initial DISi 190 µM; (C) low initial DISi = 61 µM, 65 µM Si spiked on day 14; (D) low initial DISi = 65 µM, 120 µM Si added on day 25. Each treatment was in triplicate. The curves are plotted by eye.

twice in medium F.

There were 4 treatments designated A, B, C and D, each in triplicate. Unmodified medium F was used in control designated as A. Treatment B, C and D had an initial silicate concentrations of 190, 61 and 61 μM respectively. Treatment C was spiked with additional silicate (64 μM) during early stationary phase (day 14), whereas Treatment D was spiked with additional silicate (122 μM) during late stationary phase (day 25) (Fig. 4.1).

Silicate concentrations in the culture media were monitored; as were cell concentrations, particulate chlorophyll *a*, silicon, phosphorus and domoic acid using the procedures described in Chapter 2. Growth of the cultures was described by the Gompertz model (Equation 2.11).

4.3. Results

The cell concentration increased exponentially until the onset of stationary phase 9 to 12 days after inoculation depending on the silicate regime (Table 4.1, Figs. 4.2-4.5). The onset of stationary phase in all silicate regimes coincided with a low level of silicate (<21.2 μM) in the medium. The initial silicate concentration in the medium had no significant effect on the growth rate except for Treatment B which increased growth rate by approximately 20%. Cell yields in the stationary phase were related to the total silicate supplied (Table 4.1). Cellular silicon and DA concentrations (in cells) were also dependent on the silicate concentrations in the media.

Table 4.1. Maximum growth rates, chlorophyll *a*, cell concentration, particulate silicon and DA concentration during growth of *P. pungens* f. *multiseries* under 4 different conditions. Values in parentheses give the ages (day) of the culture when these measurements were made.

Treatment	Silicate supplied (μM)	μ_{max} (d^{-1})	Chl <i>a</i> ($\mu\text{g l}^{-1}$)	Cell Conc. (10^7 cells l^{-1})	PSi (μM)	Domoic acid	
						(pg cell^{-1})	($\mu\text{g l}^{-1}$)
A	95.3	0.20	52.8 (9)	14.0 (35)	154.3 (50)	431.8 (50)	55.3 (50)
B	190.5	0.25	58.2 (12)	18.7 (35)	369.3 (20)	177.2 (41)	36.4 (41)
C	60.9	0.21	30.1 (9)	8.7 (14)	60.5 (9)	296.6 (50)	53.5 (50)
	+64		38.4 (50)	14.1 (30)	191.1 (50)		
D	60.9	0.21	58.8 (12)	9.2 (15)	124.0 (25)	143.8 (35)	19.7 (35)
	+122		66.5 (30)	15.0 (30)	185.0 (50)		

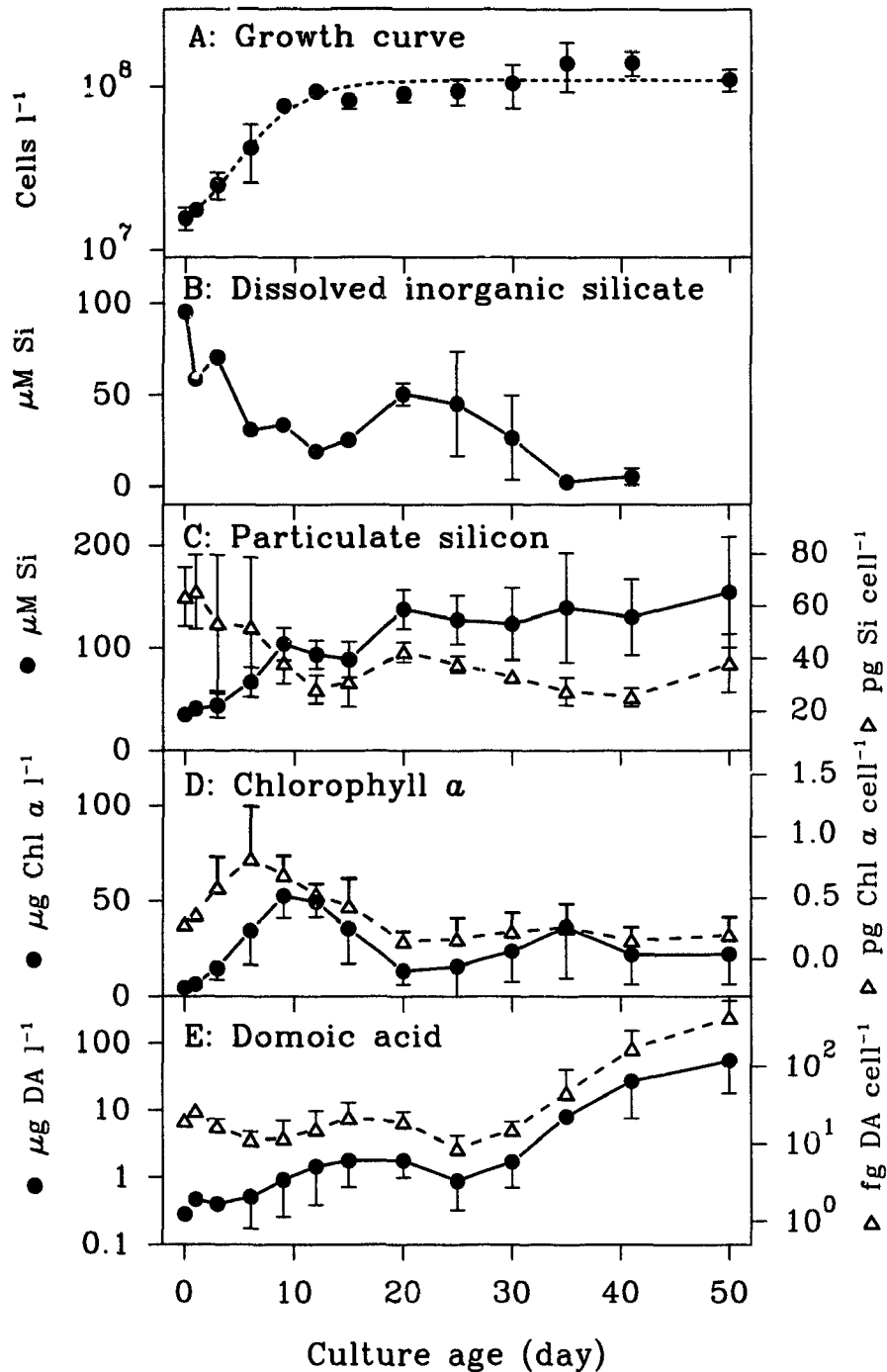


Fig. 4.2. Treatment A. Variations in (A) cell concentrations, (B) dissolved inorganic silicate, (C) particulate silicon, (D) chlorophyll *a* and (E) domoic acid concentrations during the growth cycle. Error bar = 1 standard deviation. Absence of error bar means the standard deviation was smaller than the symbol. The curve in A is fitted by Equation 2.11.

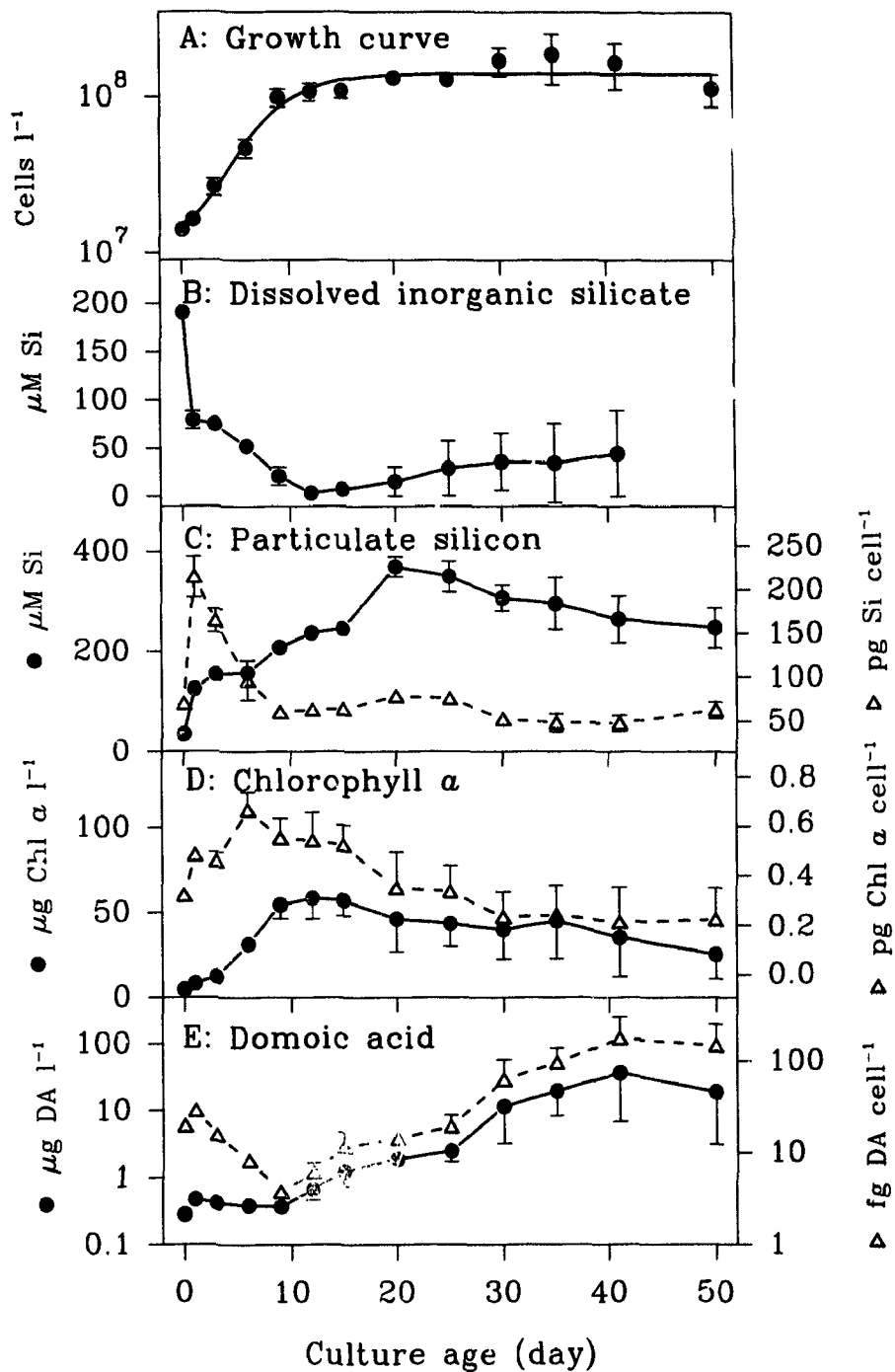


Fig. 4.3. Treatment B. Legend as in Fig. 4.2.

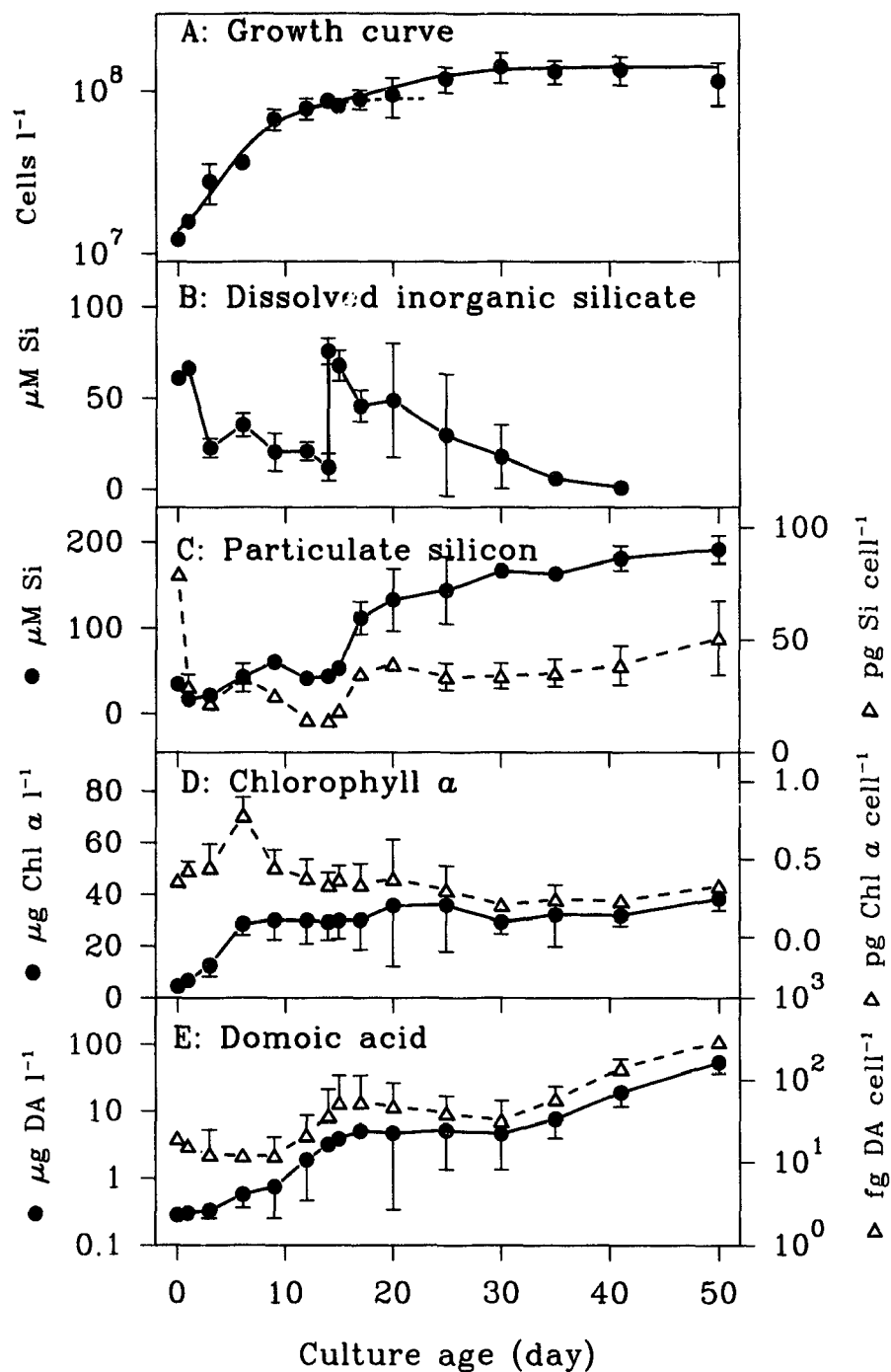


Fig. 4.4. Treatment C. (B) Silicate ($65 \mu\text{M}$) was added on day 14. Other legends as in Fig. 4.2.

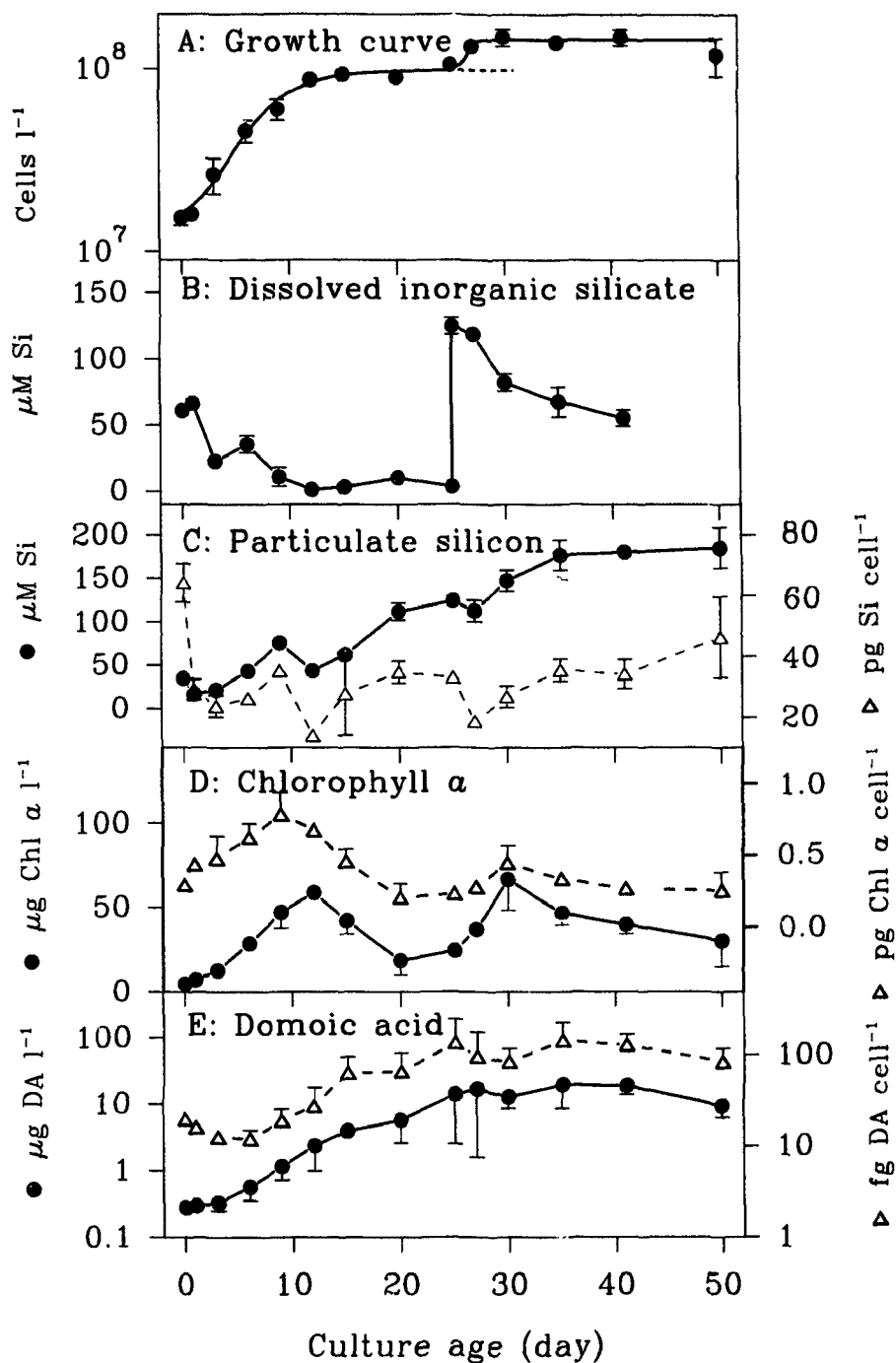


Fig. 4.5. Treatment D. (B) Silicate ($120 \mu M$) was added on day 25. Other legends as in Fig. 4.2.

4.3.1. In medium F (Treatment A)

Cell concentration increased about five-fold from an initial level of 1.5×10^7 cells l^{-1} to 9.3×10^7 cells l^{-1} on day 12 corresponding to the beginning of the stationary phase (Fig. 4.2A). During this period, silicate concentration in the medium (DISi) decreased from 95.3 to 19.2 μM . Following this, DISi increased reaching a peak of 50.4 μM on day 20 (Fig. 4.2B). Cell concentration slightly increased after day 20 following an increase in DISi and reached 14.0×10^7 cells l^{-1} on day 35. During this period, a drastic decrease in DISi from 26.3 μM on day 30 to 2.36 μM on day 35 occurred presumably reflecting the use of silicate for frustule formation.

Total particulate silicon (PSi) increased from day 0 to day 9 paralleling the increase in cell concentration (Fig. 4.2C). Subsequently, particulate silicon did not increase for 6 days probably due to the low silicate concentration in the medium, but after day 15, PSi increased following an increase in DISi (Figs. 4.2B, C). Such a variation in DISi was also found in other treatments.

Cellular silicon ranged from 25.3 to 65.7 $pg Si cell^{-1}$ (Fig. 4.2C). The silicon content of cells increased even in the first day following transfer into fresh medium when the cells were in the lag phase, but decreased subsequently during the exponential phase when growth of the culture was most rapid (Fig. 4.2C). During the stationary phase, cellular silicon levels remained low except for a slight increase on day 20.

The pattern of cellular chlorophyll *a* concentration was opposite to DISi (Fig. 4.2D) attaining a maximum (49.57 $\mu g l^{-1}$) at onset of the stationary phase, after which a decrease was observed. In late stationary phase (day 35), chlorophyll *a* increased slightly

to give a second peak ($36.43 \mu\text{g l}^{-1}$), consistent with an increase in cell concentration. Chlorophyll *a* per cell increased and reached a maximum ($0.82 \text{ pg cell}^{-1}$) at the mid-exponential phase (day 6) decreasing afterwards. Chlorophyll *a* per cell remained low and fairly constant during the stationary phase.

Two stages of DA production can be recognized. The first stage occurred during late exponential phase and corresponded to a decline in growth rate of the culture resulted from a decrease in DISi ($70.9 \mu\text{M}$ on day 3 to $30.1 \mu\text{M}$ on day 6). The DA production ($0.11 - 0.18 \mu\text{g l}^{-1} \text{ d}^{-1}$ or $1.20-2.24 \text{ fg DA cell}^{-1} \text{ d}^{-1}$) was low compared to the high DA production rates ($1.3 - 3.8 \mu\text{g DA l}^{-1} \text{ d}^{-1}$, or $10.39-25.07 \text{ fg DA cell}^{-1} \text{ d}^{-1}$) in the second stage coinciding with the lowest DISi level ($2.4 \mu\text{M}$) on day 35. This low DISi was insufficient to support any further frustule construction, but the toxin levels increased to a maximum of $55.25 \mu\text{g DA l}^{-1}$ (or $431.76 \text{ fg DA cell}^{-1}$). The DA concentration probably increased further as the production rate remained at $3.1 \mu\text{g DA l}^{-1} \text{ d}^{-1}$ (or $25.07 \text{ fg DA cell}^{-1} \text{ d}^{-1}$) during the interval day 41 to 50, but sampling was not extended beyond day 50. The initiation of DA production in both stages did not coincide with the onset of stationary phase on day 12 when DISi was $19.2 (\pm 1.94) \mu\text{M}$, however it did with drastic decreases in DISi on day 6 and day 35. Exhaustion of DISi enhanced DA production markedly during the second stage.

4.3.2. In high-Si medium (Treatment B)

High initial DISi increased maximum cell concentration (Table 4.1). Following seeding, DISi drastically decreased from $190.5 \mu\text{M}$ to $67 \mu\text{M}$ (Fig. 4.3B), while total

particulate silicon increased from 34.7 to 137.7 μM (Fig. 4.3C) accompanied by a small increase in cell number during the first day. Although the culture reached stationary phase on day 9, total particulate silicon increased continuously and attained a peak (369.3 μM) on day 20. The magnitude of the peak was more than twice the control. Cellular silicon reached a peak of 214.4 pg Si cell^{-1} at day 1 and subsequently decreased to a low (60 pg Si cell^{-1}) as the culture approached stationary phase on day 9. The DISi and cellular silicon remained low during the stationary phase.

Chlorophyll *a* concentration attained a maximum of 58.3 $\mu\text{g l}^{-1}$ on day 12 and subsequently decreased to 25.28 $\mu\text{g l}^{-1}$ on day 50. A maximum of 0.66 pg cell^{-1} was observed on day 6 (mid-exponential phase) and then decreased to 0.22 pg cell^{-1} on day 50. Maximum chlorophyll *a* concentration and chlorophyll *a* per cell were comparable to control (Table 4.1).

That DA production proceeded in two stages was also evident in this treatment. Although DISi was lowest (3.46 μM) on day 12, the PSi content per cell remained similar to day 9. The initiation of the first stage of DA production coincided with the onset of stationary phase on day 9 and a low level of DISi, but the production rate was very low (0.1 - 0.19 $\mu\text{g DA l}^{-1} \text{d}^{-1}$, 0.97-1.74 $\text{fg DA cell}^{-1} \text{d}^{-1}$). The DA production remained low until days 25-30 (Fig. 4.3E) when cellular silicon drastically decreased from 75.9 pg cell^{-1} on day 25 to 51.7 pg cell^{-1} on day 30. The concentration reached a maximum of 36.4 $\mu\text{g DA l}^{-1}$ (or 177.0 fg DA cell^{-1}) on day 41 and then decreased to 19.13 $\mu\text{g DA l}^{-1}$ (or 148.2 fg DA cell^{-1}) coinciding with an increase in cellular silicon from 47.5 pg Si cell^{-1} on day 41 to 62.9 pg Si cell^{-1} on day 50. The maximum DA concentration was about 2/3 of the

control.

4.3.3. *In low-Si medium (Treatments C and D)*

Cultures attained lower cell concentration and lower P*Si* in the medium with low initial silicate concentration (Table 4.1). Cellular silicon was 14-35 pg Si cell⁻¹, which is only half that of control. However, chlorophyll *a* concentration was comparable to control. Two stages in DA production could not be distinguished clearly. Initial DA production (0.06 - 0.19 µg DA l⁻¹ d⁻¹, or 1.16 - 2.19 fg DA cell⁻¹ d⁻¹) was 3 days earlier than in Treatment A and followed a drastic decrease of D*Si* (from 66.6 to 22.7 µM). The second stage of DA production immediately succeeded the first, reflecting the onset of the stationary phase as a result of further decrease in D*Si*. The production rates in the second stage were 0.36 to 1.64 µg DA l⁻¹ d⁻¹ (or 5.14-16.86 fg DA cell⁻¹ d⁻¹).

4.3.4. *Silicate perturbation*

Spiking the cultures with silicate (64 µM, up to the level of medium F) on day 14 (Treatment C, Fig. 4.4), cell concentration and particulate silicon increased to levels corresponding to the control. Maximum chlorophyll *a* concentration was less than that in the control at the same period. Chlorophyll *a* concentration was less variable than Treatments A and B after the cultures reached the first stationary phase. Importantly, immediately after more silicate was spiked on day 14, D*Si*, cellular silicon increased, but the second stage of DA production was interrupted, and DA concentration remained unchanged until a further silicate limitation occurred on day 35. Following that, cells

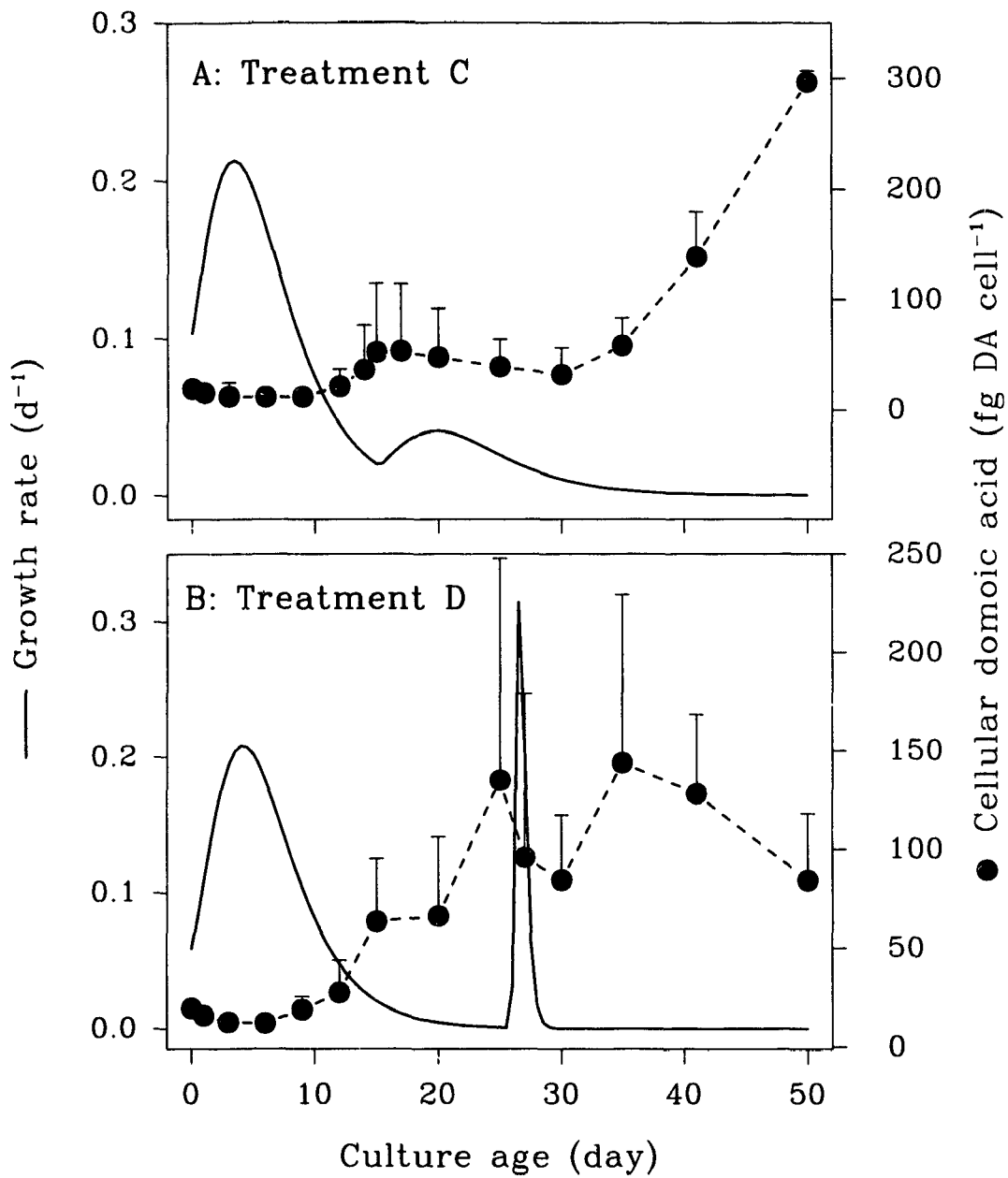


Fig. 4.6. Relationship between cellular domoic acid and growth rate during the DISi perturbation experiments.

continued to produce DA at rates of 1.9 - 3.8 $\mu\text{g DA l}^{-1} \text{d}^{-1}$ (or 14.35 - 30.20 $\text{fg DA cell}^{-1} \text{d}^{-1}$) until 53.5 $\mu\text{g DA l}^{-1}$ (or 296.6 fg DA cell^{-1}) was reached at the end of the experiment. These values were similar to those obtained from Treatment A.

In Treatment D, after addition of silicate (122 μM) on day 25, the cell concentration increased from 10.5 to 15.0 $\times 10^7 \text{ cells l}^{-1}$, chlorophyll *a* from 24.24 to 66.52 $\mu\text{g l}^{-1}$, and particulate silicon from 124 to 184 μM , but DA production ceased (Fig. 4.5). The DA production was enhanced when the cells entered the stationary phase, but stopped soon afterwards because silicate was not limiting.

In both Treatments C and D, cells started accumulating DA only when the growth rate declined (Fig. 4.6) as a result of partial or total depletion of DISi (Figs. 4.4B, 4.5B). When DISi was elevated through perturbation in the early and late stationary phases it caused cultures to resume growth, DA production stopped and did not resume until the growth rate decreased as a result of silicate stress.

4.4. Discussion

4.4.1. Growth

Cell yields of *P. pungens f. multiseriis* were proportional to supply of silicate, but growth rates were not. Cultures reached the stationary phase when low levels of silicate were present in the medium. Addition of silicate to cultures, existing in stationary phase caused by silicate limitation, facilitated further growth. These results were consistent with the work of Taguchi *et al.* (1987) on *Chaetoceros gracilis*, *Hantzschia* sp. and *Cyclotella*

sp. Cells continue to accumulate silicon even after cultures entered stationary phase, which supported further growth of the population following onset of the stationary phase (Figs. 4.2, 4.3), consistent with the observation made on *Navicula pelliculosa* (Lewin, 1957).

Chlorophyll *a* concentration is an indication of the physiological activity of an algal culture (Chapter 3). Chlorophyll *a* concentration was variable during the stationary phase in Treatments A, B, and D but not in Treatment C. This was related to the availability of silicate in the culture media. A low level of silicate in the culture media resulted in a decrease in chlorophyll *a* concentration. For example in Treatment A (Fig. 4.2), chlorophyll *a* concentration attained a peak on day 9 after DISi decreased and then declined continuously until day 20 when silicate increased probably due to the dissolution from dead cell frustules. Chlorophyll *a* increased again reaching a second peak on day 35 when DISi was exhausted. Increase of chlorophyll *a* corresponded to the increased of cell concentration (Fig. 4.2). This was consistent with the data from Treatment D (Fig. 4.5). Chlorophyll *a* concentration increased and attained a peak ($58.8 \mu\text{g l}^{-1}$) on day 12 due to the exhaustion of DISi at onset of the stationary phase and then decreased to $18.4 \mu\text{g l}^{-1}$ on day 20. No significant increase of chlorophyll *a* concentration was noticed until day 27, two days after the perturbation of DISi. In Treatments B and C, however, chlorophyll *a* was less variable in the stationary phase because silicate stress was not severe due to the high reserve of cellular silicon ($62.8 \text{ pg Si cell}^{-1}$) which was probably able to support further growth of the population (Treatment B) or the stress was rapidly released by addition of extra silicate (Treatment C) immediately after the culture

population entered the stationary phase.

4.4.2. Cellular silicon

Determination of DISi and cellular silicon demonstrated luxury uptake of silicate by *P. pungens f. multiseries*. In Treatment B (Fig. 4.3), for example, when initial silicate concentration was high at 195 μM , 59% of silicate was taken up by the diatom population in the first day although there was very little increase in cell concentration (16%). Cellular silicon increased from 69.7 to 214.4 pg Si cell^{-1} . In the control (Fig. 4.2), the initial silicate concentration was at 95.3 μM . Silicate concentration decreased by 38%, but cellular silicon increased very little (from 63.7 to 65.7 pg Si cell^{-1}). There was also an elevation in DISi after cells entered stationary phase (Fig. 4.2B) probably caused by the dissolution of silicon from dead cells. Lewin (1955) demonstrated that substantial amounts of silicon were dissolved after diatom cells died. In Treatments C and D when the initial DISi was lower (Figs. 4.4, 4.5), however, there was about a 10% increase in DISi probably due to the dissolution of silicon from dead cells present in the seeding population; following culture growth, cellular silicon dropped from 79.5 to 29.6 pg Si cell^{-1} .

The general pattern of cellular silicon was that cells in the lag or early exponential phase had higher values than cells in the later phases. Higher cellular silicon in the stationary phase was associated with higher DISi. These results were in agreement with Lewin (1957), who found that the degree of silicification of *Navicula pelliculosa* cells in culture initially fell with increasing cell number. Stationary phase cell silicon was

dependent on the initial silicate concentrations of the growth medium.

The silicon content in stationary phase cells of Treatment B (47.7 - 78.2 pg Si cell⁻¹) was comparable to the maximum levels in Treatments A, C and D (64.2 - 79.5 pg Si cell⁻¹). At these similar cell silicon levels, cells from Treatment B stopped dividing while cells from the other treatments were ready to divide. Perturbation of DISi during stationary phase did not raise cellular silicon to a level comparable to that found in the cells of Treatment B; different magnitudes of perturbation in Treatments C and D did not result in different levels of cell silicon. This suggested that the cellular silicon level was determined by the initial DISi in the fresh medium. Immediately after seeding a population into fresh medium, the cells probably adjusted their requirement for silicate according to the available resources. Perturbation had less effect on the intracellular silicon level but promoted growth of the population.

Cellular silicon varied from 14 to 214.4 pg Si cell⁻¹, which is abnormal compared to other diatoms (Table 4.2). The ratios of maximum to minimum cellular silicon (Q_{\max}/Q_{\min}) were less than 5 for most other diatoms except for *Navicula pelliculosa* and *Coscinodiscus granii*, but 15 for *P. pungens* f. *multiseries*. This suggested that *P. pungens* f. *multiseries* is better able to respond to a wide range of silicate levels than other diatoms and probably helps to explain the ubiquitous distribution of this diatom.

4.4.3. Role of silicon in cell metabolism

Diatoms require silicon not only for cell frustule formation, but also for other metabolic processes, such as DNA replication. Addition of silicate to silicon-starved

Table 4.2. Variation in the cellular silicon content in selected diatom species.

Taxa	Cell size (μm)		Q_{max}	Q_{min}	$Q_{\text{max}}/Q_{\text{min}}$	References
	width	length	(pg Si cell ⁻¹)			
Pennate	width	length				
<i>Pseudonitzschia pungens</i> <i>f. multiseries</i>	5-10	50-70	214	14	15.3	Present study
<i>Nitzschia palea</i>			62	14	4.4	Jørgensen, 1955
<i>Navicula pelliculosa</i>			3.3	0.36	9.2	Lewin, 1957
Centric	diameter	length				
<i>Skeletonema costatum</i>	4-6		7	3.8	1.8	Paasche, 1973b
	4-5	8-13	2.16	0.84	2.6	Harrison <i>et al.</i> , 1976, 1977
<i>Thalassiosira pseudonana</i>	3-6		1.81	0.6	3.0	Paasche, 1973a, b
<i>Thalassiosira decipiens</i>	17-28		330	150	2.2	Paasche, 1973b
<i>Thalassiosira nana</i>			430	89	4.8	Jørgensen, 1955
<i>Thalassiosira gravida</i>	7-9	14-24	56	30.24	1.9	Harrison <i>et al.</i> , 1977
<i>Licomphora</i> sp.	14-40		210	80	2.6	Paasche, 1973b
<i>Ditylum brightwellii</i>	13-52		900	200	4.5	Paasche, 1973b
<i>Coscinodiscus granii</i>	95-190		6412	728	8.8	Taylor, 1985
<i>Chaetoceros debilis</i>	16-20	6-9	8.46	3.11	2.7	Harrison <i>et al.</i> , 1977
<i>Chaetoceros affinis</i>	7-27		42	33	1.3	Paasche, 1980
<i>Cerataulina pelagica</i>	36-56	70-120	97	88	1.1	Paasche, 1980
<i>Rhizosolenia fragilissima</i>	12-20	42-67	51	28	1.8	Paasche, 1980

Cylindrotheca fusiformis cells caused initiation of DNA synthesis and an increased synthesis of nuclear DNA polymerases (Okita and Volcani, 1978). Therefore, silicon availability affects the cell-cycle progression in diatoms. Brzezinski *et al.* (1990) showed that silicon deprivation halted progression of the cell cycle by arresting the cells in G1, G2 and M phases in 6 of the 7 diatom species examined. Silicon starvation of diatoms leads to an accumulation of cells at the G1/S boundary and in G2 and/or M phase (Vaulot *et al.*, 1987; Brzezinski *et al.*, 1990).

Production of saxitoxins by *Alexandrium tamarense* seems to be related to the cell cycle (Anderson, 1990) and toxin synthesis occurred during the first half of the S phase but then stopped for more than 10 hours as cells went through mitosis and divided. Anderson (1990) concluded that toxin synthesis was not continuous throughout the cell cycle, but temporally linked to the pulse of DNA synthesis. Silicate availability affects the cell cycle as well as DNA synthesis. This suggests that silicate stress restrains the progression of the cell cycle and DNA synthesis, hence indirectly regulates production of toxin even though silicate plays no role in the structure and synthetic pathway of domoic acid. The relationship between domoic acid production and the cell cycle may parallel the observed relationship between saxitoxin production by *Alexandrium* sp and its cell cycle. This merits further investigation.

Lipid accumulation induced by silicon deficiency has been well documented in diatoms (Taguchi *et al.*, 1987). In *Cyclotella cryptica*, for example, this accumulation was due in part to a change in the partitioning of newly photoassimilated carbon (Roessler, 1988b); a higher proportion of the carbon was partitioned to lipid production.

This change was due to an increase in the activity of acetyl-CoA carboxylase (Roessler, 1988a), an enzyme involved in early steps of lipid synthesis. This enzyme is also believed to be associated with the early steps in the synthesis of isoprenoid (Luckner, 1984), which is believed to be an immediate precursor of DA (Fig. 1.4). Therefore, the association of silicate limitation with DA production suggests a link between DA production and lipid synthesis in *P. pungens* f. *multiseries*.

4.4.4. Production of domoic acid in relation to silicate limitation

There was a negative correlation between the final yield of domoic acid and the supply of silicate in the culture medium (Fig. 4.7). In Treatment A, the initial level of silicate in the medium was 95.28 μM , the maximum DA level attained was 55.25 $\mu\text{g DA l}^{-1}$ (or 431.76 fg DA cell⁻¹). In Treatment B with about 2 times the initial silicate concentration in the medium (196.42 μM), maximum DA level was 36.4 $\mu\text{g DA l}^{-1}$ (or 177.23 fg DA cell⁻¹). When the total supply of silicate (initial level plus spiked) was 124.55 μM in Treatment C, the maximum DA concentration attained was 53.5 $\mu\text{g DA l}^{-1}$ (or 296.55 fg DA cell⁻¹).

A two-stage DA production phenomenon was obvious in the control (Treatment A) and Treatment B but not clear in Treatments C and D. In Treatments A and B the exhaustion of DISi did not coincide with the onset of stationary phase. After initiation of the first production stage which occurred in the later exponential phase due to a decline of growth rate, the cells probably adjusted themselves to a new low silicate habitat with a new uptake kinetic strategy for further growth using the residual silicate. When silicate

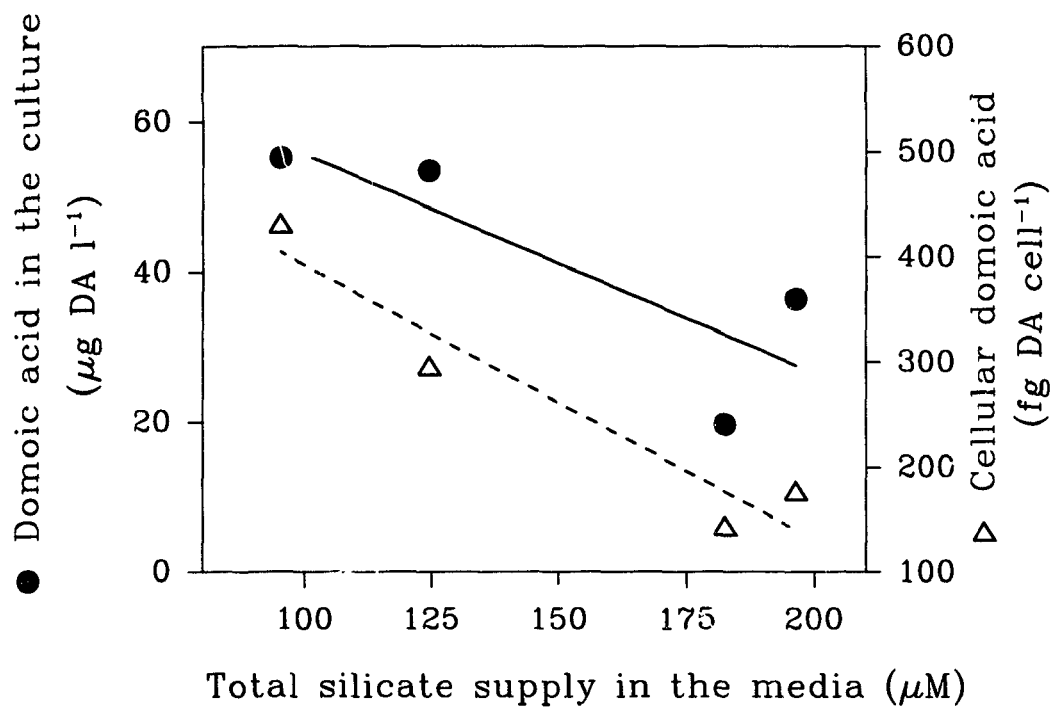


Fig. 4.7. Relationship of maximum DA concentrations in the culture and DA per cell with silicate supply. The lines are linear regressions.

was exhausted in the medium, cells were not able to adjust to permit any further growth. The cells may have been arrested at certain phase(s) in the cell cycle, which is most likely the cue for DA synthesis, and its production is enhanced. In Treatments C and D, on the other hand, DA production before silicate perturbations can not be clearly divided into two phases. Cells were not able to manage any further growth after they entered the stationary phase due to depletion of silicate. Therefore the second production stage immediately followed initiation of the first stage. This gave an image of a continuous linear increase of DA production rate. Production of DA was vigorous when cells were not able to grow further due to depletion of DISi and intracellular inorganic silicate pool.

Another noteworthy feature in the experiments was the temporal shift in the initiation of the first stage of DA production. The production started earlier as a result of decrease of initial silicate concentration in the medium. In Treatment B when the initial silicate concentration was the highest (190 μM), the first stage of DA production started on day 9 at the onset of stationary phase when growth of the culture almost stopped. In the control (Treatment A) when the initial silicate concentration was 95 μM , the first stage of DA production was initiated on day 6 at late exponential phase when growth of the culture was declining. In the Treatments C and D, the first stage of DA production was initiated on day 3 at the mid exponential phase when growth of the culture was at the peak or just started to decline (Fig. 4.6). This suggests that DA production is not necessarily associated with cessation of cell division, but triggered by physiological stress such as silicate limitation.

Subba Rao *et al.* (1990) and Bates *et al.* (1991) concluded that DA production

occurs only after cell division stopped. More silicate may have been contributed by the soil extract which made the initial silicate concentration higher in the FE medium used by Subba Rao *et al.* (1990) than in medium F or to the level comparable to Treatment B in the present study, i.e. initiation of the first DA production stage coincided with onset of the stationary phase. On the other hand, the initial silicate in F/2 medium used by Bates *et al.* (1991) was comparable to that in Treatments C and D in the present study, i.e. first DA production stage preceded onset of stationary phase. The DA production during the first stage in their cultures might have been too low to be noticed.

Interestingly, addition of silicate to a silicate-exhausted culture facilitated further growth and simultaneously interrupted DA production (Figs. 4.4, 4.5). The production resumed when growth of the population declined due to further silicate stress (Fig. 4.6). Production of DA, both before and after silicate perturbation, was initiated at decline of growth rate. This suggests there could be an inverse correlation between DA production and growth rate, even when the culture is maintained at a constant growth rate in a continuous culture. This possibility is investigated in Chapter 5.

CHAPTER 5

SILICATE LIMITATION AND DOMOIC ACID

PRODUCTION IN

CHEMOSTAT CONTINUOUS CULTURES

5.1. Introduction

In batch cultures, domoic acid (DA) production generally occurs in the stationary phase when cells stopped dividing. This is probably because cells are arrested at a certain phase of the cell cycle, such as G1 or S phase (Chapter 4), in which DA is produced. During the growth cycle of a batch culture, the physiological stage of the population is always changing. The onset of stationary phase is due to a variety of factors that restrict the further growth of a population.

Silicon plays an important role in diatom cell metabolism. In *Navicula pelliculosa*, a freshwater diatom, synthesis of RNA, protein, carbohydrate and chlorophyll ceases 5 to 7 hours after deprivation of silicate in the medium, while syntheses of DNA and lipid continue (Coombs *et al.*, 1967). In *Pseudonitzschia pungens f. multiseries*, DA was produced when cells were stressed by silicate limitation in batch culture and the production was enhanced when cell division stopped in the stationary phase (Chapter 4).

However, the first stage of DA production coincided with the later exponential phase when growth was proceeding although more slowly (Chapter 4). This implies that the toxin production is not necessarily associated with cessation of cell division, and the diatom is able to produce DA when cells are dividing but under silicate stress.

In this chapter, I raised *P. pungens* f. *multiseries* cultures in chemostats under silicate limitation and investigate the kinetics of DA production in dividing cells and its relationships with cell chemical composition and nutrient uptake kinetics of this diatom. The objective is to understand the relationships between DA production and silicate limitation in a dividing population.

5.2. Materials and Methods

5.2.1. Chemostat system

The continuous culture system is shown in Fig. 2.1 and is described in Section 2.10. Six chemostat chambers were set up simultaneously. One of them, a blank glass chamber under the same conditions, served as control to monitor the silicate level. The cultures and the control were exposed to a bank of $290 (\pm 50) \mu\text{mol m}^{-2} \text{s}^{-1}$ continuous cool white fluorescent light and the temperature was maintained at $15 (\pm 0.2) ^\circ\text{C}$.

5.2.2. Preparation of culture medium and stock culture

Mid-Atlantic oceanic sea water was collected during BIO JGOFS cruise (April, 1991) and settled for two years before the experiment. Deionized water (super Q) was

added to the seawater to lower the salinity to 27‰, comparable to that on the coast of Prince Edward Island. This sea water was further enriched to make medium H (Table 2.2) with a silicate concentration of 56.2 (± 3.4) μM . It was then dispensed (600 ml each) into 1-litre polycarbonate culture flasks and autoclaved for 15 minutes at 15 Psi.

For the medium in the reservoirs, 10 L of the same mid-Atlantic sea water was diluted and enriched as above in a 20-litre carboy and autoclaved for 20 minutes at 15 Psi. Soon after autoclaving, while it was still very hot, 2 carboys of the medium were aseptically pooled into a 20-litre reservoir. Glass tubes were positioned with intakes 5 cm above the bottom. After 24 to 36 hours at 10 °C, when the medium was cooled and became clear (precipitated), the reservoirs were connected to the peristaltic pumps that supplied this medium to each culture chamber at a different flow rate.

In the chemostat experiment I (Experiment I hereafter, Fig. 5.1), the reservoir medium was prepared and autoclaved in 20-litre glass carboys. In addition to the 56.2 (± 3.4) μM silicate (Na_2SiO_3) added, more than 100 μM silicon was released from the glass carboy into the medium during autoclaving and brought up the final concentration to 165.4 (± 9.0) μM . Silicate concentration was monitored in reservoirs and in the control; further release of silicon from the glassware during the experiments was negligible (Appendix C1).

After 10 steady state experiments, the reservoir medium was prepared again and the experiments progressed into chemostat experiment II (Experiment II hereafter, Fig. 5.1). Instead of the glass carboys, 20 litre polycarbonate carboys were used for autoclaving and storage of reservoir medium. No significant change in silicate

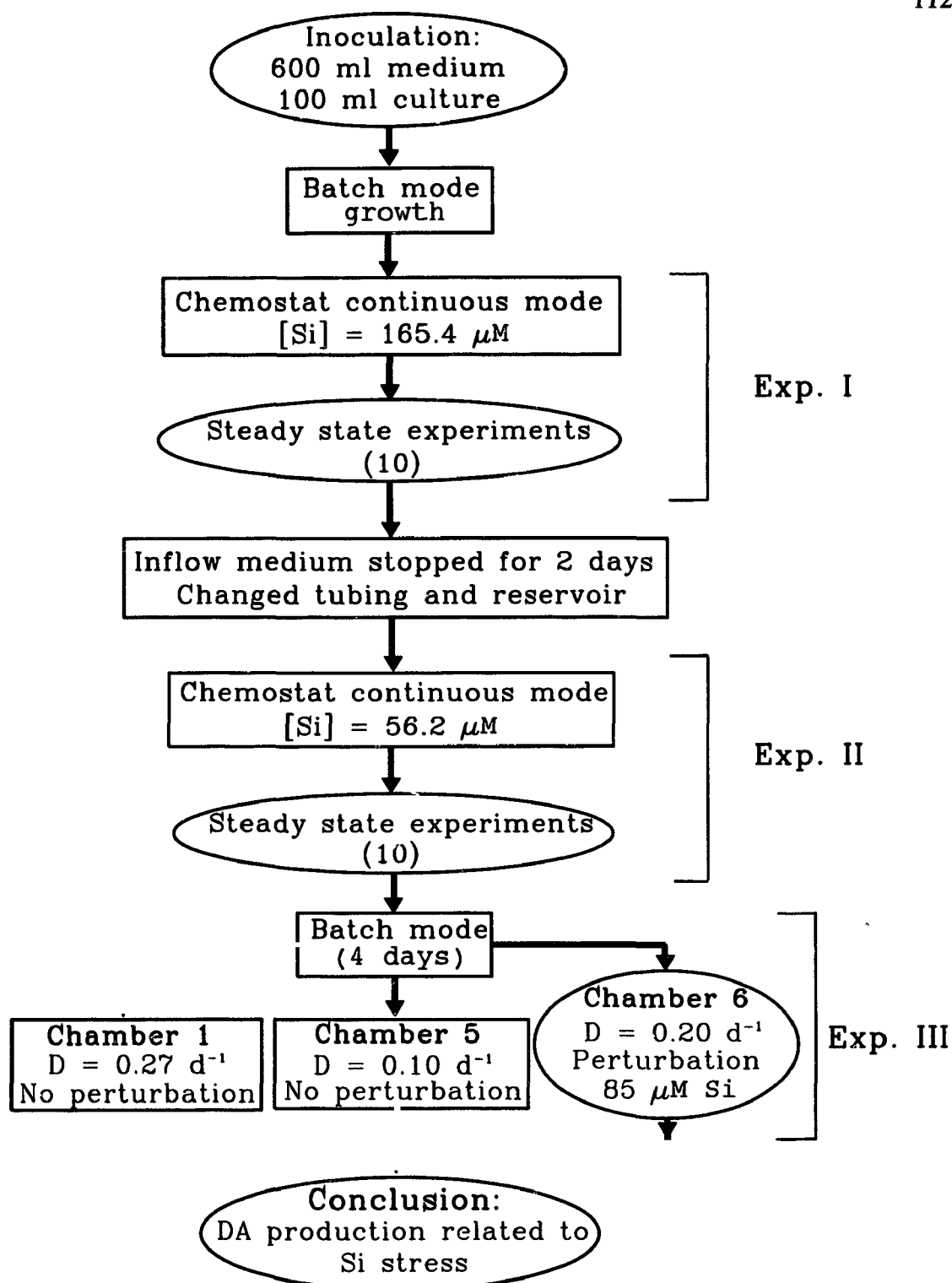


Fig. 5.1. Schematic procedures for experiments. See text for details.

concentration occurred ($56.2 \pm 3.4 \mu\text{M}$) either during autoclaving or during the experiment in the control chemostat or in the reservoirs.

Stock culture of *Pseudonitzschia pungens* f. *multiseries* (KP-59 strain) was grown in the silicate-reduced H medium prepared with Mid-Atlantic seawater for 10 days before being inoculated into the chemostat culture chambers. This stock culture was subcultured twice during the 10 day period and maintained in batch culture at 15 °C under $320 \mu\text{mol m}^{-2} \text{s}^{-1}$ continuous cool white fluorescent light.

5.2.3. Procedures for experiments

The experiments were divided into 3 parts (Fig. 5.1). The first two parts (Experiments I and II) were identical chemostat cultures except that different kinds of carboys were used for autoclaving and storage of reservoir medium. As stated earlier, the use of different carboys in the medium preparation resulted in marked differences in silicate concentration. The last part (Experiment III) was a batch mode extension after steady state experiments when addition of reservoir medium was stopped.

At the beginning of the experiments, 600 ml of medium were aseptically added to each chemostat chamber and left for 4 hours before inoculating with 100 ml of the stock culture. The culture was agitated and aerated immediately. Inflow of reservoir medium ($[\text{Si}] = 165.4 (\pm 9.0) \mu\text{M}$) was started when growth of the cultures was significant (checked visually) 2 days later, and continued until the end of the experiments. The culture population was monitored daily by measuring *in vivo* chlorophyll *a* fluorescence. After the measurement of fluorescence, a 10-ml sample was preserved (section 2.3) in a

20 ml plastic vial and served as backup for the measurement of population size. Steady state was defined as described in Section 2.10. A sample of 300 ml was collected in the steady state. Sub-samples were collected on the filters and analyzed as described in Chapter 2 for particulate silicon and phosphorus, carbon and nitrogen, ATP, domoic acid (DA) and chlorophyll *a* within 1 hour. Filtrate (1.0 μm) was collected for determinations of dissolved silicate, phosphate and DA in the medium as detailed in Chapter 2. After the samples were taken, the inflow rate was changed and the next steady state was usually attained in ≥ 8 days. A total of 10 such steady state experiments were conducted in 5 of the 6 chemostats in Experiment I.

At the end of Experiment I, the peristaltic pumps were stopped immediately after the last steady-state experiment. All the tubing for supplying reservoir medium were changed aseptically and the reservoir medium was freshly prepared in the plastic carboys.

Experiment II started 2 days later. Addition of medium ($[\text{Si}] = 56.2 (\pm 3.4) \mu\text{M}$) from the reservoirs was started and the inflow rates were randomly set disregarding the pre-history of the dilution rate. A total of 10 steady state experiments were conducted and sub-samples were collected as in Experiment I except for the additional samples for bacteria quantification as described below.

In Experiment III, the peristaltic pumps were stopped after the last steady state of Experiment II, changing the cultures into batch mode. Samples were taken and analyzed for the same variables as those in Experiment II from Chambers 1, 5, and 6 (Fig. 5.1) the next day and 4 days later. The previous dilution rates for these three chambers were 0.27, 0.10 and 0.20 d^{-1} respectively. Of the three chambers, silicate concentration in Chamber

6 was raised by 85 μM at the beginning of the batch mode.

During Experiments II and III, samples were collected for quantification of bacteria. An 18-ml sample was preserved in a 20-ml clean glass vial with 0.36 ml filtered (0.2 μm) formalin and refrigerated for less than two weeks. Triplicate subsamples of 5 ml were taken from each vial, 0.5 ml DAPI (3.3% diamidino-2-phenylindole dihydrochloride) stain was added. The samples were kept in the dark at room temperature for 12 minutes before filtering through 0.2 μm nuclepore filters. The filters were collected and mounted in immersion oil on microscopic slides and refrigerated in the dark within two hours. The sample was then enumerated under an epi-fluorescence microscope within two months. The excitation and emission wavelengths were <380 and 520 nm respectively.

5.3. Results

5.3.1. *Experiment I: continuous culture*

Biomass in the steady state was comparable ($72\text{-}105 \times 10^6$ cells l^{-1}) at different specific growth rates except for the one at the highest rate (0.669 d^{-1}) when cell concentration was significantly reduced (48×10^6 cells l^{-1}). Growth rates in the 10 steady states ranged from 0.09 to 0.67 d^{-1} . There was a negative correlation between growth rate and biomass ($n=10$, $p<0.05$) (Table 5.1a). As growth rate increased, (1) carbon assimilation (P^B_m) increased; (2) cellular phosphorus and ATP decreased, but cellular silicon and chlorophyll *a* increased; (3) C:Chl *a*, N:Chl *a*, P:Chl *a* and N:Si decreased,

while C:P, N:P and Si:P ratios increased. C:Si ratios were less variable and slightly decreased as growth rate increased. C:N ratios were relatively constant with a mean of 9.85 (Table 5.2a).

Domoic acid concentrations in the cultures ranged from 1.6 to 135.9 $\mu\text{g l}^{-1}$ (0.02 to 1.00 pg cell^{-1}), and were highest at low growth rates but exponentially decreased when growth rate increased (Figs. 5.2A, B). Similar patterns were found for DA production (Fig. 5.2C). The relationship between DA (production and concentrations) and growth rates can be described by:

$$DA = DA_m \exp(-a\mu) \quad (5.1)$$

Where DA is domoic acid (production or concentration) at growth rate of μ . DA_m is the maximum DA at $\mu=0$. a is the negative initial slope of the exponential curve.

Dissolved inorganic silicate concentration (DISi) in the culture medium of steady states ranged from 2.4 to 106.2 μM in this experiment (Table 5.1a), and positively correlated with growth rate (Fig. 5.2D). Concentration of DA was negatively correlated with silicate and phosphate in the culture medium ($n=10$ $p<0.02$) but positively correlated ($p<0.02$) with ATP concentration (Fig. 5.3, Table 5.1a). Similar to growth rate, carbon assimilation negatively correlated with DA concentration and its production ($n=10$, $p<0.05$). In addition, DA production also positively correlated with the concentrations of particulate carbon and nitrogen (Table 5.1a).

Table 5.1a. Experiment I: measured variables, their statistics and their correlation with growth rate, DA production and concentrations

Parameters	Mean	Min	Max	Correlation coefficient R (n=10)		
				Growth rate	DA prod	Total DA
Growth rate (d ⁻¹)	0.322	0.092	0.669	1.00	-0.61	-0.74
10 ⁶ Cell l ⁻¹	80.82	48.28	104.67	-0.64	0.35	0.45
DA production (µg l ⁻¹ d ⁻¹)	7.62	0.55	16.79	-0.61	1.00	0.79
Total DA (µg l ⁻¹)	42.70	1.60	135.90	-0.74	0.79	1.00
(pg DA cell ⁻¹)	0.38	0.02	1.00	-0.75	0.87	0.97
DA in filtrate (µg l ⁻¹)	9.92	0.00	36.00	-0.65	0.64	0.96
P _m ^B (µg C [µg Chl a] ⁻¹ h ⁻¹)	1.58	0.61	2.98	1.00	-0.59	-0.74
Chl a (µg l ⁻¹)	60.55	47.00	76.04	-0.28	0.32	-0.12
(pg Chl a cell ⁻¹)	0.77	0.51	1.01	0.45	-0.06	-0.51
PC (µM)	632.33	418.17	811.08	-0.71	0.63	0.39
(p ₂ C cell ⁻¹)	94.99	76.49	124.68	-0.06	0.38	-0.03
PN (µM)	75.27	45.28	98.61	-0.77	0.65	0.49
(pg N cell ⁻¹)	11.23	9.42	14.24	-0.28	0.56	0.15
PSi (µM)	124.30	84.58	161.23	-0.51	0.49	0.23
(pg Si cell ⁻¹)	43.78	34.18	53.93	0.32	0.07	-0.31
PISi (µM)	2.02	0.85	3.78	-0.74	0.36	0.31
DISi (µM)	48.10	2.40	106.20	0.97	-0.61	-0.74
DSi (µM)	48.20	4.00	113.20	0.97	-0.62	-0.74
DIP (µM)	23.14	20.31	28.06	0.54	-0.67	-0.68
PP (µM)	4.33	2.07	6.85	-0.82	0.39	0.39
(pg P cell ⁻¹)	1.65	1.22	2.40	-0.64	0.31	0.20
ATP (nM)	9.17	1.05	21.86	-0.74	0.43	0.63
(fmol cell ⁻¹)	0.109	0.012	0.226	-0.68	0.40	0.58

Table 5.1b. Experiment II: legend as Table 5.1a.

Parameters	Mean	Min	Max	Correlation coefficient R (n=10)		
				Growth rate	DA prod.	Total DA
Growth rate (d^{-1})	0.183	0.061	0.441	1.00	0.01	-0.69
10^6 Cell l^{-1}	54.46	26.62	71.44	-0.53	0.40	0.60
DA production ($\mu g\ l^{-1}\ d^{-1}$)	40.57	16.97	90.35	0.01	1.00	0.51
Total DA ($\mu g\ l^{-1}$)	287.70	45.00	553.20	-0.69	0.51	1.00
($pg\ DA\ cell^{-1}$)	2.79	1.10	5.62	-0.07	0.94	0.56
DA in filtrate ($\mu g\ l^{-1}$)	129.70	2.40	399.20	-0.76	-0.17	0.74
P_m^B ($\mu g\ C\ [\mu g\ Chl\ a]^{-1}\ h^{-1}$)	0.77	0.28	1.87	0.99	0.04	0.62
Chl a ($\mu g\ l^{-1}$)	69.26	52.53	87.10	-0.05	0.47	-0.06
($pg\ Chl\ a\ cell^{-1}$)	1.36	0.74	2.23	0.62	-0.25	-0.64
PC (μM)	595.00	505.25	771.42	-0.40	0.75	0.77
($pg\ C\ cell^{-1}$)	139.10	102.80	227.80	0.52	-0.19	-0.37
PN (μM)	79.93	52.14	106.71	-0.69	0.44	0.88
($pg\ N\ cell^{-1}$)	21.15	13.11	32.88	-0.00	-0.11	0.07
PSi (μM)	53.83	46.39	61.08	-0.19	0.17	0.23
($pg\ Si\ cell^{-1}$)	29.36	21.95	51.23	0.69	-0.42	-0.62
PISi (μM)	0.98	0.73	1.20	0.01	0.07	0.10
DISi (μM)	0.52	0.12	1.29	0.19	-0.08	0.01
DSi (μM)	2.56	0.97	4.29	-0.47	-0.18	0.39
DIP (μM)	28.86	23.03	34.46	0.66	0.13	-0.56
PP (μM)	5.36	4.72	6.19	0.09	0.68	0.17
($pg\ P\ cell^{-1}$)	3.26	2.31	5.79	0.71	-0.26	0.60
ATP (nM)	8.39	1.20	15.02	-0.18	0.56	0.14
($fmol\ cell^{-1}$)	0.156	0.045	0.330	-0.16	0.32	0.00
Bacteria ($10^3\ ml^{-1}$)	222.8	159.5	354.1	0.04	0.94	0.59

Table 5.2a. Experiment I: cellular chemical compositions of *P. pungens* f. *multiseries* expressed as ratios at various growth rates, their correlations (R) with DA production ($\mu\text{g DA l}^{-1} \text{d}^{-1}$) and concentration ($\mu\text{g DA l}^{-1}$).

μ (d^{-1})	C:Chl <i>a</i>	N:Chl <i>a</i>	Si:Chl <i>a</i>	P:Chl <i>a</i>	C:N	C:Si	C:P	N:P	N:Si	Si:P	
	(weight)				(atomic)						
0.092	675.3	20.01	67.06	3.04	9.24	5.51	134.5	14.56	0.60	24.40	
0.130	596.1	17.68	66.82	2.78	9.48	5.02	133.6	14.09	0.53	26.62	
0.160	779.4	14.56	53.23	2.85	10.04	5.49	113.8	11.33	0.55	20.71	
0.229	637.8	14.77	53.32	2.30	9.94	5.51	141.3	14.22	0.55	25.66	
0.239	811.1	15.56	59.37	2.19	9.60	5.03	150.8	15.72	0.52	29.98	
0.310	770.8	14.15	53.59	1.87	10.23	5.39	170.8	16.72	0.53	31.66	
0.320	554.6	14.53	57.52	2.07	9.67	4.88	149.9	15.51	0.51	30.71	
0.519	563.8	13.40	49.37	1.73	9.48	5.14	162.2	17.13	0.54	31.56	
0.539	516.0	13.42	68.56	1.89	9.99	3.91	156.7	15.69	0.39	40.10	
0.669	418.2	11.56	50.38	1.37	10.78	4.94	201.8	18.73	0.46	40.81	
Mean	632.3	14.96	57.92	2.21	9.85	5.08	151.5	15.37	0.52	30.22	
Std	120.9	2.25	6.86	0.51	0.43	0.46	22.8	1.91	0.05	6.10	
R	DA prod.	0.63	0.59	0.24	0.38	-0.32	0.46	-0.18	-0.11	0.52	-0.39
	$\mu\text{g DA l}^{-1}$	0.39	0.92	0.56	0.71	-0.56	0.43	-0.40	-0.29	0.61	-0.52
	μ (d^{-1})	-0.71	-0.84	-0.37	-0.92	0.60	-0.58	0.83	0.78	-0.73	0.90
C:Si:N:P = 151:29:15:1											

Table 5.2b. Experiment II: legend as Table 5.2b

μ (d ⁻¹)	C:Chl <i>a</i>	N:Chl <i>a</i>	Si:Chl <i>a</i>	P:Chl <i>a</i>	C:N	C:Si	C:P	N:P	N:Si	Si:P	
	(weight)				(atomic)						
0.061	647.8	27.85	29.85	3.14	6.21	11.57	121.6	19.62	1.87	10.51	
0.085	550.3	12.14	18.06	1.93	7.66	10.28	106.4	13.90	1.34	10.34	
0.094	567.8	20.04	24.65	2.52	6.84	11.11	120.4	17.62	1.63	10.84	
0.101	633.5	19.17	19.16	2.27	6.56	13.13	122.4	18.66	2.00	9.33	
0.095	575.3	14.66	23.69	2.45	7.81	9.64	103.1	13.23	1.24	10.69	
0.137	613.6	15.21	22.64	2.23	7.86	10.55	118.6	15.09	1.34	11.24	
0.202	771.4	17.18	17.83	2.19	7.22	13.91	125.6	17.41	1.93	9.03	
0.265	552.2	13.14	18.79	2.78	8.52	11.90	89.2	10.48	1.40	7.49	
0.299	532.9	11.39	24.26	2.25	9.30	8.73	104.0	11.20	0.94	11.92	
0.441	505.3	12.28	22.94	2.59	9.71	10.37	101.7	10.49	1.07	9.80	
Mean	595.0	16.31	22.19	2.44	7.77	11.12	111.3	14.77	1.48	10.12	
Std	72.5	4.77	3.59	0.33	1.08	1.49	11.4	3.26	0.35	1.20	
R	DA prod.	0.75	0.05	-0.31	-0.10	-0.13	0.55	0.31	0.18	0.34	-0.31
	$\mu\text{g DA l}^{-1}$	0.77	0.80	0.29	0.26	-0.82	0.52	0.76	0.83	0.74	0.05
	μ (d ⁻¹)	-0.40	-0.61	-0.13	0.05	0.90	-0.23	-0.56	-0.77	-0.61	-0.19
C:Si:N:P = 111:10:15:1											

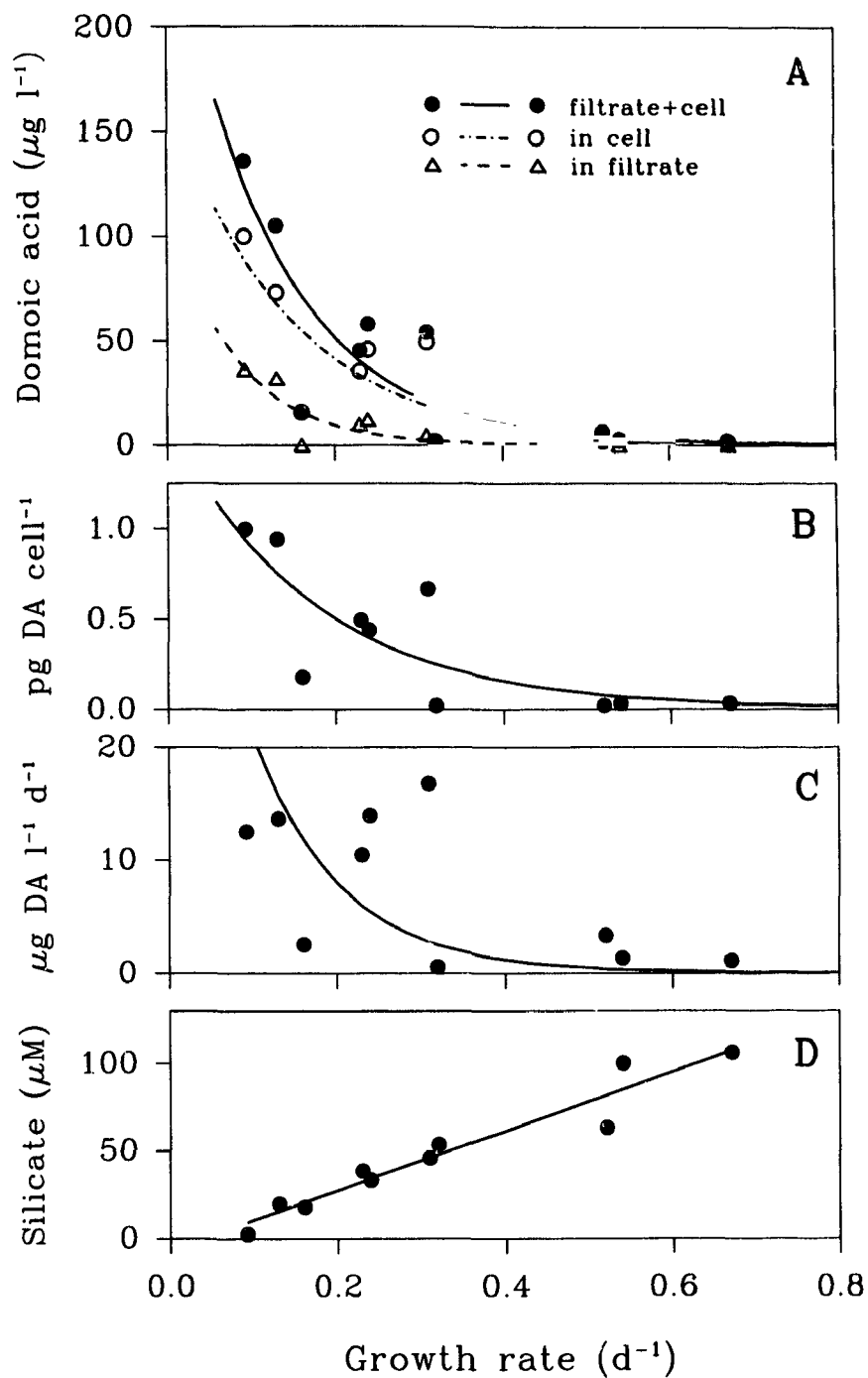


Fig. 5.2. Experiment I. Variations with growth rate: (A) DA concentration, (B) cellular DA, (C) DA production rate, and (D) DISi. Silicate concentration in the reservoir was $165.4 (\pm 9.0) \mu M$. The curves in A, B, C, are fitted by Equation 5.1.

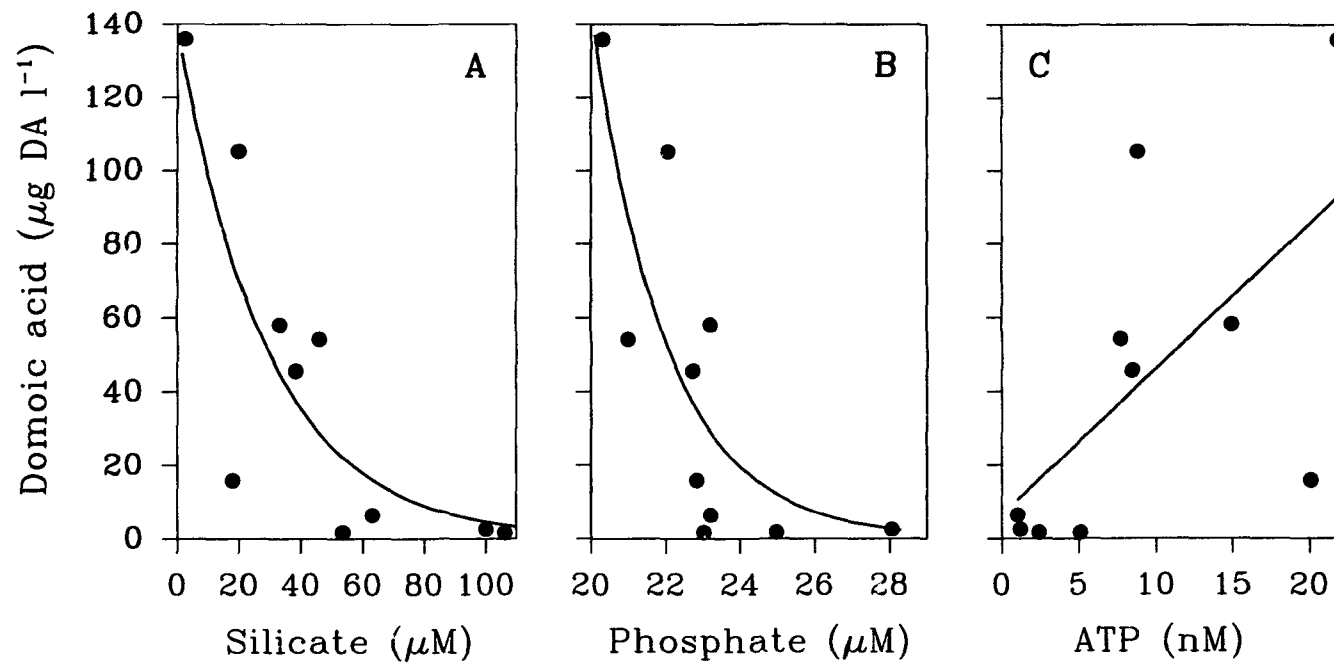


Fig. 5.3. Experiment I. Relationships of domoic acid with (A) silicate, (B) phosphate in the culture medium, and (C) ATP concentrations in the cells. The curves in A and B are fitted by an exponential function like Equation 5.1 and the line in C is a linear regression.

5.3.2. Experiment II: continuous culture

Experiment II was characterized by low DISi (56.2 μM) in the inflow medium and low cellular silicon. Cell concentrations were low and less variable ($41 - 71 \times 10^6 \text{ l}^{-1}$) except for the highest growth rate (0.441 d^{-1}) when cell concentration was significantly reduced ($26.6 \times 10^6 \text{ cells l}^{-1}$). Otherwise, cellular chlorophyll *a*, carbon, nitrogen, phosphorus and ATP were higher than those in Experiment I, but silicon was lower (Table 5.1). As growth rate increased, the following features were observed: (1) carbon assimilation increased. (2) cellular chlorophyll *a*, carbon, silicon and phosphorus increased, but cellular nitrogen was not affected (Table 5.1b). (3) C:Chl *a*, N:Chl *a*, C:P, N:P and N:Si ratios decreased, while the C:N ratio increased. Si:Chl *a*, P:Chl *a*, C:Si, and Si:P were relatively insensitive to growth rate (Table 5.2b).

Another feature in the Experiment II was high DA concentration ($45\text{-}553 \mu\text{g DA l}^{-1}$, $1.1\text{-}5.6 \text{ pg DA cell}^{-1}$) and production ($17\text{-}90 \mu\text{g DA l}^{-1} \text{ d}^{-1}$, or $0.31\text{-}1.35 \text{ pg DA cell}^{-1} \text{ d}^{-1}$) which was due to low silicate supply rates ($3.4\text{-}24.8 \mu\text{mol l}^{-1} \text{ d}^{-1}$). However, the relationships between DA and growth rate can not be simply described by equation 5.1. At very low growth rate, DA in cells and DA production rates increased as growth rate increased, reaching a peak at $\mu = 0.20 \text{ d}^{-1}$. Following this, DA production decreased exponentially similar to the pattern in Experiment I (Figs. 5.4A, B, C). At low growth rates, cells tend to release DA into the medium (Fig. 5.4A).

Abundance of bacteria followed the same pattern as DA production in relation to growth rate (Fig. 5.4D). Domoic acid and its production seem to be correlated ($p < 0.05$) with bacterial concentrations (Table 5.1b).

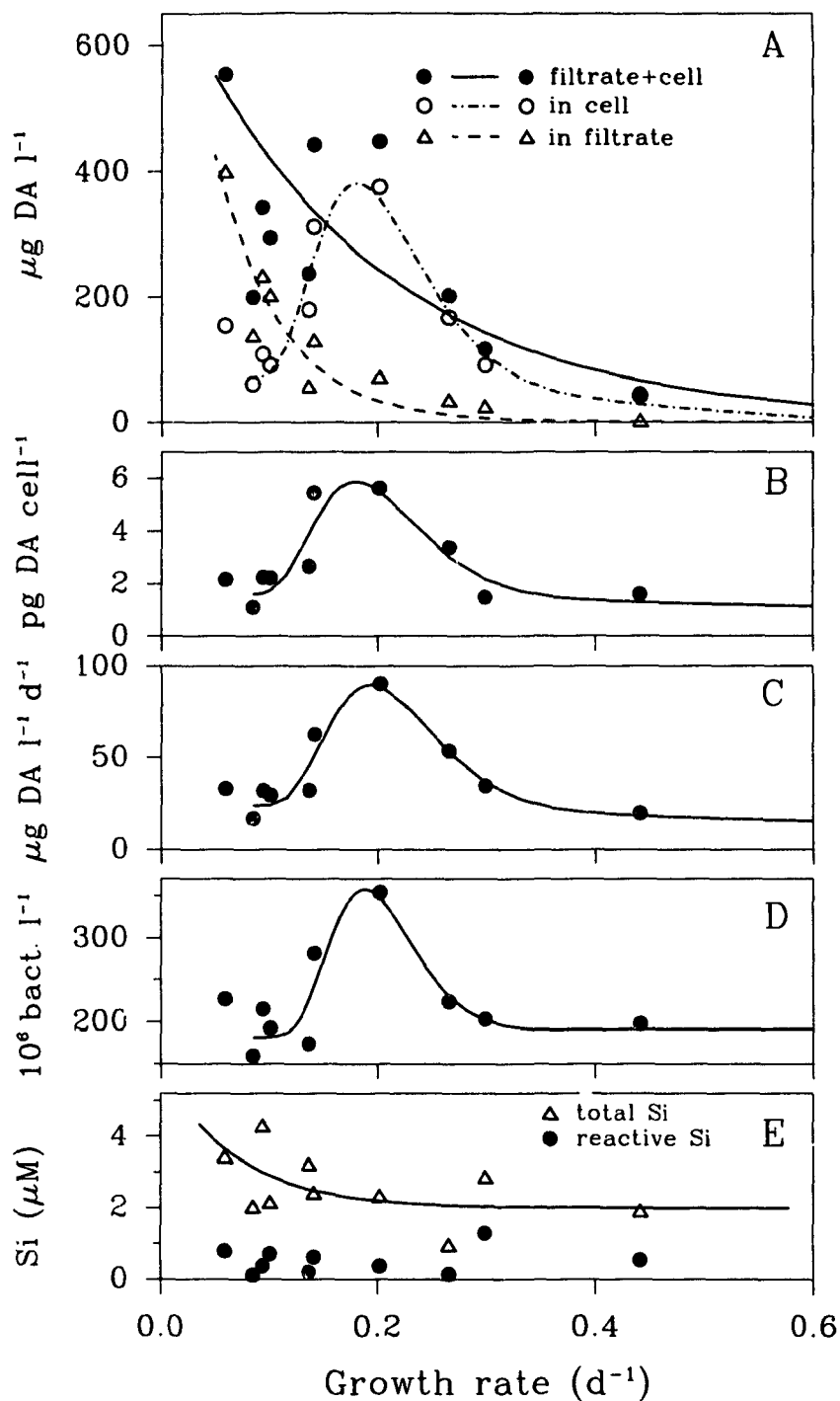


Fig. 5.4. Experiment II. Variations with growth rate: (A) DA concentration, (B) cellular DA, (C) DA production rate, (D) bacterial abundance, and (E) DISi and DSi. Silicate concentration in the reservoir was $56.2 (\pm 3.4) \mu\text{M}$. The curves are fitted by Equation 5.1 or by eye.

DISi in the culture medium at the steady state (Fig. 5.4E) remained low and unaffected by the growth rates. However, when growth rates were less than 0.14 d^{-1} , total dissolved silicon in the culture medium increased as growth rate decreased, which implies the dissolution of silica from cell walls.

Table 5.3. Common changes of chemical properties in Experiments I and II as a result of increase in growth rate

Variables	Increase	Decrease
Cell concentrations		+
Carbon assimilation (P_m^B)	+	
DA concentration and production		+
Particulate nitrogen		+
Particulate carbon		+
Particulate inorganic phosphate	+	
pg Si cell ⁻¹	+	
pg Chl <i>a</i> cell ⁻¹	+	
C:N ratio	+	
C:Chl <i>a</i> ratio		+
N:Chl <i>a</i> ratio		+
N:Si ratio		+

The common characteristics between Experiments I and II were (1) coupling of growth with carbon assimilation (P_m^B , $p < 0.0001$) and both were negatively correlated with the DA concentration ($p < 0.05$, Table 5.1). When data from both Experiments I and II were pooled, the relationship between DA concentration and growth rate can be described by a single curve of equation 5.1 (Fig. 5.5). (2) Growth rates were also

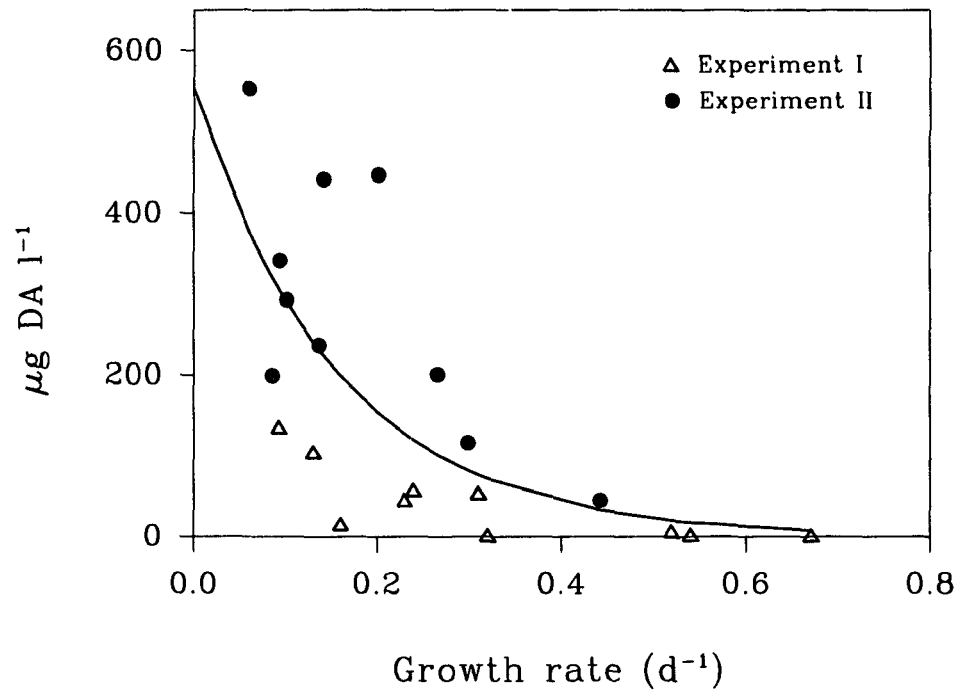


Fig. 5.5. Experiments I + II. Domoic acid concentration (filtrate + cells) in relation to growth rate. The curve is fitted by Equation 5.1.

correlated negatively with N:Chl *a* and N:P, but positively with C:N ratio (Table 5.2). (3) C:Chl *a* ratio positively correlated with DA production. (4) DA concentration correlated positively with N:Chl *a* and N:Si ratios but negatively with C:N ratio. In conclusion, any factor with a positive effect on growth and carbon assimilation exerted negative effects on DA concentration and/or its production (Tables 5.1, 5.2, 5.3).

5.3.3. Experiment III: extended batch culture

When addition of medium from the reservoir ceased in the extended batch mode, cell concentration increased or not, depending on the previous steady state growth rate. For example in Chamber 1 (Fig. 5.6), cell concentration increased from 49×10^6 cells l^{-1} to 60×10^6 cells l^{-1} in the first 21 hours. This increase was comparable to the specific growth rate in the steady state ($\mu=0.265$ d^{-1}). Further population growth was prevented by stoppage of silicate supply essential for cell frustule formation. Production rate of DA had been 53.6 μg DA $l^{-1} d^{-1}$ (or 1.09 pg DA $cell^{-1} d^{-1}$) during the previous steady state. The production was enhanced by a factor of 3 during the first 21 hours after the curtailment of silicate supply, DA concentration increased by 151.5 μg DA l^{-1} (from 201.5 to 353.0 μg DA l^{-1} , or 3.17 pg DA $cell^{-1} d^{-1}$). The production continued at a slightly reduced rate (138.5 μg DA $l^{-1} d^{-1}$, or 2.41 pg DA $cell^{-1} d^{-1}$) during the following 3 days. The total DA concentration at the end of the experiment was 768.5 μg DA l^{-1} , the highest ever reported for *P. pungens* f. *multiseries*. Of this 768.5 μg DA l^{-1} , 124.5 μg DA l^{-1} occurred in the filtrate, the concentration in the cells was 11.9 pg DA $cell^{-1}$.

In Chamber 5, the steady state growth rate was the lowest 0.10 d^{-1} and the DA

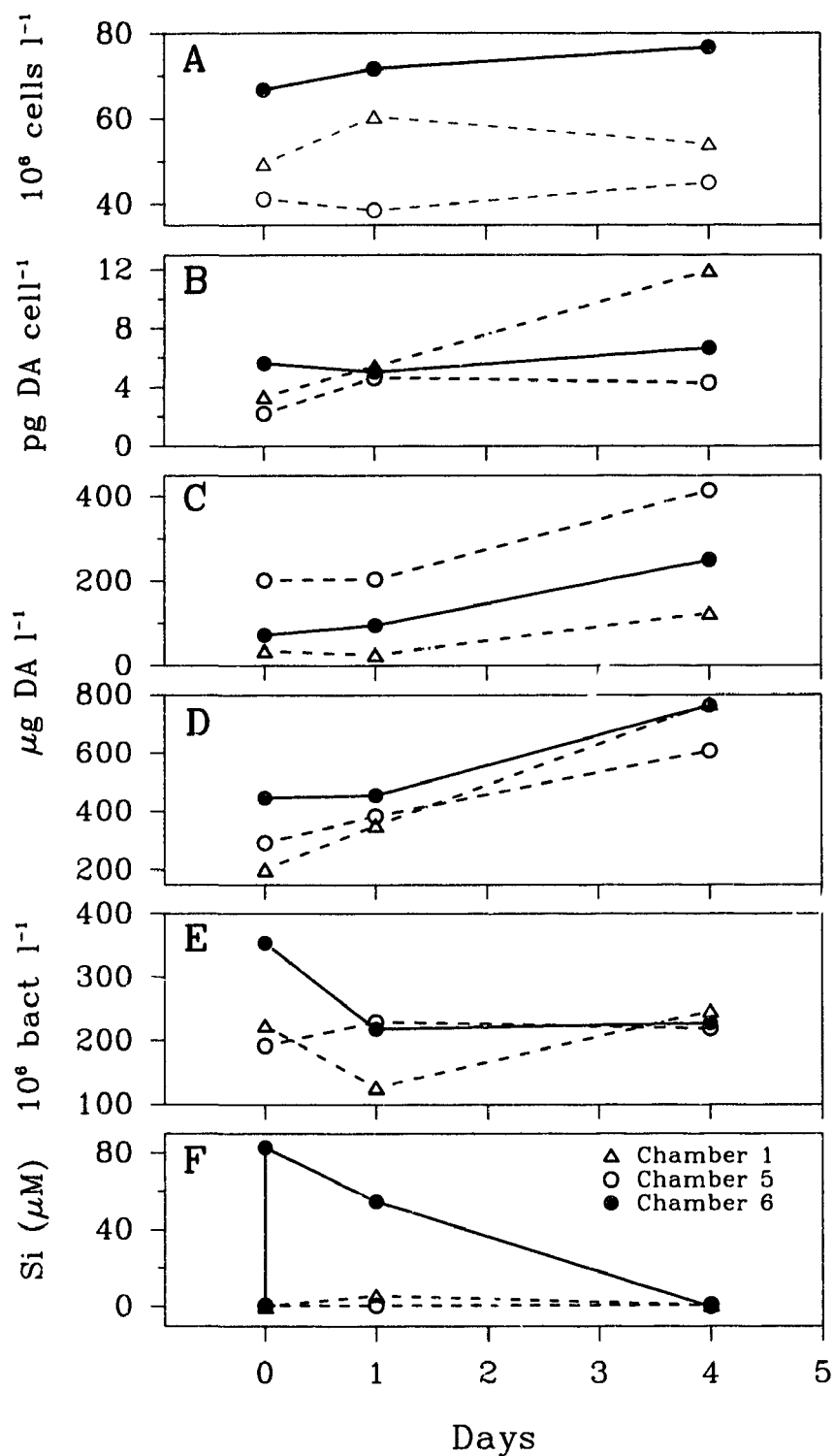


Fig. 5.6. Experiment III. Variations with time in (A) cell concentration, (B) DA per cell, (C) DA in filtrate, (D) DA in cells + filtrate, (E) bacterial abundance, and (F) DiSi.

production was $29.6 \mu\text{g DA l}^{-1} \text{d}^{-1}$ ($0.72 \text{ pg DA cell}^{-1} \text{d}^{-1}$). No substantial increase in cell concentration was observed, but an increase in DA production rate was also evident (Fig. 5.6). During the first 21 hours it was $90.5 \mu\text{g DA l}^{-1}$ (from 293.3 to $383.8 \mu\text{g DA l}^{-1}$, or $2.60 \text{ pg DA cell}^{-1} \text{d}^{-1}$), enhanced by more than 3 times. During the following 3 days, DA production continued at $74.4 \mu\text{g l}^{-1} \text{d}^{-1}$ ($1.78 \text{ pg DA cell}^{-1} \text{d}^{-1}$). Note the production rate was also slightly reduced.

In Chamber 6, the steady state growth rate was 0.20 d^{-1} and DA production was $90.35 \mu\text{g DA l}^{-1} \text{d}^{-1}$ ($1.35 \text{ pg DA cell}^{-1} \text{d}^{-1}$); $85 \mu\text{M}$ silicate was added to the culture immediately after the steady state and addition of medium from the reservoir was stopped (Fig. 5.6F). Cell concentration increased from 66.7 to $71.6 \times 10^6 \text{ cells l}^{-1}$ during the first 21 hours and attained $76.7 \times 10^6 \text{ cells l}^{-1}$ 3 days later. On the other hand, no substantial increase of DA was found ($447.3 - 455.4 \mu\text{g DA l}^{-1}$) in this culture during the first 21 hours. But an increase in DA production during the following 3 days was obvious ($455.4-763.5 \mu\text{g DA l}^{-1}$, or $1.39 \text{ pg DA cell}^{-1} \text{d}^{-1}$) due to the drastic decrease in silicate concentration (from 57.5 to $1.8 \mu\text{M}$).

Unlike in the steady state, bacterial abundance did not increase during this extended batch mode (Fig. 5.6E) although DA production substantially increased. On the other hand, increase or decrease of bacteria concentration seems to be inversely related to the change in population size of *P. pungens* f. *multiseries* (Figs. 5.6A, E). The bacterial effects on DA production is further discussed in the Appendix C3.

5.3.4. Growth kinetics

There have been conflicts over whether external or internal concentration of nutrient controls growth rate of phytoplankton in steady state of continuous culture (Droop, 1973, 1983). For the silicate limited continuous culture of *P. pungens* f. *multiseries*, Droop's (internal) model (Equation 5.2) is better suited for expressing the kinetic data than Monod's (external) model. However because of the scatter in the data and the clustering of the data points in the region of low growth rate (Fig. 5.7), interpretation of the results (Table 5.4) is difficult.

$$\mu = \mu_{max}' (Q - k_q) / Q \quad (5.2)$$

where, μ is growth rate, μ_{max}' is the *potential* maximum growth rate, Q is the measured cell quota corresponding to measured μ , and k_q is the minimum cell quota, *i.e.* the cell quota at $\mu = 0$. No significant differences were found in the fitted parameters between the two chemostat experiments (Table 5.4), but the coefficient of variation was very high (23-64%).

Table 5.4. Growth kinetics in chemostat cultures (function: $\mu = \mu_{max}' (Q - k_q) / Q$). Values in parentheses are standard deviations.

Parameter	Experiment I (n=10)	Experiment II (n=10)	Experiment I & II (n=20)
μ_{max}' (d ⁻¹)	0.68 (0.43)	0.55 (0.17)	0.58 (0.12)
k_q (pg Si cell ⁻¹)	22.44 (12.94)	18.53 (3.09)	19.12 (3.20)

The data showed that growth rate was not only controlled by cell quota but also

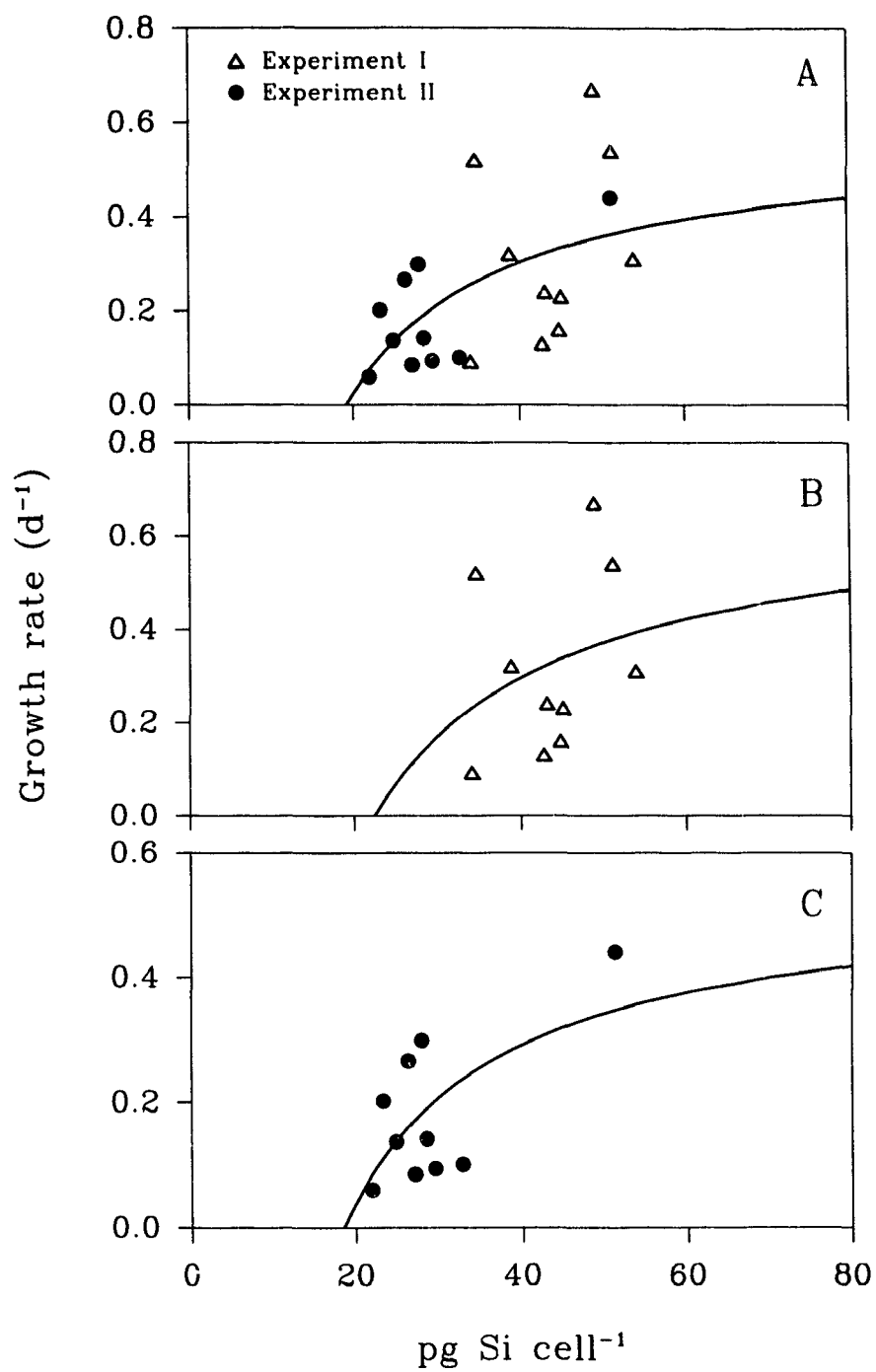


Fig. 5.7. Growth kinetics fitted with Droop's cell quota model: $\mu = \mu_{max} (Q - K_q)/Q$. (A) Experiments I and II, (B) Experiment I, and (C) Experiment II.

related to the external concentration of silicate (Fig. 5.2D). Goldman (1977) suggested that growth was controlled by uptake rate and proposed an equation (Equation 5.3), essentially a combination of the Monod and Droop equations, to describe his results from phosphate limited continuous culture of the chrysophyte *Monochrysis lutheri* Droop.

$$\mu = \mu_{max}' U / (K_U + U) \quad (5.3)$$

where U is the uptake rate (pg Si cell⁻¹ d⁻¹), K_U is the half saturation coefficient for growth with respect to uptake rate. This equation also satisfactorily described the kinetic data of *P. pungens* f. *multiseries* from my silicate-limited continuous culture.

Table 5.5. Growth kinetics in chemostat cultures. Data were from the direct fitting equation 5.3 to experimental data points. Values in parentheses are standard deviations.

Parameter	Experiment I (n=10)	Experiment II (n=10)	Experiment I & II (n=20)
μ_{max}' (d ⁻¹)	2.67 (1.59)	0.76 (0.10)	1.43 (0.33)
K_U (pg Si cell ⁻¹ d ⁻¹)	100.1 (72.7)	15.27 (3.08)	42.54 (14.27)

Direct fitting equation 5.3 to my data points did not give satisfactory results (Table 5.5) due to lack of points at high growth rates. To solve this problem, I determined μ_{max}' and K_U by first performing linear regression analysis on the cell quota (Q) vs. U data and then by fine-tuning with nonlinear regression analysis directly on μ vs. U data in equation 5.3 following the method of Goldman and McCarthy (1978). Adjustments to both parameters were within limits of one standard error from linear regression. μ_{max}' and K_U

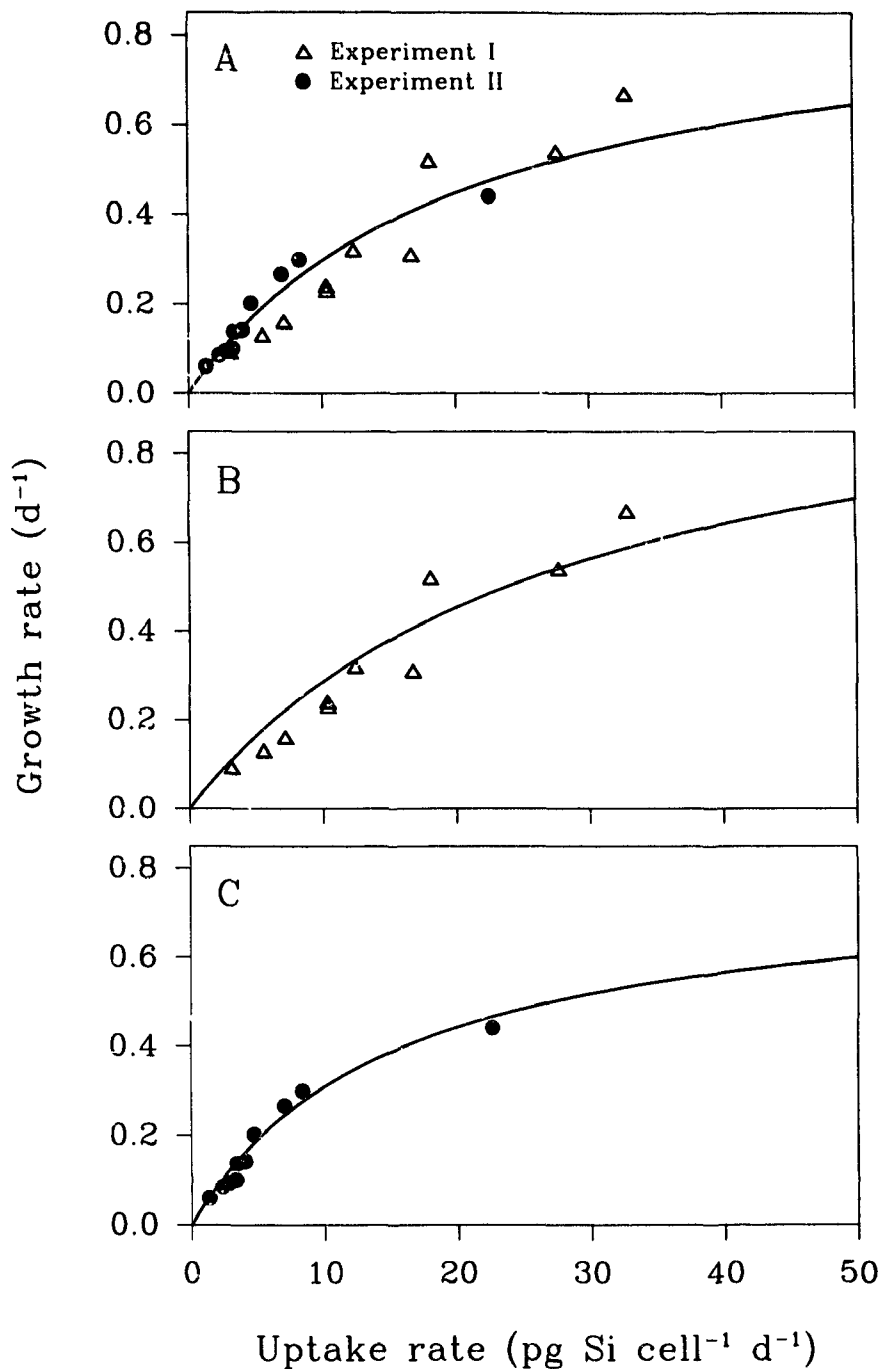


Fig. 5.8. Growth kinetics fitted with Goldman equation: $\mu = \mu_{max} U / (K_U + U)$. (A) both Experiments I and II, (B) Experiment I, and (C) Experiment II.

were finally determined by the criteria of least square of fitting (Marquardt, 1963). Coefficients of variation for both μ_{max}' and K_U in all the data sets were significantly reduced (Table 5.6) compared to Table 5.5. The results were consistent (Fig. 5.8, Table 5.6) as evident from μ_{max}' that was comparable to the μ_{max} values obtained from batch culture experiments (Chapters 3, 4) and slightly higher than the highest μ values of this continuous culture study.

Table 5.6. Growth kinetics in chemostat cultures. Data were determined first by performing linear regression on Q vs. U , and then by fine-tune fitting equation 5.3 to experimental data points. Values in parentheses are standard deviations.

Parameter	Experiment I (n=10)	Experiment II (n=10)	Experiment I & II (n=20)
μ_{max}' (d ⁻¹)	1.10 (0.20)	0.78 (0.088)	0.92 (0.012)
K_U (pg Si cell ⁻¹ d ⁻¹)	28.25 (0.84)	15.34 (2.81)	21.00 (0.47)

5.4. Discussion

5.4.1. Growth and uptake kinetics in relation to DA production

At very low growth rate in Experiment I and most steady states in Experiment II, there were still measurable quantities, of the order of 0.5 - 2 μ M, of reactive silicate left in the medium (Figs. 5.2D, 5.4E). This is consistent with the results of Paasche (1973a) on *Thalassiosira pseudonana* Hasle and Heimdal. Paasche demonstrated 4 possible mechanisms regarding this phenomenon: (1) lack of a component essential for full

utilization of silicate, such as phosphate, (2) dissolution of the silica wall, (3) binding factor and (4) existence of non-utilizable reactive silicate. The *P. pungens* f. *multiseries* cultures had enough other essential compounds in the medium that addition of silicate during the extended batch mode enabled further growth of the population. So mechanism 1 is not applicable. Mechanisms 2, 3 and 4 are possible. Dissolution of cell silicon has been demonstrated during the stationary phase of batch culture (Figs. 4.2B, 4.3B) and also found in this experiment (Fig. 5.4E). Adding a large quantity of filtrate from an old *Rhizosolenia alata* culture has been shown to inhibit growth of *P. pungens* f. *multiseries* (Subba Rao *et al.*, 1994). Besides the allelopathic effect, in the filtrate, existence of some other inhibitor of nutrient uptake similar to the "binding factor" in *Monochrysis lutheri* (Droop, 1968) is possible. Besides the monomeric Si(OH)_4 , sea water medium may contain non-utilizable low polymers of silicate, which are reactive in analysis.

Pooling the data from Experiments I and II, a single curve of equation 5.1 described them well (Fig. 5.5). However Experiment I data consisted of the lower portion, while Experiment II data the upper. This suggested the existence of different kinetics of DA production in these two Experiments. Experiments I and II differed in silicate concentration in the reservoir medium, which resulted in significant difference in kinetics of growth (Table 5.6) and DA production (Figs. 5.2, 5.4). Over a wide range of growth rates in the silicate limited continuous culture of *Skeletonema costatum*, Harrison *et al.* (1976) divided the growth kinetics into 4 regions: (1) at very low dilution rate ($<0.7 \text{ d}^{-1}$) the effluent silicate concentration increased with decreasing dilution rate; (2) silicate concentration remained at a minimum over a range of dilution rate ($0.7-1.2 \text{ d}^{-1}$); (3) a

subsequent small increase in dilution rate resulted in a large increase in effluent silicate concentration; and (4) at very high dilution rate ($>1.4 \text{ d}^{-1}$), a large increase in dilution rate resulted in a relatively small increase in silicate concentration. Experiment I results of *P. pungens* f. *multiseries* were similar to region 3 or 4 of *S. costatum*. Growth rates increased from 0.09 to 0.67 d^{-1} when residual silicate increased from 2.4 to $106.2 \text{ }\mu\text{M}$. This region was located at growth rate $>0.83 \text{ d}^{-1}$ for *S. costatum*. But the growth rate of *P. pungens* f. *multiseries* in Experiment I ranged from 0.09 to 0.67 with a wide portion overlapped with Experiment II data, while DA concentration markedly differed from Experiment II. The population size of the culture was relatively constant. This suggested that (1) silicate was not the limiting factor in Experiment I because there was sufficient silicate in the medium except when the growth rate was very low ($< 0.09 \text{ d}^{-1}$, Fig. 5.2D), (2) growth kinetics of the culture population not only differed in separate regions of growth rate but also in various reservoir concentrations of substrate, *i.e.* the supply rate of silicate. Nitrogen and phosphorus and vitamins were in excess. Carbon was not the limiting factor because the system was continuously aerated and pH was always below 9. Although there was sufficient silicate for further growth of the population, the population size never reached more than $1.05 \times 10^8 \text{ l}^{-1}$, which was comparable to the data from batch culture experiments (Figs. 4.2A-4.5A). Light was not likely limiting compared with the low light grown population (Fig. 3.9). This suggests that population size is probably restricted by some intrinsic physiological mechanism. This intrinsic factor in regulating the population size is common for continuous cultures and for the late exponential phase of batch cultures. The DA production was initiated when this intrinsic

restriction was effective.

A large supply of silicate resulted in high cellular silicon and low DA production in Experiment I, which was consistent with the batch culture study (Fig. 4.2). Cellular silicon was less variable and was independent of growth rate. Production of DA, however, was negatively correlated with growth rate (Fig. 5.2), similar to the first stage DA production in the batch culture study (Chapter 4).

In Experiment II, a low silicate supply resulted in less cellular silicon, which was positively correlated with growth rate (Table 5.1b). Growth rate was no longer a major factor influencing DA production (Fig. 5.4). The DA production was enhanced by a low uptake of silicate (Fig. 5.9). The differences in mechanism and magnitude of DA production in chemostat Experiments I and II, parallel the differences between first and second stage DA production in batch cultures (Table 5.7). However, DA production declined when the silicate uptake rate was too low ($<3.26 \text{ pg Si cell}^{-1} \text{ d}^{-1}$, Fig. 5.9C). This implies that cells produce less DA under critical stress. This result is in agreement with the decline of DA content in the cell in the senescent phase of batch culture of the same species (Subba Rao *et al.*, 1990, Bates *et al.*, 1991). In the senescent phase of batch culture (silicate exhausted, Bates *et al.*, 1991) and at extreme low uptake rate of silicate (Fig. 5.4) in continuous culture, cells tended to release DA into the culture medium. This may be because the critical silicate stress not only weakened the cell frustules as in *Navicula pelliculosa* (Lewin, 1957) but also restrained both DA production and the activity of the cell membrane. Very likely, domoic acid - a small molecular water soluble compound - is transported passively through the membranes. However when cells are not

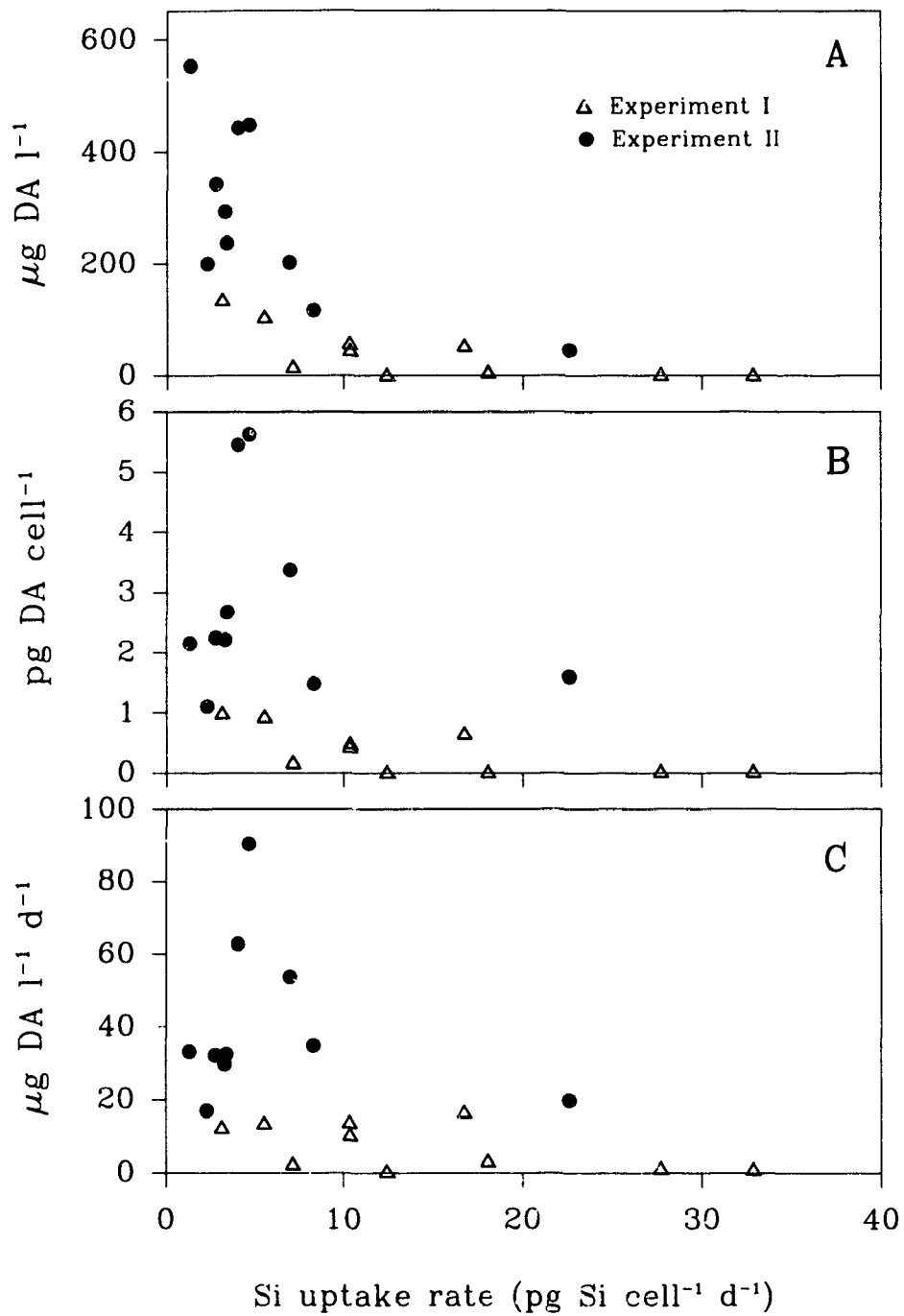


Fig. 5.9. Domoic acid in relation to silicate uptake rate. (A) DA in the whole culture, (B) DA in cells, and (C) DA production rate. Curves fitted by Equation 5.1.

severely stressed, the membrane probably limits this transport and contains most of the DA in the cells.

Experiment II cultures of *P. pungens* f. *multiseries* resemble the regions 1 and 2 of *S. costatum* (Harrison *et al.*, 1976). At very low growth rate ($\mu < 0.14 \text{ d}^{-1}$), total silicon in the medium increased although the reactive silicate remained relatively constant when growth rate decreased (Fig. 5.4D). This suggested dissolution of silicon from the cell wall when the growth rate is low which is consistent with the results from batch culture (Figs. 4.2, 4.3). Simultaneously, DA production decreased and tended to be released from cells into the medium (Fig. 5.4A). Release of DA coincided with dissolution of silicon from the cell frustule.

Table 5.7. Comparison of DA production in steady-state continuous cultures with the production in batch cultures under silicate limitation.

DA production	Batch culture	Continuous culture
No production	Early exponential phase	Approaching μ_m
Low	Late exponential phase (first stage)	High silicate supply Experiment I
High	Stationary phase (second stage)	Low silicate supply Experiment II

When growth rate was greater than 0.20 d^{-1} in Experiment II, silicon in the medium remained relatively constant as growth rate increased, which was similar to the region 2 in *S. costatum* (Harrison *et al.*, 1976). The relationship between growth rate and DA was similar to that in the Experiment I, i.e. DA production decreased as growth rate increased, but the magnitude was higher (Figs. 5.2, 5.4).

At the same growth rate, differences in silicate supply resulted in differences in silicate uptake rate and DA production. For example, at growth rate of 0.09 d^{-1} , the supply rates were 15.22 and $5.28 \mu\text{mol l}^{-1} \text{ d}^{-1}$ in Experiment I and II respectively. The corresponding uptake rates of silicate were 3.14 and $2.78 \text{ pg Si cell}^{-1} \text{ d}^{-1}$, and cellular DA and its production were 0.996 , $2.245 \text{ pg DA cell}^{-1}$ and 12.50 , $32.15 \mu\text{g DA l}^{-1} \text{ d}^{-1}$ (or 0.125 , $0.664 \text{ pg DA cell}^{-1} \text{ d}^{-1}$) respectively. At higher growth rate, the differences were also obvious. For example, at a growth rate of 0.31 or 0.30 d^{-1} , the silicate supply rate, silicate uptake rate, cellular DA, and DA production in Experiment I were $51.27 \mu\text{mol l}^{-1} \text{ d}^{-1}$, $16.72 \text{ pg Si cell}^{-1} \text{ d}^{-1}$, $0.667 \text{ pg DA cell}^{-1}$ and $16.79 \mu\text{g DA l}^{-1} \text{ d}^{-1}$ ($0.226 \text{ pg DA cell}^{-1} \text{ d}^{-1}$) respectively. The corresponding values in Experiment II were $16.80 \mu\text{mol l}^{-1} \text{ d}^{-1}$, $8.35 \text{ pg Si cell}^{-1} \text{ d}^{-1}$, $1.485 \text{ pg DA cell}^{-1}$ and $34.83 \mu\text{g DA l}^{-1} \text{ d}^{-1}$ ($0.569 \text{ pg DA cell}^{-1} \text{ d}^{-1}$). At the same growth rate, DA production was higher in Experiment II under more severe silicate limitation.

Domoic acid production was enhanced by a factor of 3 (Fig. 5.7) when the steady state continuous cultures were shifted to batch mode. The dynamics of DA production during this transition period is of great interest. During the first day after the transition, silicate stress became pronounced. There was a surge in DA production soon after cessation of silicate uptake followed by a slightly decline. The DA production was slightly reduced and the proportion of DA released from the cells into medium increased by more than 100% (Fig. 5.6C) as a result of the critical silicate stress similar to that in the steady states at very low growth rate.

With silicate perturbation in Chamber 6, on the other hand, there was a surge in

silicate uptake similar to that of *S. costatum* (Conway *et al.*, 1976). The uptake rate increased from 4.68 pg Si cell⁻¹ d⁻¹ in the steady state to 16.10 pg Si cell⁻¹ d⁻¹ during the first day in batch mode. However, DA production ceased at this moment. During the following 3 days, silicate uptake rate was reduced to 8.85 pg Si cell⁻¹ d⁻¹ and DA production resumed (Fig. 5.6D) at a rate of 102.7 µg DA l⁻¹ d⁻¹ (1.39 pg DA cell⁻¹ d⁻¹). These surges in DA production and in silicate uptake were probably higher in the first few hours after the shift from the steady state continuous to batch cultivation. Short term kinetics of silicate uptake and DA production need further investigation.

Domoic acid episodes recurred in the bays around Prince Edward Island in late fall and winter during 1987-1991. Silicate concentration is much lower in the natural sea water than in the culture, but DA levels were generally higher. These culture experiments show that cells produce more DA under lower supply of silicate even at the same growth rate. It is very likely that in natural sea water, *P. pungens* f. *multiseries* is severely silicate stressed and would therefore produce more DA under such conditions.

5.4.2. Cellular chemical composition and DA production

Biomass and cellular chemical composition varied with silicate availability. Except for silicon, concentrations of particulate chlorophyll *a*, carbon, nitrogen, phosphorus, and ATP in the culture were comparable between Experiments I and II. However, individual cells in Experiment I contained less of these constituents than those in Experiment II (Table 5.1). This suggested that silicate-limited cultures attain a smaller population size at steady state, but each cell contains more of these cellular components.

Cellular chlorophyll *a* ranged from 0.45 to 2.23 pg Chl *a* cell⁻¹ and was comparable to the results from batch culture (Figs. 3.3, 4.2 - 4.5). Cells in Experiment I contained less chlorophyll *a* than those in Experiment II (Table 5.1). This also agreed with the results from batch culture (Chapter 4). In batch culture, the maximum cellular chlorophyll *a* on day 6 was 0.82 pg Chl *a* cell⁻¹ in the controls (Fig. 4.2) while 0.66 pg Chl *a* cell⁻¹ in Treatment B (Fig. 4.3). This suggested a negative relationship between cellular chlorophyll *a* and the supply of silicate in the medium. However, this relationship was not shown in either Experiment I or II because of the positive correlation between cellular chlorophyll *a* and growth rate (Table 5.1).

Cellular carbon ranged from 76.5 to 227.8 pg C cell⁻¹ and nitrogen from 9.42 to 32.9 pg N cell⁻¹. These values were comparable to the cells in late exponential phase and stationary phase of batch cultures (Fig. 3.3). C:N ratios differed in the two continuous culture experiments, 9.24 - 10.78 for Experiment I and 6.21 - 9.71 for Experiment II. Higher ratios and less variability were characteristics of Experiment I cells and lower ratios and high variability for Experiment II cells. The ratios of Experiment I cells are comparable to those cells at late exponential phase while Experiment II cells are comparable to stationary phase cells (Fig. 3.4). This similarity between continuous cultures and batch cultures was also valid for DA production discussed in Section 5.4.1. High C:N ratios are an indication of stressed cells (Goldman *et al.*, 1979, Pan *et al.*, 1991, Subba Rao and Pan, 1993). The high C:N ratios in Experiment I cells (Table 5.2) suggested that although sufficient silicate existed for further growth of the population, the cells were stressed due to a factor not determined. The low C:N ratios in Experiment II,

on the other hand, do not necessarily indicate that the culture was less stressed than Experiment I cells. In fact, they were more severely stressed by silicate limitation. The low C:N ratios in Experiment II were attributed to the faster increase in cellular nitrogen relative to carbon (Table 5.1) under silicate limitation.

Redfield *et al.* (1963) demonstrated atomic ratios of C:Si:N:P = 106:15:16:1 based on the data from the Western Atlantic. Silicon appears to enter the biochemical cycle in about the same proportion as nitrogen (Richards, 1958). In *P. pungens* f. *multiseries*, the mean elemental ratio (atomic) of C:Si:N:P in Experiment I was 151:29:15:1 and in Experiment II 111:10:15:1 (Table 5.2). Silicate entered the cells faster than nitrogen in Experiment I but slower in Experiment II. N:P ratios (atomic) were similar in the two experiments although both N and P were much lower in the cells from Experiment I cells. Ratios of C:P, P:Si, C:Si and N:Si were significantly different ($p < 0.001$, $n=10$) between these two experiments. The higher ratios of P:Si, C:Si and N:Si were associated with high DA production in Experiment II (Fig. 5.10) strongly suggesting that DA production was enhanced by silicate limitation. When this stress was eased during the extended batch mode period in Chamber 6 by addition of silicate, DA production was interrupted (Fig. 5.7). However, DA production increased 3 times when more severe stress was applied in Chambers 1 and 5. This further confirmed the association of DA production with silicate limitation consistent with the results from perturbation of batch culture (Figs. 4.4, 4.5).

Low silicon per cell and high DA production characterized Experiment II (Fig. 5.10A). The marked difference in the relative content of silicon in cells from

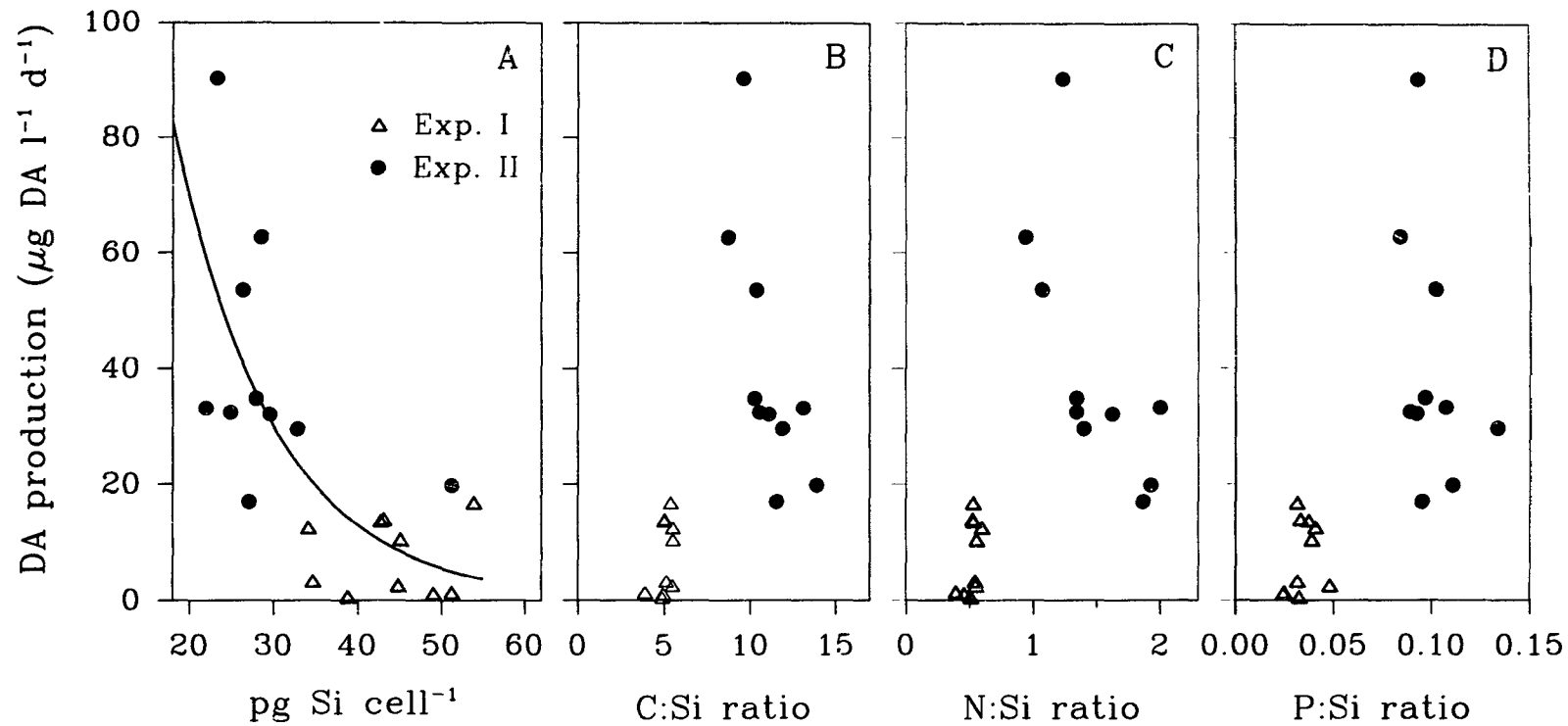


Fig. 5.10. Relationships between domoic acid production and cell chemical composition. The curve in A is fitted by Equation 5.1.

Experiments I and II (Figs. 5.10B, C, D) provided another evidence of the association of high DA production with silicate limitation. Therefore, silicon metabolism is the major factor controlling high DA production.

In Experiment II, highest DA production at $\mu=0.20 \text{ d}^{-1}$ coincided with the highest C:Chl *a*, C:Si and C:P ratios (Table 5.2b) reflecting the high particulate carbon in the culture (771.4 μM). In both Experiments I and II, C:Chl *a* ratios were positively correlated with DA production (Table 5.2) but negatively correlated with growth rate. C:Chl *a* ratio in this study ranged from 418 to 811, which is an order of magnitude higher than that for other non-toxic diatoms such as *S. costatum*, *Chaetoceros debilis*, *Thalassiosira gravida* (Harrison, *et al.*, 1977). This ratio generally varies by a factor of 2 ranging from 20 to 60 in healthy, natural non-toxic populations.

Higher C:Chl *a* ratios are associated with silicon or nitrogen limitation in diatoms. For example, in *Thalassiosira gravida* (Harrison *et al.*, 1977), C:Chl *a* of silicate-limited cells increased from 26 to 46 and in ammonium-limited cells from 26 to 55. Similarly in batch cultures of *P. pungens* f. *multiseries* (Fig. 3.4), stationary phase cells have higher C:Chl *a* ratios than exponential phase cells; in continuous culture (Table 5.2), Experiment II cells have higher C:Chl *a* than Experiment I cells.

Ratios of N:Chl *a* were negatively correlated with growth rate in both Experiments I and II, with higher values in Experiment II cells than in Experiment I cells. This was primarily due to the higher cellular nitrogen in Experiment II cells than Experiment I cells by a factor of 2 (Table 5.1). The higher nitrogen content in Si-limited cells is consistent with other non-toxigenic diatoms such as *Chaetoceros debilis* and *Thalassiosira gravida*

(Harrison *et al.*, 1977). In addition, P:Chl *a*, Si:Chl *a*, C:N and other chemical ratios were related to silicate limitations (Table 5.2).

5.4.3. Domoic acid production in relation to nutrient metabolism

Domoic acid was significantly produced when growth was low in the steady state continuous culture, or completely stopped in the stationary phase of batch cultures. This is similar to the general pattern of secondary metabolism (Vining, 1986). At high growth rates, carbon assimilation, nitrogen, phosphorus and silicate uptake rates were high, establishing a higher demand for metabolic energy and resulting in less free energy in the form of adenosine triphosphate (ATP). Fast-growing cells contained less ATP (Fig. 5.11A). Production of DA could have been inhibited partly because of the deficiency of free energy (Fig. 5.11C).

Carbon assimilation rates (P_m^B) in continuous cultures ranged from 0.2 to 2.9 $\mu\text{g Chl } a^{-1} \text{ h}^{-1}$, and were comparable with the results from batch culture (Figs. 3.7A, 3.13A, 3.18A). The photo-chemical (energy assimilation) process may be less influenced by nutrients except for phosphate. When carbon assimilation was reduced at low growth rate, chlorophyll *a* concentration was not affected (Table 5.1). This suggested that the photochemical process was still in progress at a similar rate. The photo-assimilated energy was used less for carbon assimilation and the increase in the residual free energy (ATP) was beneficial to DA production (Fig. 5.11A). The negative relationship between P_m^B and DA concentration (Fig. 5.12A) was found in both Experiments I and II. The DA production was interrupted in the stationary culture of *P. pungens* f. *multiseriis* when

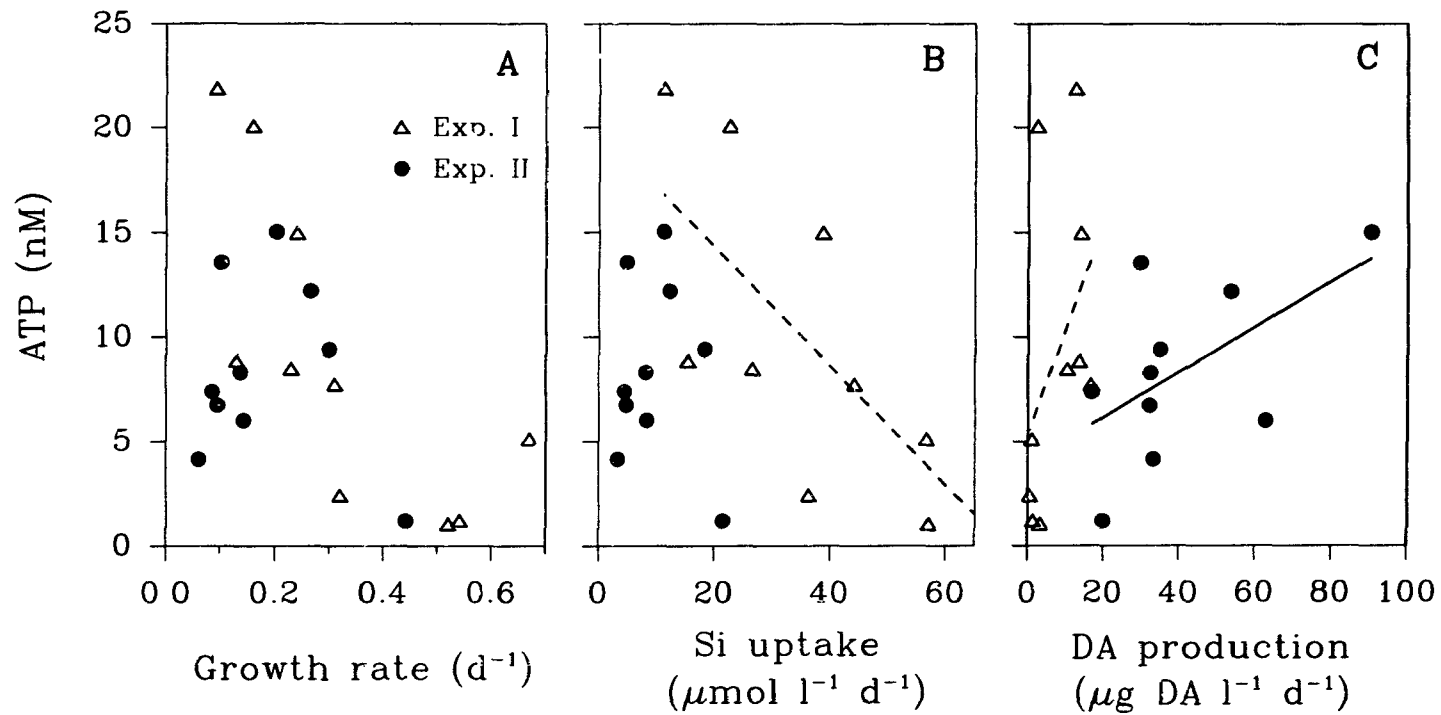


Fig. 5.11. ATP concentrations in relation to (A) growth rate, (B) silicic uptake, and (C) DA production. The lines are linear regressions, broken lines corresponding to open triangles, solid line to filled circles.

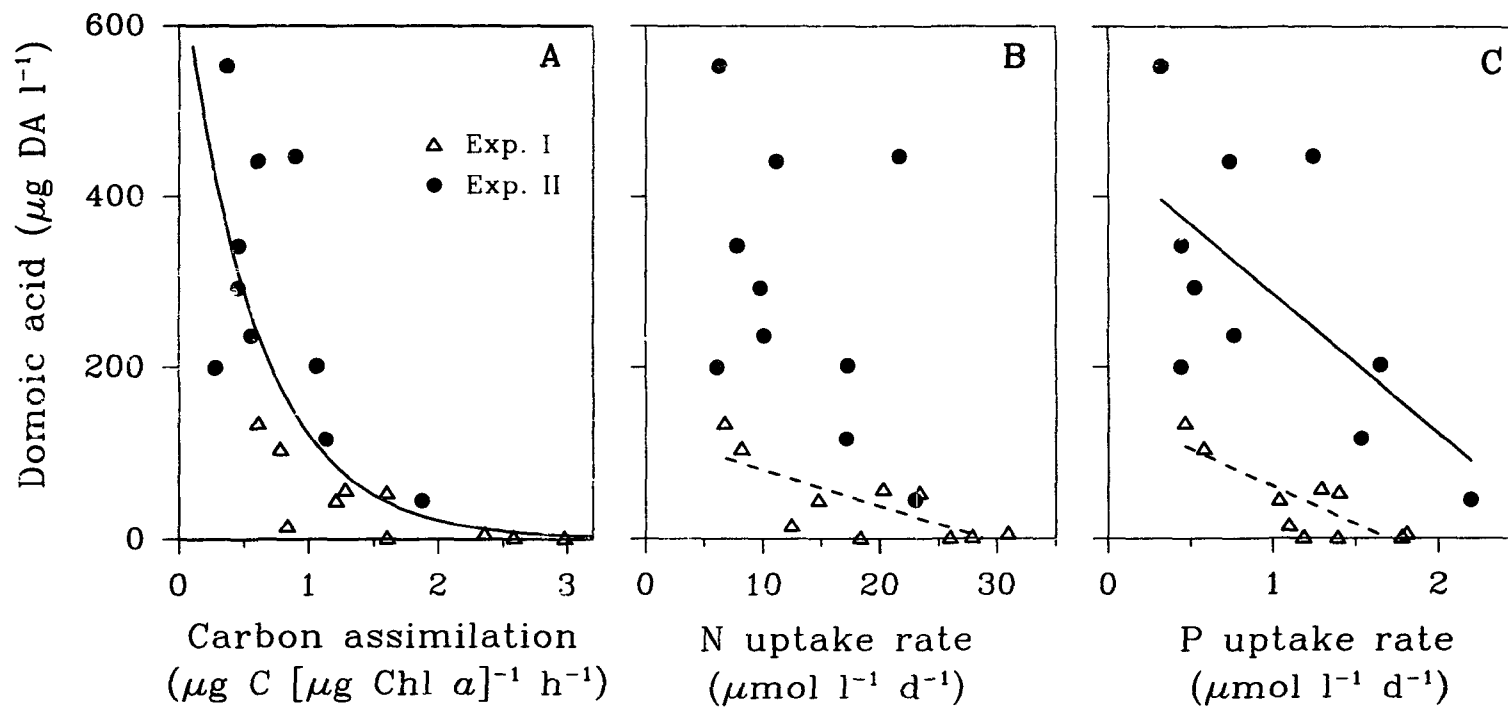


Fig. 5.12. Relationships between domoic acid concentration and other cell metabolism. The curve in A is fitted by an exponential function, as in Equation 5.1. The lines in B and C are linear regressions corresponding to open triangles (broken lines) and filled circles (solid line).

DCMU was used to block the photophosphorylation (Bates *et al.*, 1991). Production of DA was shown to depend on photo-assimilated energy. Differences in energy partitioning existed when growth rate were low and high.

Uptake of silicate requires energy. In the freshwater diatom *Navicula pelliculosa*, for example, silicate uptake was coupled with aerobic respiration (Lewin, 1955). The respiration quotient (R.Q.) was high in Si-replete cells but low in Si-depleted cells. In *P. pungens f. multiseriis*, ATP concentration was reduced at high Si uptake rates (Fig. 5.11B) due to consumption by this metabolic process. Under silicate stress, there would be less demand for energy from this metabolic process. Besides the possible connection between DA production and lipid synthesis (Section 4.4.3), energy availability was beneficial to DA production (Fig. 5.11C).

Domoic acid levels were slightly higher when nitrogen uptake was low (Fig. 5.12B). This phenomenon was significant in Experiment I. The DA production by *P. pungens f. multiseriis* was reduced when nitrogen (nitrate or ammonium) concentration in the medium was less than 110 μM (Bates *et al.*, 1993). However, in both Experiments I and II, nitrogen concentrations were never below 1000 μM . The reduced uptake rate was due to less demand for nitrogen at the low growth rate, and consequently, reduced energy consumption.

Domoic acid levels were also negatively correlated with phosphate uptake (Fig. 5.12C) although phosphate in the culture medium was never lower than 20 μM . In certain chemical respects, orthosilicate resembles orthophosphate, for example, they both react with ammonium molybdate to form a yellow complex (Section 2.5.2). Possible silicon-

phosphorus interactions have been investigated. In wheat plants, the uptake of silicate was slightly depressed in the presence of phosphate, while the uptake of phosphate was slightly enhanced when silicate was present (Rothbuhr and Scott, 1957). In *P. pungens* f. *multiseries*, uptake of phosphate was coupled with silicate. However, Experiment II cells contained twice as much phosphate as Experiment I cells (Tables 5.1a, b). The phosphate reserve was enhanced by silicate depletion. In Experiment I, DA concentration in the cultures increased when silicate as well as phosphate concentration decreased in the medium. This suggests that under phosphate limitation, DA production is also enhanced. Details of this aspect will be studied in Chapter 6.

In general, when growth declined, assimilation of carbon, nitrogen, phosphorus and silicate declined; there would be less demand for energy from those primary metabolic activities. Secondary metabolism, such as domoic acid synthesis, is favoured when this free energy is available.

CHAPTER 6

**PHOSPHATE LIMITATION AND DOMOIC ACID
PRODUCTION IN
CHEMOSTAT CONTINUOUS CULTURE**

6.1. Introduction

Domoic acid production is related to phosphorus (Figs. 1.4, 5.3). Phosphorus is one of the most important cell elements playing a key role in the synthesis of lipids (Siron *et al.*, 1989; Lombardi and Wangersky, 1991) and nucleotide (Cembella *et al.*, 1984). Recently, phosphorus has been shown to interfere with production of saxitoxins by *Alexandrium tamarense* (Boyer *et al.*, 1987; Anderson *et al.*, 1990).

Phosphate is a macronutrient in the environment. It is an important limiting factor to phytoplankton production in lakes and occasionally is a limiting factor to marine phytoplankton growth. In Cardigan Bay, PEI, when the amnesic shellfish poisoning episodes occurred in 1987, phosphate concentration in the seawater was low (<0.22 μM) and N:P ratios were high (41.2-81.5, Subba Rao *et al.*, 1988b).

In this chapter, I examined the effects of phosphate limitation on the growth, cell chemical composition and DA production of *P. pungens* f. *multiseriis* in continuous

culture and the extended batch mode. Production of DA in relation to cell bioenergetics and alkaline phosphatase activity was investigated under chemostat steady state continuous culture and extended batch culture conditions.

6.2. Materials and Methods

6.2.1. Chemostat system

The chemostat system was basically the same as that described in Section 2.10 (Fig. 2.1). Six chemostats were set up simultaneously. Glass carboys of 20 litre were used as the reservoir for the medium.

6.2.2. Preparation of culture medium and stock culture

Cardigan Bay sea water was collected at 5 m depth in 1989 and stored in light proof plastic barrels until required (> 1 year). Salinity of this sea water was adjusted to 27‰ (comparable to the salinity on site) by adding deionized water (Super Q). This sea water was then enriched to the levels of medium H (Table 2.2) with modification of silicate and phosphate concentrations. In the culture of *P. pungens* f. *multiseries* in standard medium H, silicate was usually depleted first. Therefore, the concentration of silicate was fortified to 245 µM to avoid silicate depletion during the experiments, and phosphate concentration reduced to 20% of normal (10.4 µM). This enriched seawater was then autoclaved in 10-litre glass carboys each containing 6 litre medium at 15 Psi for 20 minutes. Three carboys of this autoclaved medium were aseptically transfer to a pre-

autoclaved 20-litre glass carboy immediately after autoclaving and then cooled over 24-36 hours. This served as the reservoir medium.

In addition to the reservoir medium, small batches (250, 400 ml) of the medium with slightly higher phosphate concentration ($17.3 \mu\text{M}$) were prepared in 500 ml or 1000 ml Erlenmeyer glass flasks and autoclaved for 15 minutes. These flasks of medium were employed for stock cultures used to seed continuous cultures in the chemostat chambers.

Stock culture of *P. pungens* f. *multiseries* (strain KP-59) was grown at 15°C under $420 \mu\text{mol m}^{-2} \text{s}^{-1}$ for 18 days, subcultured every 6 days. A 50 ml culture was inoculated into a flask containing 250 ml medium.

6.2.3. Procedures for experiments

The chemostat systems were maintained at $15 (\pm 0.2)^\circ\text{C}$ under $290 (\pm 50) \mu\text{mol m}^{-2} \text{s}^{-1}$ continuous light. When the temperature of the system was steady, 300 ml of the stock culture was inoculated into each chamber containing 400 ml fresh medium (Fig. 6.1). The culture was agitated and aerated as described in Section 2.10 immediately after inoculation. Inflow of the fresh medium started 3 days later when significant growth of the culture was evident (visually checked), and continued for 25-35 days. Cultures were monitored daily by *in vivo* chlorophyll *a* fluorescence; the steady state was defined as a period of 5 days in which the coefficient of variation of chlorophyll *a* fluorescence was not greater than 5%. Inflow rate (dilution rate) was confirmed by measuring the effluent daily. When steady state was achieved, 250 ml culture was taken from each chamber. Subsamples were taken for domoic acid (DA), particulate phosphorus and silicon,

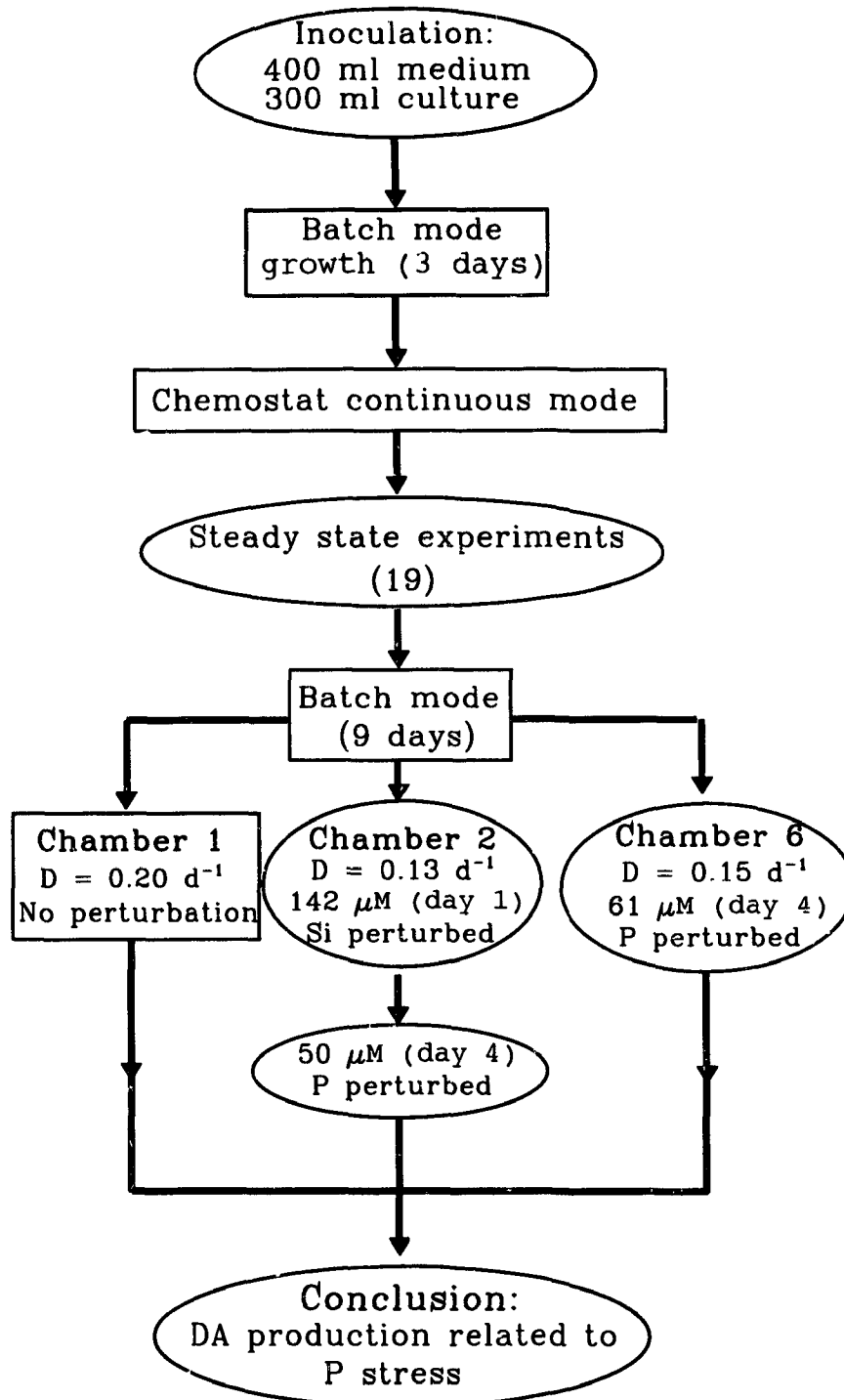


Fig. 6.1. Schematic illustration of procedures for experiments. See text for details.

particulate inorganic phosphate, chlorophyll *a*, particulate carbon and nitrogen, adenosine triphosphate (ATP), alkaline phosphatase activity (APA), and cell concentration measurements using the procedures described in Chapter 2. Filtrate (GF/F, 0.7 μm) was collected for DA and dissolved phosphorus and silicon measurements. Immediately after samples were taken, new dilution rates were established. The next steady state was usually attained in 7-9 days. A total of 19 steady state experiments were conducted from the 6 chemostats.

Immediately after the last steady state experiment, inflow of the reservoir medium was stopped and the cultures in Chambers 1, 2 and 6 were maintained under the same condition of light, temperature, aeration and agitation. The phosphate and/or silicate concentrations were perturbed in Chambers 2 and 6 (Fig. 6.1). In chamber 6, 61 μM of the phosphate was added on day 4. In Chamber 2, 142 μM silicate was added on day 1 and 50 μM phosphate was added on day 4. The cultures were kept in the batch mode for 9 days. Samples for analyses of DA, phosphate and silicate concentrations, cell concentrations and chlorophyll *a* concentration were collected daily. Other samples for particulate phosphorus and silicon, particulate inorganic phosphate, particulate carbon and nitrogen, ATP and APA were collected periodically.

6.3. Results

6.3.1. Steady states in continuous cultures

Steady state cell concentrations ranged from 8.1 to 16.7×10^7 cells l^{-1} and

increased as growth rate decreased (Table 6.1). Growth rate ranged from 0.06 to 0.62 d⁻¹, mostly <0.3 d⁻¹ (Fig. 6.2). The average growth rate of all the 19 steady state experiments was 0.25 (\pm 0.18) d⁻¹.

Growth kinetics were best described by equation 5.3 (Fig. 6.2). However, my data points were concentrated in the low growth rate portion. Direct fitting of equation 5.3 to the data points resulted in unreasonably higher values of μ_m' and K_U and huge coefficient of variation (71%-90%, Table 6.2). Therefore the highest μ_m' value, 1.10 from Chapter 5 was used as the high limit of μ_m' in the fitting, which yielded reasonable values with small standard deviations. The coefficients of variation were reduced to 2%-3.1%. The variance of fitting did increase, but the magnitude of increase was small (<8%).

Growth rate was coupled with carbon assimilation (P_m^B , Table 6.1). Growth rate increased as P_m^B increased from 0.53 to 4.46 $\mu\text{g C } [\mu\text{g Chl } a]^{-1} \text{ h}^{-1}$. This was consistent with the results earlier (Fig. 3.20, Table 5.1).

Growth rate was also correlated with phosphate and silicate concentration in the medium (Table 6.1). Dissolved phosphate increased from 0.00 to 2.97 μM while silicate increased from 1.90 to 194.1 μM as growth rate increased. When growth rate was >0.30 d⁻¹, it was most obvious that phosphate in the medium increased as growth rate increased. When growth rate <0.30 d⁻¹, on the other hand, phosphate in the medium did not change significantly (Fig. 6.3D). When growth rate was <0.14 d⁻¹, the total dissolved phosphorus slightly increased as growth decreased.

Domoic acid concentration in the culture (medium + cells) ranged from 2.2 to 474.8 $\mu\text{g l}^{-1}$, which was comparable with that in the silicate limited continuous culture

Table 6.1. Steady state experiments: measured variables, their statistics and their correlations with growth rate, DA production and concentration.

Parameters	Mean	Min	Max	Correlations (n=19)		
				Growth rate	DA prod.	Total DA
Growth rate (d ⁻¹)	0.25	0.06	0.62	1.00	-0.46	-0.57
P _m ^B (µg C [µg Chl a] ⁻¹ h ⁻¹)	1.62	0.53	4.46	0.89	-0.52	-0.55
APA (ng P [µg Chl a] ⁻¹ h ⁻¹)	79.02	16.14	194.82	-0.71	0.43	0.65
DA production (µg DA l ⁻¹ d ⁻¹)	12.31	0.99	42.42	-0.46	1.00	0.84
Total DA (µg l ⁻¹)	101.00	2.20	474.80	-0.57	0.84	1.00
Cellular DA (pg cell ⁻¹)	0.53	0.02	2.21	-0.60	0.85	0.99
DA in filtrate (µg l ⁻¹)	25.07	0.00	133.30	-0.54	0.71	0.96
10 ⁷ cells l ⁻¹	12.88	8.10	16.78	-0.65	0.58	0.51
Chl a (µg l ⁻¹)	60.32	23.01	102.30	-0.16	0.34	0.11
(pg Chl a cell ⁻¹)	0.49	0.14	0.99	0.20	-0.03	-0.18
PC (µM)	782.20	404.40	1122.90	-0.68	0.41	0.45
(pg C cell ⁻¹)	75.59	38.61	126.98	-0.07	-0.14	-0.04
PN (µM)	86.07	50.00	141.43	-0.50	0.48	0.41
(pg N cell ⁻¹)	9.66	4.45	15.15	0.07	0.05	-0.07
PSi (µM)	162.35	106.39	225.95	-0.62	0.44	0.42
(pg Si cell ⁻¹)	36.23	20.08	50.25	0.07	-0.21	-0.14
Dissolved reactive Si (µM)	63.50	1.90	194.10	0.80	-0.32	-0.46
PP (µM)	5.26	2.89	9.22	-0.42	0.19	0.09
(pg P cell ⁻¹)	1.31	0.60	2.23	0.11	-0.26	-0.31
Dissolved reactive P (µM)	0.84	0.00	2.97	0.94	-0.47	-0.45
Total dissolved P (µM)	1.64	0.51	4.61	0.76	-0.41	-0.30
Cellular PO ₄ pool (µM)	1.51	0.83	2.92	-0.31	0.02	-0.01
ATP (nM)	19.18	4.11	47.46	-0.43	0.21	0.12
(fmol ATP cell ⁻¹)	0.15	0.03	0.38	-0.30	0.01	-0.02
ATP+ADP+AMP (nM)	21.22	3.45	67.01	-0.44	0.22	0.15
Energy charge (%)	78.18	54.78	92.15	0.47	-0.27	-0.25

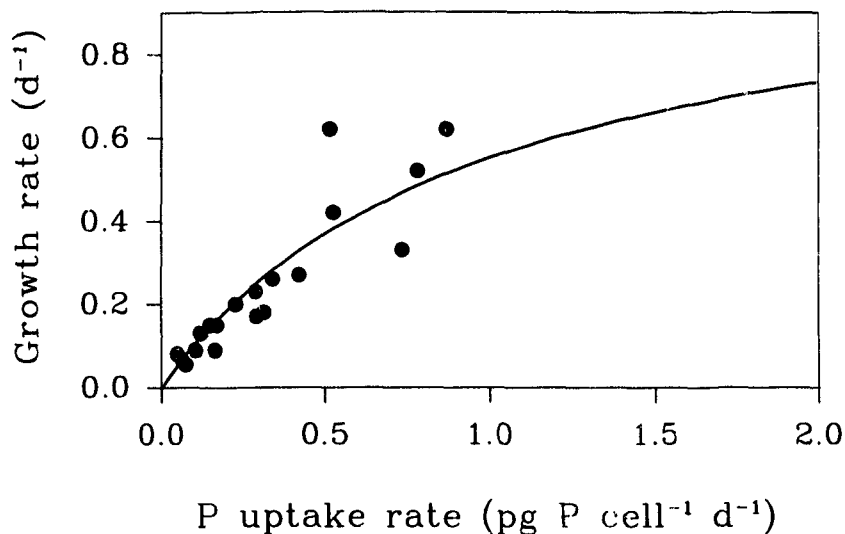


Fig. 6.2. Relationship of growth rate and phosphate uptake rate during the continuous culture. μ_m' is fixed at 1.10 d^{-1} (the maximum μ_m' from Chapter 5). $\mu = \mu_m' U/(K_U + U)$.

Table 6.2. Fitted values of Fig 6.2. During fitting, an up-limit of 1.10 d^{-1} (the μ_m' value from Chapter 5) was applied in comparison with the values obtained by directly fitting. Values in the parentheses are standard deviations of fitting.

Parameter	With limit	No limit
μ_m' (d^{-1})	1.10(0.022)	1.99(1.41)
K_U ($\text{pg P cell}^{-1} \text{ d}^{-1}$)	0.99(0.031)	2.18(1.960)
Variance of fitting	0.003291	0.00305

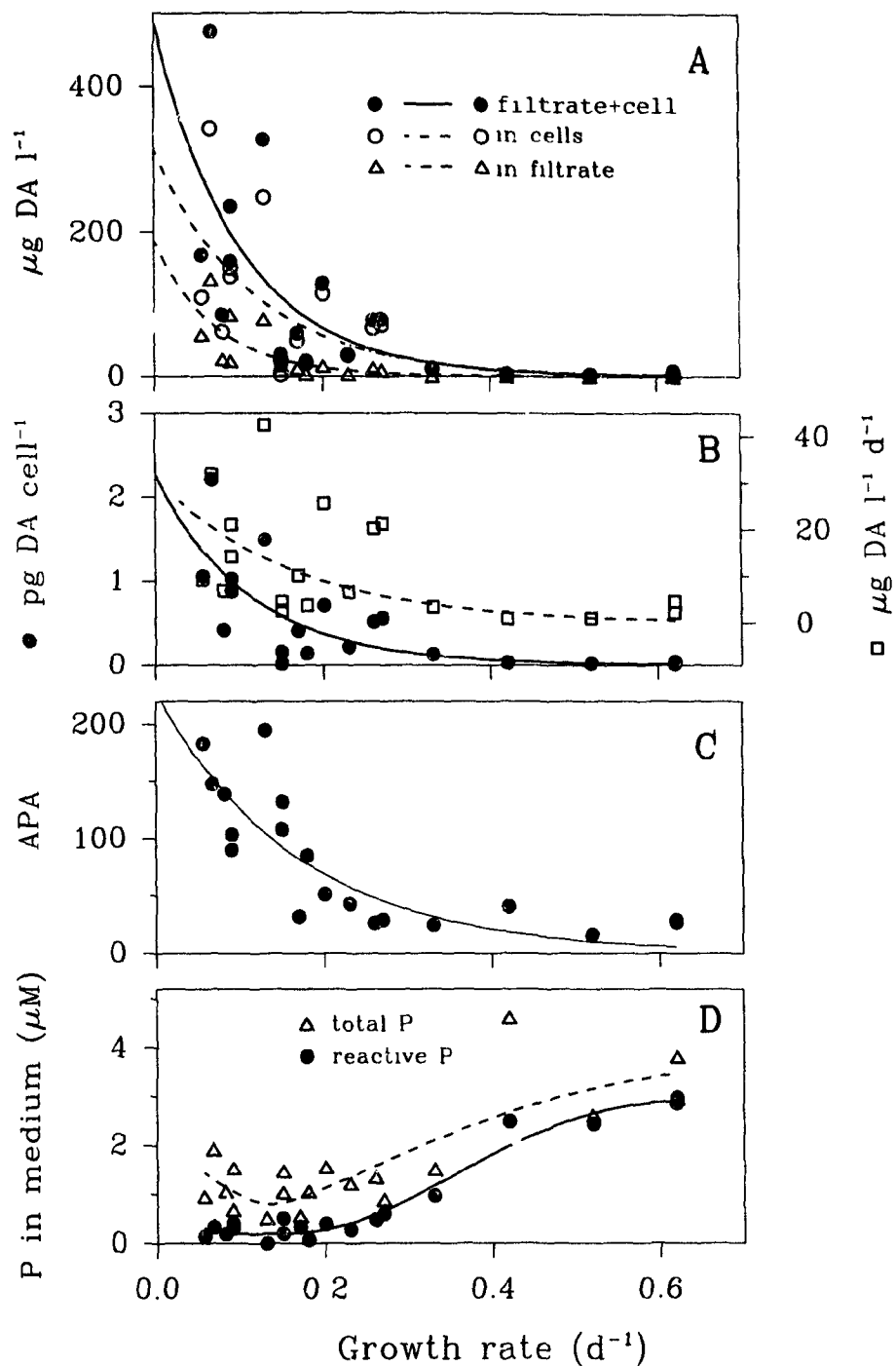


Fig. 6.3. Variation with growth rate in the steady state experiments. (A) domoic acid concentration, (B) cellular DA and its production, (C) alkaline phosphatase activity (APA, $\text{ng P } [\mu\text{g Chl } a]^{-1} \text{ h}^{-1}$), and (D) dissolved phosphorus. The curves in A, B, C are fitted by Equation 5.1 and those in D are fitted by eye.

(Chapter 5). The cellular DA levels ranged from 0.02 to 2.21 pg cell⁻¹, which were higher than those in Experiment I, but lower than those in Experiment II of the silicate limited continuous culture (Tables 5.1, 5.2). Similarly, DA production rates were 0.99-42.42 µg l⁻¹ d⁻¹ (0.012-0.257 pg DA cell⁻¹ d⁻¹), less than Experiment II value but more than those from Experiment I of the silicate limited cultures.

Concentration and production of DA were positively correlated with cell concentration, chlorophyll *a*, particulate carbon, nitrogen and silicon and APA, but negatively correlated with growth and carbon assimilation (Table 6.1). At growth rates less than 0.3 d⁻¹, DA concentration and production rate increased when growth rate decreased. At higher growth rates (> 0.3 d⁻¹), on the other hand, no change in DA occurred in relation to growth rate (Figs. 6.3A, B).

Similarly, alkaline phosphatase activity (APA) was low when growth rate was high. There was a threshold at growth rate of 0.3 d⁻¹ (Fig. 6.3C), larger than that, APA was less than 60 ng P [µg Chl *a*]⁻¹ h⁻¹ as a result of sufficient phosphate in the medium (>0.9 µM, Figs. 6.3C, D). When growth rate was lower than 0.3 d⁻¹, on the other hand, APA increased exponentially although there was detectable phosphate in the culture medium.

APA was directly related to phosphate concentration in the culture medium (Fig. 6.4). When phosphate in the culture medium was less than 1 µM, APA increased drastically from 24 to 192 ng P [µg Chl *a*]⁻¹ h⁻¹. When phosphate concentration exceeded 1.0 µM, on the other hand, APA remained relatively constant and low regardless the change of growth rate. This suggested that APA was an indicator of severity of

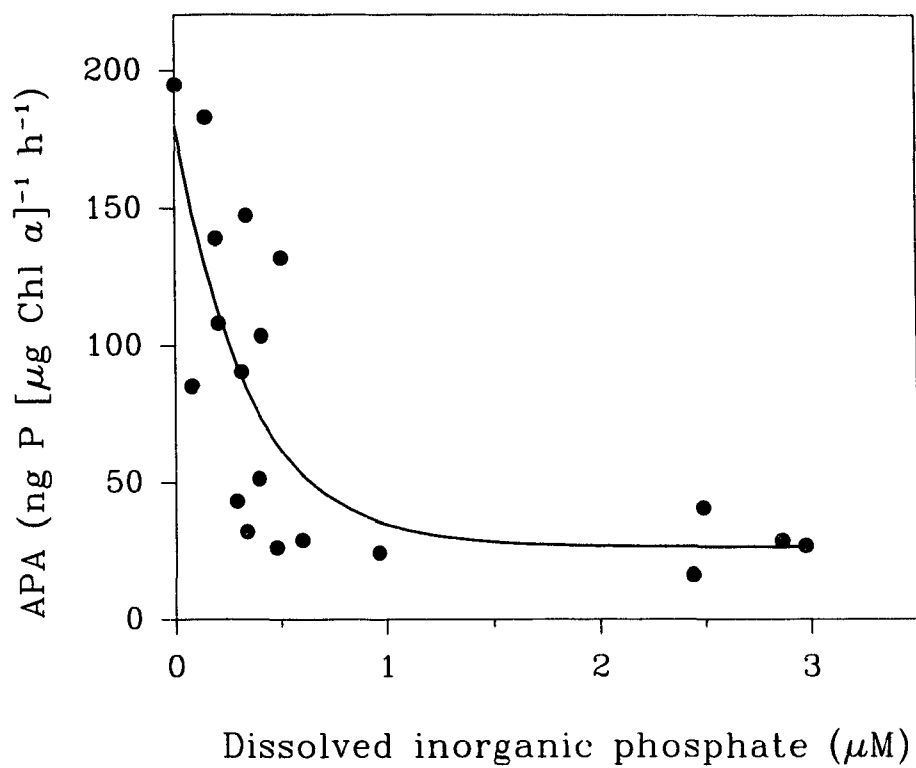


Fig. 6.4. Relationships between alkaline phosphatase activity (APA) and dissolved inorganic phosphate. The curve is fitted by Equation 5.1.

phosphate limitation and that 15 of the 19 steady states in this experiment were phosphate limited.

Domoic acid concentration was correlated with APA (Fig. 6.5, $p < 0.05$). Generally, values above $60 \text{ ng P } [\mu\text{g Chl } a]^{-1} \text{ h}^{-1}$ corresponded to high DA concentration with greater variation. The relationships between DA and N:P ratios was similar. High values of N:P (> 14) corresponded with high DA concentration (Fig. 6.6). These suggested that DA production corresponded with phosphate limitation.

Under phosphate limitation, the growth rate and the overall primary cell metabolism (P^B_m , N, P and Si uptake, etc.) were low, but DA concentration and its production were high (Fig. 6.7). This suggested a change in the energy partitioning between primary and secondary metabolism under phosphate limitation. When the growth rate was lower than 0.3 d^{-1} , ATP and total amount of ATP+ADP+AMP were generally higher but variable, which is unique in this diatom. However the adenylate energy charge (EC) was generally lower (Fig. 6.8) when growth rate was low, which was consistent with other microalgae (Cembella *et al.*, 1984). When growth rate was lower than 0.14 d^{-1} the concentration of ATP and ATP+ADP+AMP decreased, which coincided with an increase in total dissolved phosphorus. This suggested that cells were severely stressed and released phosphorus into the culture medium.

6.3.2. Principal component analysis

Table 6.1 shows that growth rate, DA concentration and its production correlated with cell concentration, dissolved phosphate and silicate and other chemical and biological

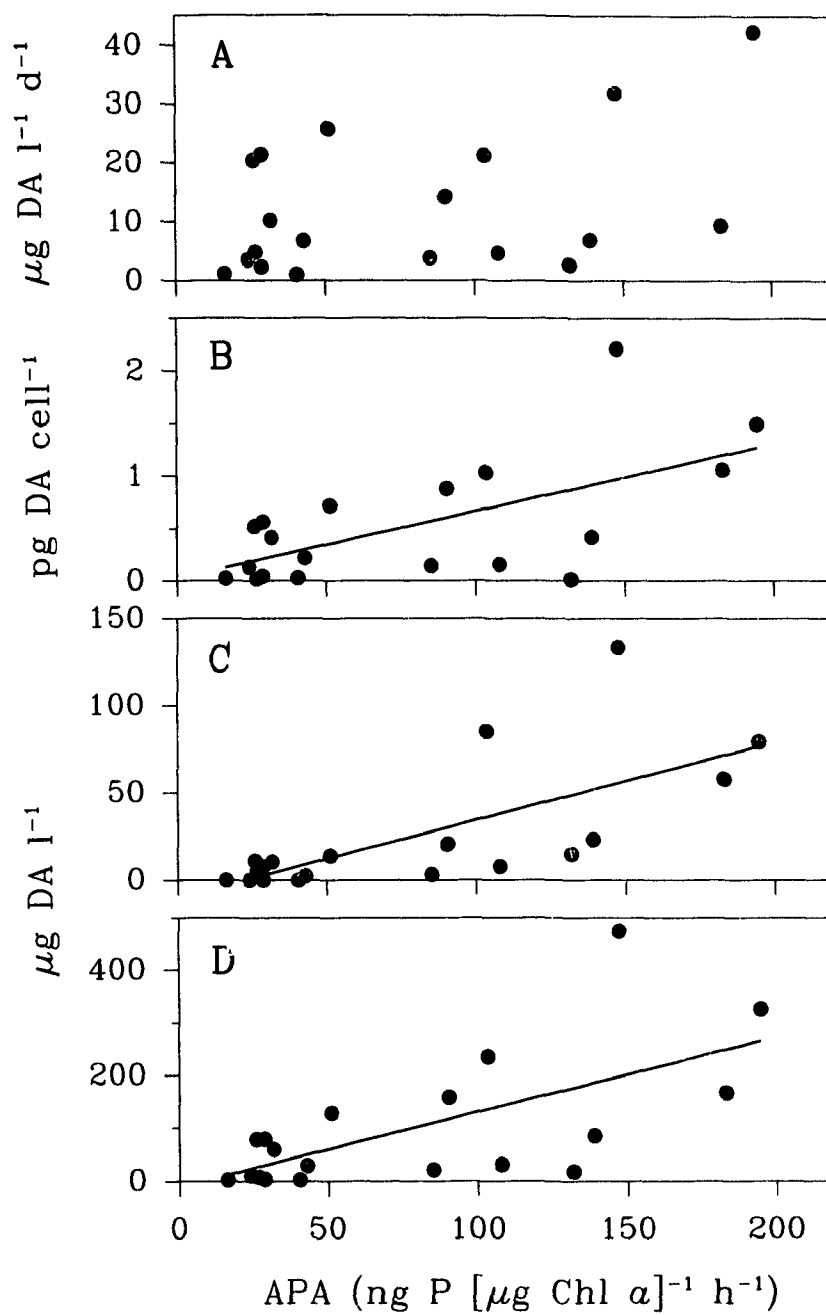


Fig. 6.5. Relationships of alkaline phosphatase activity to (A) DA production, (B) cellular DA, (C) DA in the filtrate, and (D) total DA in continuous cultures. The lines are linear regressions.

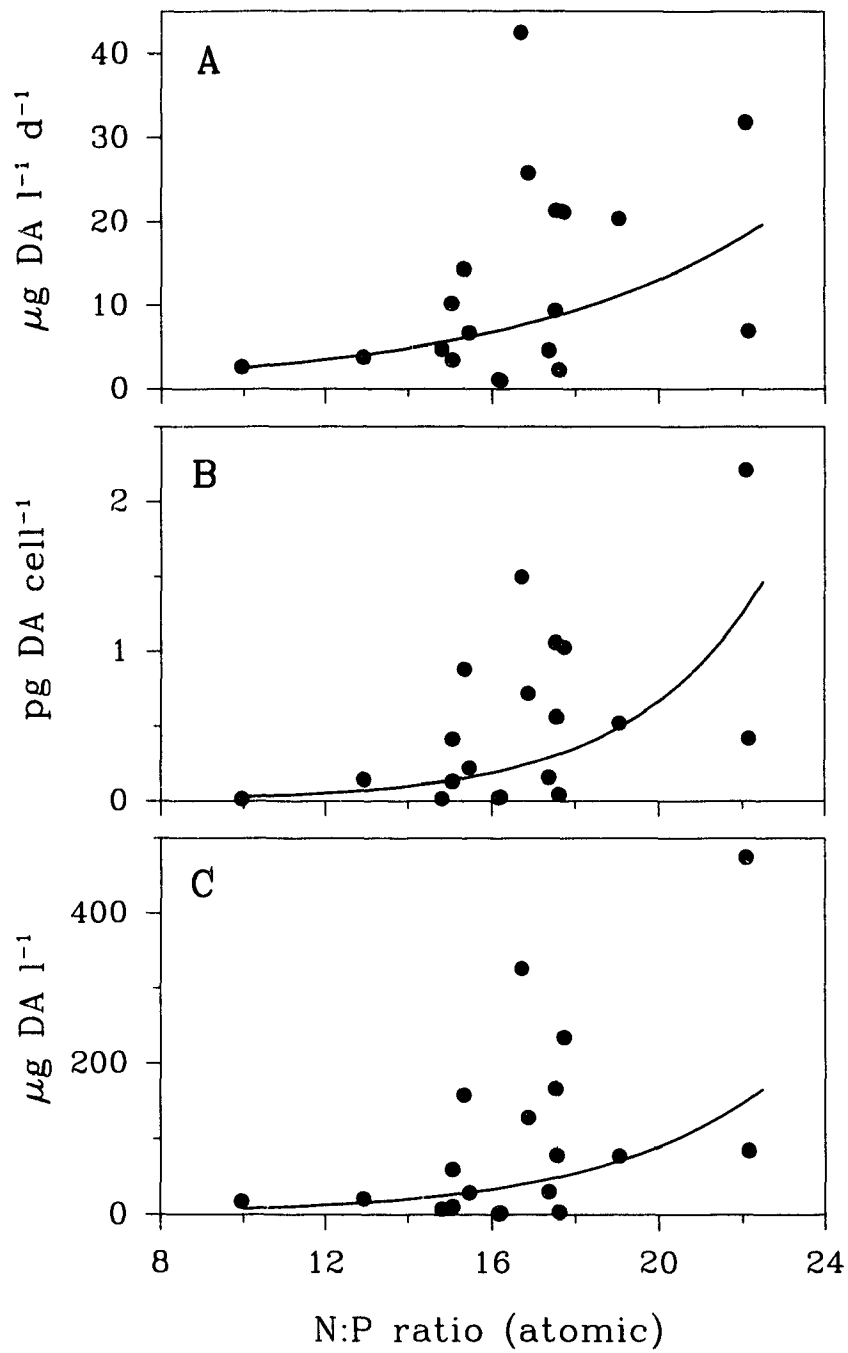


Fig. 6.6. Relationships of N:P (atomic) ratios to (A) DA production, (B) cellular DA, and (C) total DA in continuous cultures. Curves fitted by eye.

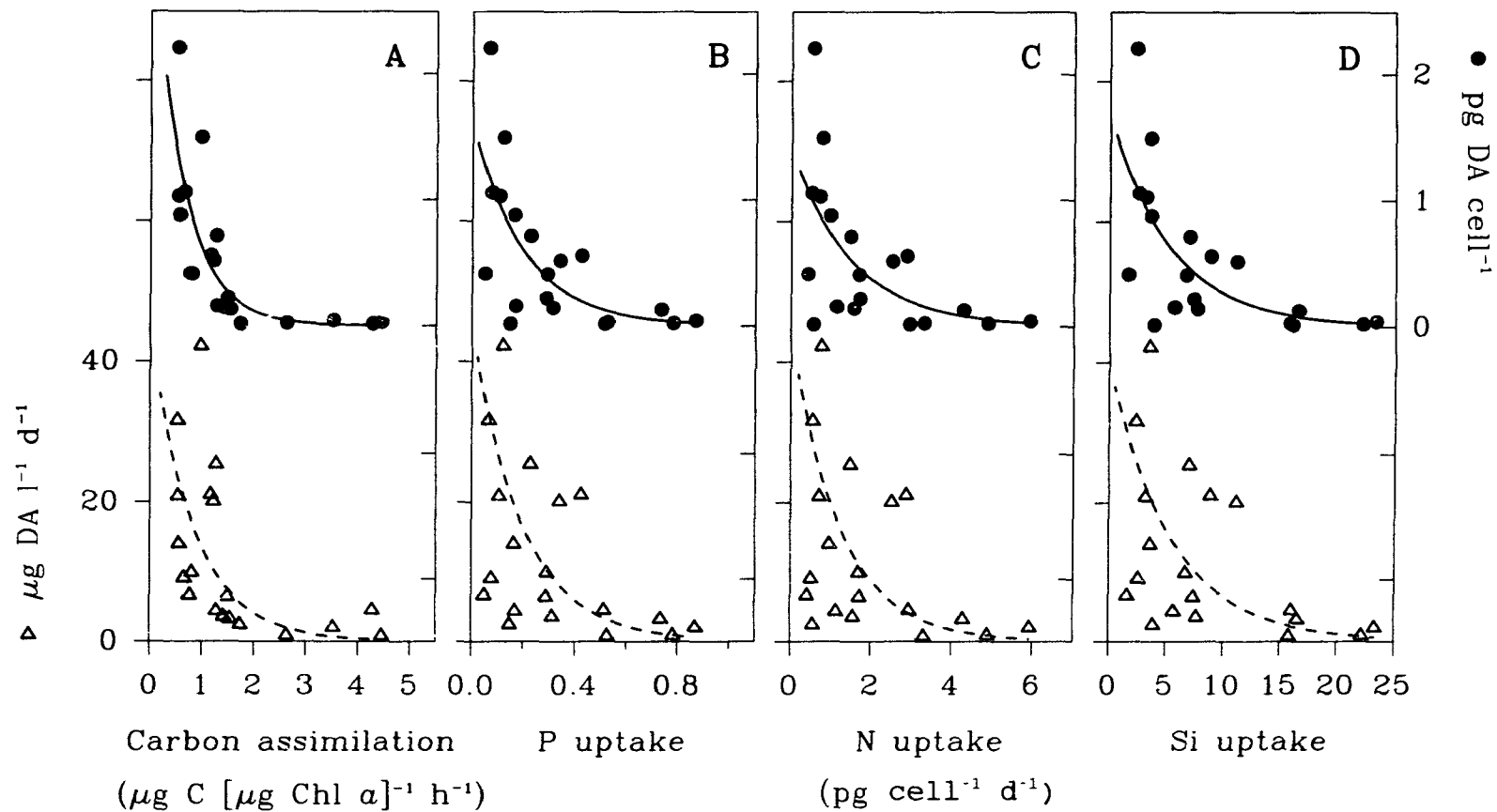


Fig. 6.7. Relationship of cellular DA (filled circle) and DA production (open triangles) with (A) carbon assimilation, uptake of (B) phosphate, (C) nitrate and (D) silicate in continuous cultures. Curves fitted by Equation 5.1.

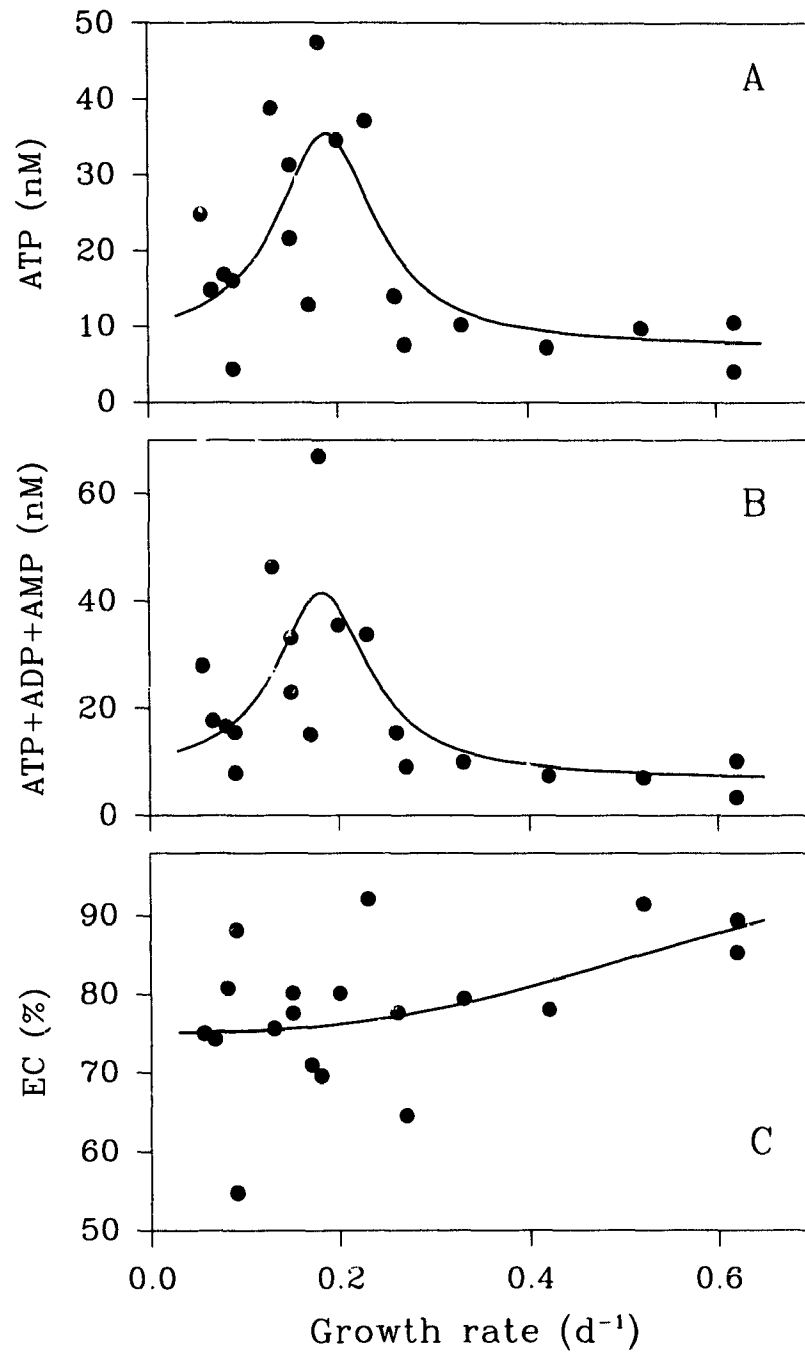


Fig. 6.8. Relationships of growth rate to (A) ATP, (B) ATP+ADP+AMP, and (C) adenylate energy charge (EC) in continuous cultures. Curves fitted by eye.

Table 6.3. Steady state experiments: results of principal component analysis of observed variables showing percentage of variance and correlation coefficients (n=19, significant level = 0.43).

Component	PC1	PC2	PC3	PC4	PC5
% variance	50	25	11	7	3
Cells ml ⁻¹	-0.31	-0.28	0.56	-0.24	0.25
APA	-0.29	-0.41	-0.08	0.53	-0.22
DIP	0.44	0.05	0.06	0.03	-0.67
PP	-0.01	0.58	-0.38	-0.07	0.23
DISi	0.39	0.13	0.44	-0.24	-0.04
PSi	-0.39	0.23	0.22	-0.25	-0.55
PC	-0.39	0.29	-0.02	0.28	-0.22
PN	-0.32	0.43	0.29	0.02	0.07
ATP	-0.27	-0.27	-0.45	-0.68	-0.18

parameters. However, use of linear regression analysis to relate biological properties could be highly suspectable due to multicollinearity problems introduced by high levels of correlations between the observed variables (Subba Rao and Smith, 1987), in this case between biomass and residual nutrient levels. Principal component analysis (Harris, 1985) of these biological and chemical parameters (except for the growth rate, DA concentration and its production) was applied to examine the integrated effect of these variables on growth and toxin productions. The first principal component (PC1) explained 50% of the variance, which was primarily contributed by dissolved inorganic phosphate (DIP); and secondarily by dissolved inorganic silicate (DISi), particulate silicon (PSi) and carbon (PC) (Table 6.3). Comparison of the newly derived variables, specifically the scores of

PC1, with the growth rate, DA concentration and its production showed high correlations ($p < 0.01$), positively with growth rate and negatively with DA and its production (Fig. 6.9). The patterns of the relationship of DA concentration and its production with PC1 resembled those with growth rate (Figs. 6.3, 6.9).

The results of principal component analysis were consistent with those of correlation analysis (Tables 6.1, 6.3). It was concluded that growth and DA production were mainly controlled by phosphate or silicate concentration in the culture medium.

6.3.3. *Extended batch mode*

When the supply of medium from the reservoir was stopped, the magnitude of increase in cell concentration was dependent on the previous steady state growth rate. In Chamber 1 (Fig. 6.10), the growth rate in the previous steady state was 0.20 d^{-1} . Cell concentration increased from 11 to $18 \times 10^7 \text{ cells l}^{-1}$ in 4 days at a slightly reduced rate ($\sim 0.12 \text{ d}^{-1}$). However, chlorophyll *a* concentration did not increase, but decreased after day 3 probably due to the exhaustion of phosphate in the culture medium.

Domoic acid increased continuously at an average production rate of $74.7 \mu\text{g DA l}^{-1} \text{ d}^{-1}$ ($0.480 \text{ pg DA cell}^{-1} \text{ d}^{-1}$), which was about 3 times of the previous steady state rate ($25.7 \mu\text{g DA l}^{-1} \text{ d}^{-1}$, or $0.170 \text{ pg DA cell}^{-1} \text{ d}^{-1}$). However, the enhanced production gradually increased during the first 4 days from 56.3 to $142.0 \mu\text{g DA l}^{-1} \text{ d}^{-1}$ (0.427 to $0.854 \text{ pg DA cell}^{-1} \text{ d}^{-1}$), followed by a reduction.

APA increased continuously from $51.6 \text{ ng P } [\mu\text{g Chl } a]^{-1} \text{ h}^{-1}$ on day 0 to $388.8 \text{ ng P } [\mu\text{g Chl } a]^{-1} \text{ h}^{-1}$ on day 9. Dissolved phosphate slightly increased during the first 2 days

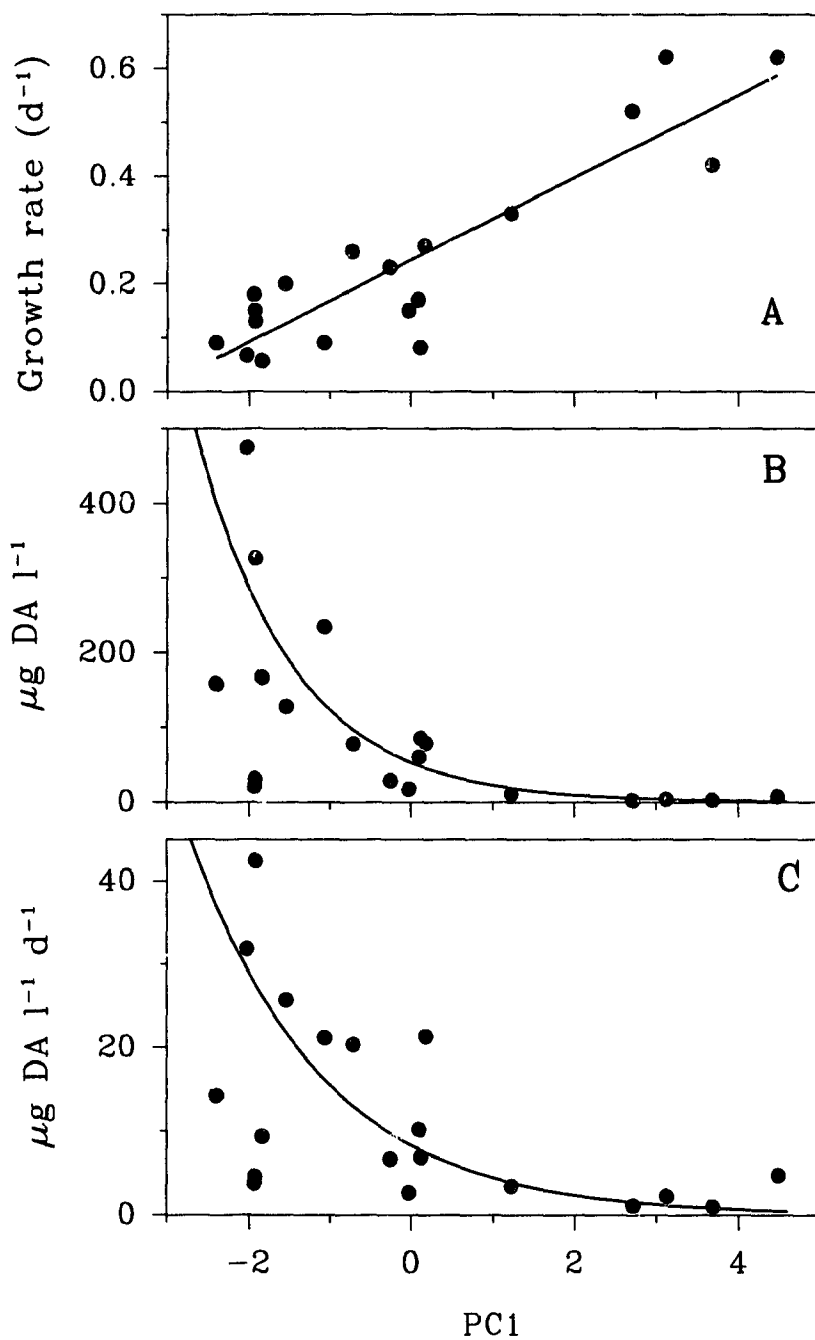


Fig. 6.9. Variations of (A) growth rate, (B) total DA in the culture and (C) DA production in relation to the scores of first principle component (PC1. Table 6.3) in continuous cultures. The line in A is linear regression and the curves in B and C are fitted by Equation 5.1.

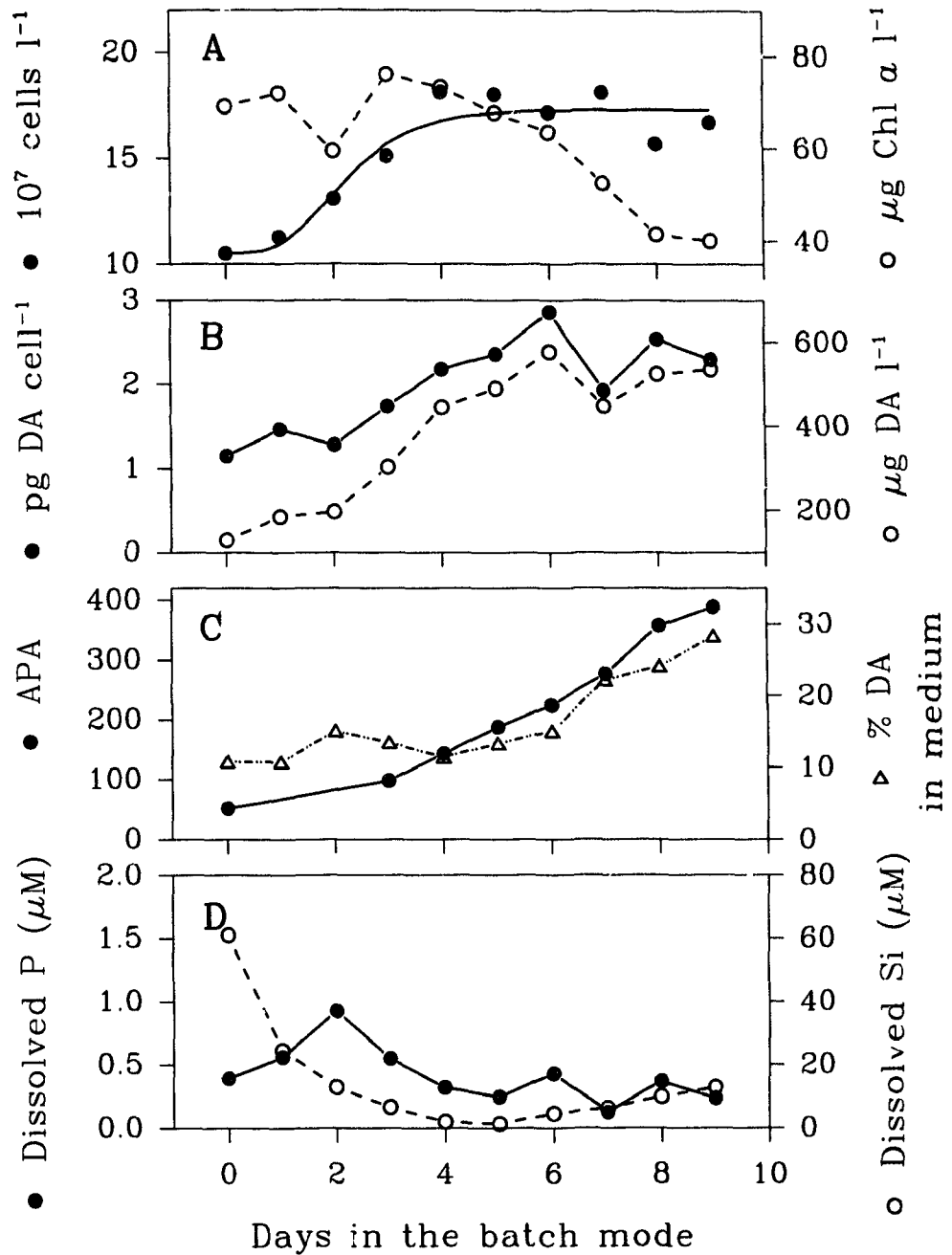


Fig. 6.10

Chamber 1 in the extended batch mode. Variations with time in (A) biomass [concentrations of cell (left) and chlorophyll *a* (right)], (B) DA [cellular DA (left) and its production (right)], (C) APA [ng P [μg Chl *a*] $^{-1}$ h^{-1} , left] and percentage of DA in the medium, and (D) dissolved phosphorus (left) and silicate (right).

(from 0.39 to 0.92 μM) and then decreased to a low on day 4 (0.32 μM). Phosphate concentration remained low from day 4 onwards (0.12-0.43 μM).

Silicate concentration in the medium decreased drastically from 61.03 μM on day 0 to 1.95 μM on day 4. From day 5 onwards, silicate concentration gradually recovered from 1.28 to 12.77 μM coincident with a decrease in particulate silicon from 233.25 to 223.45 μM . This again, suggested dissolution of cell silicon, consistent with the results from silicate limited experiments (Chapters 4, 5).

In Chamber 6 (Figs. 6.1, 6.1'), the previous growth rate was 0.15 d^{-1} . Phosphate concentration in the medium remained low (0.20-0.71 μM) during the first 4 days. Phosphate was perturbed on day 4 to a concentration of 61.36 μM , and subsequently remained high (>48.89 μM). The immediate response to phosphate perturbation was APA (Figs. 6.11C, D), which increased continuously from 108.0 $\text{ng P } [\mu\text{g Chl } a]^{-1} \text{ h}^{-1}$ on day 0 to 267.0 $\text{ng P } [\mu\text{g Chl } a]^{-1} \text{ h}^{-1}$ on day 4 and then decreased to 130.2 $\text{ng P } [\mu\text{g Chl } a]^{-1} \text{ h}^{-1}$ immediately after the perturbation. Silicate concentration decreased from 24.91 to 1.87 during the first 4 days and remained low (<3.38 μM) afterwards.

Cell concentration increased from 14.7 to 26.9 $\times 10^7$ cells l^{-1} during the 4 days, subsequently it decreased due to the exhaustion of silicate in the medium although phosphate was perturbed on day 4. On the other hand, chlorophyll *a* concentration did not change during the first 4 days but increased from day 4 onwards due to the perturbation of phosphate in the culture medium.

Domoic acid increased continuously at an average rate of 31.15 $\mu\text{g DA } \text{l}^{-1} \text{ d}^{-1}$ (0.132 $\text{pg DA cell}^{-1} \text{ d}^{-1}$). The production also continuously increased from 4.6 $\mu\text{g DA } \text{l}^{-1}$

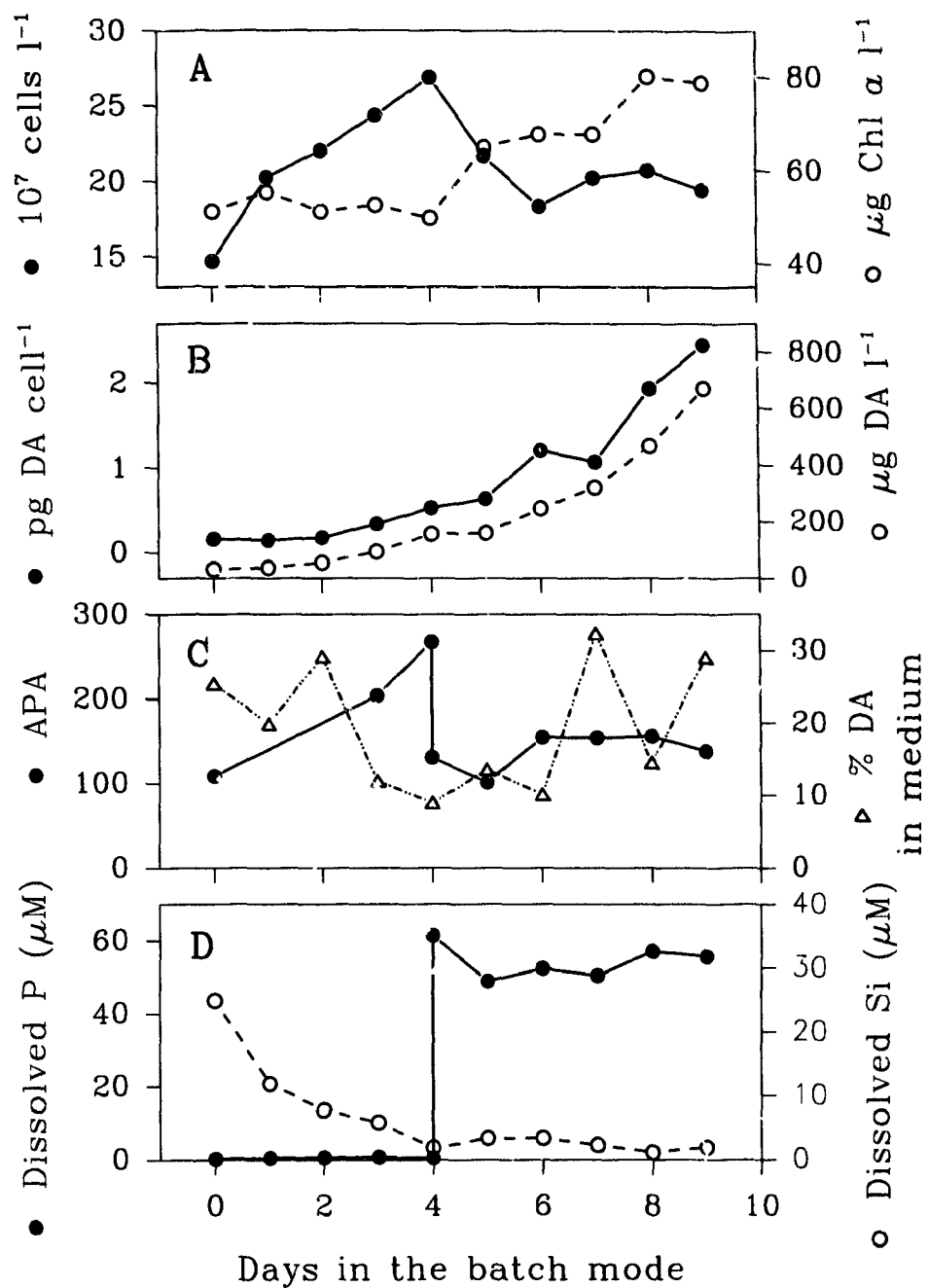


Fig. 6.11. **Chamber 6** in the extended batch mode. Legend as Fig. 6.10. **(D)** 61 μM phosphate was added to the culture on day 4.

d^{-1} ($0.31 \text{ pg DA cell}^{-1} \text{ d}^{-1}$) at steady state to $62.3 \text{ } \mu\text{g DA l}^{-1} \text{ d}^{-1}$ ($0.243 \text{ pg DA cell}^{-1} \text{ d}^{-1}$) on day 4. However, the production was interrupted on day 4 due to the perturbation of phosphate, but resumed one day later at higher rate ($87.3 \text{ } \mu\text{g DA l}^{-1} \text{ d}^{-1}$, $0.436 \text{ pg DA cell}^{-1} \text{ d}^{-1}$) coincident with the exhaustion of silicate in the medium. The production rate increased continuously to $201.7 \text{ } \mu\text{g DA l}^{-1} \text{ d}^{-1}$ ($1.004 \text{ pg DA cell}^{-1} \text{ d}^{-1}$) at the end of the experiments. Note the further enhancement of DA production when the culture was switched from phosphate limitation to silicate limitation.

At lower steady state growth (0.13 d^{-1}) in Chamber 2 (Fig. 6.12), phosphate in the culture medium was completely exhausted ($0.00 \text{ } \mu\text{M}$) but slightly increased during the first day ($0.50 \text{ } \mu\text{M}$). Phosphate concentration remained low ($<0.61 \text{ } \mu\text{M}$) during the first 4 days but after perturbed on day 4 to $49.96 \text{ } \mu\text{M}$, it remained high ($>28 \text{ } \mu\text{M}$). Silicate concentration decreased from 26.15 to $7.92 \text{ } \mu\text{M}$ during the first day, but on day 1, addition of silicate raised the concentration to $150.04 \text{ } \mu\text{M}$. Surprisingly, silicate concentration did not decrease but gradually increased to $173.34 \text{ } \mu\text{M}$ on day 4. After addition of phosphate on day 4, silicate concentration gradually decreased to $56.22 \text{ } \mu\text{M}$ by the end of the experiment.

Domoic acid concentration increased from 326.3 to $526.5 \text{ } \mu\text{g l}^{-1}$ ($1.215 \text{ pg DA cell}^{-1} \text{ d}^{-1}$) during the first day. The production was drastically reduced to $32.8 \text{ } \mu\text{g l}^{-1} \text{ d}^{-1}$ ($0.399 \text{ pg DA cell}^{-1} \text{ d}^{-1}$) during the following day immediately after the silicate addition. The DA production resumed on day 3 and day 4 at a rate of $126 \text{ } \mu\text{g DA l}^{-1} \text{ d}^{-1}$ ($0.839 \text{ pg DA cell}^{-1} \text{ d}^{-1}$). Immediately after phosphate addition on day 4, DA production was interrupted again, reduced to $13.2 \text{ } \mu\text{g DA l}^{-1} \text{ d}^{-1}$ ($0.169 \text{ pg DA cell}^{-1} \text{ d}^{-1}$). However, DA

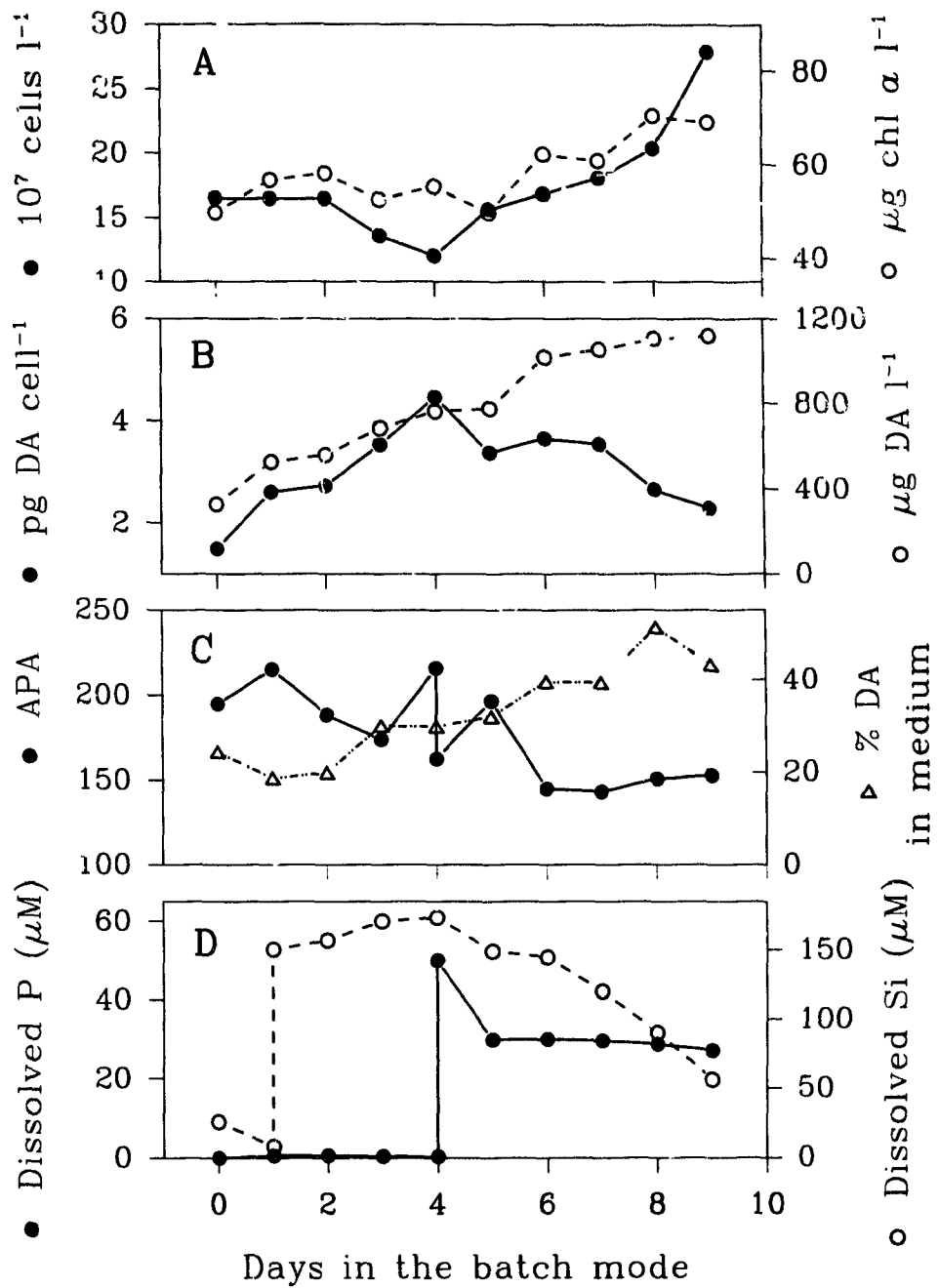


Fig. 6.12. **Chamber 2** in the extended batch mode. Legend as Fig. 6.10. **(D)** 142 μM of silicate was added to the culture on day 1 and 50 μM phosphate on day 4.

production resumed at a higher rate ($241.3 \mu\text{g DA l}^{-1} \text{d}^{-1}$, or $1.487 \text{ pg DA cell}^{-1} \text{d}^{-1}$) the next day (day 6), reduced again to $37 \mu\text{g DA l}^{-1} \text{d}^{-1}$ ($0.212 \text{ pg DA cell}^{-1} \text{d}^{-1}$) on day 7. The DA production did not recover but gradually decreased from day 7 onwards because neither phosphate nor silicate was limiting during this period.

Note, APA decreased gradually from 215.2 to 173.8 ng P [$\mu\text{g Chl } a$] $^{-1} \text{h}^{-1}$ after silicate addition and increased again on day 3 to 215.9 ng P [$\mu\text{g Chl } a$] $^{-1} \text{h}^{-1}$ on day 4 right before phosphate perturbation. APA decreased to 162.2 ng P [$\mu\text{g Chl } a$] $^{-1} \text{h}^{-1}$ immediately after the phosphate addition.

Cell concentrations slightly decreased after silicate perturbation but chlorophyll *a* concentration did not change significantly. After phosphate perturbation, both cell concentration and chlorophyll *a* increased gradually.

6.4. Discussion

6.4.1. Growth and DA production

Domoic acid was produced when growth declined. This was consistent with the results from batch (Chapter 4) and silicate limited continuous cultures (Chapter 5). The production was significantly enhanced (up to $42.4 \mu\text{g DA l}^{-1} \text{d}^{-1}$, $0.257 \text{ pg DA cell}^{-1} \text{d}^{-1}$) when growth rate was below 0.3 d^{-1} (Fig. 6.3). When growth rate was above 0.3 d^{-1} , on the other hand, DA production remained relatively constant and low ($1.0\text{-}4.7 \mu\text{g DA l}^{-1} \text{d}^{-1}$, $0.012\text{-}0.043 \text{ pg DA cell}^{-1} \text{d}^{-1}$).

At low growth rates ($< 0.3 \text{ d}^{-1}$), there was still detectable phosphate in the medium.

APA, an indication of levels of phosphate limitation, increased as did DA production when growth rate decreased. When growth rate was above 0.3 d^{-1} , however, APA was low as a result of the increase of phosphate in the medium. This suggested that DA production correlated with the severity of phosphate limitation.

Similarly, during the extended batch period, DA production significantly enhanced (by a factor of ≥ 3) soon after inflow of medium from the reservoir was stopped although the cells were still dividing (Figs. 6.10, 6.11, 6.12). Production of DA was interrupted immediately after addition of phosphate or silicate. The magnitude of enhancement in DA production at the beginning of the batch mode and the interruption of DA production by silicate and phosphate addition were in agreement with the results from the extended batch mode after silicate limited steady state studied in Chapter 5 (Section 5.3.3).

Soon after phosphate perturbation in Chamber 6 (Fig. 6.11), particulate phosphorus increased from 5.08 to $18.91 \mu\text{M}$ (or 0.59 to $2.70 \text{ pg P cell}^{-1}$). Subsequently, phosphate uptake by the cells was not significant as evident by the relative constant values of phosphate in the medium (48.89 - $57.04 \mu\text{M}$, Fig. 6.11D) and particulate phosphorus (16.04 - $18.91 \mu\text{M}$, or 2.56 - $2.70 \text{ pg P cell}^{-1}$). Domoic acid production, on the other hand, resumed one day after phosphate addition at a higher rate ($87.3 \mu\text{g DA l}^{-1} \text{ d}^{-1}$, $0.463 \text{ pg DA cell}^{-1} \text{ d}^{-1}$) and continued at a gradually accelerated rate (up to $201.7 \mu\text{g DA l}^{-1} \text{ d}^{-1}$, $1.004 \text{ pg DA cell}^{-1} \text{ d}^{-1}$). Similarly in Chamber 2 (Fig. 6.12), DA production was interrupted immediately after the phosphate addition and resumed one day later, but the DA production was low during the subsequent period. The differences in DA production during this period was probably because the former culture was simultaneously stressed

by silicate limitation but the later culture was not.

Production of DA resumed for one day in Chamber 2 probably resulted from the accumulation of DA precursors before the phosphate perturbation. The available energy would be channelled to phosphate uptake, therefore, there would be a short supply of energy for DA production and the production would be restrained. Soon after part of the energy was released, when phosphate uptake "*stopped*", DA production resumed until the available precursor was reduced. At this moment, cells were dividing as a result of sufficient phosphate and silicate in the medium. This period in Chamber 2 was similar to the early exponential phase in the batch culture. Therefore, DA production was diminished.

It is very interesting to note that DA production was interrupted immediately after silicate addition on day 1 in Chamber 2 (Fig. 6.12). Simultaneously, phosphate was limiting. The same energy partitioning theory for phosphate perturbation was applicable to the situation after silicate perturbation. Particulate silicate increased from 166.14 to 232.53 μM (or 27.36 to 39.58 $\mu\text{g Si cell}^{-1}$), while DA production reduced from 200.2 to 32.8 $\mu\text{g DA l}^{-1} \text{d}^{-1}$ (1.215 to 0.399 $\mu\text{g DA cell}^{-1} \text{d}^{-1}$). The silicate uptake rate was greatly reduced, but DA production gradually resumed to 126 $\mu\text{g DA l}^{-1} \text{d}^{-1}$ (0.839 $\mu\text{g DA cell}^{-1} \text{d}^{-1}$) one day after the perturbation (Figs. 6.12B, D).

During the continuous culture mode, when phosphate limitation relaxed in the culture, carbon assimilation increased from 1.5 to 4.5 $\mu\text{g C} [\mu\text{g Chl } a]^{-1} \text{h}^{-1}$ as the growth rate increased from 0.29 to 0.62 d^{-1} . The DA production was not significant when the culture was neither limited by phosphate nor by silicate. When the growth rate was less

than 0.30 d^{-1} , on the other hand, P_m^B was less than 1 ($0.53\text{-}0.97$) $\mu\text{g C} [\mu\text{g Chl } a]^{-1} \text{ h}^{-1}$ and DA production was significantly enhanced.

When growth rate decreased as the result of more severe phosphate limitation, Domoic acid concentration increased both in the cells and in the culture medium (Fig. 6.3A). The percentage of domoic acid in the culture medium increased significantly and ranged from 13% to 85% of total DA when the growth rate was less than 0.14 d^{-1} (Fig. 6.3A). Similarly in the batch mode, the proportion of DA in the culture medium increased from 11% to 28.3% in Chamber 1 (Fig. 6.10C), and up to 32 and 51.2% in Chambers 6 and 2 respectively (Figs. 6.11C, 6.12C). The proportion of DA in the culture medium appeared not to be affected by short term perturbation. This increase of DA in the medium was consistent with results from silicate limited continuous culture (Figs. 5.2, 5.4). Under severe phosphate limitation cell membranes might not be properly formed due to the short supply of phosphorus for the formation of lipid bilayer of the cell membrane which mainly consists of phospholipid. The resistance to the trans-membrane DA transportation might be damaged under severe phosphate stress so that DA could pass the membrane freely due to its water solubility.

6.4.2. *N:P ratios and DA production*

Table 6.4 shows cellular chemical compositions and their correlations with growth and DA production and indicates that DA production significantly correlated with N:P ratios in the cells. The concentration of nitrate (Table 2.2) and phosphate in the inflow medium were 1765 and $10.4 \mu\text{M}$ respectively resulting in a N:P ratio of 170. The Si:P

ratio in the inflow medium was 23.6. These high ratios allowed the culture to exhaust phosphate in the medium at maximum population size and created a phosphate limited environment. At this moment, the maximum particulate nitrogen in the steady state sample was 141.4 μM . Thus the dissolved nitrogen in the medium would be more than 1620 μM which resulted in extremely high values of N:P ratios, > 545.

The cellular N:P ratios in the steady state, however, changed very little, compared to the ratio in the medium. The N:P ratios ranged from 9.95 to 22.2, comparable to those from the silicate limited cultures with the mean ratios close to the optimum ratios of 10:1 proposed by Redfield *et al.* (1963). This does not necessarily mean the cultures were in the optimum N:P conditions. Optimum N:P ratios for different species typically range from 7 to 53 (Cembella *et al.*, 1984). For *P. pungens f. multiseries*, the optimum N:P ratio is around 10:1 as the uptake of phosphate did not occur in the batch culture until the cellular N:P ratios reached 10 (Pan, unpublished). After phosphate perturbation, N:P ratios dropped from 16-19 to 6-7 which coincided with the interruption of DA production in both Chambers 2 and 6. However, the continuous low ratio of N:P did not prevent the culture from producing DA in Chamber 6 because the culture was stressed by low silicate in the medium. Under more severe phosphate stress, the maximum N:P ratios of *P. pungens f. multiseries* cells was 23.3. This suggested that the N:P ratios in this diatom were conservative, which is unique in the phytoplankton. In *Thalassiosira pseudonana*, a marine diatom (Perry, 1976), N:P ratios ranged from 6.4 under nitrogen limitation to 61.1 under phosphate limitation. In *Scenedesmus* sp. a freshwater alga (Rhee, 1978), cell N:P ratios followed the N:P ratios in the inflow medium within the range of 5 to 80.

Nevertheless, one factor should not be ignored in the interpretation of the result, the phosphate concentration in the inflow medium may be still too high to create sufficiently severe phosphate stress. Although silicate concentration was fortified to 245 μM , it may still be too low to allow severe phosphate stress because silicate concentration in the medium was very low (1.89 μM) at the low growth rate 0.081 d^{-1} . But, during the extended batch mode in Chamber 2 (Fig. 6.12), cell N:P ratios did not increase after silicate addition on day 1. Still, DA production significantly correlated with cellular N:P ratios (Fig. 6.6, $p < 0.05$, $n=19$).

Production of triglycerides, a storage class of lipids is triggered in diatoms by phosphate as well as silicate limitation (Lombardi and Wangersky, 1991; Siron *et al.*, 1989; Healey and Hendzel, 1975). Parts of the biosynthetic cycle of lipids are different under silicate stress (Lombardi and Wangersky, 1991). However, Parrish *et al.* (1991) found that in batch culture of *P. pungens f. multiseries* under silicate limitation, lipid synthesis was not enhanced but a reduction was evident in late stationary phase. From the slope of the lines (broken) in Figs. 6.11B and 6.12B, we can see that DA production was triggered under stress of both nutrient limitations, up to 200 $\mu\text{g DA l}^{-1} \text{d}^{-1}$ (1.215 $\text{pg DA cell}^{-1} \text{d}^{-1}$) under phosphate limitation and to 202 $\mu\text{g DA l}^{-1} \text{d}^{-1}$ (1.004 $\text{pg DA cell}^{-1} \text{d}^{-1}$) under silicate limitation. This suggested that DA production was probably related to lipid synthesis because they have common precursors such as acetyl-CoA at the early stage of syntheses (Fig. 1.4). When DA production was vigorous under severe phosphate or silicate limitation, these precursors might be used for DA production instead of lipid synthesis in *P. pungens f. multiseries*.

Table 6.4. Steady state cultures: cellular chemical compositions and their correlation with growth rate, domoic acid and its production. Values of C:Chl *a*, N:Chl *a*, Si:Chl *a* and P:Chl *a* are $\mu\text{g}:\mu\text{g}$, and the rest are molar ratios.

Ratios	Mean	Min	Max	Correlation		
				Growth rate	DA prod.	Total DA
C:Chl <i>a</i>	172.00	103.40	279.60	-0.32	-0.25	0.07
N:Chl <i>a</i>	21.56	14.63	33.03	-0.20	-0.23	0.09
Si:Chl <i>a</i>	85.62	40.74	184.09	-0.11	-0.30	-0.05
P:Chl <i>a</i>	3.00	1.70	6.97	-0.09	-0.39	-0.20
ATP:Chl <i>a</i>	0.34	0.04	0.81	-0.39	-0.06	0.02
P:ATP	449.00	126.00	2109.00	0.08	-0.02	-0.03
C:N	9.21	7.85	13.90	-0.32	-0.16	0.02
C:Si	4.85	3.47	6.60	-0.24	0.11	0.11
C:P	153.39	102.96	243.70	-0.32	0.19	0.36
Si:N	1.93	1.32	2.94	0.01	-0.30	-0.15
Si:P	31.65	23.26	40.33	-0.16	0.21	0.43
N:P	16.62	9.95	22.15	-0.19	0.44	0.52

The enhancement of DA production in phosphate-limited cultures of *P. pungens* *f. multiseriens* is similar to that in the production of saxitoxin by *Alexandrium tamarense* (Hall, 1982; Boyer *et al.*, 1987; Anderson *et al.*, 1990). Toxin content in P-limited *A. tamarense* dramatically increased at the beginning of stationary phase, reaching levels 2 to 3 times higher than that observed in control and nitrogen-limited cultures (Boyer *et al.*, 1987). The high toxin content may be attributed partly to the generally larger cells from P-limited culture (Alam *et al.*, 1979; Boyer *et al.*, 1987), but the magnitude of increase

in toxin (by a factor of 2-3) was higher than that in cell size (by a factor of 1.5). Low phosphate batch culture of *A. fundyense* showed a very high toxin production rate (161 fmol cell⁻¹ d⁻¹).

6.4.3. Phosphate limitation and cellular chemical composition

Cellular chlorophyll *a* decreased under phosphate limitation compared to phosphate unlimited cultures (Chapters 3,4,5). During the extended batch period in Chamber 1 (Fig. 6.10), chlorophyll *a* concentration drastically decreased after day 3 when the culture was severely phosphate limited. Soon after phosphate perturbations in Chambers 6 and 2, chlorophyll *a* concentration gradually increased in spite of the decrease (Fig. 6.11) or increase (Fig. 6.12) in cell concentrations. Decrease in cellular chlorophyll *a* under nutrient stress has also been well documented in other diatoms, such as *Chaetoceros gracilis* (Lombardi and Wangersky, 1991), *C. curvisetus* and *Skeletonema costatum* (Finenko and Krupatkina-Akinina, 1974) under phosphate limitation, *Phaeodactylum tricornutum* (Roy, 1988) under nitrogen stress. In other diatoms however, cellular chlorophyll *a* content seems unaffected by phosphate stress (Cembella *et al.*, 1984). Under silicate limitation, on the other hand, cellular chlorophyll *a* increased in *P. pungens* f. *multiseries* (Chapter 5) and *Chaetoceros gracilis* (Lombardi and Wangersky, 1991).

Cellular C:Chl *a* was comparable to the results from high light batch culture experiment (Chapter 3) but was much lower (by a factor of 3) than silicate limited continuous culture (Table 5.3). This is due to the high content of carbon under silicate limitation (Tables 5.1, 5.2). In the extended batch mode in Chamber 1, for example,

silicate became exhausted in the medium after day 5, cellular carbon increased from 73 to 89 pg C cell⁻¹ and the trend for Chamber 6 was similar.

Although phosphate was the limiting factor, P:Chl *a* ratios (3.0 ± 1.16) were slightly higher than in silicate limited cultures (2.32 ± 0.45). This suggested that cellular phosphate was conservative but chlorophyll *a* was sensitive to phosphate limitation. However, this was also because that cellular chlorophyll *a* increased under silicate limitation but decreased under phosphate limitation.

Cellular nitrogen was lower (9.66 ± 2.64) than those of phosphate unlimited batch (Chapter 3) and continuous cultures (Chapter 5). Generally, P-deficiency leads to a decline of protein in phytoplankton cells, which is due to temporary impairment of protein synthesis (Cembella *et al.*, 1984). However, N:Chl *a* ratios (21.56 ± 5.07) were higher than silicate limited cultures (15.64 ± 3.89). This suggested cellular chlorophyll *a* was more sensitive to phosphate limitation than cellular nitrogen.

Cellular silicon ranged from 20.08 to 50.25 pg Si cell⁻¹, comparable to that in silicate limited steady state chemostat culture (Table 5.1). Si:Chl *a* ratios, however were 3 times higher than those in the severely silicate-limited cultures (Table 5.2b).

Although the culture was phosphate limited, cellular ATP (0.15 ± 0.09 fmol ATP cell⁻¹) was comparable with silicate limited culture (0.16 ± 0.08 fmol ATP cell⁻¹), but was higher than the cultures which were neither limited by silicate nor by phosphate (0.11 ± 0.07 fmol ATP cell⁻¹). *P. pungens* f. *multiseries* appears to be unique in this respect. Usually, cellular ATP of microalgae decreases under phosphate or other nutrient stress (Cembella *et al.*, 1984). However in the case of *P. pungens* f. *multiseries*, the pattern was

the opposite. This unique feature and its involvement in the DA production will be further discussed in Section 6.4.5.

6.4.4. Alkaline phosphatase activity and DA production

The presence of phosphate in the culture inhibited alkaline phosphatase activity (APA) in *P. pungens* f. *multiseries*. APA remained low ($<50 \text{ ng P } [\mu\text{g Chl } a]^{-1} \text{ h}^{-1}$) when phosphate concentration in the culture medium was over $1 \mu\text{M}$ at growth rate over 0.3 d^{-1} and at a phosphate supply rate larger than $2.1 \mu\text{mol l}^{-1} \text{ d}^{-1}$ (Figs. 6.3, 6.4). On the other hand, when growth rate was below 0.3 d^{-1} or phosphate supply rate was less $2.1 \mu\text{mol l}^{-1} \text{ d}^{-1}$, APA increased continuously with a decrease of phosphate in the medium. Addition of phosphate to the culture inhibited but did not suppress APA (Figs. 6.11, 6.12). In Chamber 6 (Fig. 6.11), for example, phosphate concentration reached $61.4 \mu\text{M}$ after perturbation and then decreased to $48.9 \mu\text{M}$ the next day due to the uptake by the cells. APA decreased from 267 to $130.2 \text{ ng P } [\mu\text{g Chl } a]^{-1} \text{ h}^{-1}$ immediately after perturbation and further decreased to $100.86 \text{ ng P } [\mu\text{g Chl } a]^{-1} \text{ h}^{-1}$ the next day. In Chamber 2 (Fig. 6.12), on the other hand, APA increased during the next day after a drastic decrease due to phosphate perturbation.

Such a puzzling phenomenon can be explained by difference in the phosphate demand by cell metabolism in these two populations after perturbation. In Chamber 6, the uptake was merely to replace the previous phosphate debt; the population growth was inhibited by silicate limitation simultaneously. Cellular phosphorus increased from 0.53 to $2.44 \text{ pg P cell}^{-1}$. In Chamber 2, however, high APA was due to the uptake of

phosphate for the replacement of the previous debt as well as for supplying phosphate for population growth. The population size increased by 3.6×10^7 cells l^{-1} because no other limitation existed.

Production of DA was interrupted in both Chambers 6 (Fig. 6.11) and 2 (Fig. 6.12), while cellular DA decreased in Chamber 2 but not in Chamber 6. In Chamber 6, it would be more reasonable that DA production not be interrupted because it was limited by silicate simultaneously. However, the interruption implied the existence of a time lag for transition of the population from phosphate to silicate limitation and the accompanying transition of the mechanism of DA production. Different mechanisms of DA production are associated with phosphate and silicate stresses. This difference probably paralleled their difference in the cycle of lipid synthesis discussed earlier. This merits further investigation. The other explanation would be that the available energy was partitioned to phosphate uptake, which will be discussed in section 6.4.5. The toxin production resumed at a greater rate and continuously increased after the surge uptake of phosphate stopped, but APA did not increase. Silicate limitation was under the way during this period and stimulated DA production.

In Chamber 2, APA decreased from 214.8 to 188.4 ng P [$\mu\text{g Chl } a$] $^{-1}$ h $^{-1}$ immediately after silicate perturbation on day 1 when silicate concentration in the medium increased from 7.9 to 150 μM (Fig. 6.10). Production of DA was restrained for 2 days, the rate being reduced from 200 $\mu\text{g DA } l^{-1} d^{-1}$ ($1.215 \text{ pg DA cell}^{-1} d^{-1}$) to 33 $\mu\text{g DA } l^{-1} d^{-1}$ ($0.399 \text{ pg DA cell}^{-1} d^{-1}$) and then gradually recovered. This is probably due to the chemical similarity between phosphate and silicate; e.g. they both react with ammonium

molybdate during analysis to form the yellow complex (Section 2.5). In the silicate-limited chemostat culture, under the same phosphate supply conditions, severe silicate limitation increased cellular phosphorus by a factor of 2 (Table 5.1b compared with Table 5.1a). Detailed mechanism remains obscure.

The relationship of DA concentration with APA is similar to the syntheses of other secondary metabolites such as antibiotics streptomycin by *Escherichia coli* (Martin, 1977). Formation of most other antibiotics, such as neomycin by *Streptomyces fradiae*, vancomycin by *S orientalis* and ristomycin by *Proactinomyces fructiferi* var. *ristomicini*, are also positively correlated to APA and repressible by inorganic phosphate. This suggests that similarity exists between DA production and other secondary metabolism.

6.4.5. Relationships between DA production and other primary metabolism (energy partitioning)

Synthesis of requires metabolic energy (Fig. 1.4). The same energy source is shared by primary metabolism. When primary metabolism, such as carbon assimilation, or synthesis of protein or DNA, are vigorous as cells are actively dividing, the high demand of free energy from these metabolic processes will reduce the supply of same energy for secondary metabolism such as DA production. Therefore, DA was generally produced when overall cell metabolic activity declined due to phosphate or silicate limitation. Cellular DA content and its production increased when carbon assimilation, phosphate, nitrate and silicate uptake declined (Fig. 6.7).

Cellular ATP or the ratios of ATP to other cell elements has been frequently used

to indicate cell bioenergetic state and degree of phosphate limitations in phytoplankton (Cembella *et al.*, 1984). During phosphate stress, cellular ATP may be depressed to a fraction of the value found in the exponentially growing cells (Healey, 1979). ATP levels in P-deficient cells may be, nevertheless, more than those under light- or N-limited conditions (Karl, 1980). In this study on *P. pungens* f. *multiseries*, however, cellular ATP level decreased when growth rate increased in the steady state (Table 6.1, Fig. 6.8), and this was also comparable with the levels in silicate limited cells (Table 5.1). The trend in the extended batch mode was similar; cellular ATP decreased after phosphate perturbation. It suggests a high demand of energy from primary metabolism when it is very active. In this respect, this diatom is unique.

Production of DA shares the energy source with primary metabolism. Under phosphate or silicate stress, the high content of free energy in the form of ATP is favourable for DA production. The production was interrupted due to phosphate or silicate perturbation during the extended batch mode, and then the production resumed after a day or so. Uptake of phosphate (Cembella *et al.*, 1984) and silicate (Lewin, 1955) are energy-requiring processes. When the uptake rates were high, most free energy was partitioned to uptake of phosphate or silicate leading to a decrease in the cellular ATP content and adenylate energy charge (EC) upon phosphate or silicate perturbation. After the surge of uptake following phosphate and silicate perturbation, cellular phosphorus increased by a factor of 5, then uptake decreased, i.e. the competition for the available free energy was reduced and DA production resumed. After the surge uptake of silicate, however, DA production resumed gradually because silicate uptake was still carrying on

at reduced rate.

In Chamber 2 (Fig. 6.12), although neither phosphate nor silicate was limiting after phosphate perturbation on day 5 and APA was low, the toxin production resumed at a higher rate for one day and then drastically decreased. This strongly suggested that availability of phosphate and silicate did not suppress DA production, but uptake of them competed for energy with the toxin production immediately after silicate or phosphate perturbation. As discussed earlier (Section 6.4.1), no significant uptake of phosphate or silicate was evident one day after the perturbation, which reduced the energy demand from these metabolic processes and was favourable for DA production. The resumed DA production was probably due to 1) decrease in energy demand from phosphate uptake or other primary metabolism, 2) accumulation of DA precursors.

CHAPTER 7

GENERAL DISCUSSION:

BIOCHEMICAL AND

ECOLOGICAL PERSPECTIVES

Production of domoic acid has been associated with physiological stress resulting from silicate (Chapters 4 and 5) and phosphate (Chapter 6) limitation, or with decline of growth. A change in the partitioning of biogenic energy and precursors between primary and secondary metabolism appears to be the main mechanism initiating DA production.

Decline of growth in the late exponential phase of batch culture is probably due to self-limiting regulation. During the post μ_m period, the cells reduce their division rate in response to a reduction in resources, in this case silicate, or probably to the accumulation of extracellular excreta, which inhibit growth. During this period, self-shading was not evident because significant decrease in light will result in increase in cellular chlorophyll *a* content (Chapter 3), which did not happen in the culture. The final cell yield was proportional to the added silicate, which also suggested that light was not a limiting factor. The cells may have adjusted their internal metabolism according to the changed environment. Therefore, this self-limiting regulation is both intrinsic and extrinsic. These growth kinetics suggest that *P. pungens* f. *multiseries* is probably a "K" strategist. This will be further discussed in Section 7.3.4.

Domoic acid production is greatly enhanced when a severe stress is applied after a period of active growth. The production is accelerated by a factor of 3 during the transition period from steady state growth to batch mode (Chapters 5 and 6) when growth is slowed and uptake of silicate or phosphate diminished. There was a similar trend in the early work by Bates *et al.* (1989, Table 3 in their paper). Although the authors did not mention it, their data showed higher maximum cellular domoic acid (pg DA cell⁻¹) associated with shorter duration in the exponential phase and higher population size in the stationary phase. This suggests that the accumulation of energy and precursors generated during the period of active growth is important for DA production under stress at later stages.

DA production is interrupted when growth or other specific metabolism resumes. During the perturbation experiments (Chapters 4-6), for example, DA production was reduced when the stress was eased when active uptake of nutrients, and growth, were resumed.

7.1. Biochemical perspective

The domoic acid molecule consists of two parts (Fig. 1.2). They are derived from glutamate and a C₁₀ geranyl pyrophosphate (Laycock *et al.*, 1989; Douglas *et al.*, 1992) respectively. These two parts are then condensed to form a proline ring and release 4 phosphates for each domoic acid molecule (Fig. 1.4). Biosynthesis of isopentenyl pyrophosphate from acetyl-CoA requires 2 NADPH and 3 ATP for each molecule of

isopentenyl pyrophosphate formed. This process is strongly energy consuming. The other part, glutamate derivative, is synthesized originally from α -oxoglutarate, which may be derived from the Krebs cycle (Douglas *et al.*, 1992). It is obvious that biosynthesis from α -oxoglutarate, the immediate precursor of glutamate, to proline, which requires 3 NADPH and 2 ATP molecules (Fig. 1.4), is also a high energy consumer. This part is believed to be accomplished during the period of DA production (Douglas *et al.*, 1992).

Physiological stress due to phosphate or silicate limitation restricts population growth leading to less energy demand from primary metabolism. This facilitates the synthesis of the two precursors, which are then condensed into domoic acid.

As pointed out earlier (in this chapter), active growth prior to DA synthesis is important in the production process. Exponential growth produces early precursors and assimilates energy in the form of carbon storage products (Chapter 3). The large amount of carbon assimilated during the exponential phase is not only beneficial for later survival of the population but also to DA production. Some of the precursors of DA may be produced during the exponential phase. For example, Douglas *et al.* (1992) labelled batch cultures of *P. pungens* f. *multiseries* with (1- ^{13}C -, or 1,2- ^{13}C -) acetate at the onset of, and during, the stationary phase. They found that only a very small proportion (<4.3%) of ^{13}C was incorporated into the isoprenoid part of the DA molecule, but a larger proportion (14.5-30.6%) was found in the glutamate part. Douglas *et al.* (1992) concluded that the isoprenoid precursor was probably synthesized during the period before the addition of the labelled acetate, i.e. probably during the exponentially growing period.

However, isoprenoid might be synthesized through other pathways, such as those

suggested by Luckner (1984) and Mann (1987). A number of C₅ acid (base of isoprenoid) aldehydes occur naturally and were considered as possible precursors of the isoprenoids (Mann, 1987). Isoprenoid is usually formed from acetyl-CoA, but its derivation from leucine, an α amino acid, has been found in animals and higher plants (Luckner, 1984).

Cessation of growth is not essential to DA production. Domoic acid is produced in continuously dividing cells in steady states under either phosphate or silicate limitation. Furthermore, DA production rate is higher (0.55 - 90.35 $\mu\text{g DA l}^{-1} \text{d}^{-1}$, 0.0067 - 1.35 $\text{pg DA cell}^{-1} \text{d}^{-1}$) during steady state growth (Chapters 5, 6) than that in batch cultures (0.97 - 30.20 $\text{fg DA cell}^{-1} \text{d}^{-1}$, see Chapter 4, Subba Rao *et al.* 1990 and Bates *et al.* 1991, 1993). However, the production rate is highest (up to 200 $\mu\text{g DA l}^{-1} \text{d}^{-1}$, 3.17 $\text{pg DA cell}^{-1} \text{d}^{-1}$) during batch mode after steady state growth. These differences in the production rate strongly suggest that biogenic energy and precursors during the period of growth are important in DA production. A continuous supply of energy and early precursors facilitates better DA production in the steady state under silicate or phosphate stress.

During the period of batch mode after steady state growth, when the stresses are more severe and growth declines, DA production is markedly enhanced. In batch culture (Chapter 4), DA is produced during late exponential phase (first stage) or in the stationary phase when silicate is severely limiting (second stage). The DA production rate of the second stage is much higher (0.36 - 3.8 $\mu\text{g DA l}^{-1} \text{d}^{-1}$, 5.14 - 30.20 $\text{fg DA cell}^{-1} \text{d}^{-1}$) than that of the first stage (0.06 - 0.19 $\mu\text{g DA l}^{-1} \text{d}^{-1}$, 0.97-3.67 $\text{fg DA cell}^{-1} \text{d}^{-1}$). This implies two types of conditions associated with DA production (Table 7.1) Type I condition is

essential to DA production and occurs when ambient nutrients are moderately low, while Type II condition promotes high DA production when an ambient nutrient is exhausted and the stress is severe.

Table 7.1. Characteristics of two types of conditions for DA production

Characteristics		Type I	Type II
DA production rate		Low	High
Nutrient concentration		Low	Depleted
Cell division		Yes	Yes or No
Source of the effects		External and Internal	External
Examples	Batch (Chapter 4)	First stage	Second stage
	Continuous (Chapter 5)	Experiment I	Experiment II

Condensation of the two precursors into domoic acid releases 2 pyrophosphates (or 4 phosphates). Therefore, physiological stress due to phosphate limitation not only diminishes the energy demand from primary metabolism, but also creates a low phosphate environment, which in turn feeds back to stimulate the condensation process.

There is a difference between silicate-limited (Chapter 5) and phosphate-limited (Chapter 6) cultures in the kinetics of DA production during the batch mode period after steady state growth. In the silicate-limited cultures, surge DA production is the highest during the first day after initiation of batch mode and the production declines gradually during the following 3 days. In the phosphate-limited cultures, on the other hand, the surge DA production increases gradually during first 3 or 4 days. As time progresses, the

culture becomes more severely phosphate limited, which facilitates a better feedback, creating circumstances for the condensation process in DA production.

7.2. Bioenergetics in relation to DA production

As discussed earlier (in this chapter as well as in Chapters 5 and 6), biogenic energy plays an important role in DA production. It is possibly unique to this diatom that free energy in the form of ATP increases when growth decreases. This is favourable for DA production.

The linkage between DA production and photosynthesis is obvious. Domoic acid is produced during the period of photosynthesis but stops 2 hours after transition from light to dark (Bates *et al.*, 1991). Addition of DCMU blocks the electron transport from photosystem II to photosystem I, phosphorylation is inhibited; simultaneously DA production is impeded. This suggested that photophosphorylated NADPH and ATP might be directly used for DA production.

Carbon assimilation is highest during the mid-exponential phase of batch culture (Chapter 3) and at high dilution rates in the continuous cultures (Chapters 5 and 6) when growth and other cell metabolic activities are most pronounced. Assimilation of each molecule of CO₂, requires 3 molecules of ATP and 2 of NADPH, generated from the photophosphorylation reaction (Devlin and Witham, 1983). During the period of high carbon assimilation, photophosphorylated ATP and NADPH are mainly used for this metabolic process. There would be very little, if any, of these high energy compounds

left for other related metabolism. Uptake of nutrients, such as phosphorus and silicon in the present case, also requires similar energy source.

Synthesis of one molecule of DA from the substrate produced in the Krebs cycle requires 5 ATP and 5 NADPH (Fig. 1.4), which is a strong energy consuming process. During the active growth period, the high demand for energy from the primary metabolism, such as carbon assimilation, chlorophyll *a* synthesis and nutrient uptake, restrains DA production. When energy demands from these metabolic process decline at low growth rates or at cessation of cell division, another energy consuming process, such as DA production, will be automatically favoured. Therefore, DA production is initiated when growth declines.

The low carbon assimilation in the stationary phase of batch culture or at low dilution rate in continuous cultures might be thought of as a reduction of supply of the electron acceptor NADP. Domoic acid production, on the other hand, is activated and the oxidized NADP is produced simultaneously. This continuous supply of NADP from the process of DA synthesis during the period of low carbon assimilation maintains the electron transfer process active in the photochemical reaction and creates mutually beneficial circumstances.

An active growth period is necessary for synthesis of chlorophyll pigments, the major component in the photochemical reaction. More cellular chlorophyll *a* is found in low light than in high light conditions (Figs. 3.3, 3.10). This permits comparable carbon assimilation and growth to some extent between the high and low light. Similarly, DA production is not significantly different between the incident light of 45 and 145 $\mu\text{mol m}^{-2}$

s⁻¹ (Bates *et al.*, 1991). I believe that the similar DA production is due to the differences in cellular content of chlorophyll pigments, which accomplish similar rates of photophosphorylation reactions in spite of the difference in the incident light. Similar light dependence of toxin production has been found in *Alexandrium* spp (Proctor *et al.*, 1975, Ogata *et al.*, 1987). Production of saxitoxins by *A. catenella* is proportional to the duration, but not to the intensity, of irradiance (Proctor *et al.*, 1975).

Unlike most other toxigenic micro-algae such as the dinoflagellate *Alexandrium* spp. (Anderson *et al.*, 1990) and the cyanobacterium *Microcystis* spp. (Watanabe *et al.*, 1989), which produce toxins during the exponential phase when cells are actively dividing, *P. pungens* f. *multiseries* produces toxin when cell division is restrained or stopped. This further suggests that the energy and precursor partition theory is applicable in this diatom but not in other micro-algae.

7.3. Ecological perspective

7.3.1. Effects of light and temperature

Production of DA requires energy. However, reduction of PPFD resulted in a decrease of α^B and P_m^B during the exponential phase, but not in the stationary phase (Figs. 3.12, 3.13). In fact, both α^B and P_m^B increased as PPFD decreased in the stationary phase. This is probably a survival strategy of the diatom as discussed in the Chapter 3. On the other hand, this also suggests that change in PPFD levels will not have much effect on the DA production. The results of Bates *et al.*, (1991) support this hypothesis.

In the fall-winter in PEI bays solar radiation levels are usually low (373 - 875 megajoules m⁻² per month, Atmosphere Environmental Service Canada, 1988), but this would not affect DA production. In contrast, it would reduce the metabolic cost and keep the bloom persistent for a longer period. For example, in Cardigan Bay 1987, the bloom of *P. pungens* f. *multiseries* probably started around October. It lasted until December and probably to January of 1988 (Subba Rao *et al.*, 1988b), i.e. for a period of 3 months, which is unusual for temperate diatom blooms. The duration of the bloom may explain why contamination of mussels was so severe.

Temperature is a major factor affecting cell metabolism, which in turn affects DA synthesis. Photosynthesis and other metabolic rates decrease when temperature decreases. As discussed earlier, the photochemical process is linked with DA synthesis and this process is less affected by temperature. Therefore, as a result of lowering temperature, carbon assimilation and growth were greatly reduced (Figs. 3.14, 3.18). The decrease in electron transfer and photophosphorylation may not be as significant as the decrease in carbon assimilation. That is, there could be relatively more free energy, which favours DA production as discussed earlier in Section 7.2, paralleling the increase in production of saxitoxin by *Alexandrium* spp (Boyer *et al.*, 1987) when temperature decreased.

In the fall and winter in the PEI bays, sea water temperature is around 10 °C or below (Hudson and Bernard, 1988, 1989; Bernard, 1990, 1991). This low temperature would facilitate reasonably high DA production and maintain the blooms at low metabolic cost.

However, Lewis *et al.* (1993) found enhancement of domoic acid production at

higher temperatures, which is not the case for saxitoxins. Nevertheless, synthesis of glutamate and isoprenoid involves many enzymes. For example, Mann (1987) showed that the enzymes involved in the production of 3(R)-mevalonate from acetyl-CoA are subject to very complex regulatory controls. Relatively higher temperature might favour the activity of certain enzymes, and this needs further investigation.

7.3.2. *Implication of abnormal nutrient ratios*

Diatoms require nitrogen, phosphorus and silicon in certain proportions for active growth, but the ratios differ between species (Chapters 5 and 6). *P. pungens* f. *multiseries* seems to require more phosphorus relative to nitrogen than other diatoms (Chapter 6); but it is able to grow at a similar rate under different silicate concentrations (Chapters 4 and 5). The major difference in the physiology of *P. pungens* f. *multiseries* under different silicate concentrations is that DA production rate increases as the silicate concentration decreases in the medium (Chapter 5).

The frequency of novel and toxic phytoplankton blooms has been increasing globally. Smayda (1989, 1990) documented the increases and proposed that they are due to altered nutrient compositions in aquatic ecosystems. Because of the increase in the anthropogenic enrichments of N and P but not Si due to soil fertilization and disposal of city sewage, etc., algal blooms occur more frequently. The bloom diatoms reduce the reservoir of silicate by sequestering it in benthic substrates and subsequently alter the ratios of N:P, N:Si, P:Si in lakes, coastal waters and inland seas (Conley, *et al.*, 1993). These altered nutrient ratios lead to successions of phytoplankton in which species that

are more competitive in low-silicate environments, particularly non-diatom species, are favoured.

In the culture media with various levels of silicate, cellular silica in *P. pungens* f. *multiseries* cells changed by a factor of 15 (Table 4.2), which is unusual in diatoms and suggested that *P. pungens* f. *multiseries* is a more competitive species in a low-silicate environment. When other diatom species are reduced in sea water due to insufficient concentration of silicate, *P. pungens* f. *multiseries* is probably still able to grow and simultaneously produces DA.

The abnormally wide range of cellular silica associated with *P. pungens* f. *multiseries* probably also explains the ubiquity of this species. It is able to flourish in different habitats with a wider range of silicate than other diatoms by reducing or increasing its cellular silicon (Chapters 4, 5; Table 4.2). *P. pungens* f. *multiseries* occurs between 62 °N and 40 °S in both the Atlantic and the Pacific (Table 1.1). Besides the differences in temperature and salinity over such wide geographical area, nutrient concentrations will also be different. Some waters may be rich in silicate, while others are not. It is likely that cells of *P. pungens* f. *multiseries* can establish themselves in these waters by varying their silicate demand according to the available resources as they did in culture (Chapter 4).

In 1988 in Cardigan Bay, the bloom of *P. pungens* f. *multiseries* occurred in the fall and produced DA soon after a bloom of *Skeletonema costatum* (Smith *et al.*, 1990b). A bloom of diatoms in the spring followed by a bloom of flagellates in the summer is a normal event in temperate marine habitats (Mann, 1993; Cushing, 1989), and there are

numerous examples of non-diatom blooms that have been preceded by a diatom bloom. For example, Silva (1985) found the *Prorocentrum minimum* bloom in the Obidos Lagoon (Portugal) was preceded by blooms of *S. costatum*. Maestrini and Graneli (1991) attributed the cause of a 1988 *Chrysochromulina polylepis* bloom in Scandinavian coastal waters to preceding diatom blooms.

A diatom bloom preceding a bloom of toxic dinoflagellates or *P. pungens* f. *multiseries* would obviously result in a reduction of silicate in the sea water. This is because after a diatom bloom, a large proportion of the silicate in sea water will be taken up and transported to the sediment (Conley, *et al.*, 1993). Although there is evidence of dissolution of silicon from diatom cell walls (Chapters 4, 5, Lewin, 1957), the regeneration cycle for silicate is much longer than that of nitrogen and phosphorus (Conley *et al.*, 1993). This condition obviously favours growth of dinoflagellates and some other more competitive diatoms, such as *P. pungens* f. *multiseries*. This low silicate also facilitates a better DA production as is evident from Chapters 4 and 5.

In addition to lowering the silicate concentration in the sea water, the preceding diatom blooms may also enrich the sea water in organic nutrients. This effect of enhancing dissolved organic materials in sea water by a preceding algal bloom has been termed preconditioning, implying biological effects on succeeding algal population growth (Provasoli, 1979; Barber, 1973). The presence of organic nutrients, released from the same species or from another species, may extend the duration of a bloom (Provasoli, 1979). The 1987 toxic bloom of *P. pungens* f. *multiseries* in Cardigan Bay PEI persisted for 3 month. This persistence could have been related to the organic materials produced

by the bloom itself. *P. pungens* f. *multiseries* grew better when a small proportion of the filtrate from stationary phase culture of *R. alata* was added (Subba Rao *et al.*, 1994). Results of Chapter 3 together with the unpublished work of Subba Rao and Wohlgeschaffen show that this toxigenic diatom may be able to grow and survive heterotrophically.

The production of domoic acid under nutrient depletion is similar to the situation of production of dissolved organic material, especially glycolate excretion, which has received much attention in the last 3 decades (Sharp, 1977; Harris, 1980 and reference therein). Glycolate excretion appears to be under conditions when growth rates are limited either in oligotrophic waters (Anderson and Zeutschel, 1976; Berman and Holm-Hansen, 1974) or in the populations under temporary nutrient depletion (Berman, 1976). Also, there are many reports on algal excretion during the stationary or senescent phase (Sharp, 1977; Harris 1980 and references therein). Cells under metabolic stress (Sharp, 1977) or photoinhibition (Harris, 1980) seem to excrete rapidly. Harris (1980) concluded that in all the situations described above, photosynthetic production of Calvin cycle intermediates is faster than the synthesis of carbohydrates, fats and proteins. Nutrient depletion is known to cause large changes in the pathways of carbohydrate and protein synthesis within the cells (see Chapters, 4, 5, 6 and also Harris, 1980).

Several lines of similarity between the production of domoic acid and that of glycolate are revealed. Firstly, they appear to occur in similar situations, i.e. nutrient depletion, physiological stress and growth limitation. Secondly, glycolate production is due to surplus of Calvin cycle intermediates (Harris, 1980) and DA production is

dependent on the surplus of metabolic energy and precursors (Section 7.1, 7.2). Thirdly, neither are primarily essential for overall cell metabolism, i.e. they are secondary metabolites. However, the linkage between production of these two secondary metabolites remains unclear.

When the toxigenic bloom of *P. pungens* f. *multiseries* was at its height in Cardigan Bay on December 16, 1987, silicate concentration was as low as 0.62 μM and phosphate was less than 0.22 μM (Subba Rao *et al.*, 1988b). As the bloom declined by January 7, both nitrate and silicate concentrations increased and continued until February 21, 1988, while phosphate did not clearly follow a similar pattern. This suggests that the bloom may have been limited by low phosphate or low silicate in the sea water, or by both. Production of DA is enhanced under limitation of either or both of these nutrients. The relationship between phosphate depletion and high toxin production has been reported for the dinoflagellate *A. tamarense* (Anderson *et al.*, 1990; Boyer *et al.*, 1985, 1987; Hall, 1982) and the chrysophyte *C. polylepis* (Edwardsen *et al.*, 1990; Carlsson *et al.*, 1990; Maestrini and Granéli, 1991) and is also true for *P. pungens* f. *multiseries*.

Nitrogen has often been considered a limiting nutrient for potential algal growth (Ryther and Dunstan, 1971 and others). However, there is now evidence that phosphorus is a limiting nutrient, at least regionally or during certain periods (Granéli *et al.*, 1990; Harrison *et al.*, 1992; Pan *et al.*, 1994). As a result of increasing anthropogenic disturbance, there has been increase in the nitrogen input in the coastal waters, which has altered the nutrient composition of the sea water and led to changes in the phytoplankton species composition. In the practice of controlling coastal pollution, reducing phosphorus

in waste water is easier than lowering nitrogen (Granéli *et al.*, 1990), so coastal waters are more likely to receive waste water with increasing N:P ratios. This has the potential for increasing toxic algal blooms.

7.3.3. *Implication of heavy precipitation and freshwater discharge*

In the Cardigan Bay area, upwelling usually is not evident (Drinkwater and Petrie, 1988). The significant landward current suggests a possible downwelling in this area (Lauzier, 1965, Fig. 7.1). Therefore, the main contribution of nutrients to this region is from the land nearby, carried by the Cardigan, Brudenell and Montague Rivers. Precipitation data for the September-November period from 1982 to 1987 show that 1987 was 64% above average. The magnitude of the fall-winter blooms of *P. pungens* f. *multiseries* in Cardigan Bay decreased between 1987 and 1990, and so did the September precipitation (J. C. Smith, presentation at Bedford Institute of Oceanography, February, 1991). This suggests a possible relationship between the magnitude of blooms and precipitation prior to the blooms.

Change in the direction of surface current may occur during a period of a strong freshwater runoff, which drives surface water seaward in buoyancy current and causes estuarine upwelling (Mann and Lazier, 1991). Therefore, the pre-bloom heavy precipitation would cause a stronger freshwater runoff in the Cardigan Bay area carrying nutrients from terrestrial sources. Simultaneously, strong estuarine upwelling would carry nutrients from the bottom. This is likely to stimulate an algal bloom in water derived partly from freshwater runoff and partly from estuarine upwelling.

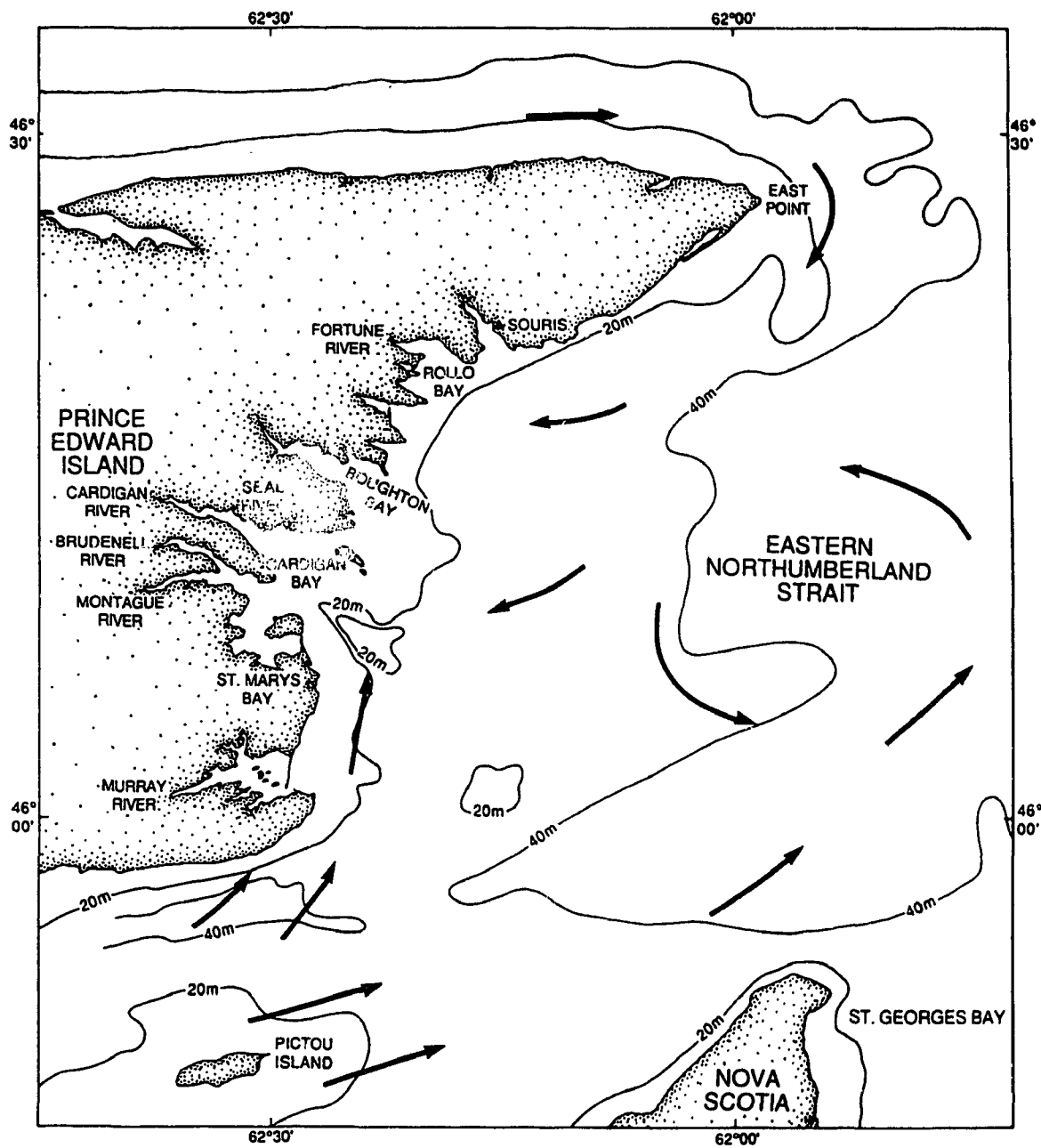


Fig. 7.1. The study area. The surface circulation pattern as described by Lauzier (1965).

The N:P and Si:P ratios in the upper reaches of the Cardigan Bay were 81.5 and 51.7 respectively, while in the lower reaches they were 41.2 and 65.6 (Subba Rao *et al.*, 1988b). This suggests that the nutrients carried by the river are not balanced for diatom growth, and a bloom in this water will ultimately be phosphate limited, which favours high production of domoic acid.

During the 3 months of the 1987 bloom in Cardigan Bay, both the concentration and flux of N, P and Si were consistently low. The phosphate and silicate limited steady growth in the continuous cultures can be considered as analogues of this bloom. The stress due to phosphate or silicate limitation in the Cardigan Bay sea water allows this diatom to produce DA continuously at a high rate similar to the continuous DA production during the steady state growth (Chapters 5 and 6).

This concept is illustrated in Fig. 7.2. Abnormally high precipitation in the fall of 1987 resulted in freshwater discharge which brought higher concentrations of nitrogen from terrestrial source to Cardigan Bay but very little phosphorus and silicate. *P. pungens* f. *multiseries* population grew and exhausted the phosphate and/or silicate in the seawater at the height of the bloom, resulting in vigorous DA production due to phosphate or silicate limitation and decline of population growth.

A toxic algal bloom following a heavy precipitation or an abnormal freshwater runoff has been a prevalent event (Shumway, 1990) and there are many examples of the association of toxic algal bloom with abnormal freshwater discharge. For example, in the lower St. Lawrence estuary in 1986, the peak of PSP toxicity and *A. tamarensis* concentration corresponded to the height of freshwater runoff (Cembella *et al.*, 1988).

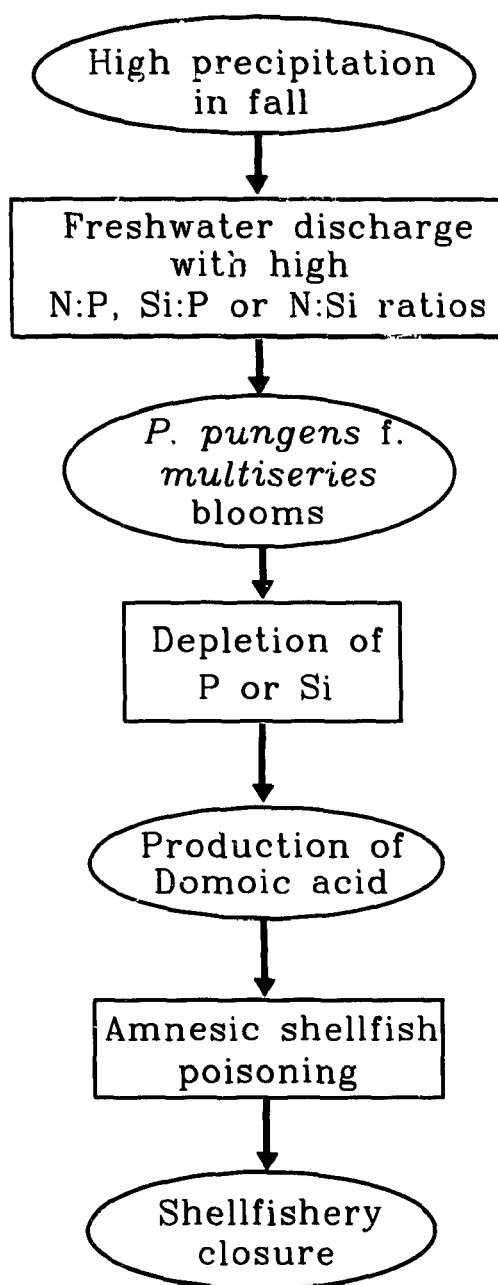


Fig. 7.2. Proposed explanation for the toxigenic blooms of *Pseudonitzschia pungens f. multiseriis* in Cardigan Bay PEI.

Blooms of *C. polylepis* in Scandinavian waters are related to abnormally high precipitation prior to the bloom (Maestrini and Granéli, 1991). The less-reported number of toxic blooms of *A. tamarense* along the coasts of Maine and Massachusetts in 1981 and absence of toxicity in the 3 salt ponds monitored by Anderson *et al.*, (1983) was attributable to the extremely low precipitation in March. Blooms of *A. tamarense* usually start in April or May in this region.

7.3.4. Population dynamics of *P. pungens* f. *multiseries* and DA production

Growth of the *P. pungens* f. *multiseries* culture population was fast in the mid-exponential phase of batch culture when the population density was at intermediate levels (Figs. 3.1, 3.2, 4.2). High growth rate in continuous culture can not be maintained when cell concentrations are high and ambient nutrients are low. This suggests that growth of *P. pungens* f. *multiseries* follows the Allee growth model (Allee, 1951), one of the three density-related population growth patterns (Odum, 1993). Growth of *P. pungens* f. *multiseries* was slow when population density was less than 10^6 cells l^{-1} in the lag phase, or larger than 10^8 cells l^{-1} (see Figs. 3.1A, 3.2A). In a mixed culture of *P. pungens* f. *multiseries* with *Rhizosolenia alata*, growth rate was highest at an intermediate density with small proportion of *R. alata* in the culture (Subba Rao *et al.*, 1994). Besides the allelopathic effects we proposed, the effects of population density in governing the population growth should not be ignored.

This population density-related growth probably relates to the self-limiting effects on population and inversely on DA production discussed earlier in this chapter. In batch

culture, DA is produced in the lag phase (Douglas and Bates, 1992, Douglas *et al.*, 1993), late exponential phase (Chapter 4) and stationary phase (Chapter 4; Subba Rao *et al.*, 1990; Bates *et al.*, 1989, 1991, 1993) when growth is slow, declining or stopped. In continuous culture, DA is produced in significant quantities when growth rate is less than 0.3 d^{-1} whether or not there is silicate or phosphate limitation (Figs. 5.2, 5.4, 6.3). However, the existence of nutrient stress due to silicate or phosphate limitation in the continuous culture greatly enhanced DA production. Similarly in batch culture, second stage DA production is about an order of magnitude higher than that in the first stage (Chapter 4). Some self-limiting factor, associated with regulation of growth rate, initiates DA synthesis, but nutrient stress is needed before DA production approaches the levels comparable to those in Cardigan Bay.

CHAPTER 8

CONCLUSIONS

Pseudonitzschia pungens f. multiseriis is an unusual diatom. It is the first diatom reported to produce toxin and its toxin production is high when cells are not actively dividing. In this respect, it differs from most other toxic algae, which produce toxin during the period of active growth. The monospecific blooms of this diatom occurred in the late fall and winter when the physical conditions are apparently not suitable for other diatom blooms. Cells of *P. pungens f. multiseriis* are more capable of adjusting their silicate reserves than most other marine diatoms. This facilitates the establishments of this diatom in various marine habitats with a wide range of silicate concentrations and allows it to be more competitive than other diatoms in low silicate habitats. The physiological and ecological characteristics of *P. pungens f. multiseriis* in relation to DA production are summarized.

- 1. Domoic acid is produced by *Pseudonitzschia pungens f. multiseriis* both in dividing and non-dividing populations.**

Production of domoic acid has been reported only after *P. pungens f. multiseriis* populations entered stationary phase when cell division has ceased (Subba Rao *et al.*,

1990, Bates *et al.*, 1989, 1991, 1993). The present study shows that both exponential and stationary populations produce domoic acid, and the cessation of cell division is not essential to DA production. The events that coincided with DA production were the decline of growth or severe external nutrient stress.

- 2. Domoic acid production in cultures of *Pseudonitzschia pungens* f. *multiseries* is greatly enhanced when the cells are stressed by limitation of nutrients, such as phosphate or silicate.**

The present study clearly demonstrates that DA production was greatly enhanced under severe phosphate or silicate limitation. The negative relationships between total silicate supply and yield of domoic acid (Fig. 4.7) in the batch culture, and the negative correlation between growth rate and DA production in continuous culture (Tables 5.1, 6.1; Figs 5.2, 5.4, 6.4) support this conclusion. Bates *et al.* (1991) reported effects of silicate limitation on DA production but they attributed the 35% enhancement in DA production to differences in the duration of the lag phase.

- 3. Conditions for DA production can be divided into two types. The first type is associated with moderately low nutrient environments and triggers low DA production. The second is a severe external stress, such as severe limitation of one nutrient when other nutrients are present in excess, and promoted high DA production.**

The two stage phenomenon in DA production in the batch cultures of *P. pungens* f. *multiseries* further facilitates our understanding of DA production both in dividing and non-dividing populations, and attributed to Type I and Type II conditions respectively (Table 7.1). When nutrients are reduced (but not exhausted) during the late exponential phase, cells adjust their internal metabolism, for example, reducing growth rate, and initiate DA production (Type I). This regulation may be intrinsic, such as genetically and enzymatically related, and extrinsic, such as population density related. When a nutrient becomes exhausted, the external stress vigorously restrains cell metabolism and promotes DA production (Type II). Type I production is low but essential, while Type II production is high (5 to 10 time higher).

- 4. Since biogenic energy is essential in DA production, partitioning of energy and precursors between primary and secondary metabolism is the main mechanism in the regulation of DA production.**

Initiation of DA production coincides with decline or stoppage of population growth. Production of DA declines when a renewed supply of phosphate and silicate leads to a resumed growth, but recommences when the surge of uptake ends. Also, DA production coincides with the period of photophosphorylation, as in Bates *et al.*, (1991). Present studies together with results in the literature suggest that changes in partitioning of photoassimilated energy and metabolic precursors between primary metabolism or secondary metabolism control DA production.

5. **The domoic acid poisoning episodes in Cardigan Bay, Prince Edward Island were due to the abnormal nutrient ratios, which ultimately resulted in the depletion of phosphorus or silicon at the height of the blooms and triggered DA production.**

The work of Subba Rao *et al.*, (1988b) showed that the N:P ratio in the Cardigan Bay sea water was very high (41-81) and silicate was low when *P. pungens* f. *multiseries* bloom was at its height. This suggests either an imbalance of nutrient composition in the fresh water runoff or an earlier diatom bloom may have stripped the water column of its silicate. This mechanism of triggering DA production is consistent with those postulated for most other toxic algal blooms (Chapter 7). The general increase of anthropogenic disturbance in coastal regions may be leading to more frequent examples of severe nutrient imbalance, often after heavy rains, and a world wide increase in the frequency of toxic algal blooms.

APPENDICES

APPENDIX A1. LIST OF PUBLICATIONS

1) Refereed journal and book publications:

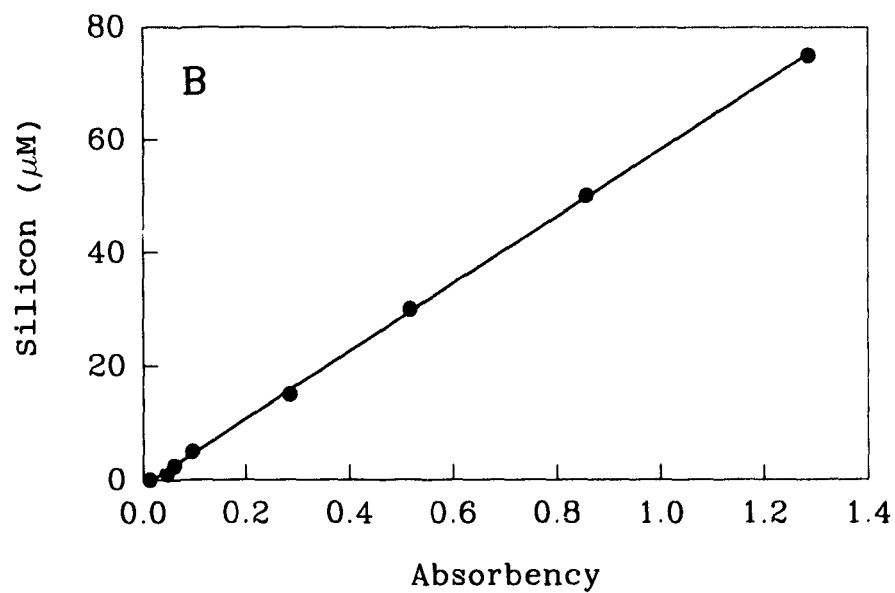
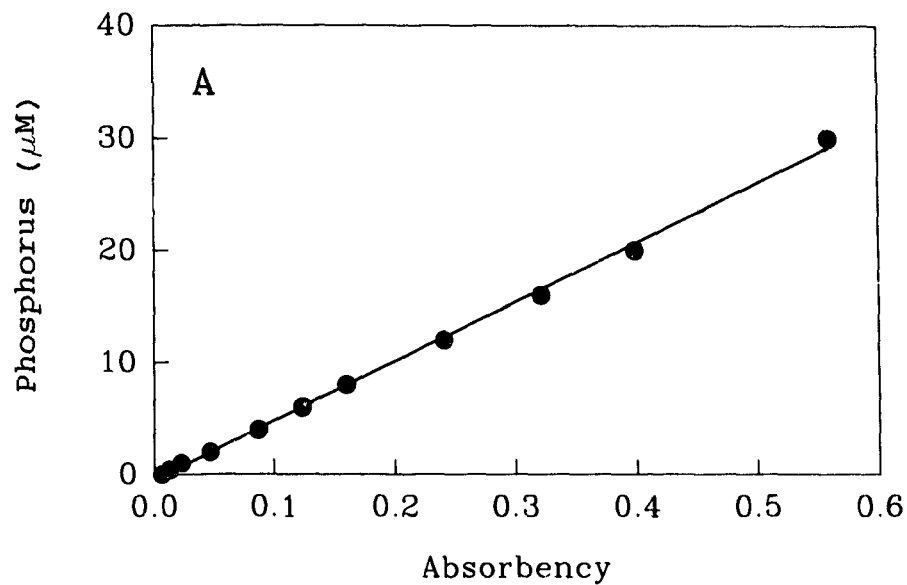
1. Subba Rao, D. V., Y. Pan and S. J. Smith, (communicated). Allelopathy between *Rhizosolenia alata* (Brightwell) and the toxigenic *Pseudonitzschia pungens* f. *multiseriis* (Hasle). *Oceanologia acta*
2. Subba Rao, D. V. and Y. Pan, (in press). Apart from toxin production, are the toxigenic algae physiologically different? In: *Proceedings of the 6th International Conference on Toxic Phytoplankton*. Nantes, France, Oct. 18-22, 1993. eds. P. Lassus *et al.*
3. Pan, Y., Y. C. Guo and C. K. Tseng, (in press). Vertical and seasonal variations of chlorophyll concentrations in the inlet of Jiaozhou Bay. *Oceanologia et Limnologia Sinica*.
4. Pan, Y., Y. C. Guo and C. K. Tseng, (in press). Annual *in situ* primary production in the inlet of Jiaozhou Bay. *Oceanologia et Limnologia Sinica*.
5. Subba Rao, D. V., Y. Pan, 1993. Photosynthetic characteristics of *Dinophysis norvegica*, Claparede & Lachmann, a red-tide dinoflagellate. *J. Plankton Res.* 15: 965-976.
6. Subba Rao, D. V., Y. Pan, V. Zitko, G. Bugden and K. Mackeigan, 1993. Diarrhetic shellfish poisoning (DSP) associated with a subsurface bloom of *Dinophysis norvegica* in the Bedford Basin, eastern Canada. *Mar. Ecol. Prog. Ser.* 97: 117-126.
7. Pan, Y., D. V. Subba Rao, K. H. Mann, W. K. W. Li and R. E. Warnock, 1993. Temperature dependence of growth and carbon assimilation in *Nitzschia pungens* f. *multiseriis*, the causative diatom of domoic acid poisoning. In: *Toxic Phytoplankton Blooms in The Sea*. eds. T. J. Smayda and Y. Shirnizu. Elsevier, Amsterdam, pp. 619-624.
8. Pan, Y., Y. C. Guo and C. K. Tseng, 1992. Carbon assimilation number of phytoplankton. In: *Ecology and Living Resources of Jiaozhou Bay*, ed. Ruiyu Liu. Science Press, Beijing, China. pp. 215-224.
9. Amadi, I., D. V. Subba Rao and Y. Pan, 1992. A *Gonyaulax digitale* red water bloom in the Bedford Basin, Nova Scotia, Canada. *Botanica Marina* 35, 451-455.
10. Guo, Y. and Y. Pan, 1992. Primary productivity in the Changjiang River estuary. *Studia Marina Sinica* 33: 191-200.

11. Pan, Y., D. V. Subba Rao and R. E. Warnock, 1991. Photosynthesis and growth of *Nitzschia pungens* f. *multiseries* Hasle, a neurotoxin producing diatom. *J. Exp. Mar. Biol. Ecol.* 154, 77-96.
12. Pan, Y., 1987. An analysis of annual observation data on transparency and submarine illumination at two stations in Jiaozhou Bay. *Marine Sciences* 1987 No. 3: 49-53.
13. Pan, Y., 1987. On chlorophyll and marine primary productivity. *Marine Sciences* 1987 No. 1: 63-65.

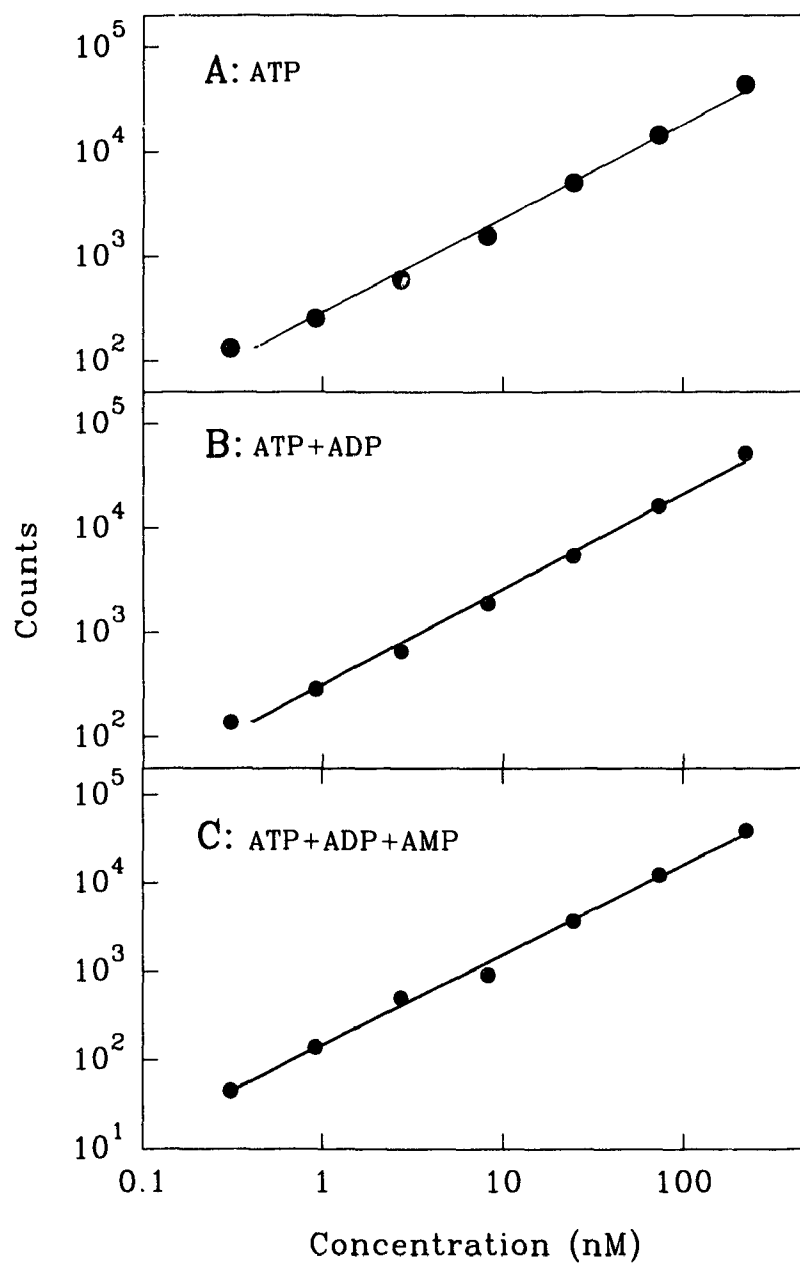
2) *non-refereed contributions*

14. Pan, Y., K. H. Mann, D. V. Subba Rao, J. Z. Zou and C. Zhang, 1994. Is there a potential for amnesic shellfish poisoning in coastal China? Poster at: *THE FIFTH INTERNATIONAL PHYCOLOGICAL CONGRESS*, Qingdao, China, June 26 - July 2, 1994
15. Pan, Y., D. V. Subba Rao and K. H. Mann, 1994. Phosphate and silicate limitation and domoic acid production by *Pseudonitzschia pungens* f. *multiseries*. Presentation at: *THE FIFTH INTERNATIONAL PHYCOLOGICAL CONGRESS*, Qingdao, China, June 26 - July 2, 1994
16. Subba Rao, D. V. and Y. Pan, 1992. Physiological ecology of *Dinophysis norvegica*, a redwater bloom species, in Bedford Basin, Nova Scotia. *Can. Tech. Rept. Fish. Aquat. Sci.* 1893: 43.
17. Pan, Y., D. V. Subba Rao, K. H. Mann, 1991. Proximate composition of *Nitzschia pungens* f. *multiseries*, a novel toxin-producing diatom. Abstract and presentation at the *Fifth International Conference on Toxic Marine Phytoplankton*, Newport, RI, USA, Oct. 28 - Nov. 1, 1991.
18. Pan, Y., D. V. Subba Rao and W. K. W. Li, 1991. Effects of growth temperature on growth and carbon assimilation in *Nitzschia pungens* f. *multiseries*. *Can. Techn. Rep. Fish. Aquat. Sci.* 1799, 15.
19. Pan, Y., D. V. Subba Rao and R. E. Warnock, 1991. Photosynthesis and growth of *Nitzschia pungens* f. *multiseries*, a neurotoxin producing diatom. *Can. Techn. Rep. Fish. Aquat. Sci.* 1799, 15.
20. Y. Pan, Guo Y. C., Z. Y. Yang and Y. S. Zhang, 1988. Study on primary productivity and chlorophyll concentration in the area around the Linshan Island. Presentation at the annual meeting of *Chinese Association of Oceanology and Limnology*, Qingdao, China, October, 1988.

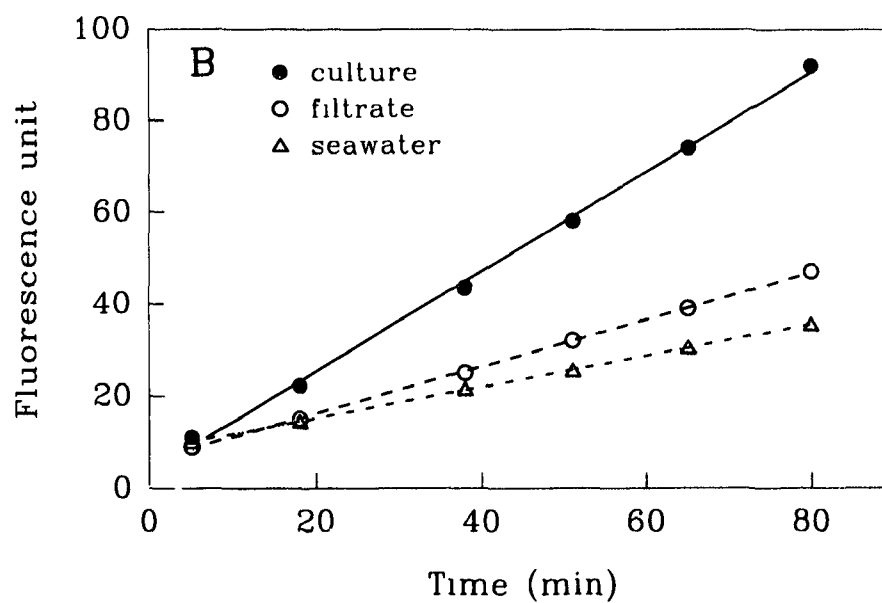
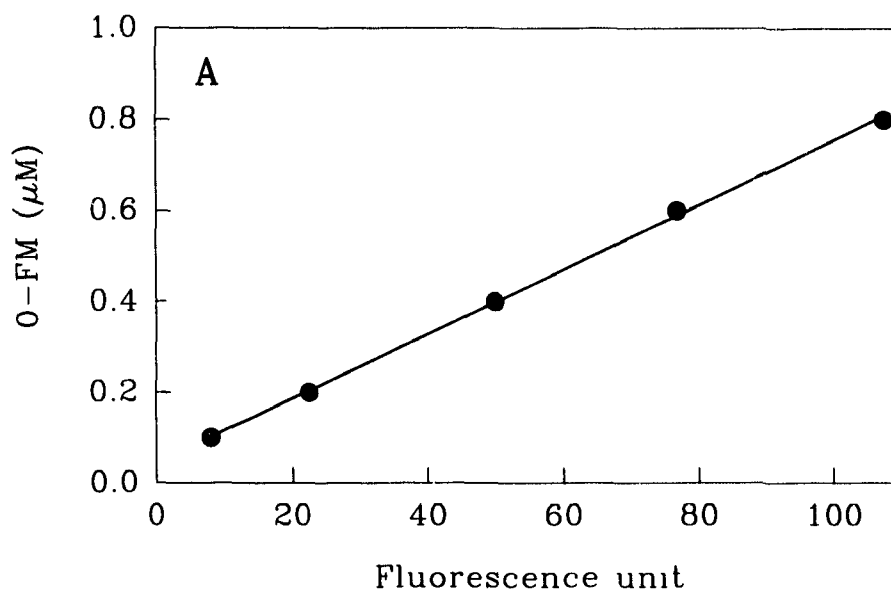
APPENDIX B1. ONE EXAMPLE OF STANDARD CURVES FOR PARTICULATE (A) PHOSPHORUS AND (B) SILICON MEASUREMENTS (CHAPTER 2).



APPENDIX B2. EXAMPLES FOR THE STANDARD CURVES FOR THE MEASUREMENTS OF ATP, ATP+ADP, ATP+ADP+AMP (CHAPTER 2).



APPENDIX B3. EXAMPLES FOR THE MEASUREMENTS OF ALKALINE PHOSPHATASE ACTIVITY. (A) STANDARD CURVE, (B) ONE EXAMPLE (JULY 13, CHAMBER 2; CHAPTERS 2,6).



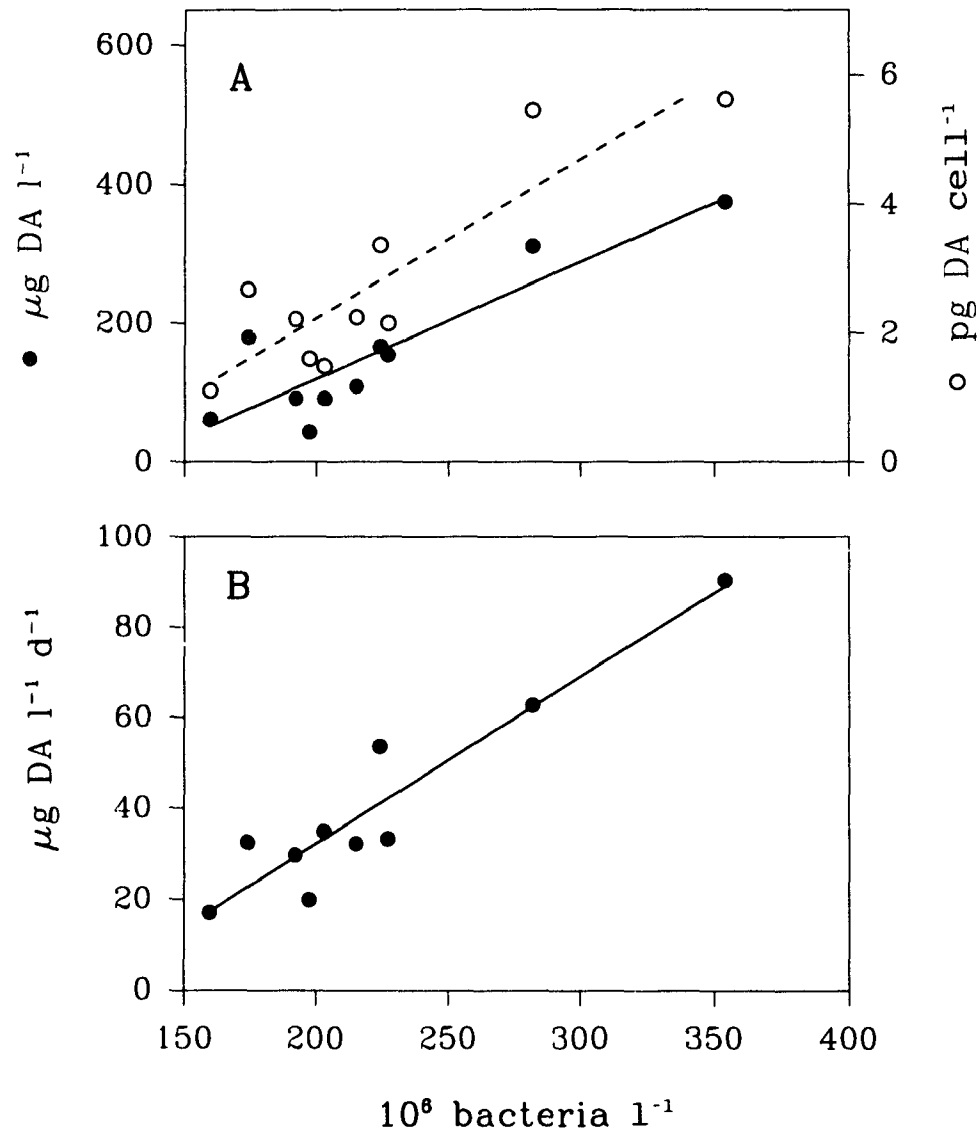
APPENDIX B4. SENSITIVITY AND COEFFICIENT OF VARIATION OF VARIOUS METHODS USED (CHAPTER 2)

Measurements	Low limit	Number of replicate per sample	Coefficient of variation (%)	
Cell conc.		5-8	5-15	
Chl <i>a</i>	0.01 ng ml	2	0-1	
PC	1 µg	2	1-3	
PN	0.05 µg	2	1-8	
PP	0.01 µM	2	0.5-5	
PSi	0.05 µM	2	0-3	
DIN	0.1 µM	2	0-2	
DIP	0.01 µM	2	0.5-1.5	
DISi	0.05 µM	2	0-1	
CO ₂		2	0-5	
DA	FMOC	2 ng	2	1-5
	DAD	0.5 µg	2	0-2
ATP		3	2-10	
APA		3	0-3	

APPENDIX C1. SILICATE CONCENTRATIONS (μM) IN THE CONTROL AND IN THE RESERVOIR DURING THE SILICATE LIMITED CONTINUOUS CULTURE EXPERIMENTS (CHAPTER 5).

	Description	Time (day)	Control	Reservoir
Exp. I	Before autoclaving			59.93
	After autoclaving	2	147.35	
		4	161.87	
		6	158.41	
		8	167.91	
		10	175.11	
		12	171.66	
	Mean		165.39	
	Std		9.01	
Exp. II	Before autoclaving			59.85
	After autoclaving	1		61.15
		3	51.97	
		5	53.70	56.49
		7	57.95	58.39
		9	58.62	57.00
		11	49.68	49.23
		13	57.16	51.02
		15	57.28	57.05
		17	53.76	57.67
		33	57.28	57.16
	Mean		55.68	56.50
	Std		2.84	3.18

APPENDIX C2. SILICATE LIMITED STEADY STATE EXPERIMENTS (CHAPTER 5). (A) DA CONCENTRATIONS (LEFT: DA IN CULTURES, RIGHT: DA PER CELL) AND (B) DA PRODUCTION, IN RELATION TO BACTERIAL ABUNDANCE.



APPENDIX C3. BACTERIAL EFFECTS ON DA PRODUCTION (CHAPTER 5).

In the silicate limited continuous cultures (Chapter 5), bacterial abundances were measured in steady state continuous cultures (Experiment II) and batch mode extension (Experiment III) in addition to other variables observed in Experiment I. In the steady states (Experiment II), as growth rate increased, the pattern of DA production matched with the variation of bacteria abundance (Figs. 5.4A, D). Bacteria concentration significantly correlated with domoic acid concentration and its production (Appendix C2). In the batch mode extension (Experiment III), on the other hand, bacterial abundance did not always follow and same pattern as domoic acid concentrations (Fig. 5.6E).

The roles of bacteria in phycotoxin production has been studied since late 1970s (Silva, 1979, 1982; Kodama *et al.*, 1989; Ogata *et al.*, 1990). However, there has been no reported study on the relationships between the bacteria abundance and phycotoxin production in culture.

Existence of bacteria enhanced domoic acid production. In *P. pungens* f. *multiseries*, Douglas and Bates (1992) found the significant difference in DA production between axenic and non-axenic batch cultures. In promoting DA production, species of bacteria may not be specific. Bacteria isolated either from *P. pungens* f. *multiseries* or from *Chaetoceros* sp. had similar enhancement in DA production when they were introduced to the axenic cultures of *P. pungens* f. *multiseries* (Bates *et al.*, 1994). DA production was related to the abundance of bacteria (Appendix C2). This suggested that

production of domoic acid probably rely on certain precursors, which existed in *P. pungens* f. *multiseries*, but bacteria may be an important supplier of this. The other alternative mechanism might be bacteria are involved in the synthesis of domoic acid. The role of bacterial might be to accelerate the synthetic process, which needs further investigation.

During the extended batch mode period, decrease of bacteria abundance corresponded to the increase of algal cell concentration, i.e. the period of population growth (Figs. 5.6A, E). For example, in Chamber 1, *P. pungens* f. *multiseries* cell concentration increased from 49.4 to 60.4 x 10⁶ cells l⁻¹, bacterial concentration dropped from 224 to 127 x 10⁶ cells l⁻¹ during the first day. In the following 3 days, on the other hand, algal concentration slightly decreased (no growth), bacterial concentration increased to 247 x 10⁶ cells l⁻¹. Similar patterns were found in Chamber 6. However, DA production differed in these two chambers. In the chamber 1, DA production was constant and its concentration increased linearly during the whole batch mode period. Whereas in Chamber 6, DA production was interrupted during the first day due to the silicate perturbation. The patterns of DA concentration and *P. pungens* f. *multiseries* concentration in Chamber 5 were the reverse of those in Chamber 1.

Bactericidal agent is reported to be produced by exponentially growing phytoplankton (Fogg, 1962; Fogg and Thake 1987). The decrease of bacterial concentration in the culture during the period when *P. pungens* f. *multiseries* was growing probably because of the effects of some bactericidal agent produced by the diatom. Further investigation is needed.

Which is the more important factor in DA production, silicate stress or existence of bacteria? DA is produced in the late exponential phase of batch culture or in Experiment I when silicate are not necessarily limiting (Figs. 4.1, 4.2, 5.2), and also in the axenic culture (Douglas and Bates, 1992; Douglas *et al.*, 1993). The action of silicate stress and bacteria are similar, i.e. they both seem to enhance domoic acid production. However the mechanisms of their action are different. Silicate stress reduces the energy demand from primary metabolism and probably induces change in the partitioning of early precursors between primary and secondary metabolism (discussed in Chapters 5 and 7). The role of bacteria is probably *i*) to supply more precursor(s) *ii*) to accelerate the process of DA synthesis or *iii*) to regenerate nutrient from organically bond compounds (Azam *et al.*, 1983; Harrison, 1992).

APPENDIX D1. FUTURE DEVELOPMENTS

D1.1. Domoic acid as a valuable compound

Amnesic shellfish poisoning has resulted in human poisoning and closure of shellfisheries and has incurred approximately \$3 x 10⁶ of economic loss. However, domoic acid is a naturally occurring neuroexcitatory amino acid. It can be used as a tool in neuro-biological research (McGeer *et al.*, 1978). It can also be used as an insecticide (Maeda *et al.*, 1984, 1987).

The high production rate of domoic acid in the silicate- or phosphate-limited continuous culture of *P. pungens* f. *multiseries* and even higher production during extended batch mode after steady state growth suggests that the synthesis of domoic acid using continuous culture of this diatom has great commercial potential. Production of DA is very high at the steady state with a growth rate between 0.15 and 0.3 d⁻¹. The surge production during the extended batch mode was up to about 200 µg DA l⁻¹ d⁻¹ (3.17 pg DA cell⁻¹ d⁻¹). Suppose a 100 litre chamber is built, up to 20 litres of the culture can be obtained every day. This culture can be left at the same condition for 2-4 day before being extracted for domoic acid. A production of 4 - 14 mg d⁻¹ domoic acid is expected from each chamber. This suggests a real potential for commercial exploitation of this diatom as a source of a valuable neurobiological compound, domoic acid.

D1.2. Further research potential

Domoic acid is produced when growth has declined or stopped under silicate limitation. Usually, lipid production in diatoms is enhanced in the stationary phase when the culture is limited by silicate as discussed in Chapter 4, while this is not the case in *P. pungens* f. *multiseries*. This suggested that biosynthesis of DA and fatty acid may share a common portion in the synthetic pathway and there must be a "switch" which manipulates the passage of substrate and energy into either fatty acid or domoic acid. This mechanism could perhaps manipulate the synthesis of isoprenoid compounds (Fig. 1.4).

Figure 1.4 suggests that part of domoic acid is derived from glutamate, which could be derived from another amino acid. Also, as discussed earlier in Section 7.1, isoprenoids could be derived from leucine. Stationary phase culture could be associated with degradation of protein to individual amino acids. Therefore, domoic acid production could also be linked to protein synthesis or degradation.

REFERENCES

- Addison, R. F., J. E. Stewart, 1989. Domoic acid and the eastern Canadian molluscan shellfish industry. *Aquaculture* 77: 263-269.
- Alam, M., C. P. Hsu and Y. Shimizu, 1979. Comparison of toxins in three isolates of *Gonyaulax tamarensis* (Dinophyceae). *J. Phycol.* 15, 106-110.
- Allee, W. C., 1951. *Cooperation Among Animal, with Human Implications*. Henry Schuman, New York.
- Anderson, D. M., 1990. Toxin variability in *Alexandrium* species. In: *Toxic Marine Phytoplankton*, eds. E. Granéli, B. Sundström, L. Edler and D. M. Anderson, Elsevier, New York, pp. 41-51.
- Anderson, D. M., S. W. Chisholm and C. J. Waters, 1983. The importance of life-cycle events in the population dynamics of *Gonyaulax tamarensis*. *Mar. Biol.* 76: 179-189.
- Anderson, D. M., D. M. Kulis, J. J. Sullivan, S. Hall and C. Lee, 1990. Dynamics and physiology of saxitoxin production by the dinoflagellates *Alexandrium* spp. *Mar. Biol.* 104: 511-524.
- Anderson, G. C. and R. P. Zeutschel, 1970. Release of dissolved organic matter by marine phytoplankton in coastal and offshore areas of the North-east Pacific Ocean. *Limnol. Oceanogr.* 15: 402-407.
- Azam, F., T. Fenchel, J. G. Field, J. S. Gray, A. A. Meyer-Reil and F. Thingstad, 1983. The ecological role of water-column microbes in the sea. *Mar. Ecol. Prog. Ser.* 10: 257-263.
- Baly, E. C. C., 1935. The kinetics of photosynthesis. *Proc. R. Soc. Lond. Ser. B*117: 218-239.
- Barber, R. T., 1973. Organic ligands and phytoplankton growth in nutrient-rich sea water. In: *Trace Metals and Metal-Organic Interactions in Natural waters*. ed. P. C. Singer, Ann Arbor Sci. Publ. Ann Arbor, Michigan. pp. 321-338.
- Baras, S. S., A. S. W. de Freitas, J. E. Milley, R. Pocklington, M. A. Quilliam, J. C. Smith and J. Worms, 1991. Controls on domoic acid production by the diatom *Nitzschia pungens* f. *multiseriis* in culture: nutrients and irradiance. *Can. J. Fish. Aquat. Sci.* 48: 1136-1144.

- Bates, S. S., J. C. Smith and J. Worms, 1993. Effects of ammonium and nitrate on growth and domoic acid production by *Nitzschia pungens* in batch culture. *Can. J. Fish. Aquat. Sci.* 50: 1248-1254.
- Bates, S. S., C. J. Bird, A. S. W. deFreitas, R. Foxall, M. W. Gilgan, L. A. Hanic, G. E. Johnson, A. W. McCulloch, P. Odense, R. Pocklington, M. A. Quilliam, P. G. Sim, J. C. Smith, D. V. Subba Rao, E. C. D. Todd, J. A. Walter and J. L. C. Wright., 1989. Pennate diatom *Nitzschia pungens* as the primary source of domoic acid, a toxin in shellfish from eastern Prince Edward Island, Canada. *Can. J. fish. Aquat. Sci.* 46, 1203-1215.
- Bates, S. S., D. J. Douglas, G. J. Doucette and C. Léger, 1994. Effect on domoic acid production of reintroducing bacteria to axenic cultures of the diatom *Pseudonitzschia pungens* f. *multiseries*. In: *Proceedings of the 6th International Conference on Toxic Marine Phytoplankton*. eds. Lasuss *et al.*, Oct. 18-22, 1993. Nantes, France (in press)
- Berman, T., 1976. Release of dissolved organic matter by photosynthesizing algae in Lark Kinneret Israel. *Freshwater Biol.* 6: 13-18.
- Berman, T. and O. Holm-Hansen, 1974. Release of photoassimilated carbon as dissolved organic matter by marine phytoplankton. *Mar. Biol.* 28: 305-310.
- Bernard, T., 1990. *P.E.I. Mussel Monitoring Program 1990*. P.E.I. Dept. Fish. Aquaculture.
- Bernard, T., 1991. *P.E.I. Mussel Monitoring Program 1991 Report*. Technical Report # 202, P.E.I. Dept. Fish. Aquaculture.
- Blackman, F. F., 1905. Optimum and limiting factor. *Ann Bot.* 19: 281-295.
- Boyer, G. L., J. J. Sullivan, R. J. Anderson, P. J. Harrison and F. J. R. Taylor, 1985. Toxin production in three isolates of *Protogonyaulax* sp. In: *Toxic Dinoflagellates*, eds. D. M. Anderson, A. W. White, D. G. Baden, Elsevier, New York. pp. 281-286.
- Boyer, G. L., J. J. Sullivan, R. J. Anderson, P. J. Harrison, F.J. R. Taylor, 1987. Effects of nutrient limitation on toxin production and composition in the marine dinoflagellate *Protogonyaulax tamarensis*. *Mar. Biol.* 96: 123-128.
- Breeuwer de Ramirez, J., 1977. Phytoplankton of the Gulf of Santa Fe and adjacent areas (1973-1974). In: *Proc. Assoc. Isl. mar. Lab. Caribb.* 12: 7.
- Brzezinski, M. A., R. J. Olson and S. W. Chisholm, 1990. Silicon availability and cell-cycle progressing in marine diatoms. *Mar. Ecol. Prog. Ser.* 67: 83-96.
- Cahet, G. M. Fiala, G. Jacques and M. Panouse, 1972. Production primaire au niveau de

la thermocline en zone néritique de Méditerranée Nord-Occidentale. *Mar. Biol.* 14: 32-40.

Caperon, J. and J. Meyer, 1972a. Nitrogen-limited growth of marine phytoplankton. I. Changes in population characteristics with steady state growth rate. *Deep-Sea Res.* 19: 601-618.

Caperon, J. and J. Meyer, 1972b. Nitrogen-limited growth of marine phytoplankton. II. Uptake kinetics and their role in nutrient limited growth of phytoplankton. *Deep-Sea Res.* 19: 619-632.

Carlsson, P., E. Granéli and P. Olsson, 1990. Grazer elimination through poisoning: one of the mechanisms behind *Chrysochromulina polylepis* blooms? In: *Toxic Marine Phytoplankton*. eds. E. Granéli, Sundström, L. Edler and D. M. Anderson, Elsevier, New York, pp. 116-122.

Cembella, A. D., N. J. Antia and P. J. Harrison, 1984. The utilization of inorganic and organic phosphorus compounds as nutrients by eukaryotic microalgae: A multidisciplinary perspective. Part 2. *CRC Critical Reviews in Microbiology* 11: 13-81.

Cembella, A. D., J. Turgeon, J-C. Therriault and P. Beland, 1988. Spatial distribution of *Protogonyaulax tamarensis* resting cysts in nearshore sediments along the north coast of the lower St. Lawrence estuary. *J. Shellfish Res.* 7: 597-609.

Cleve, P. T., 1897. A treatise on the phytoplankton of the Atlantic and its tributaries and on periodical changes of the plankton of Skagerak. *Upsala*. pp. 1-27. (ref. Hasle, 1965).

Conley, D. L., C. L. Schelske and E. F. Stoermer, 1993. Modification of the biogeochemical cycle of silica with eutrophication. *Mar. Ecol. Prog. Ser.* 101: 179-192.

Conway, H. L., P. J. Harrison and C. O. Davis, 1976. Marine diatoms grown in chemostats under silicate or ammonium limitation. II. Transient response of *Skeletonema costatum* to a single addition of limited nutrient. *Mar. Biol.* 35: 187-199.

Coombs, J., W. M. Darley, O. Holm-Hansen, B. E. Volcani, 1967. Studies on the biochemical and fine structure of silica shell formation in diatoms. Chemical composition of *Navicula pelliculosa* during silicon-starvation synchrony. *Plant Physiol.* 42: 1601-1606.

Cupp, E. E., 1943. Marine plankton diatoms of the west coast of North America. *Bull. Scripps Inst. Oceanogr. Vol. 5(1)*. 237pp. Univ. California Press, Berkeley and Los Angeles. pp. 199-207.

Cushing, D. H., 1989. A difference in structure between ecosystems in strongly stratified waters and in those that are only weakly stratified. *J. Plankton Res.* 11:1-13.

- Daigo, K., 1959. Studies on the constituents of *Chondria armata*. II. Isolation of an antihelminthical constituent. *J. Pharm. Soc. Japan* 79: 353-356.
- Darley W. M. and B. E. Volcani, 1969. Role of silicon in diatom metabolism. A silicon requirement for deoxyribonucleic acid synthesis in the diatom *Cylindrotheca fusiformis* Reimann and Lewin. *Expl. Cell Res.* 58: 334-342.
- Devlin, R. M. and F. H. Witham, 1983. *Plant Physiology (fourth edition)*. Willard Grand Press. Boston.
- Dickey, R. W., G. A. Fryxell, H. R. Grande and D. Roelke, 1992. Detection of marine toxin okadaic acid and domoic acid in shellfish and phytoplankton in Gulf of Mexico. *Toxicon* 30: 355-359.
- Douglas, D. J. and S. S. Bates, 1992. Production of domoic acid, a neurotoxic amino acid, by an axenic culture of the marine diatom *Nitzschia pungens* f. *multiseries* Hasle. *Can. J. Fish. Aquat. Sci.* 49, 85-90.
- Douglas, D. J., U. P. Ramsey, J. A. Walter and J. L. C. Wright, 1992. Biosynthesis of the neurotoxin domoic acid by the marine diatom *Nitzschia pungens* forma *multiseries*, determined with [¹³C]-labelled precursors and nuclear magnetic resonance. *J. Chem. Soc., Chem. Commun.* 1992: 714-716.
- Douglas, D. J., S. S. Bates, L. A. Bourque and R. Selvin, 1993. Domoic acid production by axenic and non-axenic cultures of the pennate diatom *Nitzschia pungens* f. *multiseries*. In: *Toxic Phytoplankton in the sea*. eds. T. J. Smayda and Y. Shimizu, Elsevier, Amsterdam. pp. 595-600.
- Drinkwater, K. and B. Petrie, 1988. Physical oceanographic observations in the Cardigan Bay region of Prince Edward Island 1982-1987. *Can. Tech. Rep. Hydrogr. Ocean Sci.* 110: 1-37.
- Droop, M. R., 1973. Some thoughts on nutrient limitation in algae. *J. Phycol.* 9: 264-272.
- Droop, M. R., 1983. 25 Years of algal growth kinetics, a personal view. *Bot. Mar.* 26: 99-112.
- Edvardsen, B., F. Moy and E. Paasche, 1990. Hemolytic activity in extracts of *Chrysochromulina polylepis* grown at different levels of selenite and phosphate. In: *Toxic Marine Phytoplankton*. eds. E. Granéli, Sundström, L. Edler and D. M. Anderson, Elsevier, New York, pp. 284-289.
- Egge, J. K. and D. J. Aksnes, 1992. Silicate as regulating nutrient in phytoplankton competition. *Mar. Ecol. Prog. Ser.* 83: 281-289.

- Enright, C. T., G. F. Newkirk, J. S. Craigie and J. D. Castell, 1986. Growth of juvenile *Ostrea edulis* L. fed *Chaetoceros gracilis* Schütt of varied chemical composition. *J. Exp. Mar. Biol. Ecol.* 96: 15-26.
- Eppley, R. W. and P. R. Sloan, 1966. Growth rates of marine phytoplankton: correlation with light absorption by cell chlorophyll *a*. *Physiol. Plant.* 19: 47-59.
- Erga, S. R., 1989. Ecological studies on the phytoplankton of Boknafjorden, western Norway. II Environmental control of photosynthesis. *J. Plankton. Res.* 11: 785-812.
- Falkowski, P. G., Z. Dubinsky, and K. Wyman, 1985. Growth-irradiance relationships in phytoplankton. *Limnol. Oceanogr.* 30: 311-321.
- Fiala, M., G. Cahat, G. Jacques, J. Neveux and M. Panose, 1976. Fertilisation de Communautés Phytoplanctoniques. I. Cas d'un milieu oligotrophe: Méditerranée Nord-occidentale. *J. Exp. Mar. Biol. Ecol.*, 24: 161-163.
- Finenko, Z. Z. and D. K. Krupatkina-Akinina, 1974. Effects of inorganic phosphorus on growth rate of diatoms. *Mar. Biol.* 26:193-201.
- Flynn K. J. and P. J. Syrett, 1986. Utilization of L-lysine and L-arginine by the diatom *Phaeodactylum tricornutum*. *Mar. Biol.* 90: 159-163.
- Fogg, G. E., 1962. Extracellular products. In: *Physiology and Biochemistry of Algae*. ed. R. A. Lewin. Academic Press, New York. pp. 475-489.
- Fogg, G. E. and B. Thake, 1987. *Algal Culture and Phytoplankton Ecology (Third edition)*. University of Wisconsin press, Madison, Wisconsin.
- Forbes J. R. and K. L. Denman, 1991. Distribution of *Nitzschia pungens* in coastal waters of British Columbia. *Can. J. Fish. Aquat. Sci.* 48: 960-967.
- Fritz, L., M. A. Quilliam, J. L. C. Wright, A. Beale and T. M. Work, 1992. An outbreak of domoic acid poisoning attributed to the pennate diatom, *Pseudonitzschia australis*. *J. Phycol.* 28: 439-442.
- Furuya, K. and R. Marumo, 1983. The structure of the phytoplankton community in the subsurface chlorophyll maxima in the western North Pacific Ocean. *J. Plankton Res.* 5: 393-406.
- Furuya, K., M. Takahashi and T. Nemoto, 1986. Summer phytoplankton community structure and growth in a regional upwelling area off Hachijo Island, Japan. *J. Exp. Mar. Biol. Ecol.* 96: 43-55.

- Garcia, V. M. T. and D. A. Purdie, 1992. The influence of irradiance on growth, photosynthesis and respiration of *Gyrodinium cf. aureolum*. *J. Plankton Res.* 14: 1251-1265.
- Garrison, D. L., S. M. Conrad, P. P. Eiles and E. M. Waladron, 1992. Confirmation of domoic acid production by *Pseudonitzschia australis* (Bacillariophyceae) in the culture. *J. Phycol.* 28: 604-607.
- Geider, R. J., B. A. Osborne and J. A. Raven, 1985. Light dependence of growth and photosynthesis in *Phaeodactylum tricornutum* (Bacillariophyceae). *J. Phycol.* 21: 609-619.
- Gilgan, M. W., B. G. Burns and G. J. Landry, 1990. Distribution and magnitude of domoic acid contamination of shellfish in Atlantic Canada during 1988. In: *Toxic Marine Phytoplankton*, eds. E. Granéli, B. Sundström, L. Edler and D. M. Anderson, Elsevier, New York, pp. 469-474.
- Glover, H. E., 1980. Assimilation number in cultures of marine phytoplankton. *J. Plankton Res.* 2: 69-79.
- Goldman, J. C., 1977. Steady state growth of phytoplankton in continuous culture: comparison of internal and external nutrient equations. *J. Phycol.* 13: 251-258.
- Goldman, J. C. and J. J. McCarthy, 1978. Steady state growth and ammonium uptake of a fast-growing marine diatom. *Limnol. Oceanogr.* 23: 695-703.
- Goldman, J. C., J. J. McCarthy and D. G. Peavey, 1979. Growth rate influence on the chemical composition of phytoplankton in oceanic water. *Nature* 279:210-215
- Gonzalez-Rodriguez, É., S. Y. Maestrini, J. L. Valentin and D. Rivera-tenebaum, 1985. Variation de la composition spécifique du phytoplancton de Cabo Frio cultivé en présence d'entichissements différentiels. *Oceanologia Acta* 8: 441-451.
- Granéli, E., K. Wallstrom, U. Larsson, W. Granéli and R. Elmgren, 1990. Nutrient limitation of primary production in the Baltic Sea area. *Ambio* 19: 142-151.
- Grunow, M. 1882. In: *Diatoms*, VI. Part no. 277-324. eds. P. T. Cleve and J. D. Möller. Upsala 1882. Esaias Kdquists Boktryokbri.
- Guillard, R. L., 1973. Division rates. In: *Handbook of Phycological Methods, Culture Methods and Growth Measurements*. ed. J. R. Stein, Cambridge Univ. Press, New York. pp. 289-311.
- Guillard, R. L. and J. H. Ryther, 1962. Studies of marine planktonic diatoms I. *Cyclotella*

- nana* Hustedt, and *Detonula confervacea* (Cleve) Gran. *Can. J. Microb.* 8: 229-239.
- Hall, S., 1982. Toxin and toxicity of *protogonyaulax* from the Northeast Pacific. *Ph.D. thesis, University of Alaska.*
- Hampson, D. R. and R. J. Wenthold, 1988. A kainic acid receptor from frog brain purified using domoic acid affinity chromatography. *J. Biol. Chem.* 263: 2500-2505.
- Harris, G. P. and B. B. Piccinin, 1977. Photosynthesis by natural phytoplankton populations. *Arch. Hydrobiol.* 80: 405-457.
- Harris, G. P., 1978. Photosynthesis, productivity and growth: The physiological ecology of phytoplankton. *Arch. Hydrobiol. Beih. Ergbn. Limnol.* 10: 1-171.
- Harris, G. P., 1980. The measurement of photosynthesis in natural populations of phytoplankton. In: *The Physiological Ecology of Phytoplankton*. ed. I. Morris. University of California Press, Berkeley, pp. 129-187.
- Harris, R. J., 1985. *A Primer of Multivariate Statistics* (Second Edition). Academic Press, Orlando.
- Harrison, P. J., H. L. Conway and R. C. Dugdale, 1976. Marine diatom grown in chemostat under silicate or ammonium limitation. I. Cellular chemical composition and steady state growth kinetics of *Skeletonema costatum*. *Mar. Biol.* 35: 177-186.
- Harrison, P. J., H. L. Conway, R. W. Holmes and C. O. Davis, 1977. Marine diatoms grown in chemostats under silicate or ammonium limitation. III. cellular chemical composition and morphology of *Chaetoceros debilis*, *Skeletonema costatum*, and *Thalassiosira gravida*. *Mar. Biol.* 43: 19-31.
- Harrison, P. J., Y. P. Yang and M. H. Hu, 1992. Phosphate limitation of phytoplankton growth in coastal estuarine waters of China and its potential interaction with marine pollutants. In: *Marine Ecosystem Enclosed Experiments*. eds. C. S. Wong and P. J. Harrison. IDRC, Ottawa, 1992. pp. 192-202.
- Harrison, W. G., 1992. Regeneration of nutrients. In: *Primary Productivity and Biochemical Cycles in the Sea*. eds. F. G. Falkowski and A. D. Woodhead. Plenum Press, New York. pp. 385-407.
- Harrison, W. G. and T. Platt, 1980. Variations in assimilation number of coastal marine phytoplankton: Effects of environmental co-variates. *J. Plankton Res.* 2: 249-.
- Harrison, W. G., E. J. H. Head, E. P. Horne, B. Irwin, W. K. W. Li, A. R. Longhurst, M. A. Paranjape and T. Platt, 1993. The western North Atlantic bloom experiment. *Deep-Sea*

Res. II 40: 279-305.

Hasle, G. R., 1965. *Nitzschia* and *Fragilariopsis* species studies in the light and electron microscopes II. The group *Pseudonitzschia*. *Skrifter utgitt av Det Norske Videnskaps-Akademi i Oslo I. Mat.-Naturv. Klasse. Ny Serie No 18. (Skr. norske Vidensk-Akad. Mat-Nat. Kl. 18)*: 1-45 + 17 plates.

Hasle, G. R., 1972. The distribution of *Nitzschia seriata* Cleve and Allied Species. In: *Beihefte Zur Nova Hedwigia* 39: 171-190. (First Symposium on recent and fossil marine diatoms. Bremerhaven, Sept. 21-26, 1970).

Hasle, G. R., 1993. Nomenclatural notes on marine planktonic diatoms. The family Bacillariacea. *Beih. Nova Hedwigia* 106: 315-321.

Healey, F. P. and L. L. Hendzel, 1975. Effect of phosphorus deficiency on two algae growing in chemostat. *J. Phycol.* 11: 303-309.

Healey, F. P., 1979. Short term responses of nutrient deficient algae to nutrient addition. *J. Phycol.* 15: 289-299.

Humphrey, G. F., 1963. Chlorophyll *a* and *c* in cultures of marine algae. *Aust. J. Mar. Freshwater Res.* 14: 148-154.

Humphrey, G. F. and D. V. Subba Rao, 1967. Photosynthetic rate of the marine diatom *Cylindrotheca closterium*. *Aust. J. Mar. Freshwater Res.* 18: 123-127.

Impellizzeri, G., S. Mangiafico, G. Oriente, M. Piattelli, S. Sciuto, E. Fattorusso, S. Magno, C. Santacroce and D. Sica, 1975. Aminoacids and low-molecular-weight carbohydrates of some marine red algae. *Phytochemistry* 14: 1549-1557.

Jørgensen, E. G., 1955. Variation in the silica content of diatoms. *Physiol. Plant.* 8: 840-845.

Judson, W. I. and T. Bernard, 1988. *Mussel Monitoring Project*. P.E.I. Dept. Fish.

Judson, W. I. and T. Bernard, 1989. *P.E.I. Mussel Monitoring Program 1989 Report*. P.E.I. Dept. Fish. Aquaculture.

Karl, D. M. and O. Holm-Hansen, 1980. ATP, ADP, and AMP determinations in water samples and algal cultures. In: *Handbook of Phycological Methods, Physiological and Biogeochemical Methods*. eds. J. A. Hellebust and J. S. Cragie. Cambridge Univ. Press, London. pp. 197-206.

Karl, D. M., 1980. Cellular nucleotide measurements and applications in microbial

ecology. *Micobiol. Rev.* 44: 739-796.

Kawamura, A. and T. Ichikawa, 1984. Distribution of diatoms in a small area in the Indian Sector of the Antarctic. In: Proceedings of the Sixth Symposium on Polar Biology. *Memoirs of National Institute of Polar Special Issue* 32: 25-38.

Kiefer, D. A. and B. G. Mitchell, 1983. A simple steady state description of phytoplankton growth rates based on absorption cross section and quantum efficiency. *Limnol. Oceanogr.* 28: 770-776.

Kodama, M. T. Ogata and S. Sato, 1989. Saxitoxin-producing bacterium isolated from *Protogonyaulax tamarensis*. In: *Red tides, Biology, Environmental Science and Toxicology*, eds. T. Okaichi, D. M. Anderson and T. Nemoto, Elsevier, pp. 363-366.

Koroleff, F., 1983a. Determination of silicon. In: *Methods of Seawater Analysis*. eds. K. Grasshoff, M. Ehrhardt, K. K. Remling, Verlag Chemie GmbH, D-6940, Weinheim, pp. 174-183.

Koroleff, F., 1983b. Determination of phosphorus. In: *Methods of Seawater Analysis*. eds. K. Grasshoff, M. Ehrhardt, K. K. Remling, Verlag Chemie GmbH, D-6940, Weinheim, pp. 125-139.

Langdon, C., 1987. On the cause of the interspecific differences in the growth-irradiance relationship for phytoplankton. Part I. A comparative study of the growth-irradiance relationship of three marine phytoplankton species: *Skeletonema costatum*, *Olisthodiscus luteus* and *Gonyaulax tamarensis*. *J. Plankton Res.* 9: 459-482.

Lauzier, L. M., 1965. Drift bottle observations in Northumberland Strait, Gulf of St. Lawrence. *J. Fish. Res. Bd. Can.* 22: 353-368.

Laws, E. and J. Caperon, 1976. Carbon and nitrogen metabolism by *Monochrysis lutheri*: measurement of growth-rate-dependent respiration rates. *Mar. Biol.* 36: 85-97.

Laws, E. A. and T. T. Bannister, 1980. Nutrient- and light-limited growth of *Thalassiosira fluviatilis* in continuous culture, with implications for phytoplankton growth in the ocean. *Limnol. Oceanogr.* 25: 457-473.

Laycock, M. V., A. S. W. de Freitas and J. L. C. Wright, 1989. Glutamate agonists from marine algae. *J. Appl. Phycol.* 1:113-122.

Lewin, J. C., 1955. Silicon metabolisms III. respiration and silicon uptake in *Navicula pelliculosa*. *J. Gen. Physiol.* 39: 1-10.

Lewin, J. C., 1957. Silicon metabolisms IV. growth and frustule formation in *Navicula*

pelliculosa. *Can. J. Microbiol.* 3: 427-433.

Lewin, J. C. and C. H. Chen, 1968. Silicon metabolism in diatom. VI. Silicic acid uptake by a colourless marine diatom, *Nitzschia alba*. *J. Phycol.* 4: 161-166.

Lewin, J. C. and B. E. F. Reimann, 1973. Silicon and plant growth. *Ann. Rev. Pl. Physiol.* 20: 289-304.

Lewin J. and J. A. Hellebust, 1978. Utilization of glutamate and glucose for heterotrophic growth by the marine pennate diatom *Nitzschia laevis*. *Mar. Biol.* 47: 1-7.

Lewis, N. I., S. S. Bates, J. L. McLachlan and J. C. Smith, 1993. Temperature effects on growth, domoic acid production and morphology of the diatom *Nitzschia pungens* f. *multiseriis*. In: *Toxic phytoplankton blooms in the sea*, eds. T. J. Smayda and Y. Shimizu. Elsevier, Amsterdam, pp. 601-606.

Li, W. K. W., 1980. Temperature adaptation in phytoplankton: cellular and photosynthetic characteristics. In: *Primary Production in the Sea*, ed. P. G. Falkowski, Plenum Publ., New York, pp. 259-279.

Li, W. K. W. and P. M. Dickie, 1987. Temperature characteristics of photosynthetic and heterotrophic activity: seasonal variations in temperatru microbial plankton. *Appl. Envir. Microb.* 53: 2282-2295.

Lin, J. and Q. Yang, 1991. Distribution of phytoplankton in Meizhou Bay, Fujian. *Journal of Oceanography in Taiwan Strait* 10: 122-126.

Lombardi, A. T. and P. J. Wangersky, 1991. Influence of phosphorus and silicon on lipid class production by the marine diatom *Chaetoceros gracilis* grown in turbidostat cage cultures. *Mar. Ecol. Prog. Ser.* 77: 39-47.

Luckner, M., 1984. *Secondary Metabolism in Microorganisms, Plants, and Animals*. 2nd ed. Springer-Verlag, New York.

Maeda, M., T. Kodama, T. Tanaka, Y. Ohfuné, K. Nomoto, K. Nishimura and T. Fujita, 1984. Insecticidal and neuromuscular activities of domoic acid and its related compounds. *J. Pesticide Sci.* 9: 27-32.

Maeda, M., T. Kodama, M. Saito, T. Tanaka, H. Yoshizumi, K. Nomoto and T. Fujita, 1987. Neuromuscular action of insecticidal domoic acid on the American cockroach. *Pesticide Biochem. Physiol.* 28: 85-92.

Maestrini, S. Y. and E. Granéli, 1991. Environmental conditions and ecophysiological mechanisms which led to the 1988 *Chrysochromulina polylepis* bloom: an hypothesis.

Oceanol. Acta 14: 397-413.

Mann, J., 1987. *Secondary metabolism* (2nd edition). Oxford Chemistry Ser. 33. Clarendon Press, Oxford.

Mann, K. H., 1993. Physical oceanography, food chains, and fish stocks: a review. *ICES J. Mar. Sci.* 50: 105-119.

Mann, K. H. and J. R. N. Lazier, 1991. *Dynamics of Marine Ecosystems: Biological-physical Interactions in the Oceans*. Blackwell, Boston.

Marquardt, D. W., 1963. An algorithm for least-squares estimation of nonlinear parameters. *J. Soc. Ind. Appl. Math.* 11: 431-441.

Marshall, H. G., 1984. Phytoplankton distribution along the eastern coast of the USA. Part V. Seasonal density and cell volume patterns for the north-eastern continental shelf. *J. Plankton Res.* 6: 169-193.

Marshall, H. G. and M. S. Cohn, 1983. Distribution and composition of phytoplankton in Northeastern coastal waters of the United States. *Estuarine, Coastal and Shelf Sciences* 17: 119-131.

Marshall, H. G. and J. A. Ranasinghe, 1989. Phytoplankton distribution along the eastern coast of the U.S.A.-VII. mean cell concentrations and standing crop. *Continental Shelf Res.* 9: 153-164.

Marshall, H. G. and M. S. Cohn, 1987a. Phytoplankton distribution along the eastern coast of the U.S.A. Part VI. Shelf waters between Cap Henry and Cape May. *J. Plankton Res.* 9: 139-149.

Marshall, H. G. and M. S. Cohn, 1987b. Phytoplankton composition of the New York Bight and adjacent waters. *J. Plankton Res.* 9: 267-276.

Martin, J. F. 1977. Control of antibiotics synthesis by phosphate. In: *Advances in Biochemical Engineering* 6, eds. T. K. Ghose, A. Fiechter, N. Blakebrough. Springer-Verlag, Berlin. pp. 105-127.

McElroy, W. D., H. H. Seliger and E. H. White, 1969. Mechanism of bioluminescence, chemi-luminescence and enzyme function in the oxidation of firefly luciferin. *Photochem. Photobiol.* 10: 153-170.

McGeer, E. G., J. W. Olney and O. L. McGeer, 1978. Kainic acid as a tool in neurobiology, Raven Press, New York.

- Miller, R. L. and D. L. Kamykowski, 1986a. Effects of temperature, salinity, irradiance and diurnal periodicity on growth and photosynthesis in the diatom *Nitzschia americana*: light-limited growth. *J. Plankton Res.* 8: 215-228.
- Miller, R. L. and D. L. Kamykowski, 1986b. Effects of temperature, salinity, irradiance and diurnal periodicity on growth and photosynthesis in the diatom *Nitzschia americana*: light-saturated growth. *J. Phycol.* 22: 339-348.
- Morel, A., L. Lassara and J. Gostan, 1987. Growth rate and quantum yield time response for a diatom to changing irradiance (energy and color). *Limnol. Oceanogr.* 32: 1066-1084.
- Navarro, J. N., 1983. A survey of the marine diatoms of Puerto Rico. VII. Suborder Raphidineae: Families Auriculaceae, Epithemiaceae, Nitzschiaceae and Surirellaceae. *Bot. Mar.* 16: 393-408.
- Odum, E. P., 1993. *Ecology and Our Endangered Life-Support Systems*. Sinauer Associates, Inc. Publishers, Sunderland, Massachusetts.
- Ogata, T., T. Ishimaru and M. Kodama, 1987. Effect of water temperature and light intensity on growth rate and toxicity change in *Protogonyaulax tamarensis*. *Mar. Biol.* 95: 217-220.
- Ogata, T., M. Kodama and T. Ishimaru, 1989. Effect of water temperature and light intensity on growth rate and toxin production of toxic dinoflagellates. In: *Red Tide: Biology, Environmental Sciences and Toxicology*, eds. T. Okaichi, D. M. Anderson and T. Nemoto, Elsevier, New York. pp. 423-426.
- Ogata T., M. Kodama, K. Komaru, S. Sakamoto, S. Sato and U. Simidu, 1990. Production of paralytic shellfish toxins by bacteria isolated from toxic dinoflagellates. In: *Toxic Marine Phytoplankton*. eds. E. Granéli, B. Sundström, L. Edler, D. M. Anderson, Elsevier, pp. 311-315.
- Okita, T. W. and B. E. Volcani, 1978. Role of silicon in diatom metabolism IX. Differential synthesis of DNA polymerase and DNA-binding proteins during silicate starvation and recovery in *Cylindrotheca fusiformis*. *Biochim. Biophys. Acta* 519: 76-86.
- Paasche, E., 1973a. Silicon and the ecology of marine plankton diatoms. I. *Thalassiosira pseudonana* (*Cyclotella nana*) grown in a Chemostat with silicate as limiting nutrient. *Mar. Biol.* 19: 117-126.
- Paasche, E., 1973b. Silicon and the ecology of marine plankton diatoms. II. Silicate uptake kinetics in five diatom species. *Mar. Biol.* 19: 262-269.

- Paasche, E., 1968. Marine plankton algae grown with light-dark cycles. II. *Ditylum brightwelli* and *Nitzschia turgidula*. *Physiologia Plantarum* 21: 66-77.
- Paasche, E., 1980. Silicon content of five marine plankton diatom species measured with a rapid filter method. *Limnol. Oceanogr.* 25: 474-480.
- Pan, Y., D. V. Subba Rao and R. E. Warnock, 1991. Photosynthesis and growth of *Nitzschia pungens* f. *multiseries* Hasle, a neurotoxin producing diatom. *J. Exp. Mar. Biol. Ecol.* 154: 77-96.
- Pan, Y., D. V. Subba Rao, K. H. Mann, W. K. W. Li and R. E. Warnock, 1993. Temperature dependence of growth and carbon assimilation in *Nitzschia pungens* f. *multiseries*, a causative diatom of domoic acid poisoning. In: *Toxic phytoplankton blooms in the sea*. eds. T. J. Smayda and Y. Shimizu. Elsevier, Amsterdam. pp. 619-624.
- Pan, Y., K. H. Mann, D. V. Subba Rao, J.-Z. Zou and C. Zhang, 1994. Is there a potential for amnesic shellfish poisoning in coastal China? Poster at: *The Fifth International Phycological Congress*, Qingdao, China, June 26 - July 2, 1994.
- Parrish, C. C., A. S. W. de Freitas, G. Bodenec, E. J. MacPherson and R. G. Ackman, 1991. Lipid composition of the toxic marine diatom, *Nitzschia pungens*. *Phytochemistry* 30: 113-116.
- Perry, M. J., 1972. Alkaline phosphatase activity in subtropical central North Pacific waters using sensitive fluorometric method. *Mar. Biol.* 15: 113-119
- Perry, M. J., 1976. Phosphate utilization by oceanic diatom in phosphorus-limited chemostat culture and in the oligotrophic waters of the central North Pacific. *Limnol. Oceanogr.* 21: 88-107.
- Platt, T. and A. D. Jassby, 1976. The relationship between photosynthesis and light for natural assemblages of coastal marine phytoplankton. *J. Phycol.* 12: 421-430.
- Platt, T., K. L. Denman and A. D. Jassby, 1975. The mathematical representation and prediction of phytoplankton productivity. *Fish. Mar. Serv. Tech. Rep.* No. 523, 110 pp.
- Platt, R., C. L. Gallegos and W. G. Harrison, 1980. Photoinhibition of photosynthesis in natural assemblages of marine phytoplankton. *J. Mar. Res.* 38: 687-701.
- Pocklington, R., J. E. Milley, S. S. Bates, C. J. Bird, A. S. W. de Freitas and M. A. Quilliam, 1990. Trace determination of domoic acid in seawater and phytoplankton by high-performance liquid chromatography of the fluorenylmethoxycarbonyl (FMOC) derivative. *Intern. J. Environ. Anal. Chem.* 38: 351-368.

- Prézelin, B. B., 1981. Light reactions in photosynthesis. In: *Physiological Bases of Phytoplankton ecology*, ed. T. Platt, pp.1-46. *Can. Bull. Fish. Aquat. Sci.* 210, Ottawa.
- Prézelin, B. B., 1982. Effects of light intensity on aging of the Dinoflagellate *Gonyaulax polyedra*. *Mar. Biol.* 69: 129-135.
- Prézelin, B. B. and H. A. Matlick, 1983. Nutrient-dependent low-light adaptation in the dinoflagellate *Gonyaulax polyedra*. *Mar. Biol.* 74: 141-150.
- Proctor, N. L., S. L. Chan and A. J. Trevor, 1975. Production of saxitoxin by cultures of *Gonyaulax catenella*. *Toxicon* 13, 1-9.
- Provasoli, L., 1979. Recent progress, an overview. In: *Toxic Dinoflagellate Blooms*. eds. D. L. Taylor and H. H. Seliger. Elsevier, New York, pp. 1-13.
- Ram, M. J. V. R. Nair, B. N. Desai, 1989. Distribution of phytoplankton off Mithapur (Gujarat). *J. Indian Fish. Assoc.* 19: 49-57.
- Redfield, A. C., B. H. Ketchum and F. A. Richards, 1963. The influence of organisms on the composition of sea-water. In: *The Sea. Ideas and observations on progress in the study of the seas*. ed. M. N. Hill. Vol. 2, John Wiley and Sons, New York. pp. 26-77.
- Rhee, C-Y., 1978. Effects of N:P ratios and nitrate limitation on algal growth, cell composition, and nitrate uptake. *Limnol. Oceanogr.* 23: 10-25.
- Richards, F. A., 1958. Dissolved silicate and related properties of some western North Atlantic and Caribbean waters. *J. Mar. Res.* 17: 449-465.
- Rivera, R. P., 1985. Chilean marine species of the genus *Nitzschia* Hasle, section Pseudonitzschia (Bacillariophyceae). *Gahana-Bot.* 42: 9-38.
- Rivkin, R. B., M. A. Voytek and H. H. Seliger, 1982a. Phytoplankton division rates in light-limited environments: two adaptations. *Science* 215: 1123-1125.
- Rivkin, R. B., H. H. Seliger, E. Swift and W. H. Biggley, 1982b. Light-shade adaptation by the oceanic dinoflagellates *Pyrocystis noctiluca* and *P. fusiformis*. *Mar. Biol.* 68: 181-191.
- Roessler, P. G., 1988a. Changes in the activity of various lipid and carbohydrate biosynthetic enzymes in the diatom *Cyclotella cryptica* in response to silicon deficiency. *Arch. Biochem. Biophys.* 267: 529-538.
- Roessler, P. G., 1988b. Effects of silicon deficiency on lipid composition and metabolism in diatom *Cyclotella cryptica*. *J. Phycol.* 24: 394-400.

- Rothbuhr, L. and F. Scott, 1957. A study of the uptake of silicon and phosphorus by wheat plant with radiochemical methods. *Biochemi. J.* 65: 241-245.
- Roy, S., 1988. Effects of change in physiological conditions on HPLC-defined chloropigment composition of *Phaeodactylum tricornutum* (Bohlin) in batch and turbidostat cultures. *J. Exp. Mar. Biol. Ecol.* 118: 137-149.
- Ryther, J. H. and W. M. Dunstan, 1971. Nitrogen, Phosphorus, and eutrophication in the coastal marine environment. *Science*, 171: 1008-1013.
- Sakshaug, E., 1977. Limiting nutrients and maximum growth rates for diatoms in Narragansett Bay. *J. Exp. Mar. Biol. Ecol.* 28: 109-123.
- Sancetta, C., 1989. Spatial and temporal trends of diatom flux in British Columbia fjords. *J. Plankton Res.* 11: 503-520.
- Scholin, C. A., M. C. Villac, K. R. Buck, G. A. Fryxell and F. P. Chavez, 1994. Domoic acid in Monterey Bay: Research trends and future directions. In: *Proceedings of Sixth International Conference on Toxic Marine Phytoplankton*, Nantes, France, Oct. 18-22, 1993. eds. Lassus *et al.* (in press).
- Sharp, J. H., 1977. Excretion of organic matter by marine phytoplankton, Do healthy cells do it? *Limnol. Oceanogr.* 22: 381-399.
- Shifrin, N. S. and S. W. Chisholm, 1981. Phytoplankton lipids: interspecific differences and effects of nitrate, silicon and light-dark cycles. *J. Phycol.* 17: 374-384.
- Shumway, S. E., 1990. A review of the effects of algal blooms on shellfish and aquaculture. *Journal of the World Aquaculture Society* 21: 65-104.
- Shuter B., 1979. A model of physiological adaptation in unicellular algae. *J. Theor. Biol.* 78: 519-552.
- Silva, E. S., 1982. Relationship between dinoflagellates and intracellular bacteria. In: *Marine Algae in Pharmaceutical Science, Vol. 2*, eds. Walter de Gruyter & Co., Berlin, New York, pp. 269-288.
- Silva, E. S., 1979. Intracellular bacteria, the origin of the dinoflagellates toxicity. In: *International IUPAC Symposium on Mycotoxins and Phycotoxins*, ed. E. S. Silva, Lausanne, Pahotox Publication. (ref. Silva 1982)
- Silva, E. S., 1985. Ecological factors related to *Prorocentrum minimum* blooms in Obidos Lagoon (Portugal). In: *Toxic Dinoflagellates*. eds. D. M. Anderson, A. White, D. G. Baden, Elsevier, New York. pp. 251-256.

- Silvert, W. and D. V. Subba Rao, 1992. Dynamics model of the flux of domoic acid, a neurotoxin through a *Mytilus edulis* population. *Can. J. Fish. Aquat. Sci.* 49, 400-405.
- Siron, R., G. Giusti and B. Berland, 1989. Changes in the fatty acid composition of *Phaeodactylum tricornutum* and *Dunaliella tertiolecta* during growth and under phosphorus deficiency. *Mar. Ecol. Prog. Ser.* 55: 95-100.
- Smayda, T. J., 1990. Novel and nuisance phytoplankton blooms in the sea: evidence for a global epidemic. In: *Toxic Marine Phytoplankton*. eds. Granéli, E. B. Sundström, L. Edler, D. M. Anderson, Elsevier, New York. pp. 29-40.
- Smayda, T. J., 1989. Primary production and the global epidemic of phytoplankton blooms in the sea: a linkage? In: *Coastal and Estuarine Studies* 35: 449-483.
- Smith, J. C., P. Odense, R. Angus, S. S. Bates, C. J. Bird, P. Cormier, A. S. W. de Freitas, C. Léger, D. O'Neil, K. Pauley and J. Worms, 1990a. Variation in domoic acid levels in *Nitzschia* species: implications for monitoring programs. *Bull. Aquacult. Assoc. Can.* 90-4: 27-31.
- Smith, J. C., R. Cormier, J. Worms, C. J. Bird, M. A. Quilliam, R. Pocklington, R. Angus and L. Hanic, 1990b. Toxic blooms of the domoic acid containing diatom *Nitzschia pungens* in the Cardigan River, Prince Edward Island, in 1988. In: *Toxic Marine Phytoplankton*, Eds. E. Granéli, B. Sundstrom, L. Edler and D. M. Anderson, Elsevier, New York, pp. 227-232.
- Smith, E. I., 1936. Photosynthesis in relation to light and carbon dioxide. *Proc. Nat. Acad. Sci. Wash.* 22: 504-511.
- Sommer, U. and H. H. Stabel, 1983. Silicon consumption and population density changes of dominant planktonic diatoms in Lake Constance. *J. Ecol.* 1983: 119-130.
- Steel, J. H., 1962. Environmental control of photosynthesis in the sea. *Limnol. Oceanogr.* 7: 137-150.
- Steemann-Nielsen, E., 1952. The use of radioactive carbon ^{14}C for measuring organic production in the sea. *J. Cons. Perm. Int. Explor. Mer.* 18: 117-140.
- Steidinger, K. A., 1979. Quantitative ultrastructure variation between culture and field specimens of the dinoflagellate *Ptychodiscus breve*. *Ph.D. thesis, University of South Florida*.
- Strickland, J. D. H. and T. R. Parsons, 1972. *A practical Handbook of Seawater Analysis*. *Fish. Res. Bd. Can. Bull.* 167.

Subba Rao, D. V., 1988. Species specific primary production measurements of arctic phytoplankton. *Br. Phycol. J.* 23: 273-282.

Subba Rao, D. V. and S. J. Smith, 1987. Temporal variation of size-fractionated primary production in Bedford Basin during the spring bloom. *Oceanologica Acta* 10: 101-109.

Subba Rao, D. V. and G. Wohlgeschaffen, 1990. Morphological variants of *Nitzschia pungens* Grunow f. *multiseries* Hasle. *Bot. Mar.* 33: 545-550.

Subba Rao, D. V., M. A. Quilliam and R. Pocklington, 1988a. Domoic acid - a neurotoxic amino acid produced by the marine diatom *Nitzschia pungens* in culture. *Can. J. Fish. Aquat. Sci.* 45: 2076-2079.

Subba Rao, D. V., P. M. Dickie and P. Vass, 1988b. Toxic phytoplankton blooms in the eastern Canadian Atlantic embayments. *International Council for the Exploration of the Sea*, C. M. 1988/L:28.

Subba Rao, D. V., A. S. W. deFreitas, M. A. Quilliam, R. Pocklington and S. S. Bates, 1990. Rates of production of domoic acid, a neurotoxic amino acid in the pennate marine diatom *Nitzschia pungens*. In: *Toxic Marine Phytoplankton*, eds. E. Granéli, B. Sundström, L. Edler and D. M. Anderson, Elsevier, New York, pp. 413-417.

Subba Rao, D. V., F. Partensky, G. Wohlgeschaffen and W. W. K. Li, 1991. Flow cytometry and microscopy of gametogenesis in *Nitzschia pungens*, a toxic, bloom-forming, marine diatom. *J. Phycol.* 27: 21-26.

Subba Rao, D. V., Y. Pan and S. J. Smith, 1994. Allelopathy between *Rhizosolenia alata* (Brightwell) and the toxigenic *Pseudonitzschia pungens* f. *multiseries* (Hasle). *Oceanologica acta* (in press).

Subba Rao, D. V. and Y. Pan, 1993. Photosynthetic characteristics of *Dinophysis norvegica* Claparede & Lachmann, a red-tide dinoflagellate. *J. Plankton Res.* 15: 965-976.

Sullivan, C. W. and B. E. Volcani, 1973. Role of silicon in diatom metabolism III. The effects of silicate on DNA polymerase, TEP kinase and DNA synthesis in *Cylindrotheca fusiformis*. *Biochim. Biophys. Acta* 308: 212-229.

Taguchi, S., J. A. Hirata and E. A. Laws, 1987. Silicate deficiency and lipid synthesis of marine diatoms. *J. Phycol.* 23: 260-267.

Taguchi, S., 1976. Relationship between photosynthesis and cell size of marine diatom. *J. Phycol.* 12: 185-189.

Takano, H. and K. Kuroki, 1977. Some diatoms in the section *Pseudonitzschia* found in

coastal water of Japan. *Bull. Tokai Reg. Fish. Res. Lab. No. 91*: 41-51.

Takemoto, T. and K. Daigo, 1958. Constituents of *Chondria armata*. *Chem. Pharmaceutical Bull.* 6: 578-580.

Taylor, D. L. 1968. In situ studies of the cytochemistry and ultrastructure of a symbiont marine dinoflagellate. *J. Mar. Biol. Ass. U.K.* 48: 349-366.

Taylor, N. J. 1985. Silica incorporation in the diatom *Coscinodiscus granii* as affected by light intensity. *Br. Phycol. J.* 20: 365-374.

Vaulot, D., R. J. Olson, S. Merkel and S. W. Chrisholm, 1987. Cell-cycle response to nutrient starvation in two phytoplankton species, *Thalassiosira weissflogii* and *Hymenomonas carterae*. *Mar. Biol.* 95: 625-630.

Verity, P. G., 1982. Effects of temperature, irradiance, and daylength on the marine diatom *Leptocylindrus danicus* Cleve. IV. Growth. *J. Exp. Mar. Biol. Ecol.* 60: 209-222.

Verity, P. G., 1981. Effects of temperature, irradiance, and daylength on the marine diatom *Leptocylindrus danicus* Cleve. I. Photosynthesis and cellular composition. *J. Exp. Mar. Biol. Ecol.* 55: 79-91.

Vining, L., 1986. Secondary Metabolism. In: *Biotechnology, Vol. 4.*, eds. H. J. Rehm and G. Reed. VCH Verlagsgesellschaft, Weinheim. pp. 19-38.

Watanabe, M. F., K. I. Harada, K. Matsuura and M. Watanabe, 1989. Heptapeptide toxin production during the batch culture of two *Microcystis* species. *J. Appl. Phycol.* 1: 161-165.

Webb, W. L., M. Newton and D. Stan, 1974. Carbon dioxide exchange of *Alnus rabra*: A mathematical model. *Oecologia* 17: 281-291.

Whyte, J. N. C., N. G. Ginther and L. D. Townsend, 1994. Accumulation and depuration of domoic acid by the mussel, *Mytilus californianus*, when fed batch culture *Pseudonitzschia pungens* f. *multiseries*. In: *Proceedings of Sixth International Conference on Toxic Marine Phytoplankton*, Nantes, France, Oct. 18-22, 1993. eds. Lassus *et al.* (in press).

Wohlgelassen, G. D., K. H. Mann, D. V. Subba Rao., R. Pocklington, 1992. Dynamics of the phycotoxin domoic acid: accumulation and excretion in two commercially important bivalves. *J. Appl. Phycol.* 4: 297-310.

Wood A. M., and L. Shapiro (eds), 1993. *Domoic acid*: final report of the workshop report. Oregon Institute of Marine Biology, Feb. 21-23, 1992. Oregon Sea Grant. ORESU-

W-93-003.

Work, T. M., A. M. Beale, L. Fritz, M. A. Quilliam, M. Silver, K. Buck and J. L. C. Wright, 1993. Domoic acid intoxication of brown pelicans and cormorants in Santa Cruz, California. In: *Toxic Phytoplankton Blooms in The Sea*. eds. T. J. Smayda and Y. Shimizu, Elsevier, Amsterdam. pp. 643-649.

Wright, J. L. C., R. K. Boyd, A. S. W. de Freitas, M. Falk, R. A. Foxall, W. D. Jamieson, M. V. Laycock, A. W. McCulloch, A. G. McInnes, P. Odense, V. P. Pathak, M. A. Quilliam, M. A. Ragan, P. G. Sim, P. Thibaut, J. A. Walter, M. Gilgan, D. J. A. Richard and D. Dewar, 1989. Identification of domoic acid, a neuroexcitatory amino acid, in toxic mussels from eastern Prince Edward Island. *Can. J. Chem.* 67: 481-490.

Yoder, J. A., 1979. Effect of temperature on light-limited growth and chemical composition of *Skeletonema costatum* (Bacillariophyceae). *J. Phycol.* 15: 263-270.

Yoo, K. I. and J. H. Lee, 1982. Studies on the planktonic diatoms in the vicinity of Kori Nuclear Power Plant. *Bull. Korea Ocean Res. Dev. Inst.* 4: 53-62.

Zou, J. Z., M. J. Zhou and C. Zhang, 1993. Ecological features of toxic *Nitzschia pungens* Grunow in Chinese coastal waters. In: *Toxic Plankton Blooms in the Sea*. eds. T. J. Smayda and Y. Shimizu. Elsevier, Amsterdam. pp. 651-656.

Zwietering, M. H., I. Jongenburger, F. M. Rombouts and K. van't Riet, 1990. Modelling of the bacterial growth curve. *Appl. Envir. Microb.* 56: 1875-1881.